



UNIVERSITY OF
LIVERPOOL

Novel Iridicycles for the Asymmetric Reduction of C=N Bonds

**This thesis is submitted in accordance with the requirements of
The University of Liverpool for the degree of**

Doctor in Philosophy

by

Jennifer Smith

September 2015

Contents

Acknowledgements.....	iv
Abstract.....	vi
Abbreviations.....	vii
Chapter 1: Introduction	1
1.1 Introduction to Chiral Amines.....	2
1.2 Asymmetric Reduction of Acyclic Imines	4
1.2.1 Asymmetric Hydrogenation of acyclic imines	4
1.2.2 Asymmetric Transfer Hydrogenation of acyclic imines.....	10
1.3 Direct Asymmetric Reductive Amination (DARA)	14
1.3.1 Asymmetric Hydrogenation for DARA.....	14
1.3.2 Asymmetric Transfer Hydrogenation for DARA	17
1.4 Asymmetric Reduction of Quinolines	20
1.4.1 Asymmetric Hydrogenation of quinolines	20
1.4.2 Asymmetric Transfer Hydrogenation of quinolines	24
1.5 Asymmetric Reduction of Pyridines.....	28
1.5.1 Asymmetric Hydrogenation of pyridines	28
1.5.2 Asymmetric Transfer Hydrogenation of pyridines	30
1.6 Aims of this thesis	31
1.7 References	34
Chapter 2: Iridicycle Development and Synthesis	43
2.1 Introduction	44
2.2 Oxazoline based complexes	44
2.2.1 Basic Oxazoline Complexes	44
2.2.2 Bulky oxazoline complex.....	47
2.3 Imidazoline complexes.....	51
2.4 Conclusions	56
2.5 Experimental	56
2.5.1 Standard Procedures.....	57
2.5.2 Analytical data.....	63
2.6 References	105
Chapter 3: Development of a Direct Asymmetric Reductive Amination System.	107
3.1 Introduction	108

3.2 Screening Iridicycles	109
3.3 Optimisation of reaction conditions	119
3.4 Substrate scope.....	125
3.4.1 Ketone variation.....	125
3.4.2 Amine variation.....	128
3.5 Conclusions	134
3.6 Experimental	134
3.6.1 Standard Procedures.....	134
3.6.2 Analytical data.....	136
3.7 References	148
Chapter 4: Asymmetric Transfer Hydrogenation of Quinolines	150
4.1 Introduction	151
4.2 Complex Screening.....	151
4.3 Additive screening.....	155
4.4 Substrate Scope	158
4.4.1 2-Substituted quinolines	158
4.4.2 3- and 4-Substituted quinolines	160
4.5 Conclusion	163
4.6 Experimental	164
4.6.1 General Procedures	164
4.6.2 Analytical data.....	165
4.7 References	171
Chapter 5: Asymmetric Transfer Hydrogenation of Pyridinium Salts.....	172
5.1 Introduction	173
5.2 Screening of Chiral Iridicycles	174
5.3 Condition Optimisation	179
5.4 Substrate Scope	184
5.5 Conclusions	187
5.6 Experimental	187
5.6.1 Standard procedures.....	188
5.6.2 Analytical data.....	189
5.7 References	200
Chapter 6: Asymmetric Hydrogenation of Acyclic Imines	201
6.1 Introduction	202

6.2 Catalyst Screening.....	202
6.3 Condition Optimisation.....	205
6.4 Substrate Screening	208
6.5 Mechanistic Investigation	211
6.5.1 Benzyl Imine AH	211
6.5.2 Modelling of the New Iridium Species	218
6.5.3 Changing Benzyl imine	222
6.5.4 Aniline Monitoring	227
6.5.5 Solvent Test.....	231
6.5.6 Proposed mechanism.....	232
6.6 Conclusions	234
6.7 Experimental	235
6.7.1 Standard Procedures.....	236
6.7.2 Analytical data.....	237
6.8 References	- 257 -
Chapter 7: Conclusions and Future Work	- 259 -

Acknowledgements

First I must thank my supervisor Professor J Xiao for the opportunity to work on this project and the endless discussions of chemistry that enabled this work to be completed. I must also thank Astra Zeneca and EPSRC for the funding that supported this project. Thanks must also go to Dr James Muir for all the help and guidance, especially during my placement at AstraZeneca.

Special thanks must go to Dr Jonathon Barnard and Dr Weijun Tang, both of whom helped greatly in the early days of this project and participated in the synthesis of ligands and complexes presented in Chapter 2. I must also thank Dr Barbara Villa Marcos and Dr Chao Wang who initiated this project synthesising a few of the chiral iridicycles. Chris Thomas is thanked for providing several oxazoline ligands for this study. The molecular modelling presented in Chapter 6, would not have been possible without Dr Neil Berry who performed the DFT calculations for me. For the high pressure NMR study (Chapter 6) Dr Jon Iggo and Alice Parry must be thanked for their knowledge, skills and time. Thanks must also be given to Michael Beaumont for his help, time and endless patience with the low pressure NMR study and teaching me manual NMR skills. Konstantin, Tony, Jean and Moya for the analytic services provided within the department. From AstraZeneca I must thank Andy Ray, for his mass spec skills and training, allowing for analysis of the iridicycles and Marc for his help with the HPLC analysis of the piperidines (Chapter 5).

Many thanks must go to the past and present members of the Xiao group, who have made these 4 years an experience I will never forget. A mention must go to Tom and Jonathon, my lab buddies who kept me entertained in the long hours in the lab. Also to the girls of the group Barbara, Angela and Zhijun, who helped to organise the group's social life, without which we would all have gone a lot crazier. I must thank Dinesh for his advice and ideas, Ste for his continued support especially in proof reading parts of this thesis and Ed who has endured the ups and downs of these 4 years with me. Also to Suleyman, Derya, Nam, Xiaofeng, Jianjun, Ziyu,

Lingjuan, Noemi, Antonio, Pinn, Mink, Emma, Ellis who shall all remain good friends, even countries apart.

I must also thank people from Macclesfield; most importantly Freda and Andrew who have proof read the entire of this thesis and made me truly welcome in Macclesfield. I would also like to thank all the first floor Etherow team who supported me through my time there; James, Ben, Danny, Mike, Jerome, Craig, Barry, Ross, Simon, Phil C, Phil, Pete and Peter.

I would also like to thank the many people outside of the group who have helped keep me going throughout this experience; Gita, Steph, Katie and all those who joined us for countless Friday nights in the AJ. I must especially thank Kathryn, Vicky and Georgie who have supported me through everything and I would not have made it to the end of this without them.

My family must also be acknowledged, even if they will only understand this section! Firstly my mum who has supported me in all things I have decided to try (no matter how annoying they were). My brother, Phil, who helped me grow as a person and is willing to listen and offer help in all things. I must thank Oliver for providing the greatest distraction from my work these last 2 years; I wouldn't have it any other way! Also to my Nan, Jo and Pete who have helped in so many little ways over the years. I would be lost without all of you.

Abstract

The asymmetric reduction of imino bonds is a well known and utilised method of chiral amine synthesis. Chapter 1 gives an insight into the published methods for a range of substrates *via* hydrogenation and transfer hydrogenation systems.

This thesis presents a range of novel iridacycles, all of which contain chiral oxazoline and imidazoline ligands. The synthesised complexes demonstrate a variety of electronic and steric properties. Their activities are presented in the latter chapters for the asymmetric reduction of C=N bonds.

Chapter 3 demonstrates the activity of the 4,5,6-trimethoxyimidazoline iridium complex for direct asymmetric reductive amination. High activity, yielding up to quantitative product is reported, under unusually mild conditions, in both aqueous and organic solvent systems. The enantioselectivities achieved were moderate to high for the substrates screened.

The use of a bulky 2,4,6-tri-*iso*-propyloxazoline iridium complex is reported for the asymmetric reduction of quinolones, *via* transfer hydrogenation conditions. The tetrahydroquinolines were produced in high yields and moderate enantioselectivities. The addition of co-solvents to the aqueous system yielded improved enantioselectivities and conversions.

For the reduction of pyridinium salts a bromo-dioxole imidazoline iridium complex presented high activity. This presents unprecedentedly mild conditions *via* a transfer hydrogenation system, producing high yields of *N*-benzyl piperidines. The enantioselectivities determined were high, although some could not be measured by the available means.

The 2,4,6-tri-*iso*-propyloxazoline iridium complex further demonstrates high activity and enantioselectivity for the asymmetric hydrogenation of acyclic imines. An NMR and mechanistic study revealed the *in-situ* formation of a new iridium species present only in TFE.

Abbreviations

2-MeTHF	2-Methyltetrahydrofuran
Å	Angstrom
AH	Asymmetric Hydrogenation
Aq	Aqueous
Ar	Aryl
ATH	Asymmetric Transfer Hydrogenation
Atm	Atmospheric pressure
BARF	Tetrakis(3,5-bis(trifluoromethyl)phenyl)borate
Bdpch	1,2-Bis(diphenylphosphinoxy)cyclohexane
Bdpp	2,4-Bis(diphenylphosphino)pentane
BINOL	1,1'-Bi-2-naphthol
Bn	Benzyl
Bppm	2-(DiphenylphosphinoMethyl)-4-(diphenylphosphino)-N-(<i>t</i> -butoxycarbonyl)pyrrolidine
CHCl ₃	Chloroform
CI	Chemical Ionisation
COD	Cyclooctadiene
Conv	Conversion
COSY	Correlation Spectroscopy
Cp*	Pentamethylcyclopentadienyl
CPME	Cyclopentyl methyl ether
Cy	Cyclohexyl

Cydn	<i>trans</i> -1,2-diaminocyclohexane
DARA	Direct Asymmetric Reductive Amination
DCE	Dichloroethane
DCM	Dichloromethane
Ddppm	1,4:3,6-dianhydro-2,5-bis(diphenylphosphino)- <i>D</i> -mannitol
DFT	Density Functional Theory
Diop	2,3- <i>O</i> -isopropylidene-2,3-dihydroxy-1,4-bis(diphenylphosphino)butane
DMSO	Dimethylsulphoxide
DPEN	1,2-Diphenyl-1,2-ethylenediamine
DRA	Direct Reductive Amination
Ee	Enantiomeric Excess
Eq	Equivalents
ESI	Electrospray Ionisation
EtOAc	Ethylacetate
EtOH	Ethanol
FT	Formic acid triethylamine complex (5:2)
h	Hour(s)
H ₂	Molecular hydrogen
HCO ₂ H	Formic acid
HEH	Hantzsch Ester
Hex	Hexane
HMQC	Heteronuclear Multiple-Quantum Correlation
HNEt ₂	Diethylamine

HPLC	High Pressure Liquid Chromatography
HRMS	High Resolution Mass Spectroscopy
Hz	Hertz
I ₂	Molecular Iodine
IPA	<i>Iso</i> -propanol
Ir	Iridium
J	Coupling constant
K	Kelvin
K ₂ CO ₃	Potassium carbonate
Kcal	Kilocalorie
m	Multiplet
MeCN	Acetonitrile
MeOH	Methanol
mg	Milligram(s)
MHz	Mega hertz
min	Minute(s)
mL	Millilitre(s)
MM	Molecular Mechanics
mmol	Millimole(s)
mol	Mole(s)
MS	Molecular sieves
Ms	mesylate
n.r	No reaction

NaCO ₂ H	Sodium formate
nbd	2,5-norbornadiene, bicyclo[2,2,1]hepta-2,5-diene
NBS	N-Bromosuccinimide
<i>n</i> -BuLi	<i>n</i> -butyllithium
NEt ₃	Triethylamine
NH ₃	Ammonia
NH ₄ CO ₂ H	Ammonia formate
Nm	Nanometre(s)
NMR	Nuclear Magnetic Resonance
NOESY	Nuclear Overhauser Effect Spectroscopy
°C	Degrees Celsius
PhMe	Toluene
PHOX	phosphinooxazoline
PMP	<i>para</i> -methoxyphenyl
PPh ₃	Triphenylphosphine
ppm	Parts per million
PTSA	<i>para</i> -toluenesulfonic acid
rt	Room temperature
SDS	Sodium dodecyl sulphate
SFC	Supercritical Fluid Chromatography
skewphos	2,4-bis(diphenylphosphino)pentane
TBAI	Tetrabutylammonium Iodide
^t Bu	<i>tert</i> -butyl

^t BuOH	<i>tert</i> -butanol
TFA	Trifluoroacetic acid
TFE	2,2,2-Trifluoroethanol
TH	Transfer Hydrogenation
THF	Tetrahydrofuran
TMS	Trimethylsilane
Tol-BINAP	2,2'-Bis(di- <i>p</i> -tolylphosphino)-1,1'-binaphthyl
TRIP	3,3'-Bis(2,4,6-triisopropylphenyl)-1,1'-binaphthyl-2,2'-diyl hydrogenphosphate
Ts	Tosyl
xyl	xylyl
α	Alpha
δ	Chemical shift

Chapter 1: Introduction

1.1 Introduction to Chiral Amines

α -Chiral amines are prevalent motifs in natural products and therapeutic agents, and are used as key building blocks in synthetic chemistry. They are utilised in multiple industries, including pharmaceuticals, fragrances and agrochemicals, and additionally show activity as chiral ligands and catalysts.

A range of important commercial chiral amines are shown in Figure 1.1. For example (*S*)-Metolachlor is widely used as a herbicide.¹⁻³ Many drugs also contain a chiral amine moiety, for example ephedrine,^{4,5} commonly used as a decongestant. Other pharmaceutically important cyclic amines appear in a number of natural products, such as tubulosine which shows activity as an antitumor drug.^{6,7}

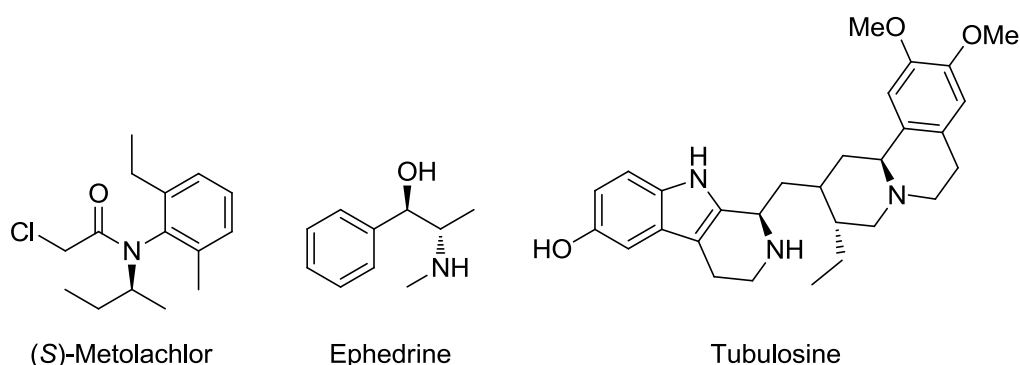


Figure 1.1 Examples of commercial chiral amines.

(*L*)-Proline is a naturally occurring amino acid (Figure 1.2) which has found extensive use as a chiral organocatalyst,⁸ with high selectivity for asymmetric aldol reactions, proceeding *via* an enamine intermediate. Chiral amines can readily coordinate to metal centres and therefore have been utilised as chiral ligands. One of the most well known examples is diphenylethylenediamine (DPEN), which can be used for a wide range of reactions, including reductions.^{9,10} They have also been

used as chiral auxiliaries, for example [1,1'-binaphthalene]-2,2'-diamine (Figure 1.2), which contains axial chirality.^{11,12}

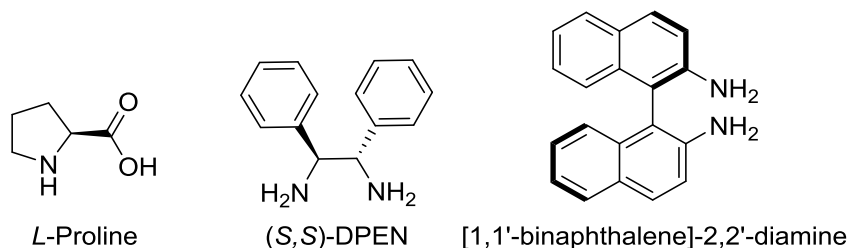
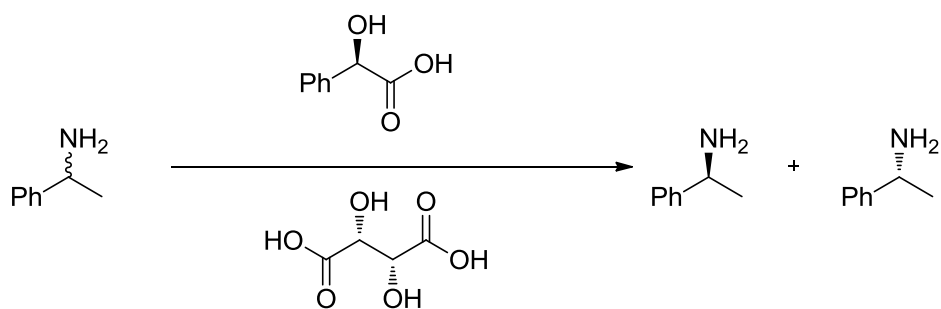


Figure 1.2 Examples of chiral amine catalysts/ligands.

The preparation and isolation of these important enantiomerically enriched amines has been widely investigated. One of the oldest systems is resolution, which is the separation of the two enantiomers from a racemic mixture. This can be achieved by reaction with a chiral agent, such as tartaric acid^{13,14} or mandelic acid,^{15,16} to form diastereomeric salts that can be crystallised for separation (Scheme 1.1). Although a relatively cheap procedure, there is significant amount of waste as the maximum isolated yield can be only 50%.



Scheme 1.1 Tartaric acid (top) and mandelic acid (bottom) for chiral resolution.

Asymmetric synthesis of chiral amines has long been explored; the most successful method is *via* reduction reactions. Whilst significant work has been performed on the reduction of unsaturated C=C and C=O bonds,^{17–19} the reduction of imines has proved one of the most difficult to achieve, compared to carbonyls^{17,18}

or olefins¹⁹. This has partially been attributed to: the difficulty in isolating the imine; the weak binding of the imine to a metal catalyst; and the strong coordination of the product amine to the metal centre, poisoning the catalysts. As a research group we are interested in the synthesis of amines *via* the reduction of imines using novel metal complexes.^{20–22} In this project, the focus will be on the development of an asymmetric version, confined to two reaction pathways: hydrogenation and transfer hydrogenation.

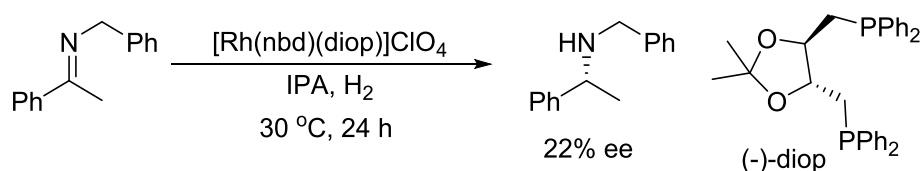
1.2 Asymmetric Reduction of Acyclic Imines

The reduction of acyclic imines is the most widely explored area in C=N bond reduction, with many reported systems using either H₂ gas or an organic hydride source, such as *iso*-propanol (IPA) and Hantzsch esters (HEH). Many issues still require attention including; the limited substrate scope, the use of harsh reaction conditions and additives.

1.2.1 Asymmetric Hydrogenation of acyclic imines

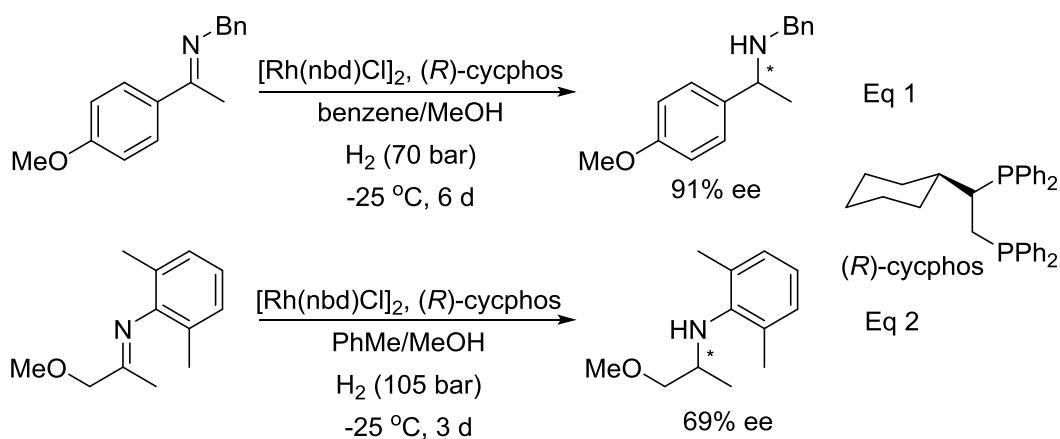
1.2.1.1 Rhodium catalysed AH

Scorrano and co-workers reported the asymmetric hydrogenation (AH) of imines in 1975, demonstrating the use of rhodium in the presence of the diphosphine ligand (-)-diop (Scheme 1.2), as well as olefin and ketone reduction.²³ Although this system yielded a low ee for the reported amine of just 22%, it set a precedent that this transformation was possible.



Scheme 1.2 First reported AH of an imine.

A significant amount of research has since been dedicated to the development of rhodium diphosphine systems. Kutney and co-workers were the first to report a high ee for these systems using (*R*)-cycphos to yield up to 91% ee for *N*-benzyl imines (Eq 1, Scheme 1.3).²⁴ This improvement in selectivity may be attributed to the low temperature of $-25\text{ }^\circ\text{C}$. *N*-aryl imines under the same conditions were only able to produce up to 69% ee (Eq 2, Scheme 1.3),^{25,26} with both substrates requiring several days for high conversions and the addition KI to activate the imine towards reduction.



Scheme 1.3 Early AH systems with high ee.

A range of chiral diphosphine ligands active in the presence of rhodium are shown in Figure 1.3.^{27–30} Notably Borner *et al.* conducted a study on a range of phosphines and phosphonites to directly compare the conversion and ee (Figure 1.3).³¹ Many of those tested showed low to moderate ee, with the highest enantioselectivity achieved with the electron poor ligand (*R,R*)-bdpch at 71% ee.

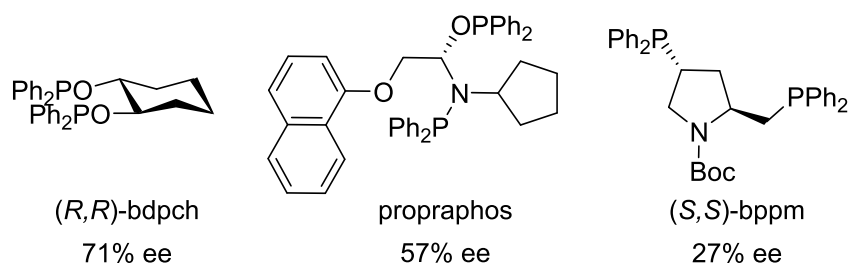
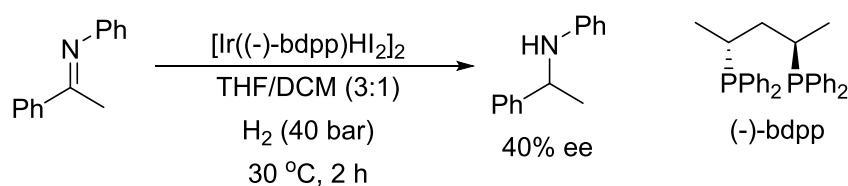


Figure 1.3 Some diphosphine ligands tested for benzyl imine AH.

1.2.1.2 Iridium catalysed AH

In the 1990's diphosphine ligands were first reported in the presence of iridium. Osborn *et al.* showed that up to 80% ee could be obtained under mild conditions, using (-)-bdpp on cyclic imines, whilst *N*-aryl imines reached just 40% ee with the same ligand (Scheme 1.4).³²



Scheme 1.4 First AH using iridium diphosphine complex.

Several groups have since reported iridium (I) diphosphine systems for *N*-aryl imine AH (Figure 1.4). Derwisi and co-workers showed that ddppm was a suitable ligand for this transformation, requiring a chlorinated solvent to yield high conversions and ee's up to 94%.³³ Imamoto *et al.* utilised (S,S) -^tBu-BisP as ligand and achieved up to 99% ee.³⁴ Ligands containing the phosphine-phosphite combination (P-OP) were also highly active. Pizzano and co-workers developed a range of these complexes and were able to provide ee's up to 85%.³⁵ More recently Hu *et al.* developed a similar phosphine-phosphoramidite ligand, containing a H8-BINOL moiety. The complex formed *in situ* achieved up to 99% ee, including for alkyl

imines.³⁶ The phenyl-ferrocenylethyl scaffold has also been reported in the presence of iridium although only one substrate is reported with an ee of 43% (Figure 1.4).^{37,38}

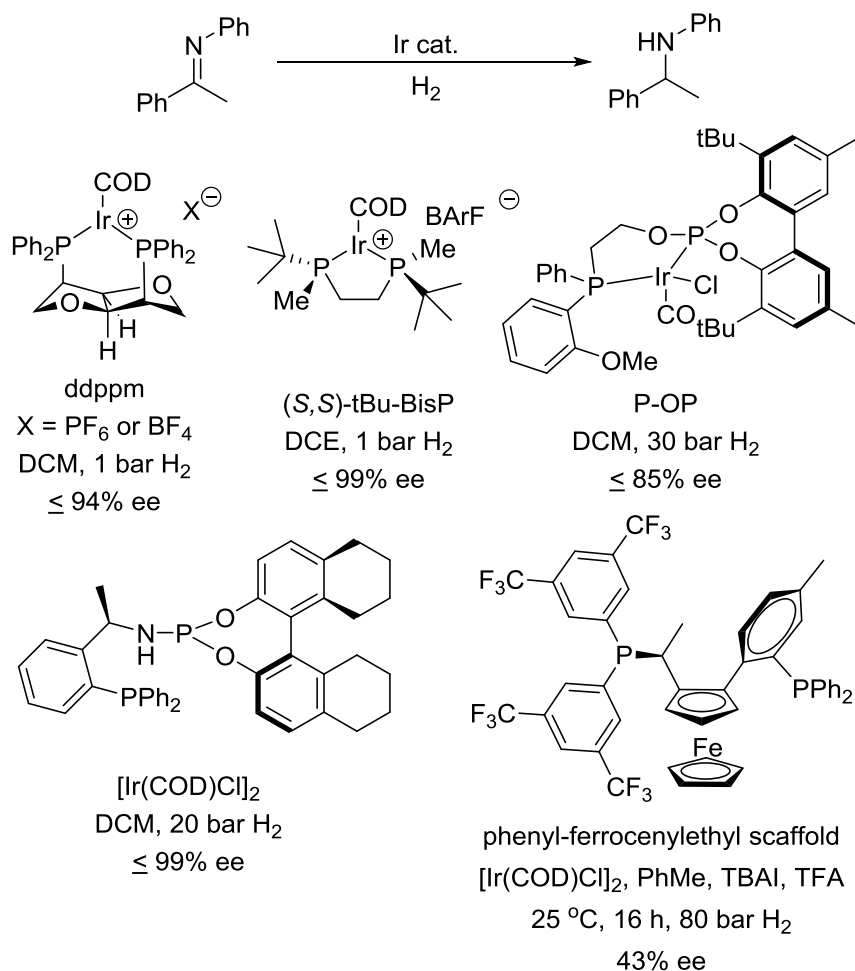


Figure 1.4 Iridium (I) complexes used for AH of imines.

Another common class of highly active ligands used with iridium for AH are phosphine oxazolines (PHOX) (Figure 1.5). An early example of their activity was shown with an *N*-benzyl imine by James *et al.* although active the enantioselectivity was moderate, with 63% ee being the highest.³⁹ Zhou and co-workers later developed a SIPHOX ligand, which completed the AH with a much greater ee of 90-97% for all substrates reported under mild conditions (Figure 1.5).⁴⁰ Andersson *et*

al. have also developed modified PHOX ligands containing an N-P bond (Figure 1.5).⁴¹ These complexes achieved up to 90% ee for *N*-aryl imines, however, they proved inactive for cyclic imines.⁴²

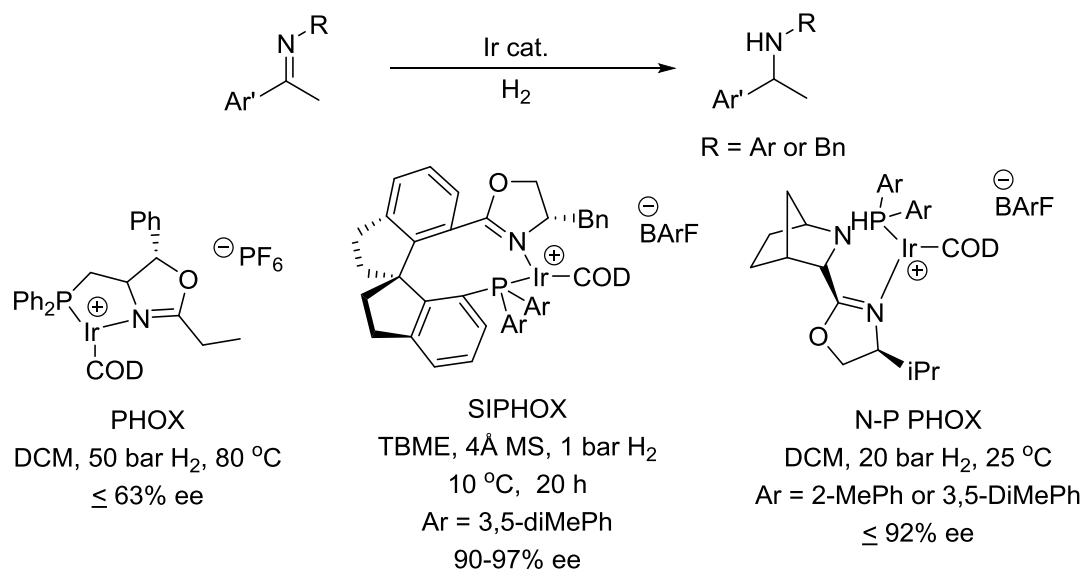
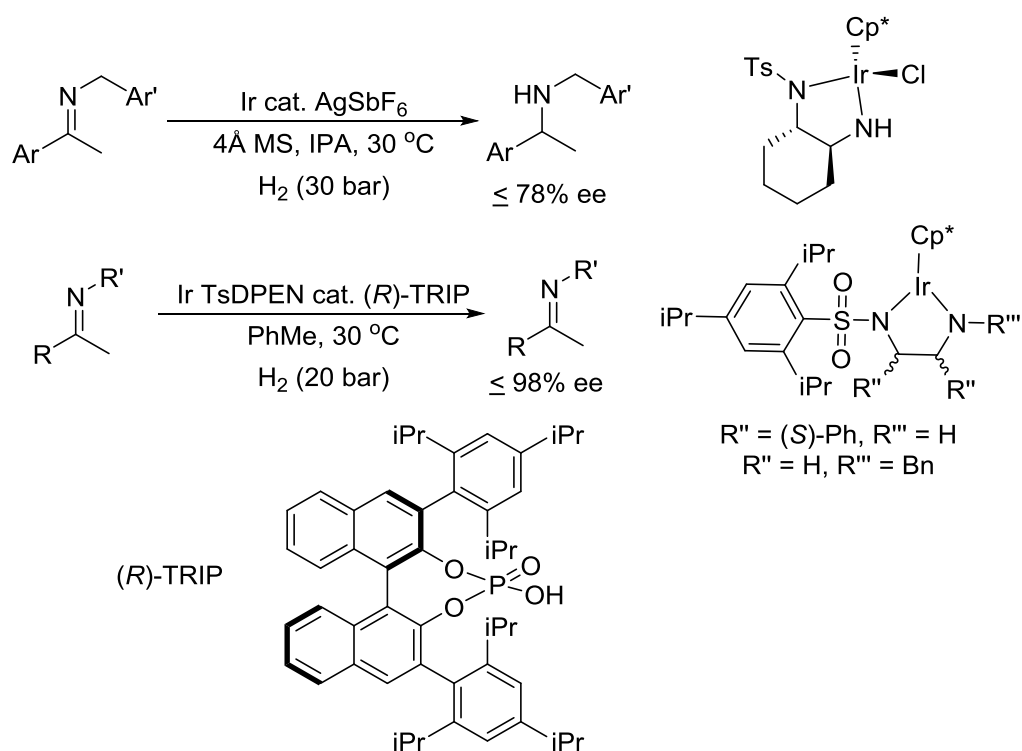


Figure 1.5 Iridium PHOX complexes employed for AH of imines.

Ikariya and co-workers demonstrated that diamine ligands were highly active for imine AH.⁴³ Silver salts were required to improve both the conversion and ee (up to 78%) with a Ts-cydn ligand (Scheme 1.5). The addition of phosphoric acids as a counter ion was able to produce high ee's up to 98%, as reported by Xiao and co-workers.⁴⁴⁻⁴⁶ Both chiral and achiral diamine ligands could be employed in the presence of (*R*)-TRIP (Scheme 1.5).



Scheme 1.5 Diamine ligands utilised with iridium for AH.

1.2.1.3 Other metal catalysed AH

Fan *et al.* showed that ruthenium cymene in the presence of the Ms-DPEN ligand can provide the desired AH in up to 99% ee, for a wide range of *N*-benzyl imines (left, Figure 1.6).^{47,48} Ohkuma and co-workers have also shown that the use of (*S,S*)-DPEN and (*S,S*)-xyl-Skewphos with a ruthenium precursor was able to achieve up to 99% ee's (centre, Figure 1.6).⁴⁹ Beller *et al.* has also demonstrated that (*S*)-TRIP is highly selective in the presence of Knolker's iron complex, achieving up to 98% ee (right, Figure 1.6).⁵⁰

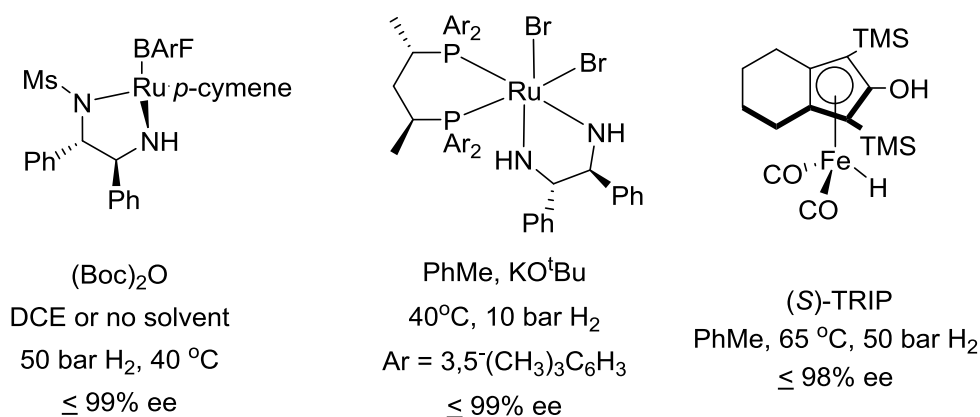
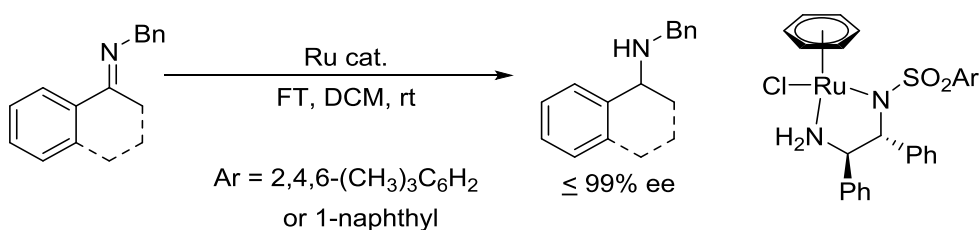


Figure 1.6 Ruthenium and Iron complexes used for AH of imines.

1.2.2 Asymmetric Transfer Hydrogenation of acyclic imines

1.2.2.1 Metal catalysed ATH

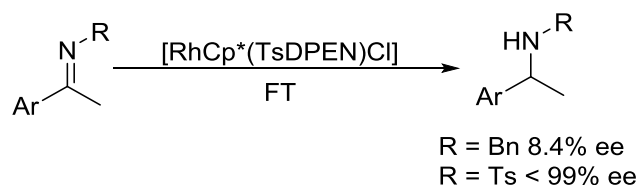
Transfer hydrogenation for imine reduction, using an organic hydride source is less well explored. First reported by Noyori in 1996, a formic acid triethylamine 5/2 complex (FT) was employed as the hydride source.⁵¹ The ATH system was catalysed by a ruthenium Ts-DPEN complex and produced ee's as high as 89%, although it proved more selective for cyclic imines (Scheme 1.6).^{52–54} A study conducted into the *N*-benzyl imine indicated that the lower selectivity is caused by isomerisation of the imine, with reduction of the *E* isomer leading to enantiopure (*S*)-amine, whilst the *Z* imine produces a lower purity of the (*R*)-amine.⁵⁵



Scheme 1.6 Noyori's ATH of imines utilising Ru-TsDPEN.

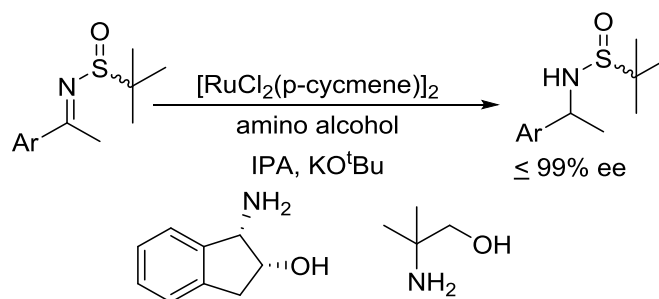
Switching to a rhodium metal centre showed a detrimental effect on the selectivity, although high activity was maintained (Scheme 1.7).⁵⁶ Cyclic examples

maintained a high selectivity (< 99% ee), whilst acyclic imines resulted in a drop of enantioselectivity to 8.4%. Reduction of sulfonated imines under this system yielded up to 99% ee.⁵⁷



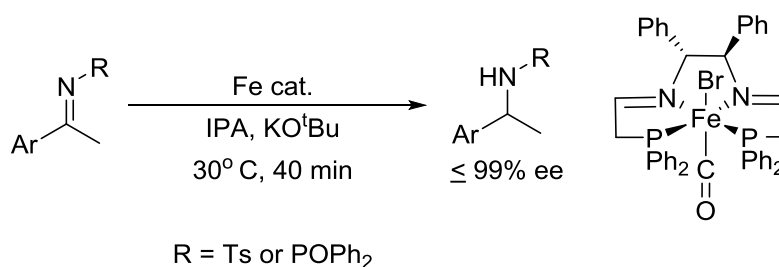
Scheme 1.7 ATH of imines utilising a rhodium TsDPEN complex.

Chiral amino alcohols also show high activity for the reduction of sulfonated imines. Yus *et al.* utilised (1*S*,2*R*)-1-amino-2-indanol in the presence of ruthenium, which produced ee's as high as 99% (Scheme 1.8).^{58,59} A racemic ligand, namely 2-amino-2-methyl-1-propanol, could also be used if a chiral sulfonate was placed on the imine, achieving similarly high conversions and ee's.^{60–63}



Scheme 1.8 Use of amino alcohol ligands with ruthenium for sulfonated imines.

Morris *et al.* has demonstrated the use of iron PNP pincer complexes on a range of protected imines (Scheme 1.9).^{64–66} *N*-diphenylphosphenoyl imines, as well as *N*-tosyl imines and ketones, can be reduced effectively to yield high conversion and selectivity under these conditions.

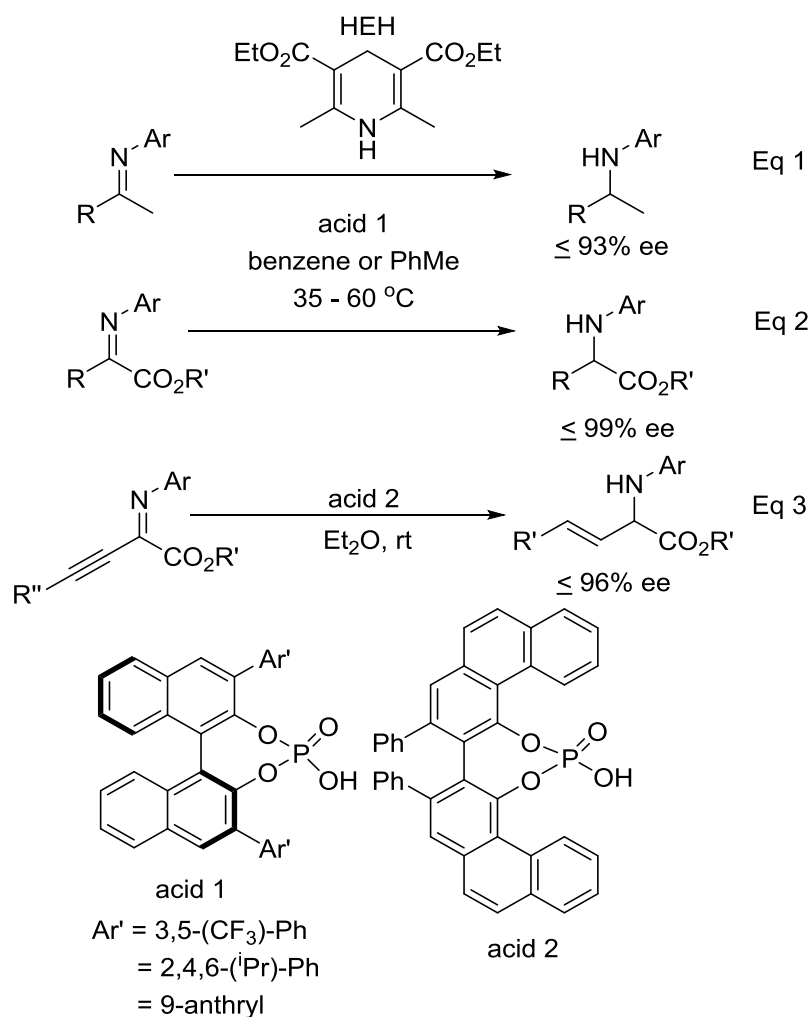


Scheme 1.9 Iron catalysed ATH of imines.

1.2.2.2 Organocatalytic ATH

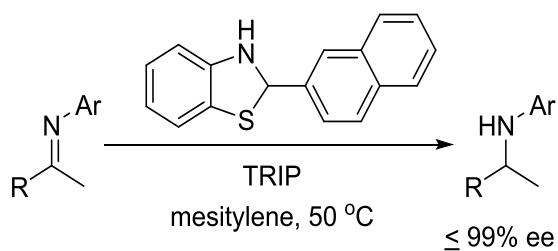
Chiral phosphoric acids also demonstrate catalytic activity for ATH in their own right, providing alternative metal-free systems; however, these systems are generally slower than their metalated counter-parts. The Brønsted acid protonates the imine, therefore activating it for reduction and forming a chiral ion pair.

This was first reported in 2005 by the groups of Rueping and List. Both groups showed the activity of chiral phosphoric acids for the ATH of *N*-aryl imines (Eq 1, Scheme 1.10) to afford amines in high ee's of 70 to 93%, utilising a Hantzsch ester (HEH) as the hydride source.^{67,68} α -Imino-esters could also undergo ATH in the presence of chiral phosphoric acids, leaving the ester group intact (Eq 2, Scheme 1.10).^{69,70} However, the alkenyl functionality proved susceptible to reduction forming an olefin (Eq 3, Scheme 1.10).⁷¹



Scheme 1.10 Brønsted acid catalysed reduction of imines.

Benzothiazolines have also shown activity as a hydride source in the presence of Brønsted acid catalysts (Scheme 1.11). Akiyama *et al.* reported in 2009 complete conversion with 98% ee being achieved in 24 hours, with the benzothiazoline premade or formed *in situ*.



Scheme 1.11 Use of benzothiazoline for ATH of imine.

1.3 Direct Asymmetric Reductive Amination (DARA)

Direct asymmetric reductive amination (DARA) is a more economical route for the synthesis of chiral amines. This is the one-pot reaction of a pro-chiral ketone with an amine to form the imine *in situ*, before a reduction reaction occurs, eliminating the challenging isolation of the imine intermediate (Figure 1.7). Despite its appeal this transformation is less well documented, due to the competition between ketone and imine reductions, as well as potential poisoning of the catalyst by the amine substrate and products.

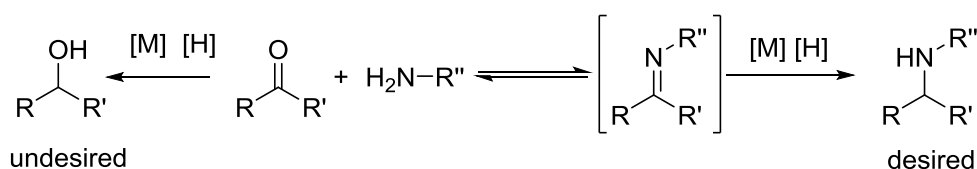
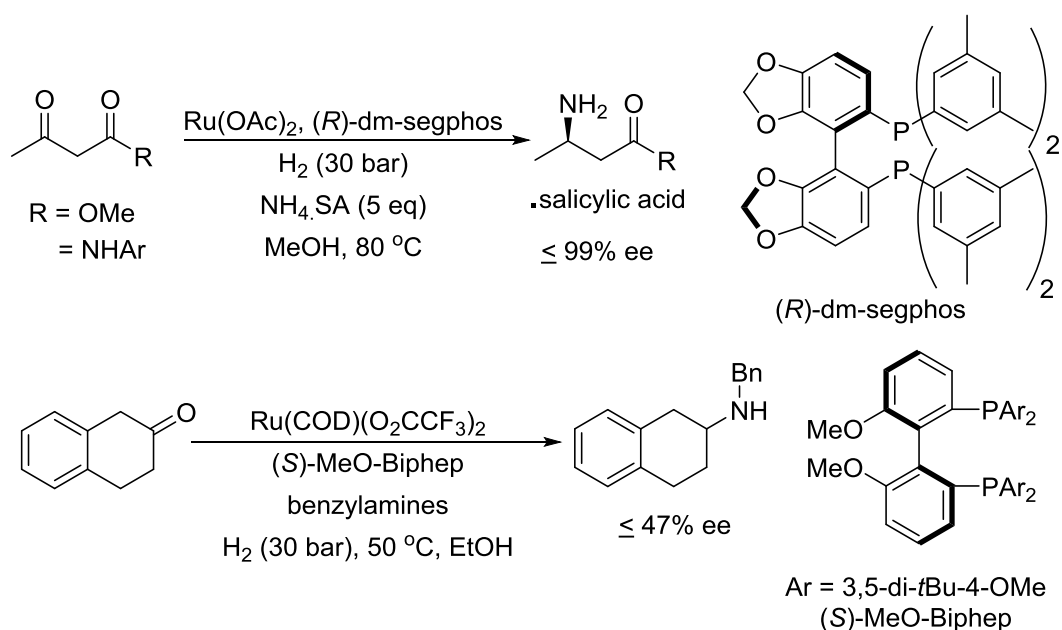


Figure 1.7 Reductive amination vs. ketone reduction.

1.3.1 Asymmetric Hydrogenation for DARA

1.3.1.1 Ruthenium catalysed DARA

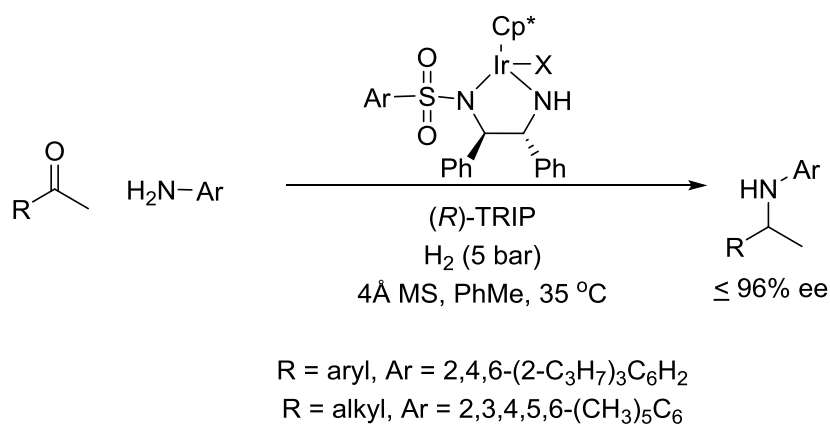
An early report of DARA was in 2009 by Saito and co-workers employing ruthenium diacetate with (*R*)-DM-segphos to synthesise sitagliptin and several derivatives (Scheme 1.12).⁷² The DARA could be performed between β -keto amides or β -keto esters⁷³ with ammonium salicylate, to directly produce primary amines with up to 99% ee. Utilising (*S*)-MeO-BiPhep, in the presence of ruthenium, tetralones could undergo DARA with benzylamine to produce secondary amines with up to 47% ee.⁷⁴



Scheme 1.12 DARA utilising ruthenium diphosphine complexes.

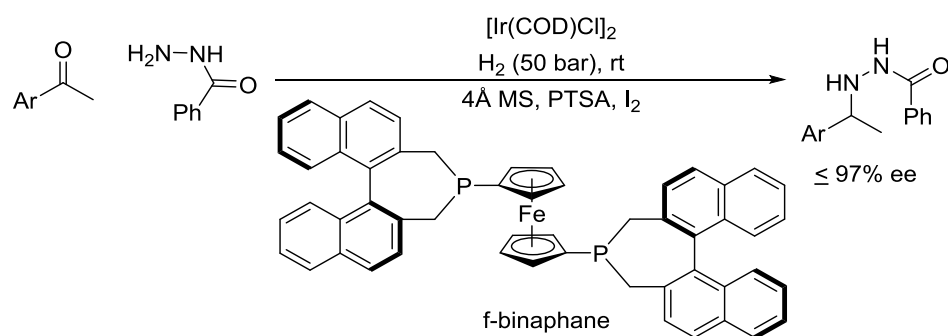
1.3.1.2 Iridium catalysed DARA

A more versatile system was reported by Xiao *et al.* (Scheme 1.13), under similar conditions to those reported above for AH of imines (Scheme 1.5).^{75,76} Utilising an iridium Ts-DPEN complex in the presence of (R) -TRIP, a wide range of substrates could undergo DARA, producing ee's up to 96%. Slight variation of the sulfonate group allowed for both alkyl and aryl ketones to be utilised.



Scheme 1.13 DARA with iridium Ts-DPEN and a chiral phosphoric acid.

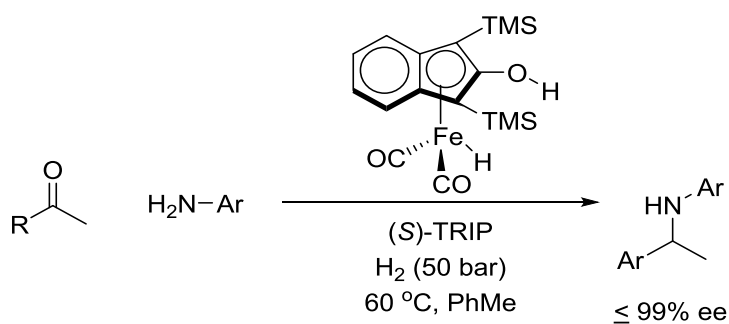
(*S,S*)-f-binaphane in the presence of iridium has also proved an active catalyst utilising phenyl hydrazine as the amine source (Scheme 1.14).⁷⁷ In the presence of several additives (4Å MS, PTSA and iodine) it was able to achieve high conversions, with ee's up to 97%.



Scheme 1.14 DARA with phenyl hydrazine using iridium.

1.3.1.3 Iron catalysed DARA

Beller and co-workers reported a unique system for DARA employing the achiral Knölker's iron complex in the presence of (*S*)-TRIP (Scheme 1.15).⁷⁸ This system proved highly effective, with a large substrate scope, capable of DARA with both alkyl and aryl ketones in the presence of anilines, producing ee's up to 99%.

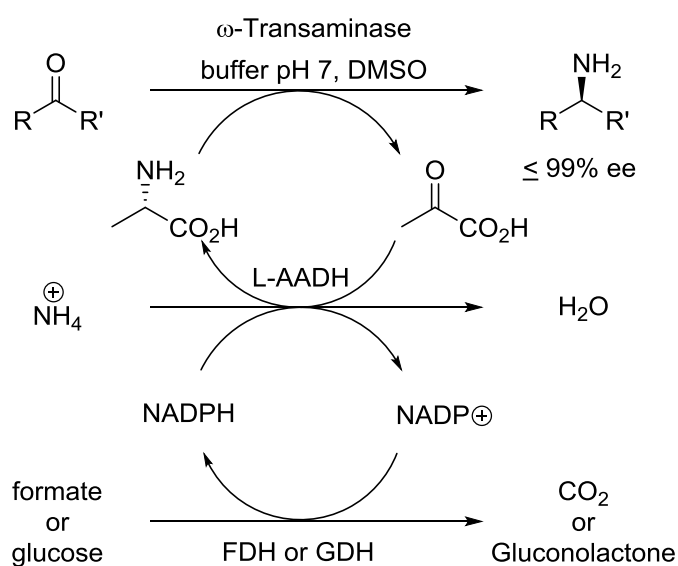


Scheme 1.15 DARA using an iron complex with a chiral phosphoric acid.

1.3.2 Asymmetric Transfer Hydrogenation for DARA

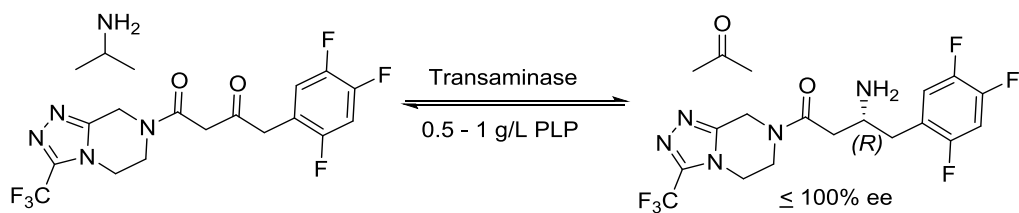
1.3.2.1 Enzymatic routes for DARA

Natural enzymes are capable of DARA, utilising chiral amino acids to create a pocket in which the reaction may occur. Several enzymes have undergone directed evolution to render them more stable and reusable. Kroutil *et al.* reported the use of both aryl and alkyl ketones to yield primary amines, one of the few successful systems capable of producing 99% ee (Scheme 1.16).⁵³ However, this system required a complicated setup; using three separate enzymes, along with both *L*-alanine and NADH as hydrogen sources.



Scheme 1.16 Three enzyme system for DARA.

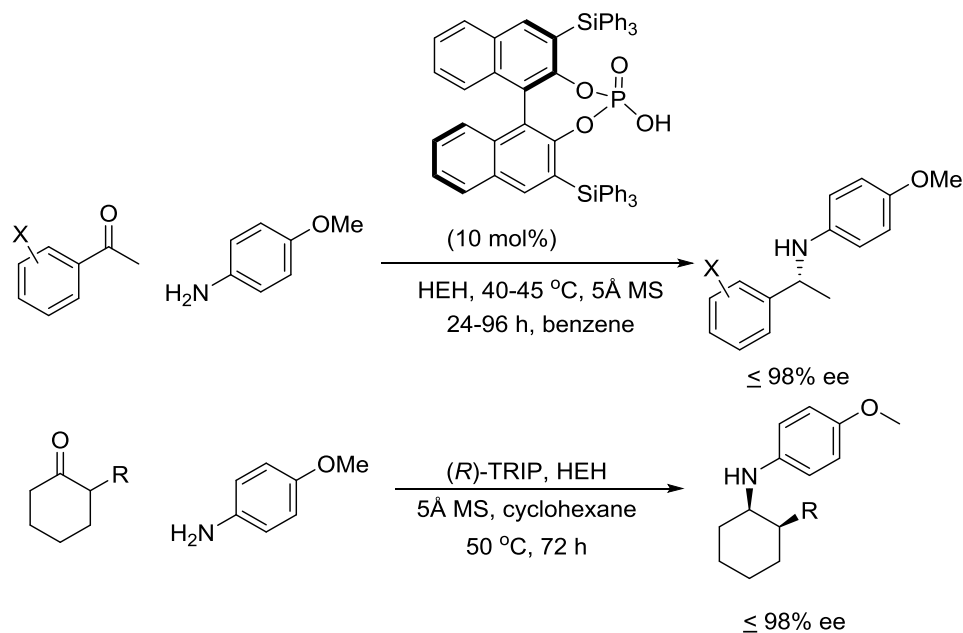
Hughes and co-workers have also reported the directed evolution of an enzyme, *via* 27 mutations, to develop an enzyme capable of producing up to 100% ee on an industrial scale.⁵⁴ Pyridoxal-5'-phosphate (PLP) promotes this reaction by forming a Schiff base and transferring a hydride from a lysine residue on the catalyst to the substrate (Scheme 1.17).



Scheme 1.17 Modified transaminase for DARA.

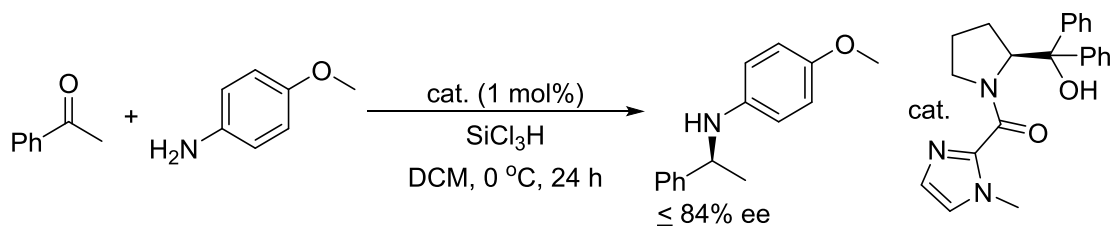
1.3.2.2 Organocatalytic DARA

MacMillan *et al.* reported the use of a chiral BINOL phosphoric acid catalyst and a HEH, although a slow reaction (1-4 days) high ee's of up to 97% could be obtained (Scheme 1.18).⁸¹ A limited substrate scope was also observed; functionalities larger than a methyl were not tolerated and only a few alkyl substrates were reported. List and co-workers have reported similar conditions utilising (*R*)-TRIP as the phosphoric acid (Scheme 1.18).⁸² A range of cyclic α -substituted ketones were reported, with ee's up to 98% and diastereoselectivities ranging from 5:1 to 99:1, with a preference for the *cis* amine product.



Scheme 1.18 Phosphoric acid catalysed DARA in the presence of HEH.

An imidazole based catalyst was also shown to be active for this transformation by Martin and co-workers. Utilising trichlorosilane as a hydride source with up to 70% conversion and 84% ee being obtained (Scheme 1.19).⁸³ However, alkyl amines proved difficult, requiring tandem reaction conditions and microwave irradiation to promote imine formation.

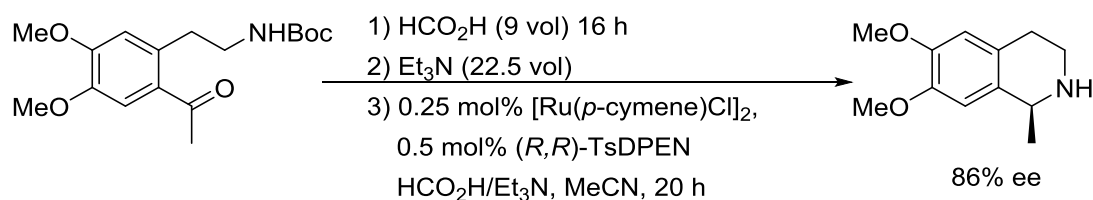


Scheme 1.19 Organocatalytic system using trichlorosilane.

1.3.2.3 Metal-Catalysed DARA

Whilst enzymatic and organocatalytic DARA has proved successful for ATH, they still have many drawbacks, predominantly the high catalyst loading, long reaction time and substrate specificity.

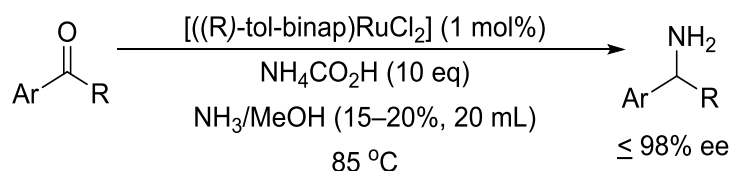
The first metal catalysed system was published by Wills *et al.* utilising a ruthenium Ts-DPEN complex in the presence of FT (Scheme 1.20).⁸⁴ A single chiral cyclic amine was produced in 86% ee.



Scheme 1.20 First ATH transition metal catalysed DARA.

The most successful system published to date by Riermeier *et al.*⁸⁵ has shown to be active for a wide range of ketones, producing a mix of primary amines and acetylated amines. A ruthenium tol-BINAP catalyst was employed, in the

presence of a large excess of ammonium formate with ammonia in methanol, as the hydride source and solvent, to yield complete conversion and up to 98% ee (Scheme 1.21).



Scheme 1.21 Most successful metal catalysed DARA reported to date.

1.4 Asymmetric Reduction of Quinolines

The asymmetric reduction of heterocycles is less well developed. Nearly all reported systems have the same major drawback whereby chirality can only be installed in the 2-position, with very limited reports for the 2,3-position and just one report for chirality in the 4-position.

1.4.1 Asymmetric Hydrogenation of quinolines

1.4.1.1 Iridium catalysed AH

The first reported AH was by Zhou *et al.* which detailed the use of $[\text{Ir}(\text{COD})\text{Cl}]_2$, with a chiral diphosphine ligand ((*R*)-MeO-BiPhep) (Figure 1.8).⁸⁶ This system yielded tetrahydroquinolines in up to 96% ee and high conversions, carried out in the presence of iodine, this system was also active on exocyclic enamines.⁸⁷ C₃-TunePhos also proved an active ligand under similar conditions, producing up to 92% ee and giving complete conversion, for a limited range of substrates (Figure 1.8).⁸⁸

Benzyl chloroformate⁸⁹ and piperidinium triflate⁹⁰ have both been used as alternatives for iodine, activating the quinoline towards reduction (Figure 1.8). In

the presence of $[\text{Ir}(\text{COD})\text{Cl}]_2$ and SegPhos these additives enable the synthesis of tetrahydroquinolines in up to 92% ee. Switching to a (*S*)-H8-BINAPO ligand in either THF or DMPEG/hexane as solvent was able to yield up to 96% ee (Figure 1.8).⁹¹ Similarly (*R*)-P-Phos (Figure 1.8) proved active in these reaction solvents, with up to 92% ee. In the latter solvent system the complex was immobilised allowing for easy recyclability.⁹²

Further work by Zhou *et al.* on quinoline reduction led to the development of modified BiPhep diphosphine ligand to produce an immobilised complex (Figure 1.8)⁹³ forming a more stable catalyst that was able to hydrogenate the quinoline. The use of this immobilised complex is advantageous for being recyclable with activity proven for 5 runs with only a small drop in conversion and enantioselectivity (< 10% drop).

The use of electron withdrawing ligands were able to improve conversion. Commercially available (*R*)-difluoroPhos (Figure 1.8) was able to offer much higher conversions,⁹⁴ allowing for a reduction in catalysts loading, although this system once more required the addition of iodine for activation of the quinoline. Zhou developed (*R*)- CF_3O -BiPhep⁹⁵ which led to a greater increase in activity with this complex (Figure 1.8), producing similar ee's and yields, whilst using a much lower catalyst loading of 0.0005 mol %.

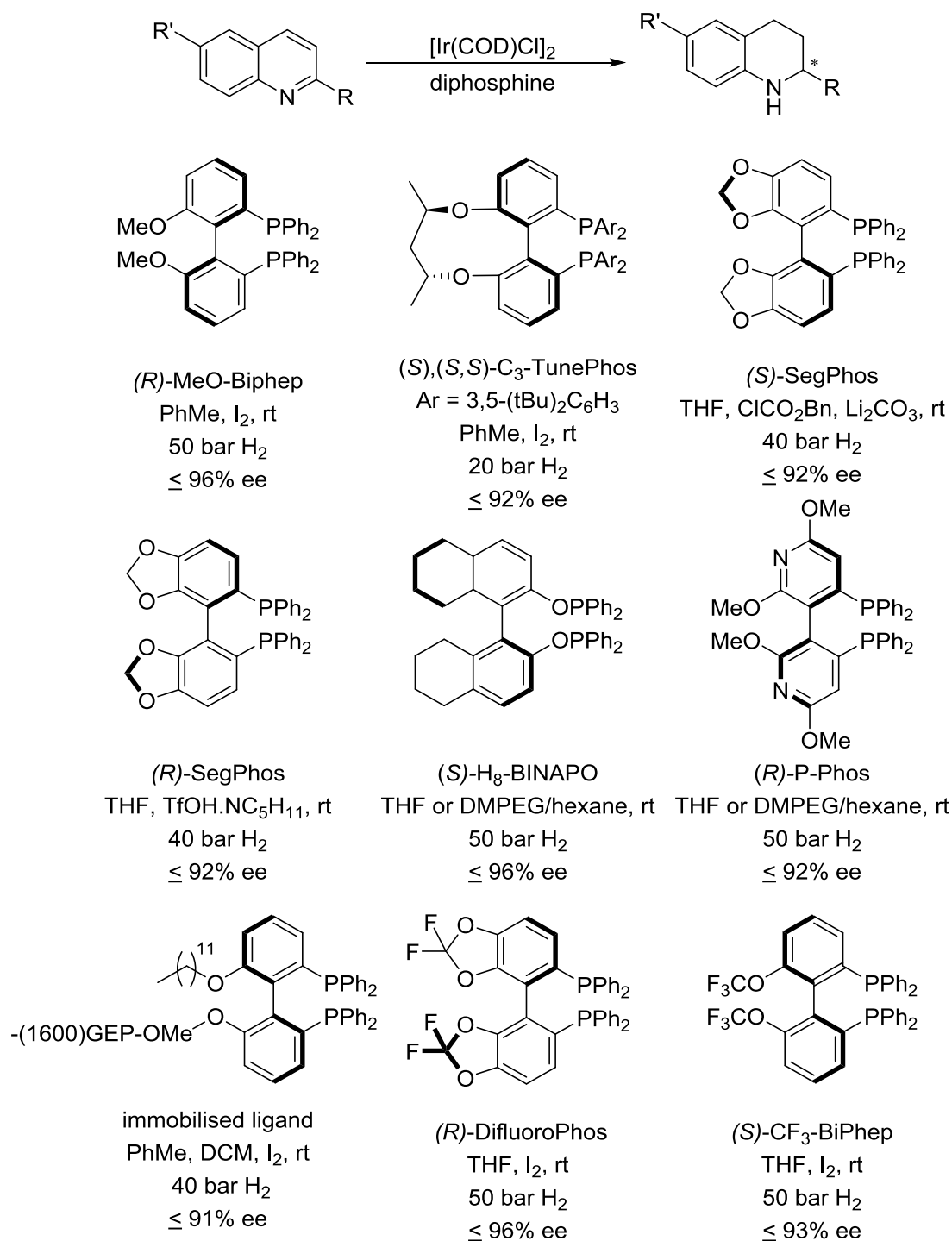
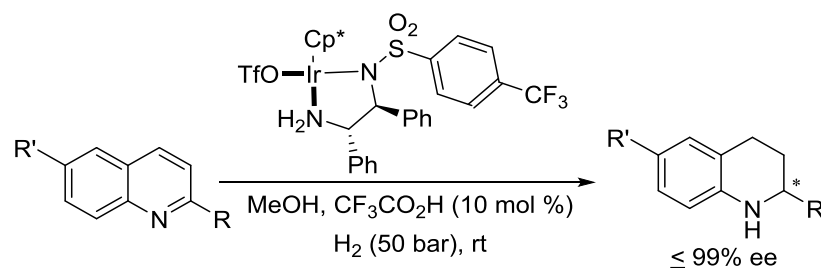


Figure 1.8 A range of diphosphine ligands active with iridium COD chloride for quinoline AH.

Noyori's Ts-DPEN ligand, in the presence of iridium is also active for the AH of quinolines. Xu and co-workers showed that the [IrCp*(CF₃TsDPEN)OTf] complex

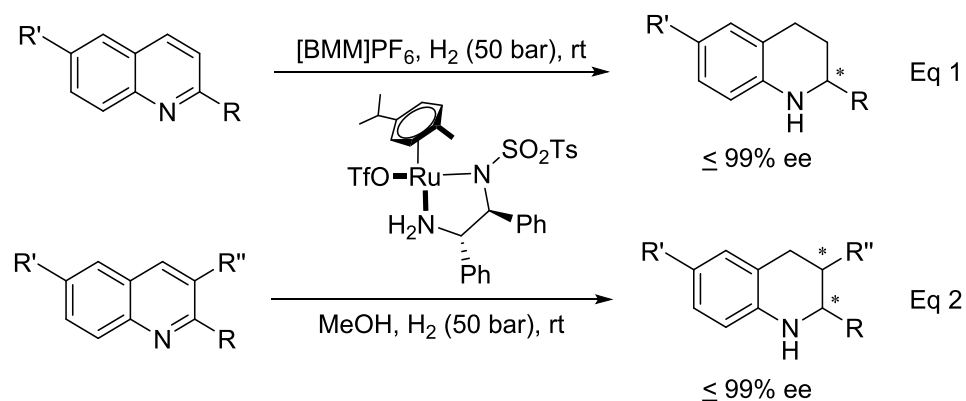
in the presence of a catalytic amount of trifluoroacetic acid yielded up to 99% ee (Scheme 1.22).⁹⁶



Scheme 1.22 Iridium TsDPEN complex for AH of quinolines.

1.4.1.2 Ruthenium catalysed AH

Chan *et al.* continued their work utilising ruthenium with Ts-DPEN ligands (Eq 1, Scheme 1.23), reporting the transformation in neat ionic liquids.⁹⁷ The catalytic system afforded excellent selectivity for all substrates published with up to 99% ee, whilst allowing the catalyst to be recycled for 8 runs. The same complex was also active in alcoholic solvents, allowing for 2,3-disubstituted quinolines to be reduced in moderate to high enantioselectivities (Eq 2, Scheme 1.23).⁹⁸ An in-depth mechanistic study was reported, indicating that the reaction proceeds *via* a 1,4-hydride addition to the quinoline salt, followed by isomerisation of this product, setting up a 1,2-hydride addition to yield the final tetrahydroquinoline (Figure 1.9).



Scheme 1.23 Ruthenium DPEN complexes for AH of quinolines.

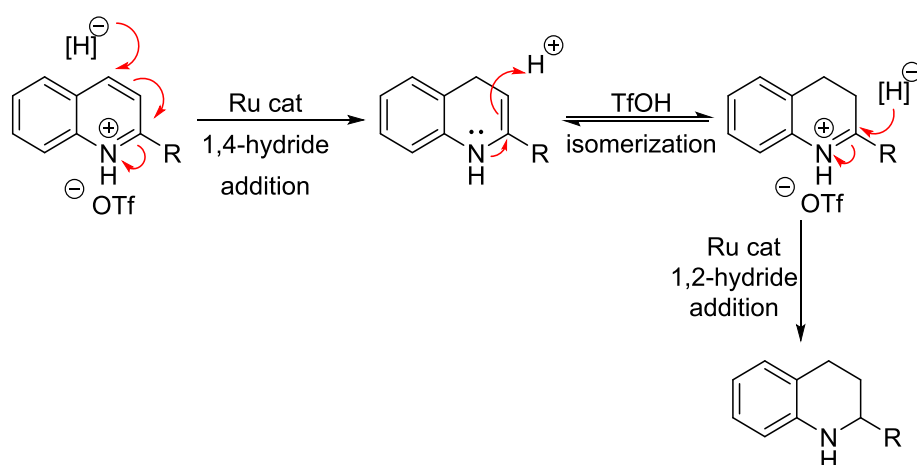
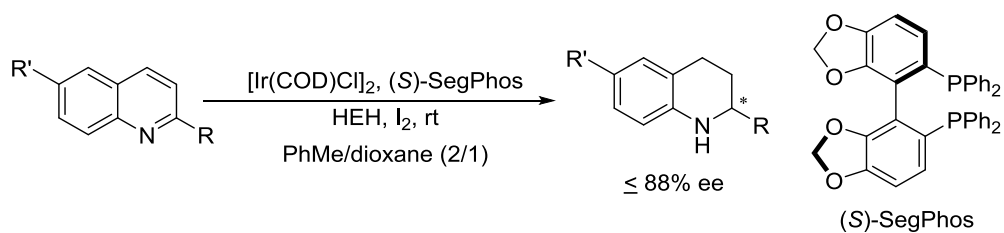


Figure 1.9 Proposed mechanism for AH of 2-substituted quinoline.

1.4.2 Asymmetric Transfer Hydrogenation of quinolines

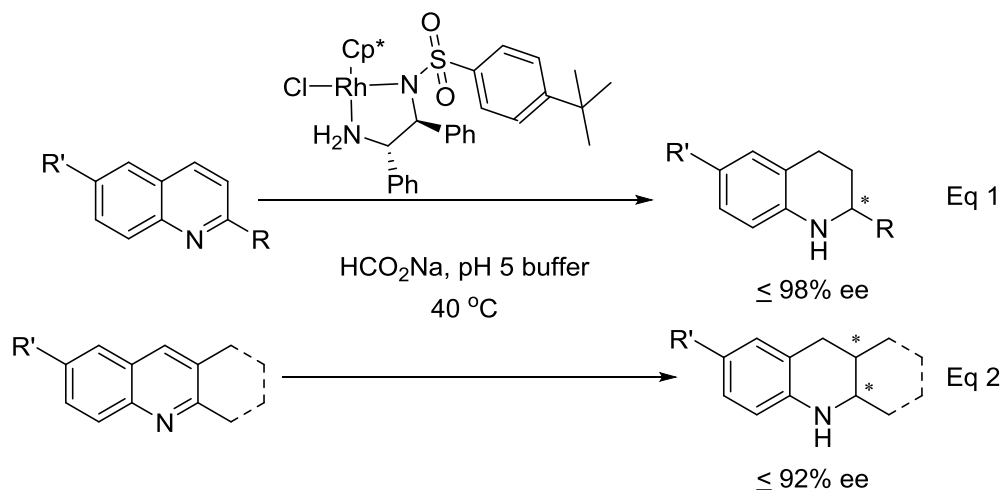
1.4.2.1 Metal catalysed ATH

Zhou *et al.* reported a metal catalysed ATH, similar to their hydrogenation system, utilising $[\text{Ir}(\text{COD})\text{Cl}]_2$, mixed with (*S*)-SegPhos to obtain up to 88% ee over two days (Scheme 1.24).⁹⁹ As in the AH system iodine was required to activate the substrate, but a HEH was used in place of the hydrogen gas.



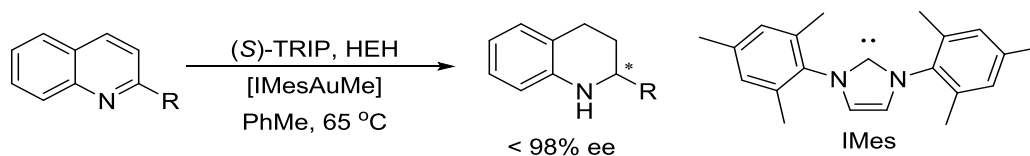
Scheme 1.24 First metal catalysed ATH of quinolines.

Xiao *et al.* developed a system using rhodium in aqueous reaction conditions, utilising a buffered sodium formate solution as hydride source and solvent (Eq 1, Scheme 1.25).¹⁰⁰ This system also allowed for the reduction of a couple of 2,3-disubstituted quinolines with high ee and dr (Eq 2, Scheme 1.25).



Scheme 1.25 Best metal catalysed ATH of quinolines.

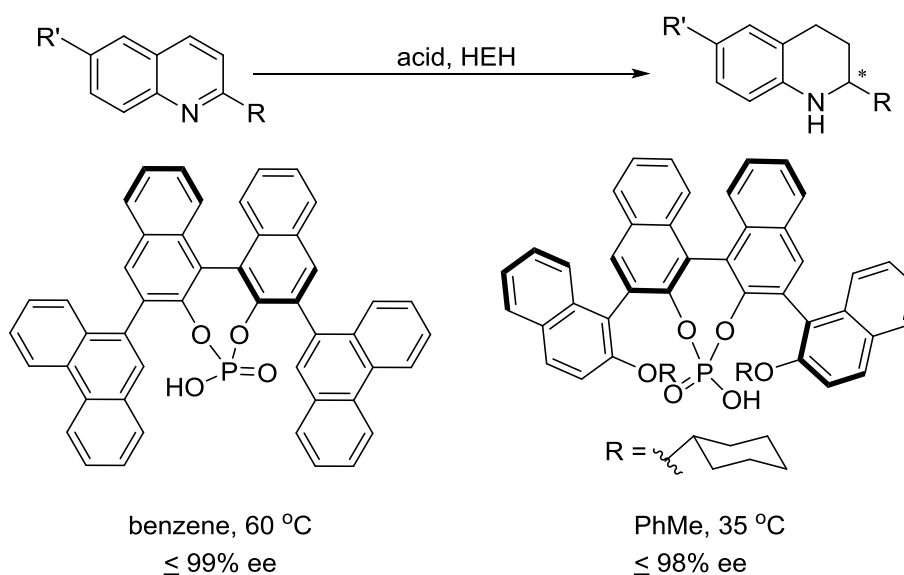
A combination of TRIP with a racemic NHC gold complex was reported by Gong and co-workers (Scheme 1.26).¹⁰¹ The system worked well in the presence of HEH, at low temperatures and reasonable times, achieving up to 98% ee with quantitative conversion.



Scheme 1.26 ATH system using an achiral gold and chiral phosphoric acid.

1.4.2.2 Organocatalytic ATH of quinolines

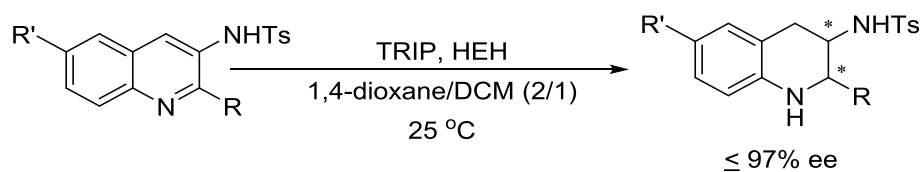
The first of these metal free systems was reported by Theissrmann *et al.* using a bulky 9-phenanthryl substituted phosphoric acid (left, Scheme 1.27), achieving up to 99% ee, although up to 60 hours were required for high conversions.¹⁰² Xu and co-workers were able to reduce the reaction temperature and time whilst still maintaining excellent ee's (up to 98%), using a modified bulky phosphoric acid containing cyclohexyloxy group (right, Scheme 1.27).¹⁰³



Scheme 1.27 First chiral acid catalysed ATH of quinolines.

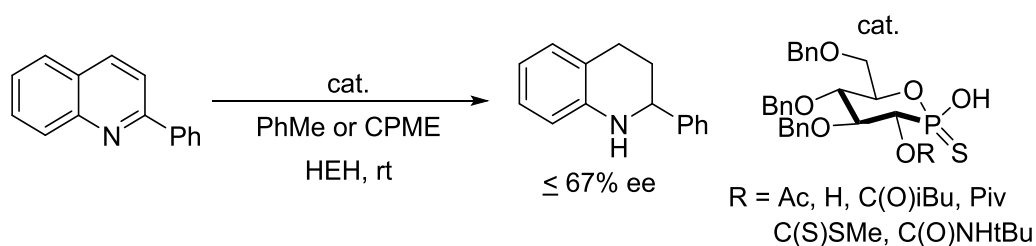
A recent system published by Zhou *et al.* in 2014 has proven successful at producing 2,3-disubstituted tetrahydroquinolines, using TRIP as the catalyst (Scheme 1.28).¹⁰⁴ Only quinoline-3-tosylamines are suitable substrates for ATH

producing up to 97% ee, indicating that the tosyl group is crucial for chiral induction with the acid.



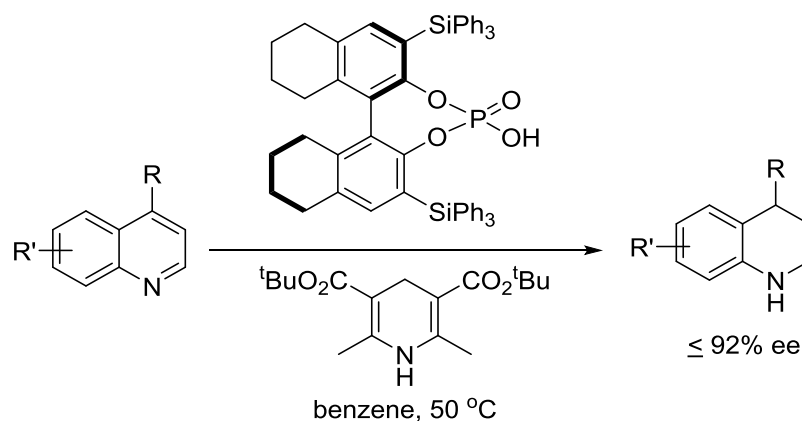
Scheme 1.28 Quinoline-3-amine ATH using chiral phosphoric acid.

Novel P-chiral thiophosphoric acids bearing a sugar backbone are also capable of catalysing the reduction of 2-phenylquinolines in the presence of a HEH in moderate ee's of up to 67% (Scheme 1.29).



Scheme 1.29 ATH of 2-phenylquinoline by a chiral thiophosphoric acid.

Only one successful system for the asymmetric reduction of 4-substituted quinolines has been reported (Scheme 1.30). This system requires the use of an octahydro-BINOL-phosphate bearing triphenylsilyl residues, in the presence of a bulky HEH to give a range of 4-substituted products of up to 92% ee.¹⁰⁵



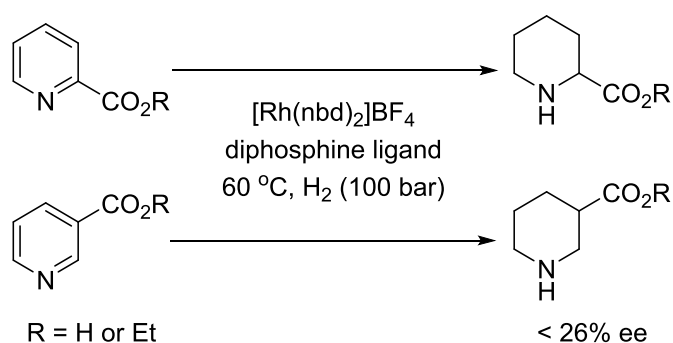
Scheme 1.30 ATH of 4-substituted quinolines.

1.5 Asymmetric Reduction of Pyridines

Pyridine reduction is one of the most difficult C=N bond reductions to perform, with few chiral examples reported. The majority of those prove to be very substrate specific or require harsh conditions, such as high pressure.

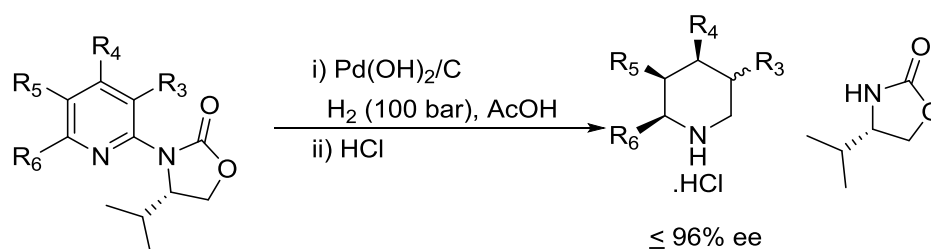
1.5.1 Asymmetric Hydrogenation of pyridines

The first report came in 2000 by Blaser *et al.* in which only four pyridine substrates were reported, all of which were carboxyl substituted (Scheme 1.31).¹⁰⁶ The AH was performed using a rhodium complex in the presence of various diphosphine ligands, but was only able to produce a maximum of 26% ee.



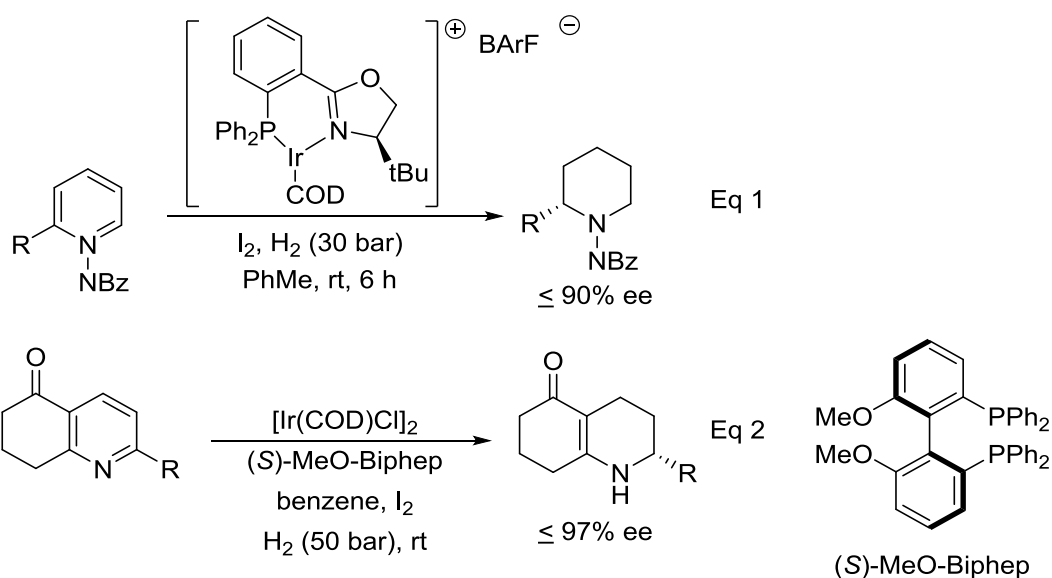
Scheme 1.31 First AH of pyridine.

Lehmann and co-workers greatly improved the ee to 96%, for polysubstituted pyridine rings (Scheme 1.32) by utilising a chiral auxiliary in the 2-position, which was removed under the acidic workup conditions.¹⁰⁷ A high pressure was required in the presence of palladium hydroxide on carbon.



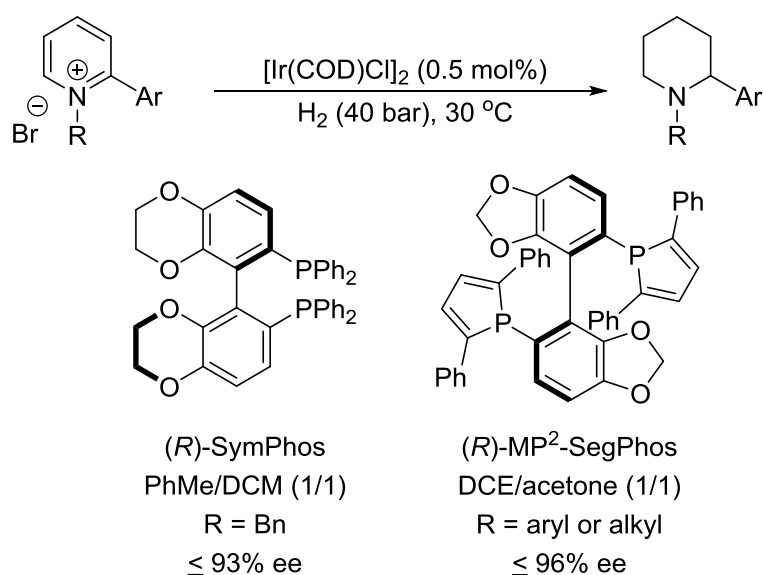
Scheme 1.32 AH of pyridines with a chiral auxiliary.

The pressure required for the hydrogenation was eventually reduced by Charette *et al.* however, these conditions were specific for *N*-benzyolimino-pyridinium ylides, utilising $[\text{Ir}(\text{COD})\text{Cl}]_2$ combined with a PHOX ligand to yield up to 90% ee (Eq 1, Scheme 1.33).¹⁰⁸ Zhou utilised (*S*)-MeO-BiPhep in the presence of iridium, to partially reduce 7,8-dihydro-quinolin-5-(6H)-ones producing ee's up to 97%.¹⁰⁹ (Eq 2, Scheme 1.33).



Scheme 1.33 AH of pyridines using iridium COD.

Building on their quinoline reduction work, Zhou *et al.* produced 2-substituted piperidines in high yield and enantioselectivities (up to 93% ee), once more utilising $[\text{Ir}(\text{COD})\text{Cl}]_2$ with (*R*)-SymPhos (Scheme 1.34).¹¹⁰ Though this system utilised a wider scope than previous systems it was not without limits, with only one example of a 2-alkyl substituted pyridine being presented with just a 65% ee and 60% yield. Zhang *et al.* reported an improved version of this system, changing the ligand to a more bulky (*R*)-MP²-SegPhos (Scheme 1.34).¹¹¹ Although again only few 2-alkyl substituted pyridinium substrates were reported with moderate ee's, the range of protecting groups was extended from just benzyls to include alkyl protecting groups, producing high ee's.

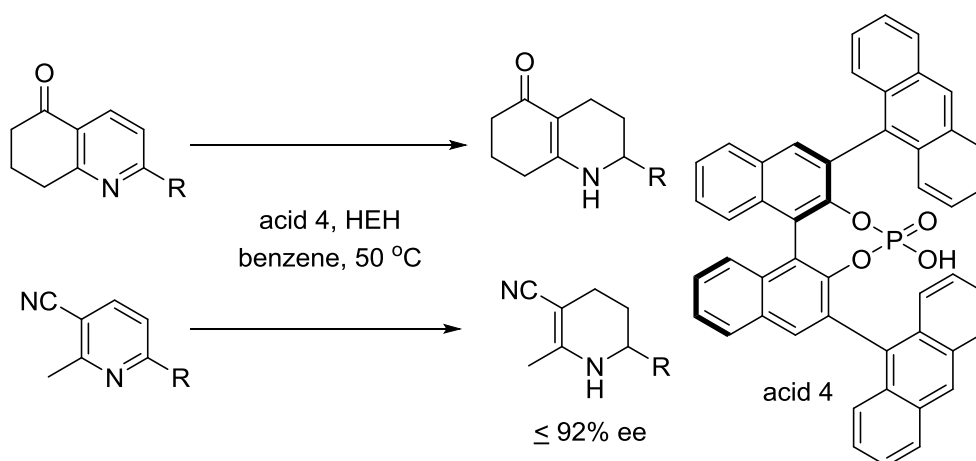


Scheme 1.34 AH of pyridinium salts.

1.5.2 Asymmetric Transfer Hydrogenation of pyridines

The ATH of pyridines has proved most difficult with just one system having been reported in 2007 by Antonchick *et al.* which required a bulky chiral phosphoric

acid in the presence of a HEH (Scheme 1.35).¹¹² This system was active only on 7,8-dihydro-quinolin-5(6*H*)-ones and 2-methyl-3-cyano-6-substituted-pyridines and only capable of partial hydrogenation, in up to 92% ee. Although racemic TH systems have been reported, ATH systems remain unexplored.



Scheme 1.35 Partial ATH of pyridine using chiral phosphoric acid catalysis.

1.6 Aims of this thesis

Previous work within the Xiao group has focused on the development of cyclometalated complexes and their uses. These iridacycles possess an iridium-nitrogen bond, which is able to stabilise the metal-carbon bond. These have proved to be extremely stable complexes, tolerant of being stored in air for extended periods of time with no signs of decomposition. They are also simple to synthesise by sodium acetate activation as previously reported (Scheme 1.39).¹¹³



Scheme 1.36 Cyclometallation to form iridacycle complex.

This class of iridacycles has proved active for a wide range of reductive and oxidative reactions. They were initially reported for direct reductive amination (DRA) *via* transfer hydrogenation^{20–22} (Eq 3, Figure 1.10), but have since been shown to be active for hydrogenation¹¹⁴ (Eq 2 and 4, Figure 1.10) as well as transfer hydrogenation of *N*-heterocycles¹¹⁵ (Eq 4, Figure 1.10) and carbonyls¹¹⁶ (Eq 1, Figure 1.10). By varying the conditions these iridacycles were also shown to be active for the dehydrogenation of *N*-heterocycles¹¹⁷ (Eq 4, Figure 1.10) and formic acid¹¹⁸ (Eq 6, Figure 1.10), as well as the dehydrogenative coupling of *N*-heterocycles¹¹⁹ (Eq 5, Figure 1.10). They have also been used for alkylation reactions, utilising a hydrogen borrowing mechanism under similar conditions (Eq 7, Figure 1.10).¹²⁰

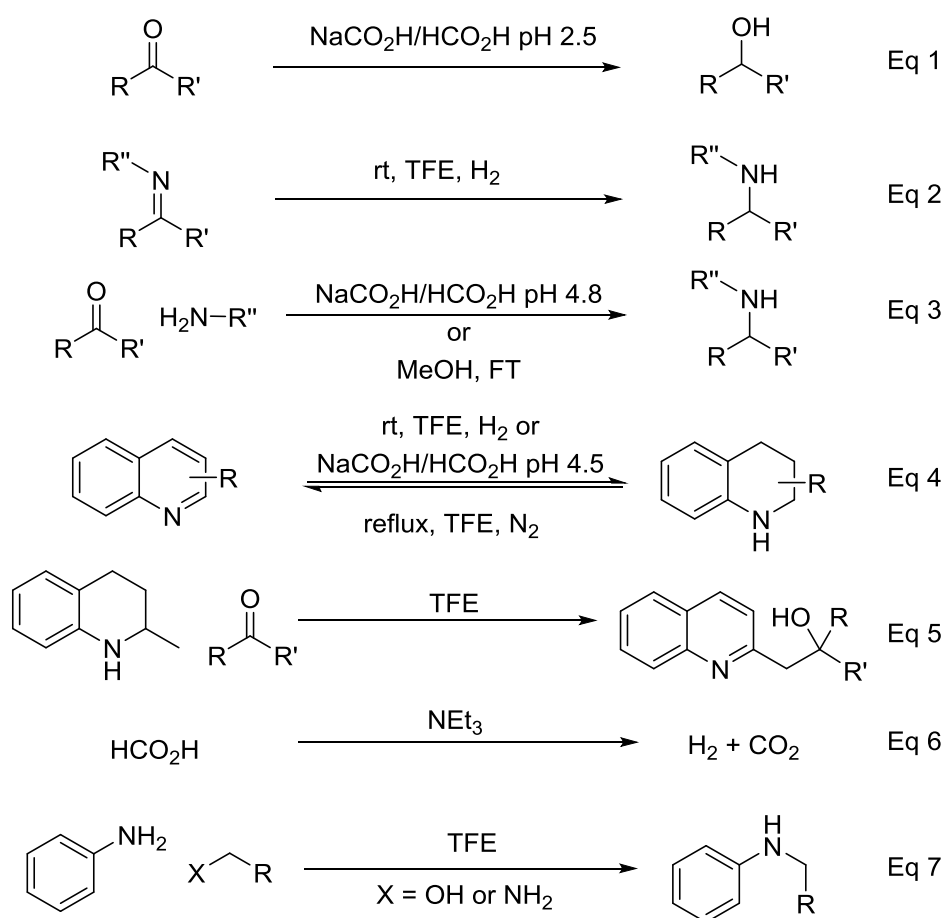


Figure 1.10 Reactions performed using the Xiao group's iridacycles.

Whilst these iridicycles have shown great activity, there has been very limited work on chiral derivatives of these species, towards the AH of a few simple imines. This shall be the aim of this thesis: to expand upon and develop a range of chiral iridicycles and to determine the extent to which they are active for a number of asymmetric reduction reactions.

1.7 References

- 1 H. Blaser, *Adv. Synth. Catal.*, 2002, **344**, 17–31.
- 2 C. J. Peter and J. B. Weber, *Weed Sci.*, 1985, **33**, 874–881.
- 3 D. Sloan M, E. Camper N, *Environ. Exp. Bot.*, 1986, **26**, 1–7.
- 4 S. Toubro, A. V Astrup, L. Breum and F. Quaade, *Int. J. Obes. Relat. Metab. Disord.*, 1993, **17 Suppl 1**, S69–72.
- 5 A. Lee, W. D. Ngan Kee and T. Gin, *Anesth. Analg.*, 2002, **94**, 920–926.
- 6 L. Carrasco, A. Jimenez and D. Vazquez, *Eur. J. Biochem.*, 1976, **64**, 1–5.
- 7 W. Ma, J. E. Anderson, A. T. McKenzie, S. R. Byrn and J. L. McLaughlin, *J. Nat. Prod.*, 1990, **53**, 1009–1014.
- 8 Z. An, W. Zhang, H. Shi and J. He, *J. Catal.*, 2006, **241**, 319–327.
- 9 T. Ohkuma, H. Doucet, T. Pham, K. Mikami, T. Korenaga, M. Terada and R. Noyori, *J. Am. Chem. Soc.*, 1998, **120**, 1086–1087.
- 10 C. J. Copley and J. P. Henschke, *Adv. Synth. Catal.*, 2003, **345**, 195–201.
- 11 S. Telfer, *Coord. Chem. Rev.*, 2003, **242**, 33–46.
- 12 J. Y. Kim and T. Livinghouse, *Org. Lett.*, 2005, **7**, 1737–9.
- 13 K. Kodama, N. Hayashi, M. Fujita and T. Hirose, *RSC Adv.*, 2014, **4**, 25609.
- 14 Z. Ren, Y. Zeng, Y. Hua, Y. Cheng and Z. Guo, *J. Chem. Eng. Data*, 2014, **59**, 2517–2522.
- 15 T. Vries, H. Wynberg, E. Van Echten, J. Koek, W. Hoeve, R. M. Kellogg, Q. B. Broxterman, A. Minnaard, S. Van Der Sluis, L. Hulshof and J. Kooistra, *Angew. Chem. Int. Ed.*, 1998, **37**, 2349–2354.

- 16 J. K. Whitesell and D. Reynolds, *J. Org. Chem.*, 1983, **48**, 3548–3551.
- 17 T. Ohkuma, *Proc. Japan Acad. Ser. B*, 2010, **86**, 202–219.
- 18 S. Gladiali and E. Alberico, *Chem. Soc. Rev.*, 2006, **35**, 226–36.
- 19 J. J. Verendel, O. Pa, M. Dieguez and P. G. Andersson, *Chem. Rev.*, 2014, **114**, 2130–2169.
- 20 C. Wang, A. Pettman, J. Basca and J. Xiao, *Angew. Chem. Int. Ed.*, 2010, **49**, 7548–52.
- 21 Q. Lei, Y. Wei, D. Talwar, C. Wang, D. Xue and J. Xiao, *Chem. Eur. J.*, 2013, **19**, 4021–4029.
- 22 D. Talwar, N. P. Salguero, C. M. Robertson and J. Xiao, *Chem. Eur. J.*, 2014, **20**, 245–252.
- 23 A. Levi, G. Modena and G. Scorrano, *J. Chem. Soc. Chem. Commun.*, 1975, **1975**, 6.
- 24 G. Kang, W. R. Cullen, M. D. Fryzuk, B. R. James and J. P. Kutney, *J. Chem. Soc. Chem. Commun.*, 1988, 1466–1467.
- 25 W. R. Cullen, M. D. Fryzuk, B. B. James, J. P. Kutney, G.-J. Kang, G. Herb, I. S. Thorburn and R. Spogliarich, *J. Mol. Catal.*, 1990, **62**, 243–253.
- 26 A. G. Becalski, W. R. Cullen, M. D. Fryzuk, B. R. James, G. Kang and S. J. Rettig, *Inorg. Chem.*, 1991, **30**, 5002–5008.
- 27 J. Bakos, A. Orosz, B. Heil, M. Laghmari, P. Lhoste and D. Sinou, *J. Chem. Soc. Chem. Commun.*, 1991, **4**, 1684.
- 28 Q. Zhao, J. Wen, R. Tan, K. Huang, P. Metola, R. Wang, E. V. Anslyn and X. Zhang, *Angew. Chemie . Int. Ed.*, 2014, **53**, 8467–8470.

- 29 C. Lensink and J. G. De Vries, *Tet. Asym.*, 1992, **3**, 235–238.
- 30 J. M. Buriak and J. a. Osborn, *Organometallics*, 1996, **15**, 3161–3169.
- 31 V. I. Tararov, R. Kadyrov, T. H. Riermeier, J. Holz and A. Börner, *Tet. Asym.*, 1999, **10**, 4009–4015.
- 32 Y. Ng Cheong Chan and J. A. Osborn, *J. Am. Chem. Soc.*, 1990, **112**, 9400–9401.
- 33 A. Dervisi, C. Carcedo and L. L. Ooi, *Adv. Synth. Catal.*, 2006, **348**, 175–183.
- 34 T. Imamoto, N. Iwadate and K. Yoshida, *Org. Lett.*, 2006, **8**, 2289–2292.
- 35 S. Vargas, M. Rubio, A. Suárez, D. Del Río, E. Àlvarez and A. Pizzano, *Organometallics*, 2006, **25**, 961–973.
- 36 C. J. Hou, Y. H. Wang, Z. Zheng, J. Xu and X. P. Hu, *Org. Lett.*, 2012, **14**, 3554–3557.
- 37 G. Espino, L. Xiao, M. Puchberger, K. Mereiter, F. Spindler, B. R. Manzano, F. a Jalón and W. Weissensteiner, *Dalt. Trans.*, 2009, 2751–2763.
- 38 Y. Wang, T. Sturm, M. Steurer, V. B. Arion, K. Mereiter, F. Spindler and W. Weissensteiner, *Organometallics*, 2008, **27**, 1119–1127.
- 39 M. B. Ezhova, B. O. Patrick, B. R. James, F. J. Waller and M. E. Ford, *J. Mol. Catal.*, 2004, **224**, 71–79.
- 40 S. Zhu, J. Xie, Y. Zhang, S. Li and Q. Zhou, *J. Am. Chem. Soc.*, 2006, **128**, 12886–12891.
- 41 A. Triforiová, J. S. Diesen, C. J. Chapman and P. G. Andersson, *Org. Lett.*, 2004, **6**, 3825–3827.

- 42 A. Trifonova, J. S. Diesen and P. G. Andersson, *Chem. Eur. J.*, 2006, **12**, 2318–2328.
- 43 S. Y. Shirai, H. Nara, Y. Kayaki and T. Ikariya, *Organometallics*, 2009, **28**, 802–809.
- 44 C. Li, C. Wang, B. Villa-Marcos and J. Xiao, *J. Am. Chem. Soc.*, 2008, **130**, 14450–1.
- 45 W. Tang and J. Xiao, *Synth.*, 2014, **46**, 1297–1302.
- 46 W. Tang, S. Johnston, C. Li, J. a. Iggo, J. Bacsá and J. Xiao, *Chem. Eur. J.*, 2013, **19**, 14187–14193.
- 47 F. Chen, T. Wang, Y. He, Z. Ding, Z. Li, L. Xu and Q. H. Fan, *Chem. Eur. J.*, 2011, **17**, 1109–1113.
- 48 F. Chen, Z. Ding, Y. He, J. Qin, T. Wang and Q. H. Fan, *Tetrahedron*, 2012, **68**, 5248–5257.
- 49 N. Arai, N. Utsumi, Y. Matsumoto, K. Murata, K. Tsutsumi and T. Ohkuma, *Adv. Synth. Catal.*, 2012, **354**, 2089–2095.
- 50 S. Zhou, S. Fleischer, K. Junge and M. Beller, *Angew. Chemie . Int. Ed.*, 2011, **50**, 5120–5124.
- 51 N. Uematsu, A. Fujii, S. Hashiguchi, T. Ikariya and R. Noyori, *J. Am. Chem. Soc.*, 1996, **118**, 4916–4917.
- 52 R. Noyori and S. Hashiguchi, *Acc. Chem. Res.*, 1997, **30**, 97–102.
- 53 J. Václavík, M. Kuzma, J. Přech and P. Kačer, *Organometallics*, 2011, **30**, 4822–4829.

- 54 M. Kuzma, J. Václavík, P. Novák, J. Přech, J. Januščák, J. Červený, J. Pecháček, P. Šot, B. Vilhanová, V. Matoušek, I. I. Goncharova, M. Urbanová and P. Kačer, *Dalt. Trans.*, 2013, **42**, 5174–82.
- 55 P. Šot, M. Kuzma and J. Václavík, *Organometallics*, 2012, **31**, 6496–6499.
- 56 J. Mao, D. C. Baker, R. Rhcl, C. H. C. H. C. H. Nh, S. Rhcltsdpen and C. Rhcl, *Org. Lett.*, 1999, **1**, 814–843.
- 57 S. H. Kwak, S. A. Lee and K. I. Lee, *Tet. Asym.*, 2010, **21**, 800–804.
- 58 D. Guijarro, Ó. Pablo and M. Yus, *Tet. Lett.*, 2009, **50**, 5386–5388.
- 59 D. Guijarro, O. Pablo and M. Yus, *J. Org. Chem.*, 2010, **75**, 5265–5270.
- 60 D. Guijarro, Ó. Pablo and M. Yus, *Tet. Lett.*, 2011, **52**, 789–791.
- 61 Ó. Pablo, D. Guijarro, G. Kovács, A. Lledós, G. Ujaque and M. Yus, *Chem. Eur. J.*, 2012, **18**, 1969–1983.
- 62 Ó. Pablo, D. Guijarro and M. Yus, *J. Org. Chem.*, 2013, **78**, 9181–9189.
- 63 Ó. Pablo, D. Guijarro and M. Yus, *European J. Org. Chem.*, 2014, **2014**, 7034–7038.
- 64 A. a. Mikhailine, M. I. Maishan and R. H. Morris, *Org. Lett.*, 2012, **14**, 4638–4641.
- 65 W. Zuo, A. J. Lough, Y. F. Li and R. H. Morris, *Science.*, 2013, **342**, 1080–1083.
- 66 W. Zuo and R. H. Morris, *Nat. Protoc.*, 2015, **10**, 241–257.
- 67 M. Rueping, E. Sugiono, C. Azap, T. Theissmann and M. Bolte, *Org. Lett.*, 2005, **7**, 3781–3.
- 68 S. Hoffmann, A. M. Seayad and B. List, *Angew. Chem. Int. Ed.*, 2005, **44**, 7424–7.

- 69 G. Li, Y. Liang and J. C. Antilla, *J. Am. Chem. Soc.*, 2007, **129**, 5830–1.
- 70 Q. Kang, Z.-A. Zhao and S.-L. You, *Adv. Synth. Catal.*, 2007, **349**, 1657–1660.
- 71 Q. Kang, Z. Zhao and S. You, *Org. Lett.*, 2008, **10**, 2031–2034.
- 72 D. Steinhuebel, Y. Sun, K. Matsumura, N. Sayo and T. Saito, *J. Am. Chem. Soc.*, 2009, **131**, 11316–7.
- 73 K. Matsumura, X. Zhang, K. Hori, T. Murayama, T. Ohmiya, H. Shimizu, T. Saito and N. Sayo, *Org. Process Res. Dev.*, 2011, **15**, 1130–1137.
- 74 O. Bondarev and C. Bruneau, *Tet. Asym.*, 2010, **21**, 1350–1354.
- 75 C. Li, B. Villa-Marcos and J. Xiao, *J. Am. Chem. Soc.*, 2009, **131**, 6967–9.
- 76 B. Villa-Marcos, C. Li, K. R. Mulholland, P. J. Hogan and J. Xiao, *Molecules*, 2010, **15**, 2453–2472.
- 77 M. Chang, S. Liu, K. Huang and X. Zhang, *Org. Lett.*, 2013, **15**, 4354–4357.
- 78 S. Zhou, S. Fleischer, H. Jiao, K. Junge and M. Beller, *Adv. Synth. Catal.*, 2014, **365**, 3451–3455.
- 79 D. Koszelewski, I. Lavandera, D. Clay, G. M. Guebitz, D. Rozzell and W. Kroutil, *Angew. Chem. Int. Ed.*, 2008, **47**, 9337–40.
- 80 C. K. Savile, J. M. Janey, E. C. Mundorff, J. C. Moore, S. Tam, W. R. Jarvis, J. C. Colbeck, A. Krebber, F. J. Fleitz, J. Brands, P. N. Devine, G. W. Huisman and G. J. Hughes, *Science.*, 2010, **329**, 305–9.
- 81 R. I. Storer, D. E. Carrera, Y. Ni and D. W. C. MacMillan, *J. Am. Chem. Soc.*, 2006, **128**, 84–6.
- 82 V. N. Wakchaure, J. Zhou, S. Hoffmann and B. List, *Angew. Chem. Int. Ed.*, 2010, **49**, 4612–4.

- 83 F.-M. Gautier, S. Jones, X. Li and S. J. Martin, *Org. Biomol. Chem.*, 2011, **9**, 7860–8.
- 84 G. D. Williams, R. a Pike, C. E. Wade and M. Wills, *Org. Lett.*, 2003, **5**, 4227–30.
- 85 R. Kadyrov and T. H. Riermeier, *Angew. Chem. Int. Ed.*, 2003, **42**, 5472–4.
- 86 W. Wang, S. Lu, P. Yang, X. Han and Y. Zhou, *J. Am. Chem. Soc.*, 2003, **125**, 10536–10537.
- 87 X.-B. Wang, D.-W. Wang, S.-M. Lu, C.-B. Yu and Y.-G. Zhou, *Tet. Asym.*, 2009, **20**, 1040–1045.
- 88 F. R. Gou, W. Li, X. Zhang and Y. M. Liang, *Adv. Synth. Catal.*, 2010, **352**, 2441–2444.
- 89 S.-M. Lu, Y.-Q. Wang, X.-W. Han and Y.-G. Zhou, *Angew. Chem. Int. Ed.*, 2006, **45**, 2260–3.
- 90 D.-S. Wang and Y.-G. Zhou, *Tet. Lett.*, 2010, **51**, 3014–3017.
- 91 K. H. Lam, L. Xu, L. Feng, Q.-H. Fan, F. L. Lam, W. Lo and A. S. C. Chan, *Adv. Synth. Catal.*, 2005, **347**, 1755–1758.
- 92 L. Xu, K. H. Lam, J. Ji, J. Wu, Q.-H. Fan, W.-H. Lo and A. S. C. Chan, *Chem. Commun.*, 2005, 1390–2.
- 93 X. Wang and Y. Zhou, *J. Org. Chem.*, 2008, **73**, 5640–5642.
- 94 W. Tang, Y. Sun, Lijin Xu, T. Wang, Qinghua Fan, K.-H. Lam and A. S. C. Chan, *Org. Biomol. Chem.*, 2010, **8**, 3464–71.
- 95 D.-Y. Zhang, C.-B. Yu, M.-C. Wang, K. Gao and Y.-G. Zhou, *Tet. Lett.*, 2012, **53**, 2556–2559.

- 96 Z.-W. Li, T.-L. Wang, Y.-M. He, Z.-J. Wang, Q.-H. Fan, J. Pan and L.-J. Xu, *Org. Lett.*, 2008, **10**, 5265–8.
- 97 H. Zhou, Z. Li, Z. Wang, T. Wang, L. Xu, Y. He, Q.-H. Fan, J. Pan, L. Gu and A. S. C. Chan, *Angew. Chem. Int. Ed.*, 2008, **47**, 8464–7.
- 98 T. Wang, L.-G. Zhuo, Z. Li, F. Chen, Z. Ding, Y. He, Q.-H. Fan, J. Xiang, Z.-X. Yu and A. S. C. Chan, *J. Am. Chem. Soc.*, 2011, **133**, 9878–91.
- 99 D.-W. Wang, W. Zeng and Y.-G. Zhou, *Tet. Asym.*, 2007, **18**, 1103–1107.
- 100 C. Wang, C. Li, X. Wu, A. Pettman and J. Xiao, *Angew. Chem. Int. Ed.*, 2009, **48**, 6524–8.
- 101 X.-F. Tu and L.-Z. Gong, *Angew. Chem. Int. Ed.*, 2012, **51**, 11346–9.
- 102 M. Rueping, A. P. Antonchick and T. Theissmann, *Angew. Chem. Int. Ed.*, 2006, **45**, 3683–6.
- 103 Q.-S. Guo, D.-M. Du and J. Xu, *Angew. Chem. Int. Ed.*, 2008, **47**, 759–62.
- 104 X.-F. Cai, R.-N. Guo, G.-S. Feng, B. Wu and Y.-G. Zhou, *Org. Lett.*, 2014, **16**, 2680–3.
- 105 M. Rueping, T. Theissmann, M. Stoeckel and A. P. Antonchick, *Org. Biomol. Chem.*, 2011, **9**, 6844–6850.
- 106 M. Struder, C. Wedemeyer-exl, F. Spindler and H.-U. Blaser, *Monatshefte für Chemie*, 2000, **131**, 1335–1343.
- 107 F. Glorius, N. Spielkamp, S. Holle, R. Goddard and C. W. Lehmann, *Angew. Chem. Int. Ed.*, 2004, **43**, 2850–2.
- 108 C. Y. Legault and A. B. Charette, *J. Am. Chem. Soc.*, 2005, 8966–8967.
- 109 X.-B. Wang, W. Zeng and Y.-G. Zhou, *Tet. Lett.*, 2008, **49**, 4922–4924.

- 110 Z.-S. Ye, M.-W. Chen, Q.-A. Chen, L. Shi, Y. Duan and Y.-G. Zhou, *Angew. Chem. Int. Ed.*, 2012, **51**, 10181–4.
- 111 M. Chang, Y. Huang, S. Liu, Y. Chen, S. W. Krska, I. W. Davies and X. Zhang, *Angew. Chem. Int. Ed.*, 2014, **53**, 12761–4.
- 112 M. Rueping and A. P. Antonchick, *Angew. Chem. Int. Ed.*, 2007, **46**, 4562–5.
- 113 Y. Boutadla, D. L. Davies, R. C. Jones and K. Singh, *Chemistry*, 2011, **17**, 3438–48.
- 114 J. Wu, J. H. Barnard, Y. Zhang, D. Talwar, C. M. Robertson and J. Xiao, *Chem. Commun.*, 2013, **49**, 7052–4.
- 115 D. Talwar, H. Y. Li, E. Durham and J. Xiao, *Chem. Eur. J.*, 2015, **21**, 5370–5379.
- 116 Y. Wei, D. Xue, Q. Lei, C. Wang and J. Xiao, *Green Chem.*, 2013, **15**, 629–634.
- 117 J. Wu, D. Talwar, S. Johnston, M. Yan and J. Xiao, *Angew. Chemie . Int. Ed.*, 2013, **52**, 6983–6987.
- 118 J. H. Barnard, C. Wang, N. G. Berry and J. Xiao, *Chem. Sci.*, 2013, **4**, 1234.
- 119 D. Talwar, A. Gonzalez-de-Castro, H. Y. Li and J. Xiao, *Angew. Chemie Int. Ed.*, 2015, **54**, 5223–5227.
- 120 Q. Zou, C. Wang, J. Smith, D. Xue and J. Xiao, *Chem. Eur. J.*, 2015, **21**, 9656–9661.

Chapter 2: Iridicycle Development and Synthesis

2.1 Introduction

Cyclometalated complexes have long been known as versatile catalysts, utilising a number of transition metals, including iridium, ruthenium and palladium.^{1,2} These complexes are capable of catalysing many transformations, including reductions.

A large amount of work has been conducted by Xiao *et al.* utilising cyclometalated iridium complexes (Figure 2.1).³⁻¹³ These complexes have been shown to be efficient and highly chemoselective catalysts for a range of reduction and oxidation reactions. The aim in this chapter is to build upon this chemistry and develop a wide range of chiral analogues for testing in later chapters.

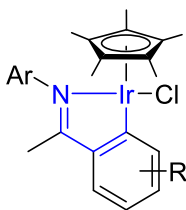


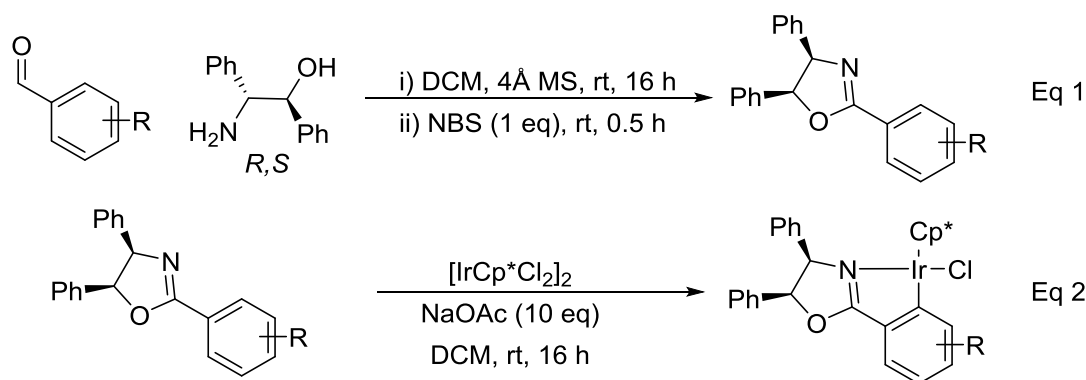
Figure 2.1 General structure of achiral iridacycles.

2.2 Oxazoline based complexes

2.2.1 Basic Oxazoline Complexes

The most effective method for installing chirality into the racemic motif (Figure 2.1) was to lock the imine into a ring, containing chiral substituents (Scheme 2.1). This could be achieved with readily available chiral amino alcohols and also diamines (Chapter 2.3). The ligands were produced *via* a condensation reaction between 2-amino-1,2-diphenylethanol and a benzaldehyde derivative, following a procedure published by Glorius (Eq 1, Scheme 2.1).¹⁴ Once the ligand was obtained the cyclometalation was performed under the mild conditions reported (Eq 2,

Scheme 2.1).² Upon running ^1H NMR analysis of the complex two diastereoisomers were observed (**Ir 1-a** and **b**), indicating that the chirality at the iridium centre was undefined (Figure 2.2). This should have little impact upon the catalytic activity, as the chloride must be lost to activate the complex, forming a pro-chiral iridium centre. For the basic oxazoline motif, both the *R,S* (**Ir 1**) and *S,S* (**Ir 2**) amino alcohols were used (Figure 2.3); however, the catalytic results reported later (Chapter 3.2) showed the *R,S*-ligand produced higher ee's, so was selected for the remaining oxazoline complexes.



Scheme 2.1 General procedure for the synthesis of oxazolines and standard conditions for the cyclometalation reaction.

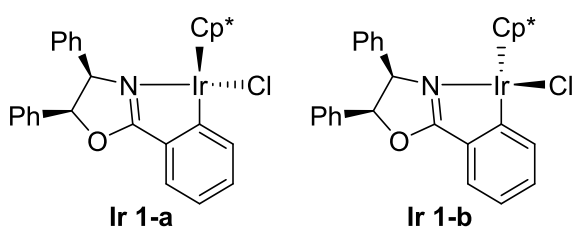


Figure 2.2 (*R,S*)-Oxazoline complex showing chirality at the iridium centre.

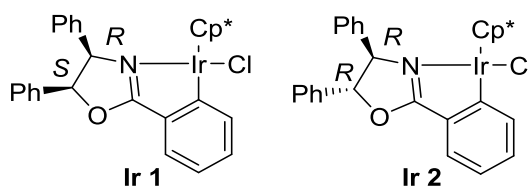
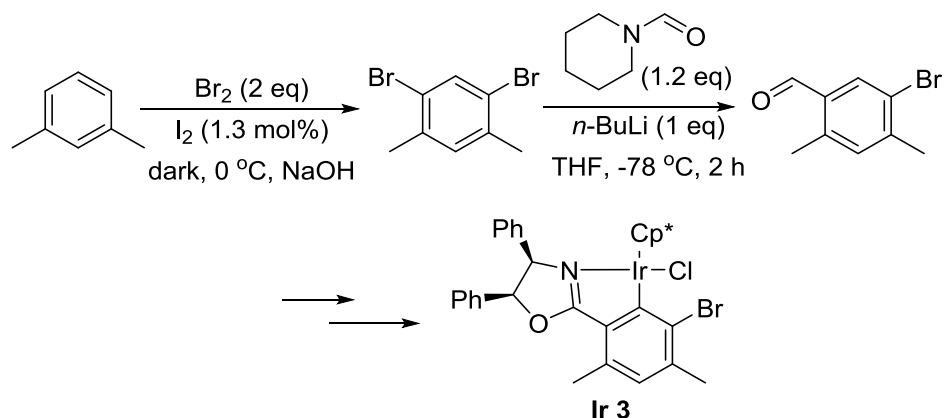


Figure 2.3 Simple oxazoline complexes from commercial benzaldehyde and the *R,S* and *R,R* amino alcohol.

2,4-Dimethyl-5-bromobenzaldehyde was synthesised to determine the effect of steric bulk *ortho* to the iridium centre (Scheme 2.2). This was done by bromination of *m*-xylene to afford 1,5-dibromo-2,4-dimethylbenzene.¹⁵ The product underwent a selective acylation to afford the desired benzaldehyde,¹⁶ which was subjected to the standard condensation and cyclometalation conditions to produce **Ir 3** (shown in Scheme 2.1).



Scheme 2.2 Synthesis of 2,4-dimethyl-5-bromobenzaldehyde.

To incorporate electron donating substituents, commercially available methoxybenzaldehydes were used for the synthesis of oxazoline ligands (**Ir 4** and **Ir 5**, Figure 2.4). Two 2-phenol based oxazolines using the amino alcohol valinol, were obtained from the group of Dr H. Aspinall within the department,¹⁷ allowing for comparison of different substituents in subsequent studies. Following analysis these

were also subjected to cyclometalation to form the iridicycles, **Ir 7** and **Ir 8** (Figure 2.4).

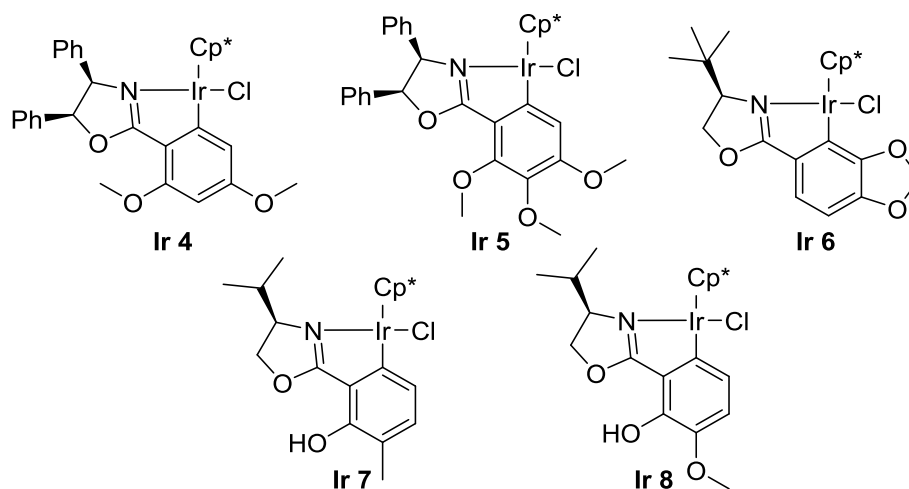


Figure 2.4 Electron rich oxazoline complexes.

2.2.2 Bulky oxazoline complex

The crystal structures obtained (by C Wang of the Xiao group)¹⁸ of the simple oxazoline complexes show a large empty pocket where the chloride sits around the iridium (Figure 2.6). Bulky ligands may therefore offer a higher enantioselectivity, due to the tighter space available around the iridium centre, limiting the possible approaches of the substrates to the active iridium centre.

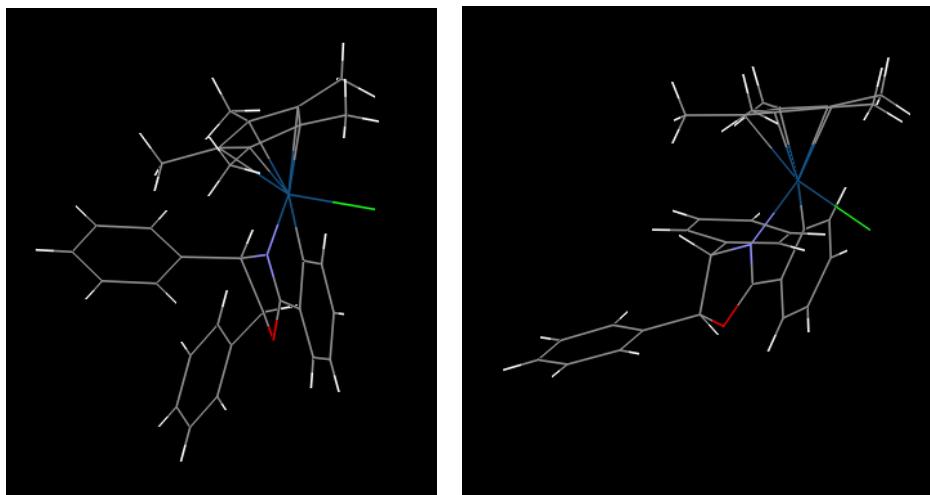


Figure 2.5 Crystal structures of the basic oxazoline complexes (left *R,S*, right *R,R* (shown in Figure 2.3)), with chloride shown in green.

Commercially available 4-*iso*-propyl and 4-*tert*-butylbenzaldehyde were used as bulky substrates to test steric effects (**Ir 9** and **Ir 10**, Figure 2.6). Bulkier aldehydes were prepared in order to evaluate the effect of sterics on catalytic activity, the first of which was the addition of a sterically hindered 2,4,6-*iso*-propylbenzene ring in the 4-position of benzaldehyde as initially synthesised by B. V. Marcos of the Xiao Group¹⁹ (Scheme 2.3). This was synthesised from its bromide through Suzuki coupling with 4-formylphenylboronic acid.²⁰ The aldehyde could then undergo the standard condensation to afford the desired ligand before being subjected to the cyclometalation conditions, yielding **Ir 11**.

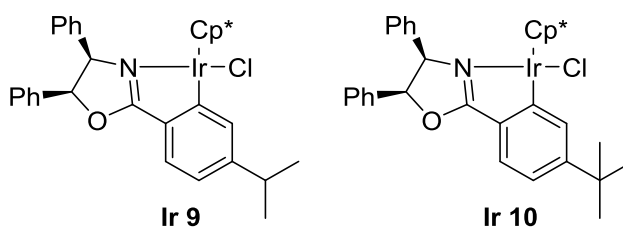
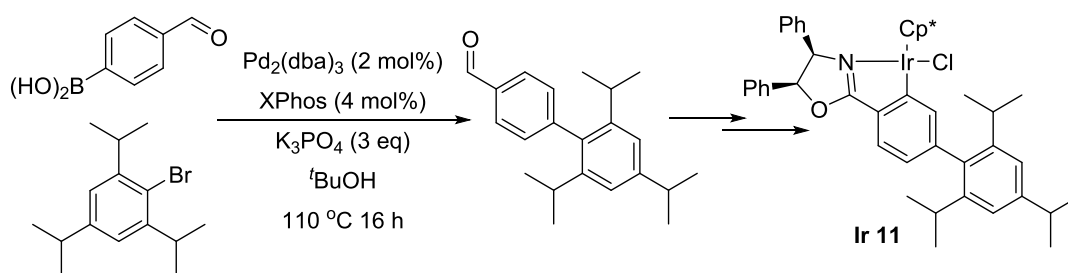
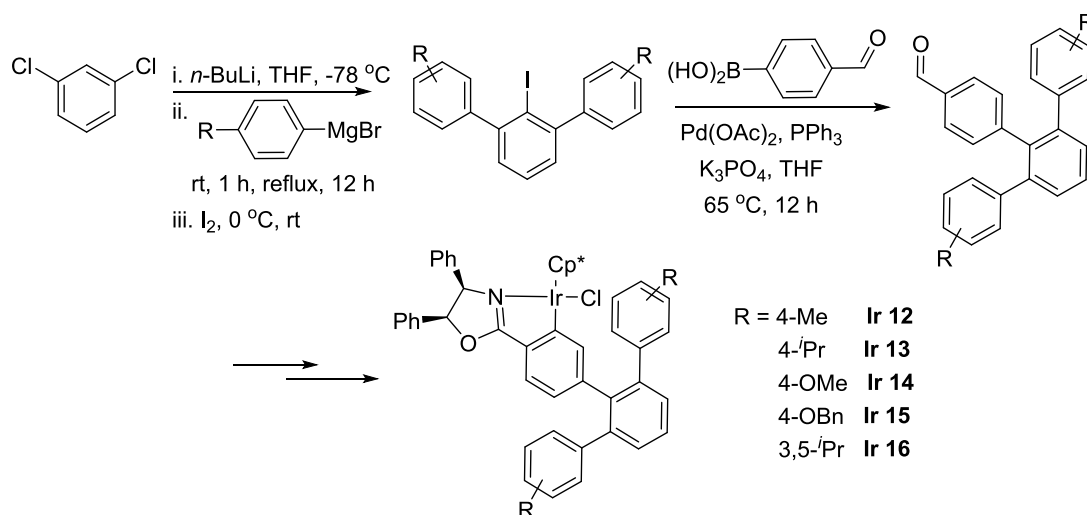


Figure 2.6 Bulky oxazoline complexes synthesised from commercial benzaldehydes.



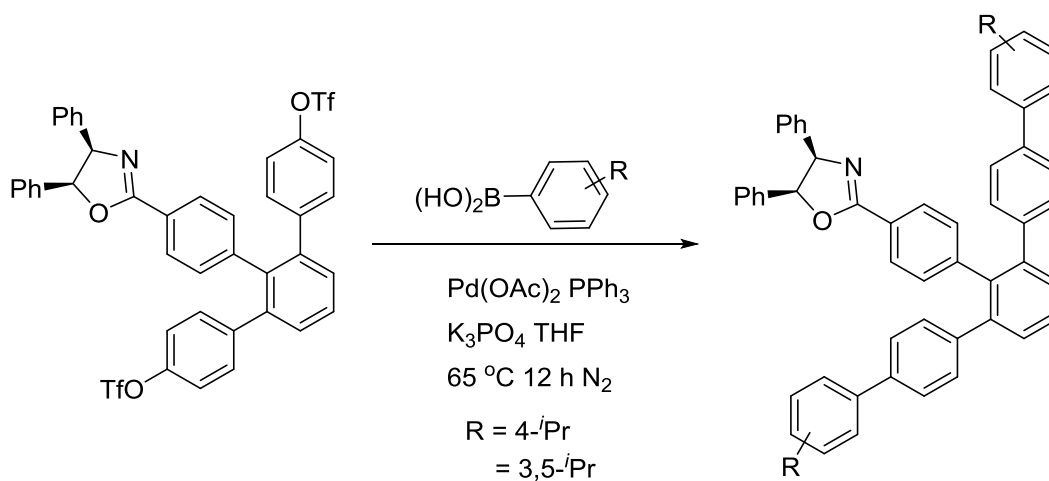
Scheme 2.3 Synthesis of 2,4,6-isopropyl complex.

These complexes concentrated their steric hindrance away from the chiral centres, it was therefore decided that a *meta*-terphenyl motif might offer more promise. This motif could spread closer to the metal centre, potentially forming a pocket and forcing the substrates closer to the chiral environment. The terphenyl ligands were synthesised (with assistance of Dr W. Tang within the Xiao group) from 1,3-dichlorobenzene (Scheme 2.4), which was treated with *n*-BuLi to form the 2-lithium salt.^{21–23} The salt reacted with a freshly prepared Grignard solution in THF of the desired aryl substrate *in situ* and upon quenching with iodine, afforded the desired 2-iodo-terphenyl product. This was then subjected to a Suzuki coupling with 4-formylphenylboronic acid as described earlier, before undergoing a standard condensation with the amino alcohol. Due to the steric bulk, some of these complexes required harsher cyclometalation conditions of heating to 50 °C under a sealed nitrogen atmosphere to produce **Ir 12–16**.



Scheme 2.4 General synthesis of *meta*-terphenyl aldehyde for oxazoline complexes.

Larger ligands were synthesised by the addition of a further aryl group upon the terphenyl. This was achieved once more by palladium catalysed coupling of the aryl boronic acid with a triflate (provided by a Dr W. Tang within the group) (Scheme 2.5). The resulting iridium complexes (**Ir 17** and **Ir 18**) are shown in Figure 2.7.



Scheme 2.5 Addition of extra aryl group *via* Suzuki coupling.

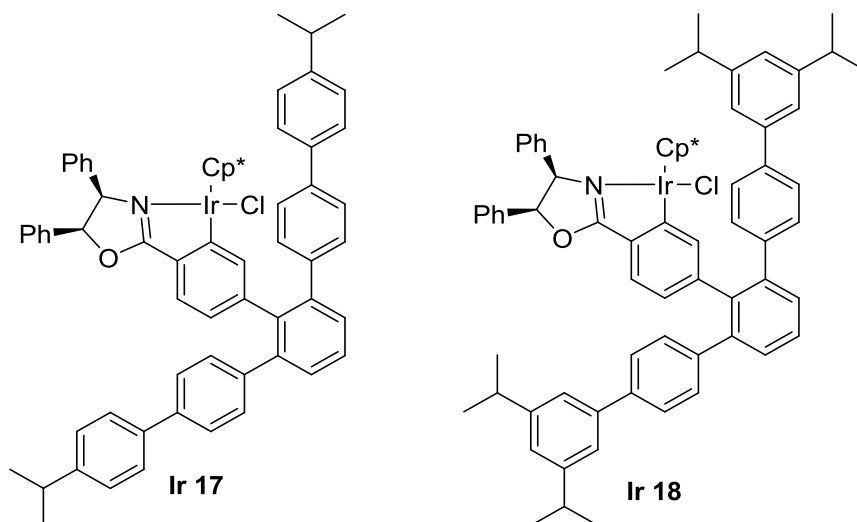
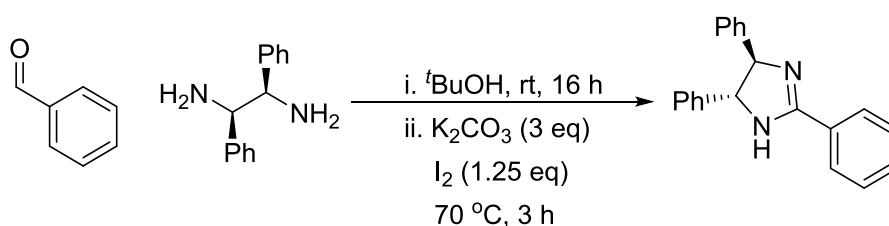


Figure 2.7 Diaryl *meta*-terphenyl complexes.

2.3 Imidazoline complexes

A second class of ligands was prepared by replacing the amino alcohols with diamines. The condensation conditions to form the imidazolines were mild (Scheme 2.6) and the simplest imidazoline ligand was synthesised using benzaldehyde and (*R,R*)-DPEN. Upon cyclometalation three resonances were observed by ^1H NMR, **Ir 19-a**, **b** and **c**. As before two diastereoisomers resulted from chirality at the iridium centre, however, a regioisomer was formed through cyclometalation onto the DPEN ring **Ir 19-c** (Figure 2.8).



Scheme 2.6 General conditions for the synthesis of imidazoline ligands.

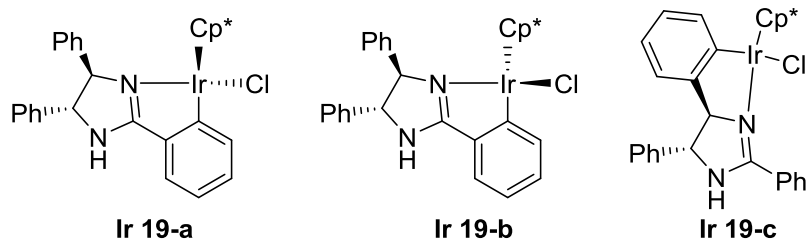
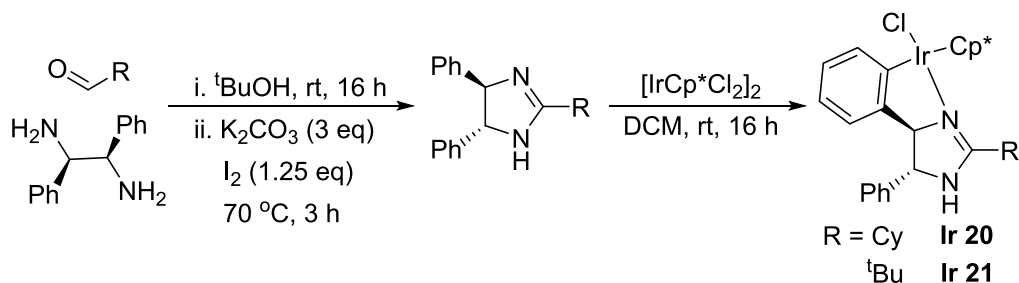


Figure 2.8 Various positions of cyclometalation of standard imidazolines.

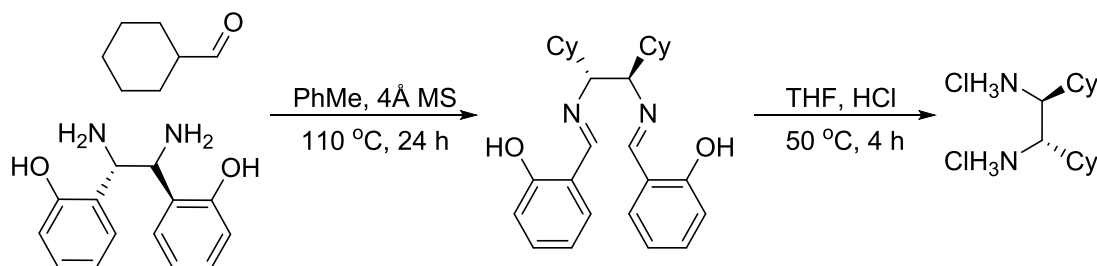
In order to determine if **Ir 19a-c** complex would be selective or even active in reduction reactions, a number of these complexes were prepared **Ir 20** and **Ir 21** (Scheme 2.7). This was done by switching the benzaldehyde for an aliphatic aldehyde, resulting in just one phenyl ring being present for cyclometalation. Both the condensation and cyclometalation reaction occurred readily, yielding the desired complexes. With these complexes containing a chiral centre within the iridicycle, they may offer a higher selectivity if active.



Scheme 2.7 Synthesis of iridicycles with a chiral centre.

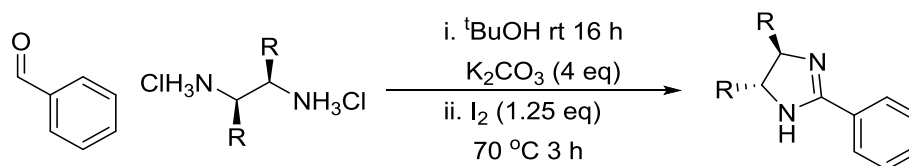
To further determine the effect of the cyclometalation onto the aryl ring of the DPEN, the phenyl rings were removed. This was achieved by synthesising (*S,S*)-1,2-bis(cyclohexyl)-1,2-diaminoethane,²⁴ *via* a Diaza-Cope rearrangement (Scheme 2.8), with the aid of Dr J Barnard. To achieve this bis-1,2-(2-hydroxydiphenyl)-1,2-diaminoethane reacted with cyclohexanecarboxaldehyde, to yield the intermediate

(*S,S*)-*N,N'*-bis(salicylidene)-1,2-cyclohexyl-1,2-diaminoethane. After treatment with hydrochloric acid, the dihydrochloride salt of the diamine could be isolated.



Scheme 2.8 Synthesis of 1,2-bis(cyclohexyl)-1,2-diaminoethane hydrochloride.

With this diamine in hand it was reacted with benzaldehyde (**Ir 22**, Figure 2.9), under similar conditions as previously stated, except the potassium carbonate was added in the first step, to allow for free-basing *in situ* (Scheme 2.9). Upon cyclometalation the resulting complex was similar to the oxazoline complexes, with just the 2 diastereoisomers being obtained. The diamine then reacted with a number of commercial benzaldehydes, with various substitution patterns and electronic effects. 3,5-Bromobenzaldehyde was used (**Ir 23**, Figure 2.9), as this would show the effect of placing an electron withdrawing group *ortho* to the iridium. When piperonal was used, cyclometalation occurred solely in the most hindered position on the ring (**Ir 24**, Figure 2.10). When a dioxane ring (6-membered) was present cyclometalation became unselective with an inseparable mixture of both regioisomers being observed (**Ir 25**, Figure 2.9).



Scheme 2.9 General synthesis of the imidazoline from a diamine salt.

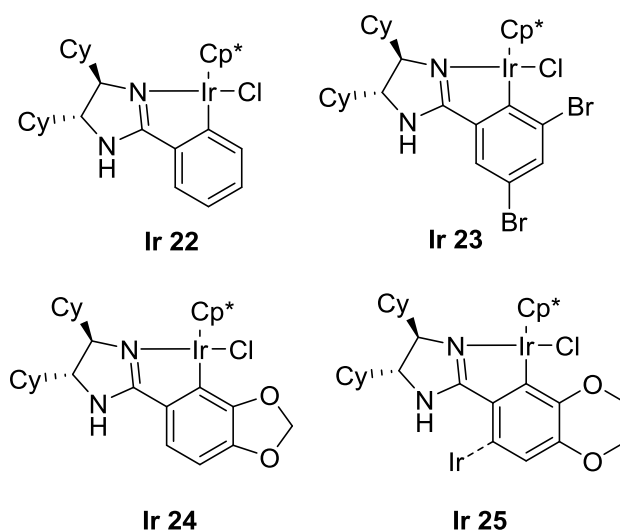
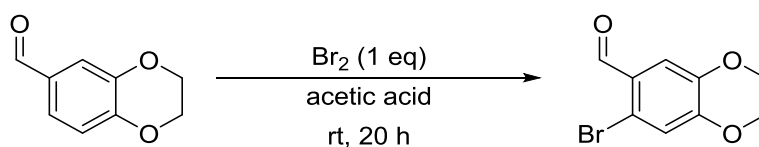


Figure 2.9 Dicyclohexyl diamine based imidazoline complexes.

The dicyclohexyldiamine was expensive and challenging to synthesise, therefore further analogues were made from DPEN, with a focus on oxygenated complexes. This was initiated with a focus on commercial benzaldehydes. A number of methoxy containing complexes were synthesised (**Ir 26** - **Ir 29**, Figure 2.10), along with a range of 5-membered rings, such as dioxolane (**Ir 30** - **Ir 32**) and furan (**Ir 33**) based complexes (Figure 2.10). Despite the dioxolane and furan rings offering the opportunity to undergo cyclometalation in two positions, once cyclometalation only occurred in the more hindered position, producing the standard three complexes. Expanding the ring to dioxane (a 6-membered ring) previously had shown a loss in selectivity upon cyclometalation; which occurred in both the 2 and 6 positions. This was overcome by performing a selective bromination on the benzaldehyde (Scheme 2.10), to block the 2 position; forcing cyclometalation to occur solely in the 6 position (**Ir 34**), once the ligand had been formed.



Scheme 2.10 Selective bromination on the 2 position of 2,3-dihydrobenzo[b][1,4]dioxine-6-carbaldehyde.

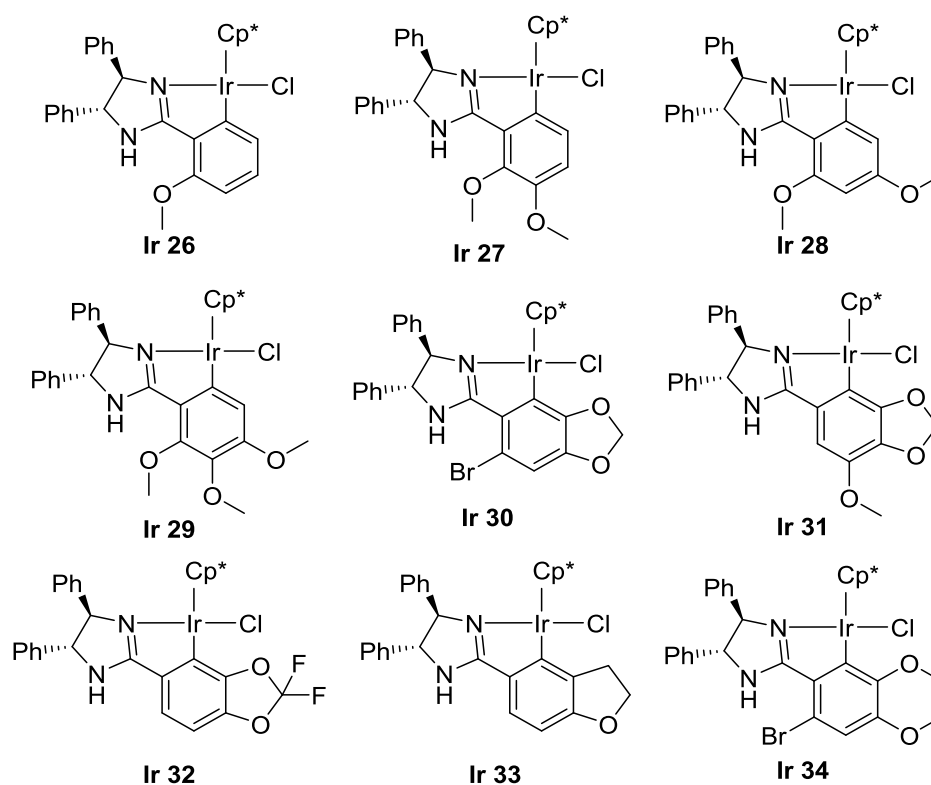


Figure 2.10 A range of oxygen rich imidazoline complexes.

Further variation of the DPEN group was achieved using commercially available substituted *para*-methoxy and *ortho*-chloro DPEN salts. Condensation using the conditions shown in Scheme 2.9, with 2,3,4-trimethoxybenzaldehyde was successful, although slightly harsher conditions were required once more for the cyclometalation (**Ir 35** and **Ir 36**, Figure 2.11).

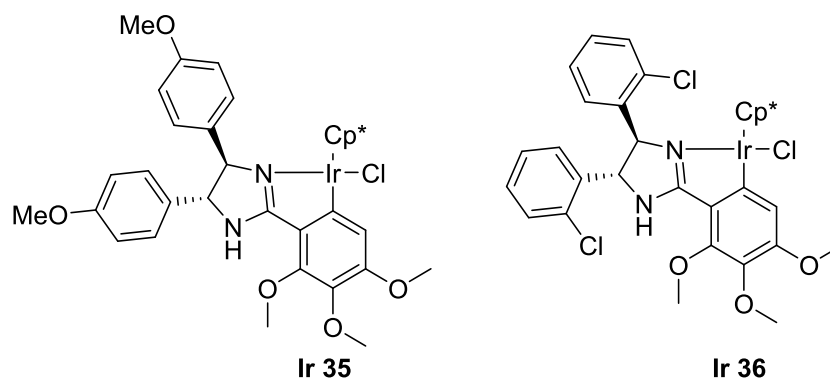


Figure 2.11 Complexes bearing substitution on the imidazoline aryl rings.

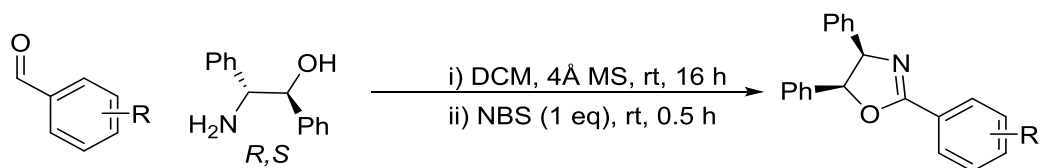
2.4 Conclusions

During this chapter a large number of novel chiral ligands and their corresponding cyclometallated iridium complexes were synthesised and characterised. A diverse range of stereo and electronic properties was incorporated into these iridicycles, with bulky and electron rich complexes being the two most abundant classes of complexes synthesised. These complexes are being utilised in the following chapters to determine their activity and selectivity for a range of reductive transformations, in both hydrogenation and transfer hydrogenation conditions.

2.5 Experimental

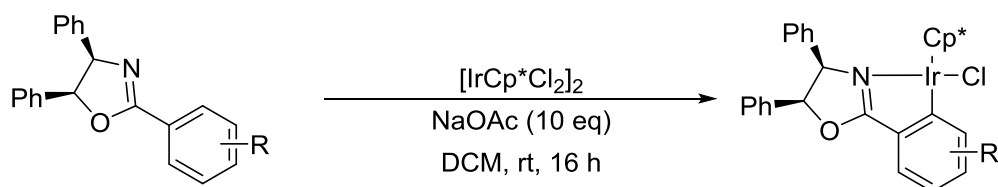
THF was dried over sodium with benzophenone indicator, DCM and toluene were dried on an MB-SPS 800 solvent drying system, methanol was dried over magnesium and iodine. 4Å MS were activated in an oven overnight; all other chemicals were used as purchased. NMR spectra were recorded on a Bruker 400 MHz NMR spectrometer, with TMS as internal standard.

2.5.1 Standard Procedures



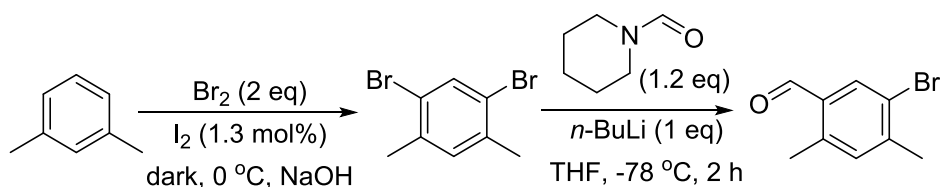
Amino alcohol condensation¹⁴

A round bottom flask was charged with amino alcohol (1 eq, 1 mmol), benzaldehyde (1 eq, 1 mmol), 4Å MS and a stirrer bar. DCM (5 mL) was added and the reaction was stirred at room temperature for 16 h. NBS (1 eq, 1 mmol) was added slowly (exothermic reaction) to the flask, producing an orange/yellow solution, which was stirred for a further 30 min. The reaction mixture was filtered and washed with aq NaHCO₃ (10 mL x 3) and water (10 mL). The organics were dried over MgSO₄ and concentrated under vacuum. The resulting residue was purified by column chromatography in 10% EtOAc in hexane, to give 60-80% isolated yields.



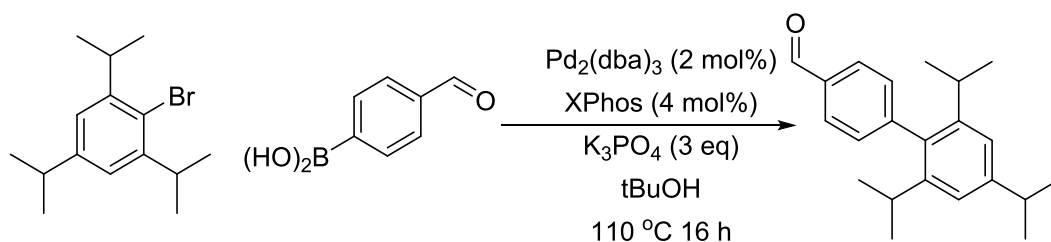
Standard cyclometalation²

A glass vial was charged with [IrCp*Cl₂]₂ (1 eq), ligand (2 eq), NaOAc (10 eq) and a stirrer bar. DCM was added and the resulting orange solution was left to stir at room temperature for 16 h. The reaction mixture was filtered through Celite and the solvent was removed under vacuum. The complex was recrystallised from DCM/hexane to yield a yellow solid, in quantitative yield.



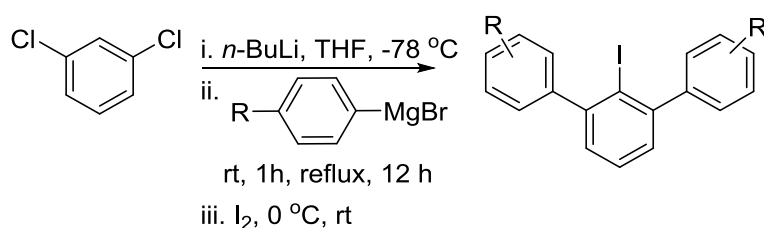
2,4-Dimethyl-5-bromobenzaldehyde synthesis^{15,16}

A round bottomed flask was charged with a stirrer bar and *m*-xylene (1 eq, 10 mmol). Bromine (2.2 eq) was then added over 5 min, iodine (1.5 mol%) was then added slowly over 30 min and the resulting solution was stirred for 3 h at room temperature. The reaction was quenched by the addition of aq NaOH (4 M, 10 mL) and stirred for 30 min. The resulting precipitate was then filtered off and recrystallized from EtOH, to yield the desired 1,5-dibromo-2,4-dimethylbenzene. A round bottomed flask was charged with the 1,5-dibromo-2,4-dimethylbenzene and a stirrer bar, followed by THF (10 mL). The flask was then cooled to -78°C , *n*-BuLi (1.6 M, 1 eq) was added and allowed to stir for 30 min. DMF (2 eq) in THF (5 mL) was then added and the mixture stirred at -78°C for 30 min, then warmed to room temperature and allowed to stir for 2 h. The reaction was quenched by addition of aq NaOH and the organics were extracted into Et₂O (10 mL) x 3. The organics were then dried over MgSO₄ and evaporated under vacuum. The resulting residue was purified by column chromatography in 10% EtOAc in hexane, in an overall yield of 75%.



Suzuki Coupling for the synthesis of 2',4',6'-triisopropyl-[1,1'-biphenyl]-4-carbaldehyde

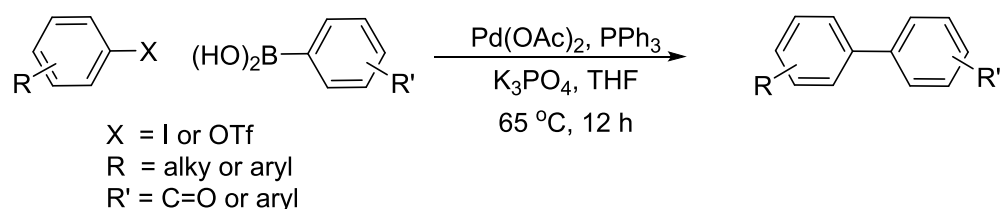
A glass reaction tube was charged with $\text{Pd}_2(\text{dba})_3$ (2 mol%), XPhos (4 mol%), K_3PO_4 (3 eq), 4-formylphenylboronic acid (2 eq), 2,4,6-triisopropylbromide (1 eq, 0.5 mmol) and a stirrer bar. The reaction tube was then flushed with nitrogen and *t*-amylalcohol (10 mL) was added. The reaction mixture was heated to $110\text{ }^\circ\text{C}$ and left to stir 16 h. Once cooled to room temperature the reaction was diluted with water (20 mL), and extracted into EtOAc (10 mL x 3). The organics were dried over MgSO_4 and evaporated under vacuum. The resulting residue was purified by column chromatography using 5% EtOAc in hexane and isolated in a yield of 70%.



Terphenyl synthesis

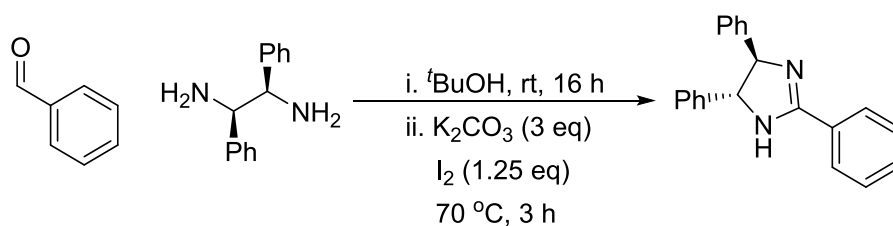
A two necked round-bottomed flask, equipped with a condenser and stirrer bar, was flushed with nitrogen and sealed. 1,3-Dichlorobenzene (10 mmol) and THF (15 mL) were added and the flask was cooled to $-78\text{ }^\circ\text{C}$. To this *n*-BuLi (1.6 M, 0.8 mL) was added and allowed to stir for 2 h. After this time the desired freshly prepared aryl magnesium bromide (synthesised from the bromide and magnesium, in the

presence of iodine at reflux in THF) (3 eq) was added and allowed to warm to room temperature with stirring overnight. Once complete the reaction mixture was cooled to 0 °C, and iodine (3 eq) in THF (10 mL) was injected and the mixture was stirred at room temperature for 30 min. The reaction was then quenched with aq Na₂S₂O₄ (50 mL) and extracted with Et₂O (30 mL x 3). The organics were then washed with water (30 mL) and brine (30 mL), dried over MgSO₄ and evaporated under vacuum. The resulting residue was then purified by column chromatography, using neat hexane and isolated in 40-60% yields.



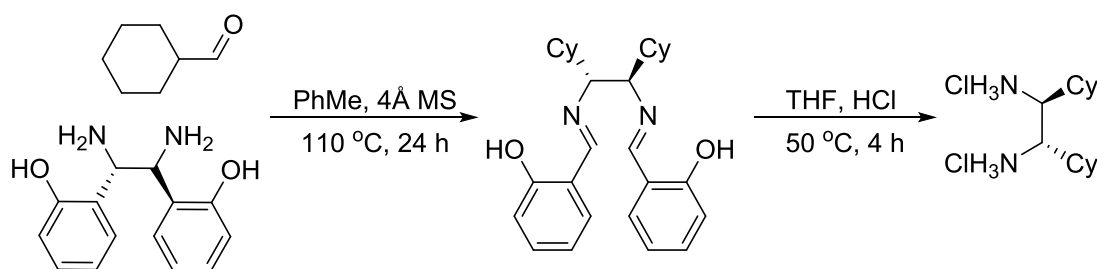
General Suzuki coupling

A glass reaction tube was charged with Pd(OAc)₂ (5 mol%), PPh₃ (10 mol%), K₃PO₄ (4 eq), boronic acid (3 eq), the desired triflate or halide (1 eq, 0.1 mmol) and a stirrer bar. The reaction tube was then flushed with nitrogen and THF (3 mL) was added. The reaction mixture was heated to 65 °C and left to stir for 12 h. Once cooled the reaction mixture was filtered through Celite and evaporated under vacuum. The resulting residue was purified by column chromatography using 20% EtOAc in hexane. The products were isolated in 50-85% yield.



Diamine condensation

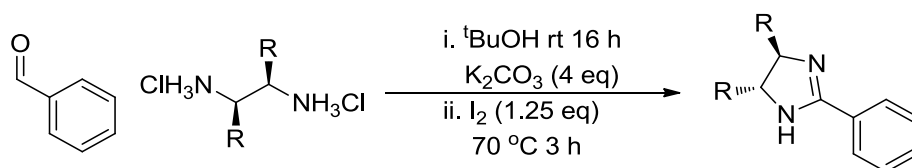
A reaction tube was charged with diamine (1 eq, 1 mmol), benzaldehyde (1 eq, 1 mmol) and a stirrer bar, *t*BuOH (5 mL) was then added and the resulting mixture stirred at room temperature for 16 h. K_2CO_3 (3 eq, 3 mmol) and I_2 (1.25 eq, 1.15 mmol) were then added and the resulting dark orange solution was heated to 70 °C and stirred for 3 h. Once cooled the reaction was quenched by addition of saturated aq $\text{Na}_2\text{S}_2\text{O}_4$ (10 mL) and the organics extracted with EtOAc. The organic layer was washed with water (10 mL x 3) and dried over MgSO_4 . The solvent was then removed under vacuum and the residue purified by column chromatography in 50% EtOAc in hexane. The products were isolated in 60-85% yields.



(*S,S*)-1,2-Bis(cyclohexyl)-1,2-diaminoethane synthesis

A glass reaction tube was charged with 4Å MS, bis-1,2-(2-hydroxydiphenyl)-1,2-diaminoethane (1 eq, 1 mmol), cyclohexanecarboxaldehyde (2.4 eq, 2.4 mmol) and a stirrer bar. Dry toluene was then added (5 mL) and this was stirred at 115 °C for 24 h. After cooling the reaction mixture was evaporated under vacuum and methanol

was added to precipitate the intermediate, which was isolated by filtration. The intermediate was then loaded into a glass reaction tube along with a stirrer bar. To this THF (5 mL), followed by aq HCl (2M, 10 mL) was added and this was heated to 50 °C and stirred for 3 h. After cooling and filtration the diamine 2HCl salt was isolated as a white solid, in 60-70% yield.



Diamine hydrochloride salt condensation

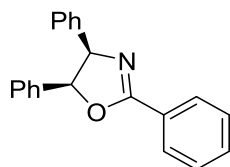
A reaction tube was charged with diamine (1 eq, 1 mmol), K₂CO₃ (4 eq, 4 mmol) benzaldehyde (1 eq, 1 mmol) and a stirrer bar, ^tBuOH (5 mL) was added and the resulting mixture stirred at room temperature for 16 h. I₂ (1.25 eq, 1.15 mmol) was added and the resulting dark orange solution was heated to 70 °C and stirred for 3 h. Once cooled the reaction was quenched by addition of aq Na₂S₂O₄ (10 mL) and the organics extracted with EtOAc. The organic layer was washed with water (10 mL x 3) and dried over MgSO₄. The solvent was removed under vacuum and the residue purified by column chromatography in 50% EtOAc in hexane. The product was isolated in yields of 50-80%.

Bromination reaction

A round bottomed flask was charged with 1,4-benzodioxan-6-carboxaldehyde (1 eq, 1 mmol) and a stirrer bar was placed under a nitrogen atmosphere. To this acetic acid (4 mL) was added followed by bromine (1 eq), and the resulting mixture was stirred at room temperature for 20 h. After completion the reaction mixture was

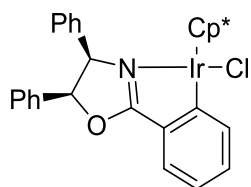
cooled in an ice bath and water added (10 mL). The resulting product was then isolated by filtration.

2.5.2 Analytical data



(4R,5S)-2,4,5-Triphenyl-4,5-dihydrooxazole¹⁸ In accordance with published data.

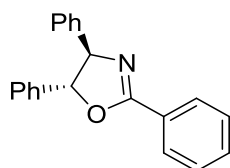
White solid. ¹H NMR (CDCl₃, 400 MHz) δ (ppm) 8.19-8.17 (m, 2H), 7.59-7.55 (m, 1H), 7.52-7.48 (m, 2H), 7.09-7.00 (m, 6H), 6.99-6.92 (m, 4H), 6.02 (d, J = 10.0 Hz, 1H), 5.75 (d, J = 10.0 Hz, 1H). ¹³C NMR (CDCl₃, 100 MHz) δ (ppm) 165.3, 138.1, 137.0, 132.2, 129.0, 128.9, 128.3, 128.1, 127.9, 127.8, 126.8, 85.7, 74.9. HRMS (ESI) [M+H]⁺ calculated 300.1388; found 300.1384.



Ir 1¹⁸ In accordance with published data.

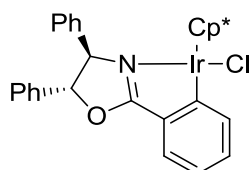
Yellow solid. ¹H NMR (CDCl₃, 400 MHz) δ (ppm) 7.86 (d, J = 7.7 Hz, 0.7H), 7.80 (d, J = 7.6 Hz, 0.3H), 7.65 (d, J = 7.6 Hz, 0.7H), 7.59 (d, J = 7.6 Hz, 0.3H), 7.34-7.29 (m, 1H), 7.10-7.03 (m, 9H), 6.96-6.89 (m, 2H), 6.28 (d, J = 9.1 Hz, 0.7H), 6.23 (d, J = 10.0 Hz, 0.3H), 5.80 (d, J = 10.0 Hz, 0.3H), 5.42 (d, J = 9.1 Hz, .07H), 1.55 (s, 5H), 1.50 (s, 10H).

¹³C NMR (CDCl₃, 100 MHz) δ (ppm) 135.7, 134.3, 132.37, 128.0, 127.8, 127.6, 126.9, 126.3, 121.9, 88.3, 87.6, 72.0, 9.4, 9.1.



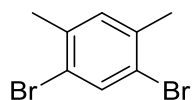
(4*R*,5*R*)-2,4,5-Triphenyl-4,5-dihydrooxazole¹⁸ In accordance with published data.

White solid. **¹H NMR** (CDCl₃, 400 MHz) δ (ppm) 8.15-8.13 (m, 2H), 7.56-7.29 (m, 13H), 5.41 (d, *J* = 7.6 Hz, 1H), 5.22 (d, *J* = 7.6 Hz, 1H). **¹³C NMR** (CDCl₃, 100 MHz) δ (ppm) 164.5, 142.2, 140.9, 132.1, 129.4, 129.3, 129.1, 128.9, 128.8, 128.2, 127.9, 127.2, 126.1, 89.4, 79.5. **HRMS** (ESI) [*M*+*H*]⁺ calculated 300.1388; found 300.1385. **CHN** calculated C, 84.25; H, 5.72; N, 4.58; found **C**, 84.58; **H**, 5.78; **N**, 4.60.



Ir 2¹⁸ In accordance with published data.

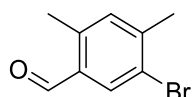
Yellow solid. **¹H NMR** (CDCl₃, 400 MHz) δ (ppm) 7.83 (dd, *J* = 17.3, 7.9 Hz, 1H), 7.57-7.53 (m, 2H), 7.45-7.41 (m, 4H), 7.38-7.28 (m, 6H), 7.05 (d, *J* = 6.4 Hz, 1H), 5.52 (d, *J* = 11.4 Hz, 1H), 5.19-5.14 (m, 1H), 1.56 (s, 6H), 1.51 (s, 9H). **¹³C NMR** (CDCl₃, 100 MHz) δ (ppm) 130.8, 129.1, 129.1, 128.9, 127.2, 126.5, 121.8, 119.3, 92.7, 88.2, 87.6, 9.4, 9.2.



1,5-Dibromo-2,4-dimethylbenzene

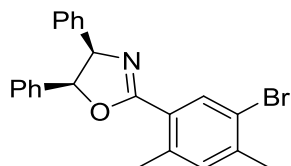
White solid. $^1\text{H NMR}$ (CDCl_3 , 400MHz) δ (ppm) 7.66 (s, 1H), 7.08 (s, 1H), 2.30 (s, 6H).

$^{13}\text{C NMR}$ (CDCl_3 , 100MHz) δ (ppm) 136.9, 134.9, 132.6, 122.1, 22.3.



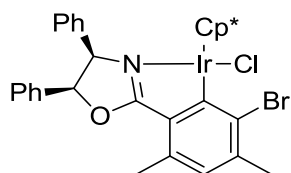
5-Bromo-2,4-dimethylbenzaldehyde

Yellow solid. $^1\text{H NMR}$ (CDCl_3 , 400 MHz) δ (ppm) 10.13 (s, 1H), 7.90 (s, 1H), 7.12 (s, 1H), 2.57 (s, 3H), 2.41 (s, 3H). $^{13}\text{C NMR}$ (CDCl_3 , 100 MHz) δ (ppm) 190.9, 144.2, 139.4, 135.4, 134.2, 133.5, 122.4, 23.1, 18.9. **HRMS** (CI) calculated $[\text{M}+\text{H}]^+$ 230.0175, found $[\text{M}+\text{H}]^+$ 230.0165.



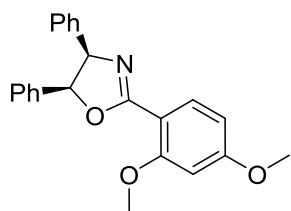
(4R,5S)-2-(5-Bromo-2,4-dimethylphenyl)-4,5-diphenyl-4,5-dihydrooxazole

White solid. $^1\text{H NMR}$ (CDCl_3 , 400 MHz) δ (ppm) 8.24 (s, 1H), 7.19 (s, 1H), 7.08-7.01 (m, 6H), 6.96-6.93 (m, 4H), 5.95 (d, $J = 10.1$ Hz, 1H), 5.77 (d, $J = 10.1$ Hz, 1H), 2.68 (s, 3H), 2.43 (s, 3H). $^{13}\text{C NMR}$ (CDCl_3 , 100 MHz) δ (ppm) 164.1, 141.0, 138.6, 137.8, 136.6, 133.9, 133.8, 127.9, 127.8, 127.7, 127.5, 127.0, 126.4, 125.9, 121.7, 84.7, 75.0, 22.9, 21.9. **HRMS** (ESI) found $[\text{M}+\text{H}]^+$ 406.0805.



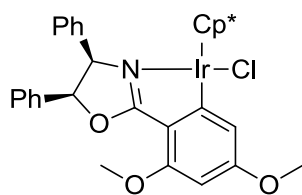
Ir 3

Yellow solid. **¹H NMR** (CDCl₃, 400 MHz) δ (ppm) 7.23-6.91 (m, 11H), 6.19 (d, J = 9.1 Hz, 0.7H), 5.99 (d, J = 10.1 Hz, 0.3H), 5.79 (d, J = 9.1 Hz, 0.7H), 5.30 (d, J = 9.1 Hz, 0.3H), 2.54-2.51 (m, 6H), 1.55 (s, 9H), 1.51 (s, 6H). **¹³C NMR** (CDCl₃, 100 MHz) δ (ppm) 162.1, 129.2, 128.2, 128.1, 127.9, 127.8, 127.7, 127.6, 127.5, 126.7, 126.4, 126.1, 85.6, 20.1, 10.1, 9.8, 9.0. **MS** (ESI) calculated [M+H]⁺ 769.22, found [M+H]⁺ 769.30.



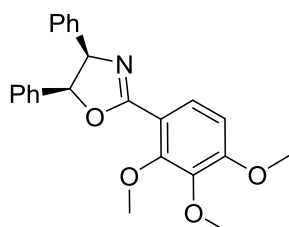
(4*R*,5*S*)-2-(2,4-Dimethoxyphenyl)-4,5-diphenyl-4,5-dihydrooxazole

Yellow solid. **¹H NMR** (CDCl₃, 400 MHz) δ (ppm) 7.95 (d, J = 8.6 Hz, 1H), 7.04-6.92 (m, 10H), 6.57-6.54 (m, 2H), 5.92 (d, J = 10.1 Hz, 1H), 5.73 (d, J = 10.1 Hz, 1H), 3.92 (s, 3H), 3.84 (s, 3H). **¹³C NMR** (CDCl₃, 100 MHz) δ (ppm) 163.6, 163.5, 160.5, 138.2, 137.0, 132.9, 128.0, 128.0, 127.7, 127.6, 127.6, 127.4, 127.2, 126.9, 126.8, 126.5, 109.7, 99.1, 84.4, 74.8, 56.1, 55.6.



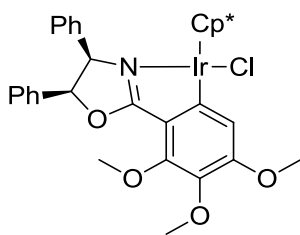
Ir 4

Yellow solid. ^1H NMR (CDCl_3 , 400 MHz) δ (ppm) 7.39 (d, J = 6.9 Hz, 1H), 7.12-6.93 (m, 11H), 6.23 (d, J = 9.1 Hz, 0.6H), 6.18 (d, J = 9.9 Hz, 0.4H), 5.68 (d, J = 9.9 Hz, 0.4H), 5.30 (d, J = 9.1 Hz, 0.6H), 3.93 (s, 3H), 3.83 (s, 1.8H), 3.82 (s, 1.2H), 1.48 (s, 9H), 1.46 (s, 6H). ^{13}C NMR (CDCl_3 , 100MHz) δ (ppm) 180.5, 164.0, 160.7, 136.9, 135.2, 134.8, 129.6, 128.5, 127.9, 127.9, 127.7, 127.7, 127.6, 127.5, 127.2, 127.0, 126.5, 113.1, 112.6, 112.2, 93.2, 93.1, 90.7, 88.4, 88.0, 87.7, 72.5, 71.0, 55.3, 55.2, 9.4, 9.1. MS (ESI) calculated $[\text{M}+\text{H}]^+$ 721.31; found $[\text{M}+\text{H}]^+$ 721.10. CHN $\text{C}_{33}\text{H}_{35}\text{ClIrNO}_3$ calculated C, 54.92; H, 4.89; N, 1.94; found C, 55.71; H, 4.84; N, 2.26.



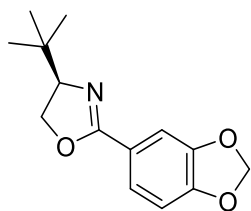
(4R,5S)-4,5-Diphenyl-2-(2,3,4-trimethoxyphenyl)-4,5-dihydrooxazole

Yellow solid. ^1H NMR (CDCl_3 , 400 MHz) δ (ppm) 7.74 (d, J = 8.9 Hz, 1H), 7.08-6.95 (m, 10H), 6.77 (d, J = 8.9 Hz, 1H), 5.98 (d, J = 10.2 Hz, 1H), 5.73 (d, J = 10.2 Hz, 1H), 4.01 (s, 3H), 3.93 (s, 3H), 3.92 (s, 3H). ^{13}C NMR (CDCl_3 , 100 MHz) δ (ppm) 163.7, 156.4, 154.0, 143.1, 138.0, 136.9, 127.9, 127.8, 127.7, 127.6, 127.3, 126.9, 126.4, 126.3, 115.2, 107.3, 74.5, 61.9, 61.1, 56.5.



Ir 5

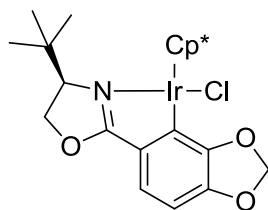
Yellow solid. $^1\text{H NMR}$ (CDCl_3 , 400 MHz) δ (ppm) 7.4 (d, $J = 7.1$ Hz, 1H), 7.15 (s, 1H), 7.10-6.95 (m, 9H), 6.27 (d, $J = 9.1$ Hz, 0.6H), 6.19 (d, $J = 9.9$ Hz, 0.4H), 5.71 (d, $J = 9.9$ Hz, 0.4H), 5.32 (d, $J = 9.1$ Hz, 0.6H), 4.01 (s, 3H), 3.99 (s, 1.8H), 3.92 (s, 1.2H), 3.87 (s, 1.2H), 3.86 (s, 1.8H), 1.49 (s, 9H), 1.46 (s, 6H). $^{13}\text{C NMR}$ (CDCl_3 , 100 MHz) δ (ppm) 180.4, 160.0, 157.7, 157.1, 153.2, 137.5, 157.4, 136.7, 135.1, 134.9, 134.7, 129.6, 128.5, 128.0, 128.0, 127.9, 127.8, 127.8, 127.6, 127.5, 127.3, 126.9, 126.3, 117.1, 114.1, 113.8, 90.8, 88.3, 88.0, 87.7, 72.5, 71.2, 62.2, 62.1, 60.9, 60.9, 55.8, 9.4, 9.1. **MS** (ESI) found $[\text{M}+\text{H}]^+$ 751.3. **CHN** $\text{C}_{34}\text{H}_{37}\text{ClIrNO}_4$ calculated C, 54.35; N, 4.96; H, 1.86; found C, 54.27; H, 5.25; N, 1.64.



(*R*)-2-(Benzo[d][1,3]dioxol-5-yl)-4-(*tert*-butyl)-4,5-dihydrooxazole

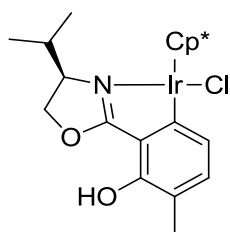
White solid. $^1\text{H NMR}$ (CDCl_3 , 400 MHz) δ (ppm) 7.50 (d, $J = 8.0$ Hz, 1H), 7.43 (s, 1H), 6.81 (d, $J = 8.0$ Hz, 1H), 6.00 (s, 2H), 4.33-4.28 (m, 1H), 4.20 (t, $J = 8.1$ Hz, 1H), 4.01 (dd, $J = 10, 7.6$ Hz, 1H), 0.94 (s, 9H). $^{13}\text{C NMR}$ (CDCl_3 , 100 MHz) δ (ppm) 162.7, 150.0, 147.5, 123.0, 121.9, 108.5, 107.9, 101.4, 76.0, 68.7, 34.0, 25.8. **HRMS** (ESI) found

[M+H]⁺ 248.1285. **CHN** C₁₄H₁₇NO₃ calculated C, 68.00; H, 6.93; N, 5.66; found C, 67.43; H, 6.87; N, 5.55.



Ir 6

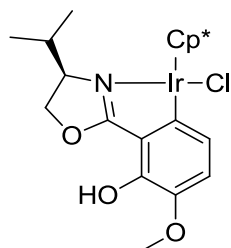
Yellow solid. **¹H NMR** (CDCl₃, 400 MHz) δ (ppm) 7.05 (d, J = 7.0 Hz, 1H), 6.53 (d, J = 7.0 Hz, 1H), 6.02 (d, J = 1.5 Hz, 1H), 5.97 (d, J = 1.5 Hz, 1H), 4.77 (dd, J = 9.2, 4.0 Hz, 1H), 4.55 (t, J = 8.8 Hz, 1H), 3.96 (dd, J = 9.4, 4.0 Hz, 1H), 1.75 (s, 15H), 1.09 (s, 9H). **¹³C NMR** (CDCl₃, 100 MHz) δ (ppm) 179.5, 162.1, 150.7, 149.5, 141.4, 138.9, 124.9, 122.8, 103.3, 100.0, 99.4, 87.8, 72.3, 70.9, 58.6, 35.8, 25.7, 9.6. **MS** (ESI, EtOAc) [M+H]⁺ 609.3. **CHN** C₁₄H₁₆ClIrNO₃ calculated C, 47.32; H, 5.18; N, 2.30; found C, 46.26; H, 5.06; N, 1.72.



Ir 7

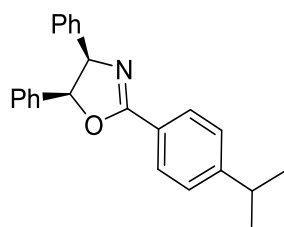
Yellow solid. **¹H NMR** (CDCl₃, 400 MHz) δ (ppm) 7.38 (d, J = 7.0 Hz, 1H), 7.12 (d, J = 7.0 Hz, 1H), 4.46-4.43 (m, 1H), 4.30-4.19 (m, 2H), 2.68-2.56 (m, 1H), 2.93 (s, 3H), 1.61 (s, 15H), 0.91 (dd, J = 24.1, 7.7 Hz, 6H). **¹³C NMR** (CDCl₃, 100 MHz) δ (ppm) 160.8, 133.6, 131.0, 126.5, 113.4, 108.2, 84.3, 74.2, 67.4, 29.7, 19.5, 17.8, 14.8, 9.0.

MS (ESI) found $[M+H]^+$ 582.5. **CHN** $C_{23}H_{34}ClIrNO_2$ calculated C, 47.53; H, 5.38; N 2.41; found C, 45.92; H, 5.38; N, 1.82.



Ir 8

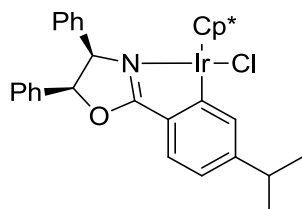
Yellow solid. $^1\text{H NMR}$ (CDCl_3 , 400 MHz) δ (ppm) 7.14 (d, $J = 7.1$ Hz, 1H), 6.77 (d, $J = 7.1$ Hz, 1H), 4.44-4.41 (m, 1H), 4.33-4.28 (m, 1H), 4.27-4.21 (m, 1H), 3.80 (s, 3H), 2.73-2.58 (m, 1H), 1.6 (s, 15H), 0.89 (dd, $J = 33.17, 7.80$ Hz, 6H). $^{13}\text{C NMR}$ (CDCl_3 , 100 MHz) δ (ppm) 159.5, 152.9, 120.8, 114.9, 113.2, 109.7, 84.5, 73.9, 87.9, 56.5, 29.6, 19.5, 9.2, 9.0. **MS** (ESI) found $[M+H]^+$ 597.29. **CHN** $C_{23}H_{34}ClIrNO_3$ calculated C, 46.26; H, 5.23; N 2.35; found C, 45.46; H, 5.27; N, 1.69.



(4*R*,5*S*)-2-(4-Iso-propylphenyl)-4,5-diphenyl-4,5-dihydrooxazole¹⁹ In accordance with published data.

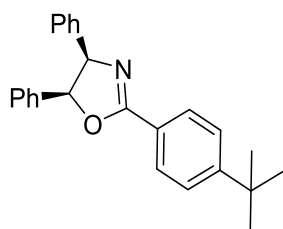
White solid. $^1\text{H NMR}$ (CDCl_3 , 400 MHz) δ (ppm) 8.03 (d, $J = 8.3$ Hz, 2H), 7.27 (d, $J = 8.3$ Hz, 2H), 6.98-6.91 (m, 6H), 6.88-6.83 (m, 4H), 5.91 (d, $J = 10.0$ Hz, 1H), 5.65 (d, $J = 10.0$ Hz, 1H), 2.91 (dt, $J = 13.9, 6.9$ Hz, 1H), 1.22 (d, $J = 6.9$ Hz, 6H). $^{13}\text{C NMR}$ (CDCl_3 , 100 MHz) δ (ppm) 165.1, 153.2, 137.8, 136.7, 128.8, 127.9, 127.8, 127.7, 127.7,

127.6, 127.5, 127.4, 127.0, 126.8, 126.7, 126.5, 125.0, 85.3, 85.3, 76.9, 74.5, 74.4, 34.4, 34.3, 24.0, 23.9. **HRMS** (ESI) calculated $[M+H]^+$ 342.1858; found $[M+H]^+$ 342.1865.



Ir 9¹⁹ In accordance with published data.

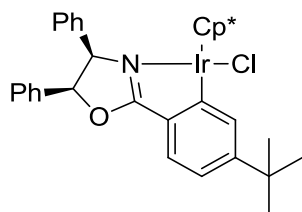
Yellow solid. **¹H NMR** (CDCl₃, 400 MHz) δ (ppm) 7.65 (s, 0.7H) 7.59 (s, 0.3H), 7.52 (d, J = 7.8 Hz, 0.7H), 7.45 (d, J = 7.8 Hz, 0.3H), 7.33 (d, J = 7.0 Hz, 1H), 7.01-6.88 (m, 10H), 6.48 (d, J = 9.1 Hz, 0.7H), 6.12 (d, J = 10 Hz, 0.3H), 5.70 (d, J = 10 Hz, 0.3H), 6.33 (d, J = 9.1 Hz, 0.7H), 2.93 (dt, J = 13.7, 6.8 Hz, 1H), 1.42 (s, 15H), 1.27 (d, J = 6.8 Hz, 6H). **¹³C NMR** (CDCl₃, 100 MHz) δ (ppm) 134.0, 128.1, 128.0, 127.8, 128.6, 126.9, 126.3, 120.5, 90.6, 71.9, 34.7, 23.7, 9.4, 9.2.



(4R,5S)-2-(4-(*tert*-butyl)phenyl)-4,5-diphenyl-4,5-dihydrooxazole¹⁹ In accordance with published data.

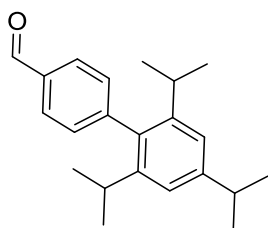
White solid. **¹H NMR** (CDCl₃, 400 MHz) δ (ppm) 8.11 (d, J = 8.4 Hz, 2H), 7.52 (d, J = 8.4 Hz, 2H), 7.06-7.01 (m, 6H), 6.96-6.92 (m, 4H), 6.00 (d, J = 10.0 Hz, 1H), 5.73 (d, J = 10.0 Hz, 1H), 1.38 (s, 9H). **¹³C NMR** (CDCl₃, 100 MHz) δ (ppm) 165.0, 155.3, 137.9,

136.8, 128.5, 127.9, 127.7, 127.6, 127.3, 127.0, 126.4, 125.6, 124.7, 85.2, 74.5, 35.1, 31.3. **HRMS** (ESI) calculated $[M+H]^+$ 356.2010; found $[M+H]^+$ 356.2012.



Ir 10¹⁹ In accordance with published data.

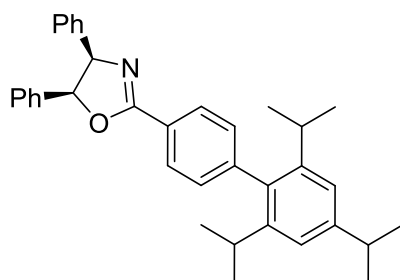
Yellow solid. **¹H NMR** (CDCl₃, 400 MHz) δ (ppm) 7.91 (s, 0.7H), 7.85 (s, 0.3H), 7.60 (d, J = 8.0 Hz, 1H), 7.53 (d, J = 8.0 Hz, 1H), 7.15-7.03 (m, 10H), 6.26 (d, J = 9.1 Hz, 0.7H), 6.19 (d, J = 9.9 Hz, 0.3H), 5.77 (d, J = 9.9 Hz, 0.3H), 5.40 (d, J = 9.1 Hz, 0.7H), 1.50 (s, 10H), 1.49 (s, 5H), 1.42 (s, 9H). **¹³C NMR** (CDCl₃, 100 MHz) δ (ppm) 193.3, 154.8, 151.0, 136.3, 134.5, 132.6, 129.6, 129.2, 128.6, 128.1, 128.0, 127.8, 126.9, 126.5, 126.3, 125.6, 119.7, 90.7, 88.2, 88.0, 87.6, 76.3, 71.9, 35.3, 31.6, 9.5, 9.2. **HRMS** (ESI) found $[M+H]^+$ 717.3455.



2',4',6'-triisopropyl-[1,1'-biphenyl]-4-carbaldehyde¹⁹ In accordance with published data.

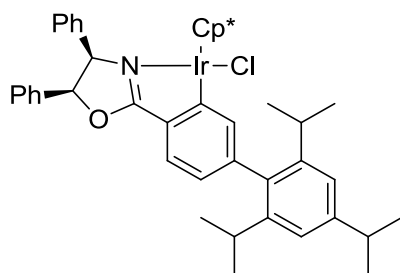
White solid. **¹H NMR** (CDCl₃, 400 MHz) δ (ppm) 10.01 (s, 1H), 7.87-7.84 (m, 2H), 7.31-7.29 (m, 2H), 7.00 (s, 2H), 2.88 (septet J = 6.9 Hz, 1H), 2.43 (septet, J = 6.9 Hz, 2H), 1.24 (d, J = 6.9 Hz, 6H), 1.01 (d J = 6.9 Hz, 12H). **¹³C NMR** (CDCl₃, 100 MHz)

δ (ppm) 191.0, 147.6, 147.1, 145.0, 134.7, 133.9, 129.6, 128.4, 119.7, 33.3, 29.4, 23.1, 23.0. **HRMS** (CI) calculated $[M+H]^+$ 309.2213; found $[M+H]^+$ 309.2223.



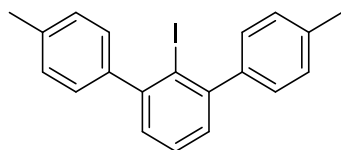
(4*R*,5*S*)-4,5-Diphenyl-2-(2',4',6'-triisopropyl-[1,1'-biphenyl]-4-yl)-4,5-dihydrooxazole¹⁹ In accordance with published data.

White solid. **¹H NMR** (CDCl₃, 400 MHz) δ (ppm) 8.20 (d, *J* = 8.1 Hz, 2H), 7.33 (d, *J* = 9.2 Hz, 2H), 7.08-6.97 (m, 12H), 6.05 (d, *J* = 10.1 Hz, 1H), 5.78 (d, *J* = 10.1 Hz, 1H), 2.95 (septet, *J* = 6.9 Hz, 1H), 2.63 (septet, *J* = 6.9 Hz, 2H), 1.32 (d, *J* = 6.9 Hz, 6H), 1.11 (d, *J* = 6.9 Hz, 12H). **¹³C NMR** (CDCl₃, 100 MHz) δ (ppm) 165.0, 148.3, 146.3, 145.0, 137.8, 136.7, 136.2, 130.2, 128.3, 128.0, 127.7, 127.7, 127.4, 127.0, 126.4, 125.7, 120.7, 85.4, 74.6, 23.3, 30.4, 24.2, 24.1. **HRMS** (ESI) calculated $[M+H]^+$ 502.3110; found $[M+H]^+$ 502.3109. **CHN** C₃₆H₃₄NO calculated C, 86.18; H, 7.84; N, 2.79; found C, 85.48; H, 7.79; N, 2.88.



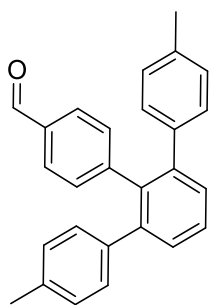
Ir 11¹⁹ In accordance with published data.

Yellow solid. **¹H NMR** (CDCl₃, 400 MHz) δ (ppm) 7.68 (d, *J* = 7.7 Hz, 0.7H), 7.62 (s, 0.7H), 7.58 (d, *J* = 7.7 Hz, 0.3H) 7.56 (s, 0.3H), 7.42 (d, *J* = 7.2 Hz, 0.7H) 7.35 (d, *J* = 7.2 Hz, 0.3H), 7.12-7.02 (m, 11H) 6.90 (d, *J* = 7.7 Hz, 0.7H), 6.87 (d, *J* = 7.7 Hz, 0.3H), 6.30 (d, *J* = 9.2 Hz, 0.7H), 6.27 (d, *J* = 10.4 Hz, 0.3H), 5.80 (d, *J* = 10.4 Hz, 0.3H), 5.47 (d, *J* = 9.2 Hz, 0.7H), 3.03-2.69 (m, 3H), 1.58 (s, 3H), 1.50 (s, 12H), 1.36 (d, *J* = 6.8 Hz, 6H), 1.20-1.09 (m, 12H). **¹³C NMR** (CDCl₃, 100 MHz) δ (ppm) 181.1, 163.2, 147.5, 145.9, 137.8, 137.3, 136.2, 134.4, 128.1, 128.0, 127.8, 126.3, 123.7, 120.7, 120.2, 90.7, 88.2, 87.5, 72.1, 34.2, 30.5, 30.2, 25.0, 24.6, 24.0, 23.9, 9.4, 9.1. **HRMS** (ESI) found [M+H]⁺ 863.5543. **CHN** calculated C, 63.98; H, 6.19; N, 1.62; found C, 63.78, H, 6.27; N, 1.45.



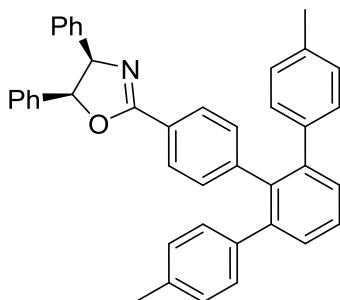
2'-iodo-4,4''-dimethyl-1,1':3',1''-terphenyl

White solid. **¹H NMR** (CDCl₃, 400 MHz) δ (ppm) 7.57-7.75 (m, 4H), 7.37-7.3 (m, 1H), 7.25-7.23 (m, 2H), 6.93-6.91 (m, 4H), 2.29 (s, 6H). **¹³C NMR** (CDCl₃, 100 MHz) δ (ppm) 137.6, 135.4, 131.6, 130.6, 129.2, 127.3, 90.6, 21.4.



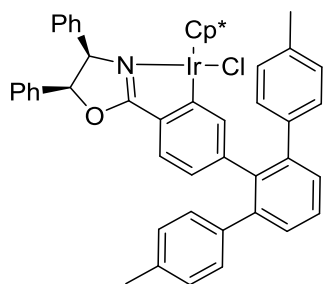
4''-Methyl-6'-(p-tolyl)-[1,1':2',1''-terphenyl]-4-carbaldehyde

Yellow solid. $^1\text{H NMR}$ (CDCl_3 , 400 MHz) δ (ppm) 10.04 (s, 1H), 7.97-7.92 (m, 4H), 7.75-7.73 (m, 3H), 7.55-7.53 (m, 4H), 7.30-7.27 (m, 4H), 2.41 (s, 6H). $^{13}\text{C NMR}$ (CDCl_3 , 100 MHz) δ (ppm) 192.3, 147.6, 138.9, 137.2, 135.4, 130.7, 130.2, 128.9, 128.1, 127.8, 127.6, 125.9, 21.6.



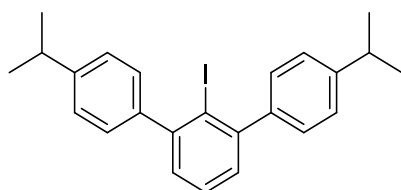
(4R,5S)-2-(4''-Methyl-6'-(p-tolyl)-[1,1':2',1''-terphenyl]-4-yl)-4,5-diphenyl-4,5-dihydrooxazole

Yellow solid. $^1\text{H NMR}$ (CDCl_3 , 400 MHz) δ (ppm) 8.26-8.17 (m 2H), 7.74-7.68 (m, 3H), 7.58-7.51 (m, 2H), 7.29-7.27 (m, 3H), 7.09-7.93 (m, 15H), 6.03 (d, $J = 10.1$ Hz, 1H), 5.76 (d, $J = 10.1$ Hz, 1H), 2.4 (s, 6H). $^{13}\text{C NMR}$ (CDCl_3 , 100 MHz) δ (ppm) 165.3, 144.9, 138.4, 138.2, 137.7, 137.1, 130.1, 129.5, 128.3, 128.1, 127.8, 127.7, 127.4, 126.8, 126.4, 85.8, 74.9, 32.02, 23.1.



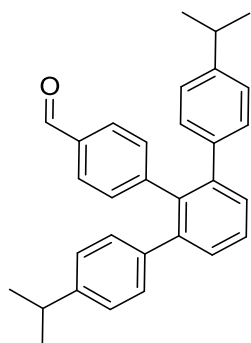
Ir 12

Yellow solid. $^1\text{H NMR}$ (CDCl_3 , 400 MHz) δ (ppm) 8.05-8.0 (m, 1H), 7.71 (d, $J = 7.8$ Hz, 1H), 7.64 (dd, $J = 8.1, 3.7$ Hz, 1H), 7.60 (d, $J = 8.1$ Hz, 4H), 7.43-7.41 (m, 2H), 7.28 (d, $J = 7.8$ Hz, 3H), 7.11-7.08 (m, 6H), 7.05-7.01 (m, 6H), 6.3 (d, $J = 9.0$ Hz, 0.7H), 6.23 (d, $J = 9.9$ Hz, 0.3H), 5.82 (d, $J = 9.9$ Hz, 0.3H), 5.43 (d, $J = 9.0$ Hz, 0.7H), 2.43 (s, 3H), 2.28 (s, 3H), 1.52 (s, 10H), 1.51 (s, 5H). $^{13}\text{C NMR}$ (CDCl_3 , 100 MHz) δ (ppm) 180.01, 144.54, 139.27, 137.16, 136.16, 134.33, 129.6, 129.4, 128.6, 128.2, 128.0, 127.9, 127.9, 127.5, 126.9, 126.3, 126.1, 90.8, 90.1, 88.4, 87.7, 85.8, 72.0, 21.3, 21.2, 9.5, 9.2. **MS** (ESI) found $[\text{M}+\text{H}]^+$ 919.3.



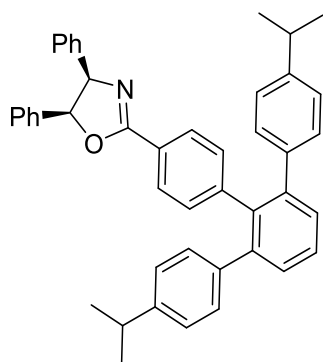
2'-Iodo-4,4''-diisopropyl-1,1':3',1''-terphenyl

White solid. $^1\text{H NMR}$ (CDCl_3 , 400 MHz) δ (ppm) 7.41-7.27 (m, 11H), 3.01 (dt $J = 13.8, 7.0$ Hz, 2H), 1.34 (d, $J = 7.0$ Hz, 12H). $^{13}\text{C NMR}$ (CDCl_3 , 100 MHz) δ (ppm) 148.1, 148.1, 143.1, 129.3, 127.5, 125.9, 104.0, 76.7, 33.9, 24.0.



4''-Isopropyl-6'-(4-isopropylphenyl)-[1,1':2',1''-terphenyl]-4-carbaldehyde

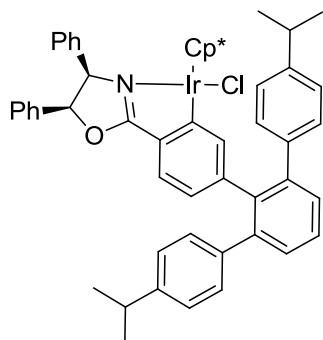
White solid. ^1H NMR (CDCl_3 , 400 MHz) δ (ppm) 7.54-7.45 (m, 5H), 7.06-6.98 (m, 10H), 2.89-2.82 (m, 2H), 1.23 (d, $J = 7.1$ Hz, 12H). ^{13}C NMR (CDCl_3 , 100 MHz) δ (ppm) 192.4, 162.1, 147.1, 141.8, 138.7, 137.8, 133.8, 132.5, 129.8, 129.7, 128.6, 127.9, 125.8, 33.6, 23.9. HRMS (CI) found $[\text{M}+\text{H}]^+$ 419.2385.



(4R,5S)-2-(4''-Isopropyl-6'-(4-isopropylphenyl)-[1,1':2',1''-terphenyl]-4-yl)-4,5-diphenyl-4,5-dihydrooxazole

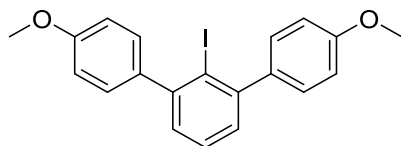
Yellow solid. ^1H NMR (CDCl_3 , 400 MHz) δ (ppm) 7.86-7.79 (m, 2H), 7.50-7.47 (m, 5H), 7.11-7.06 (m, 12H), 6.99-6.91 (m, 4H), 5.99 (d, $J = 9.9$ Hz, 1H), 5.72 (d, $J = 9.9$ Hz, 1H), 2.91-2.88 (m, 2H), 1.26 (d, $J = 6.8$ Hz, 12H). ^{13}C NMR (CDCl_3 , 100 MHz) δ (ppm) 182.8, 162.1, 146.9, 141.9, 139.0, 132.0, 129.8, 129.6, 127.9, 127.7, 127.6, 127.4, 127.0, 126.3, 125.8, 85.1, 37.9, 33.7, 24.0, 17.2. HRMS (ESI) found $[\text{M}+\text{H}]^+$

612.3276. **CHN** C₄₅H₄₁NO calculated C, 88.34; H, 6.75; N, 2.79; found C, 85.48; H, 7.79; N, 2.88.



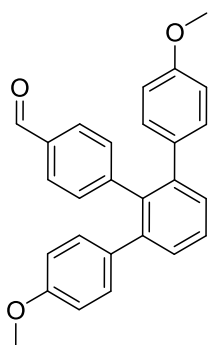
Ir 13

Yellow solid. **¹H NMR** (CDCl₃, 400 MHz) δ (ppm) 7.48-7.46 (m, 3H), 7.42 (d, J = 1.0 Hz, 1H), 7.38 (d, J = 1.0 Hz, 1H), 7.22 (d, J = 8.6 Hz, 2H), 7.10-7.02 (m, 14H), 6.87-6.84 (m, 2H), 6.63-6.55 (m, 1H), 6.26 (d, J = 9.3 Hz, 0.65H), 6.13 (d, J = 9.8 Hz, 0.4H), 5.74 (d, J = 9.8 Hz, 0.4H), 5.37 (d, J = 9.3 Hz, 0.6H), 2.89-2.78 (m, 2H), 1.22 (s, 15H), 1.20 (s, 12H). **¹³C NMR** (CDCl₃, 100 MHz) δ (ppm) 181.1, 162.1, 146.5, 143.8, 142.7, 142.6, 141.1, 140.0, 139.8, 139.5, 139.3, 138.8, 136.4, 134.9, 134.6, 130.1, 129.8, 129.7, 129.6, 129.2, 129.1, 128.2, 128.1, 128.0, 127.9, 127.8, 127.8, 127.5, 127.3, 126.8, 126.3, 126.0, 125.9, 125.7, 90.4, 88.0, 87.2, 73.2, 72.0, 33.7, 24.3, 24.1, 24.0, 23.8, 23.7, 9.2, 9.0. **MS** (ESI) found [M+H]⁺ 973.8. **CHN** calculated C, 67.84; H, 5.69; N, 1.44; found C, 67.41; H, 5.66; N, 1.30.



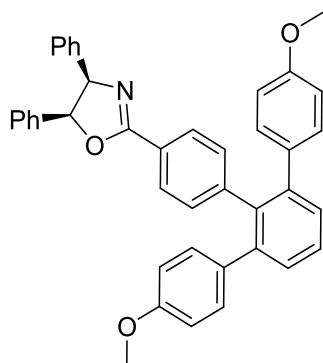
2'-Iodo-4,4''-dimethoxy-1,1':3',1''-terphenyl

White solid. $^1\text{H NMR}$ (CDCl_3 , 400 MHz) δ (ppm) 7.40-7.37 (m, 1H), 7.34-7.32 (m, 4H), 7.26-7.25 (m, 2H), 7.01-6.97 (m, 4H), 3.89 (s, 6H). $^{13}\text{C NMR}$ (CDCl_3 , 100 MHz) δ (ppm) 159.0, 147.8, 138.4, 130.6, 128.6, 12.5, 113.2, 105.1, 55.3.



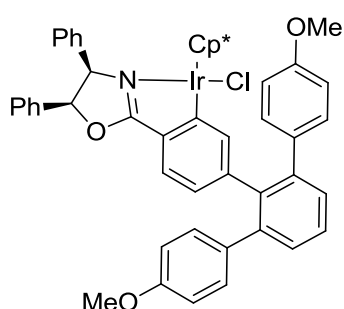
4''-Methoxy-6'-(4-methoxyphenyl)-[1,1':2',1''-terphenyl]-4-carbaldehyde

Yellow solid. $^1\text{H NMR}$ (CDCl_3 , 400 MHz) δ (ppm) 9.89 (s, 1H), 7.57-7.43 (m, 5H), 7.07 (d, $J = 7.8$ Hz, 2H), 6.99 (d, $J = 8.6$ Hz, 4H), 6.72 (d, $J = 8.6$ Hz, 4H), 3.77 (s, 6H). $^{13}\text{C NMR}$ (CDCl_3 , 100 MHz) δ (ppm) 192.2, 158.3, 147.2, 141.4, 137.8, 133.7, 132.4, 131.0, 129.5, 128.8, 128.0, 113.2, 55.1. **HRMS** (ESI) found $[\text{M}+\text{Na}]^+$ 417.1473.



(4*R*,5*S*)-2-(4''-Methoxy-6'-(4-methoxyphenyl)-[1,1':2',1''-terphenyl]-4-yl)-4,5-diphenyl-4,5-dihydrooxazole

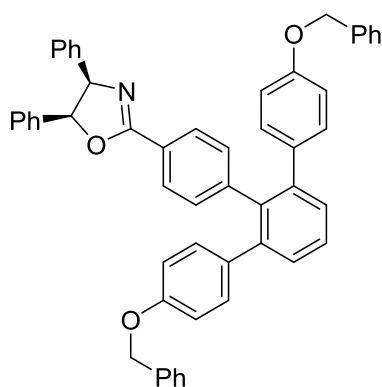
Yellow solid. ^1H NMR (CDCl_3 , 400 MHz) δ (ppm) 7.84-7.82 (m, 2H), 7.52-7.43 (m, 4H), 7.10-6.96 (m, 15H), 6.79-6.76 (m, 4H), 5.99 (d, $J = 10.1$ Hz, 1H), 5.72 (d, $J = 10.1$ Hz, 1H), 3.81 (s, 6H). ^{13}C NMR (CDCl_3 , 100 MHz) δ (ppm) 182.8, 165.1, 162.1, 158.2, 144.0, 141.5, 137.8, 136.6, 134.1, 131.9, 131.0, 129.5, 127.9, 127.7, 127.6, 127.5, 127.4, 127.0, 126.4, 124.7, 113.3, 85.2, 74.4, 55.2. HRMS (ESI) found $[\text{M}+\text{H}]^+$ 588.2545.



Ir 14

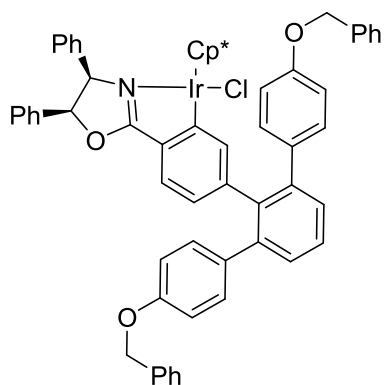
Yellow solid. ^1H NMR (CDCl_3 , 400 MHz) δ (ppm) 7.47-7.42 (m, 2H), 7.39 (dd, $J = 6.7$, 1.1 Hz, 2H), 7.31 (d, $J = 7.7$ Hz, 1H), 7.22-7.19 (m, 2H), 7.09-6.99 (m, 10H), 6.90-6.88 (m, 2H), 6.79-6.71 (m, 4H), 6.61 (dd, $J = 7.8$, 1.4 Hz, 0.7H), 6.58 (dd, $J = 7.8$, 1.4 Hz, 0.3H), 6.26 (d, $J = 9.3$ Hz, 0.7H), 6.15 (d, $J = 9.9$ Hz, 0.3H), 5.75 (d, $J = 9.9$ Hz, 0.3H),

5.37 (d, $J = 9.3$ Hz, 0.7H), 3.78 (s, 2H), 3.76 (s, 1H), 3.75 (s, 2H), 3.75 (s, 1H), 1.25 (s, 10H), 1.23 (s, 5H). ^{13}C NMR (CDCl_3 , 100 MHz) δ (ppm) 181.8, 181.1, 162.1, 158.1, 158.0, 157.9, 145.0, 143.8, 142.2, 140.9, 140.5, 140.0, 139.7, 139.4, 139.2, 126.4, 135.1, 134.8, 134.5, 133.8, 131.3, 131.1, 130.9, 129.4, 129.3, 129.3, 129.2, 129.1, 128.3, 128.2, 128.1, 127.9, 127.8, 127.8, 127.6, 127.4, 126.9, 126.3, 126.0, 125.8, 125.7, 125.4, 113.5, 113.3, 113.2, 90.5, 88.0, 87.2, 73.1, 72.0, 55.3, 55.3, 55.3, 55.2, 9.2, 8.9. **MS** (ESI) found $[\text{M}+\text{H}]^+$ 950.4. **CHN** calculated C, 64.51; H, 4.99; N, 1.48; found C, 64.00; H, 4.96; N, 1.33.



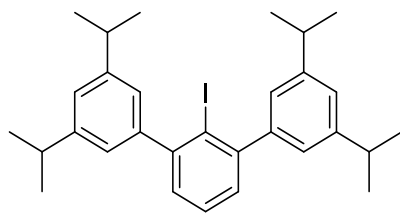
(4*R*,5*S*)-2-(4''-(Benzyloxy)-6'-(4-(benzyloxy)phenyl)-[1,1':2',1''-terphenyl]-4-yl)-4,5-diphenyl-4,5-dihydrooxazole

Yellow solid. ^1H NMR (CDCl_3 , 400 MHz) δ (ppm) 7.89 (d, $J = 8.3$ Hz, 2H), 7.54-7.38 (m, 13H), 7.12-7.06 (m, 12H), 7.02-6.98 (m, 4H), 6.89 (d, $J = 8.6$ Hz, 4H), 6.02 (d, $J = 10.0$ Hz, 1H), 5.75 (d, $J = 10.0$ Hz, 1H), 5.08 (s, 4H). ^{13}C NMR (CDCl_3 , 100 MHz) δ (ppm) 165.1, 157.5, 144.0, 141.6, 138.2, 137.9, 137.0, 136.7, 134.4, 132.0, 131.1, 129.6, 128.6, 128.0, 128.0, 127.7, 127.7, 127.4, 127.0, 126.5, 124.8, 114.3, 85.3, 70.0. **HRMS** (ESI) found $[\text{M}+\text{H}]^+$ 740.3161.



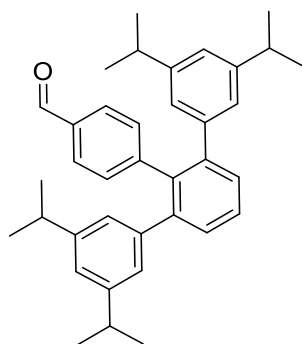
Ir 15

Yellow solid. $^1\text{H NMR}$ (CDCl_3 , 400 MHz) δ (ppm) 7.81 (d, $J = 8.3$ Hz, 1H), 7.47-7.29 (m, 22H), 7.24-7.19 (m, 2H), 7.11-6.99 (m, 15H), 6.96-6.80 (m, 10H), 6.63-6.58 (m, 1H), 6.26 (d, $J = 9.3$ Hz, 0.7H), 6.14 (d, $J = 9.8$ Hz, 0.3H), 5.97 (d, $J = 10.1$ Hz, 0.5H), 5.75 (d, $J = 9.8$ Hz, 0.3H), 5.69 (d, $J = 10.1$ Hz, 0.5H), 5.38 (d, $J = 9.3$ Hz, 0.7H), 5.04-4.99 (m, 6H), 1.26 (s, 10H), 1.23 (s, 5H). $^{13}\text{C NMR}$ (CDCl_3 , 100 MHz) δ (ppm) 181.1, 157.4, 157.3, 144.0, 143.4, 142.1, 141.5, 139.7, 139.5, 139.2, 138.2, 137.9, 137.5, 137.1, 137.0, 136.6, 136.4, 135.43, 134.6, 134.4, 134.0, 132.0, 131.4, 131.2, 131.2, 131.0, 130.9, 130.3, 129.4, 129.3, 128.7, 128.6, 128.6, 128.5, 128.5, 128.4, 128.1, 128.0, 127.9, 127.9, 127.8, 127.7, 127.6, 127.5, 127.4, 127.4, 127.0, 126.9, 126.4, 126.3, 126.0, 125.9, 114.5, 114.2, 114.1, 90.5, 88.0, 87.2, 85.2, 74.5, 72.0, 70.2, 70.1, 70.0, 19.5, 9.3, 9.0. **MS** (ESI) found $[\text{M}+\text{H}]^+$ 1104.3.



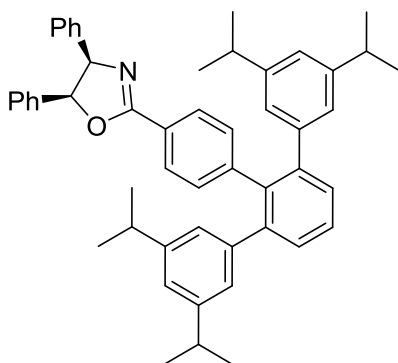
2'-Iodo-3,3'',5,5''-tetraisopropyl-1,1':3',1''-terphenyl

Yellow solid. $^1\text{H NMR}$ (CDCl_3 , 400 MHz) δ (ppm) 7.45-7.41 (m, 1H), 7.34 (s, 1H), 7.32 (s, 1H), 7.15-7.12 (m, 6H), 3.04-2.97 (m, 4H), 1.36 (d, $J = 6.8$ Hz, 24H). $^{13}\text{C NMR}$ (CDCl_3 , 100 MHz) δ (ppm) 148.8, 148.2, 145.5, 128.5, 127.5, 125.1, 124.0, 104.2, 34.2, 24.1.



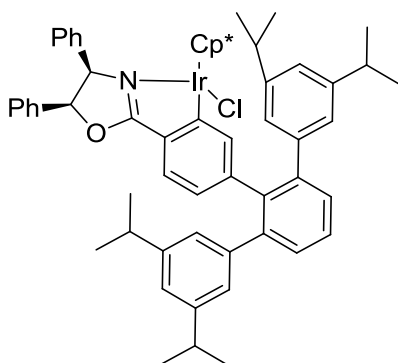
6'-(3,5-Diisopropylphenyl)-3'',5''-diisopropyl-[1,1':2',1''-terphenyl]-4-carbaldehyde

Yellow solid. $^1\text{H NMR}$ (CDCl_3 , 400 MHz) δ (ppm) 9.86 (s, 1H), 7.54-7.52 (m, 5H), 7.03 (d, $J = 8.1$ Hz, 2H), 6.87 (s, 2H), 6.78 (d, $J = 1.5$ Hz, 4H), 2.76 (dt, $J = 13.7, 7.0$ Hz, 4H), 1.08 (d, $J = 7.0$ Hz, 24H). $^{13}\text{C NMR}$ (CDCl_3 , 100 MHz) δ (ppm) 192.0, 148.2, 147.7, 142.4, 141.0, 138.0, 133.7, 132.4, 129.2, 128.6, 128.0, 125.6, 123.4, 37.9, 39.9, 23.9.



(4*R*,5*S*)-2-(6'-(3,5-Diisopropylphenyl)-3'',5''-diisopropyl-[1,1':2',1''-terphenyl]-4-yl)-4,5-diphenyl-4,5-dihydrooxazole

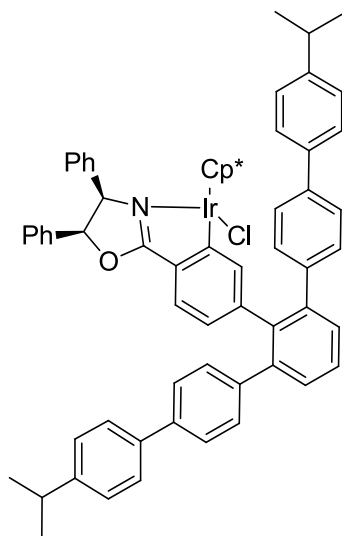
Yellow solid. ^1H NMR (CDCl_3 , 400 MHz) δ (ppm) 7.81-7.75 (m, 3H), 7.04-7.00 (m, 7H), 6.96-6.92 (m, 3H), 6.87-6.83 (m, 7H), 6.79 (d, J = 1.5 Hz, 3H), 5.92 (d, J = 9.9 Hz, 1H), 5.65 (d, J = 9.9 Hz, 1H), 2.76 (dt, J = 13.8, 6.9 Hz, 4H), 1.11 (d, J = 6.9 Hz, 24H). ^{13}C NMR (CDCl_3 , 100MHz) δ (ppm) 148.1, 147.1, 142.5, 141.2, 131.9, 129.2, 129.1, 127.9, 127.8, 127.7, 127.6, 127.6, 127.4, 126.9, 126.3, 125.7, 125.1, 123.3, 74.4, 71.8, 34.0, 24.0, 23.0. HRMS (ESI) calculated $[\text{M}+\text{H}]^+$ 696.4205; found $[\text{M}+\text{H}]^+$ 696.4191.



Ir 16

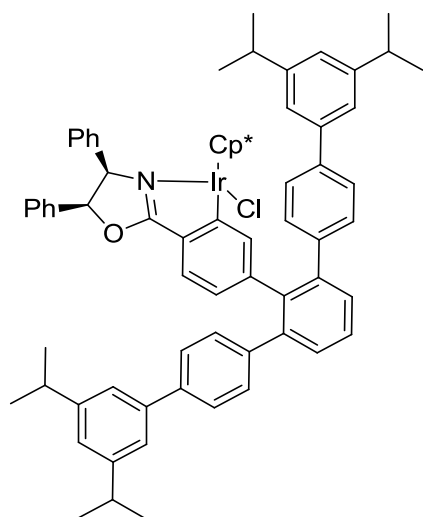
Yellow solid. ^1H NMR (CDCl_3 , 400 MHz) δ (ppm) 7.5-7.48 (m, 2H), 7.4 (s, 1H) 7.19 (d, J = 7.8 Hz, 1H), 7.07-6.98 (m, 10H), 6.89-6.78 (m, 7H), 6.61 (dd, J = 6.9 Hz, 1H), 6.14

(m, 1H), 5.73 (d, $J = 9.9$ Hz, 0.4H), 5.31 (d, $J = 9.9$ Hz, 0.6H), 2.88-2.74 (m, 4H), 1.21 (s, 8H), 1.19 (s, 7H), 1.17-1.08 (m, 24H). ^{13}C NMR (CDCl_3 , 100 MHz) δ (ppm) 148.2, 148.2, 147.8, 128.1, 128.0, 127.9, 127.8, 126.9, 126.2, 126.0, 126.0, 125.9, 87.8, 87.1, 73.1, 71.8, 34.1, 34.0, 33.9, 33.8, 31.0, 24.4, 24.3, 24.2, 24.1, 24.0, 23.9, 23.8, 9.2, 9.0. **MS** (ESI) found $[\text{M}+\text{H}]^+$ 1058.8.



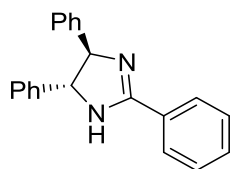
Ir 17

Yellow solid. ^1H NMR (CDCl_3 , 400 MHz) δ (ppm) 7.91-7.79 (m, 2H), 7.72-7.58 (m, 4H), 7.52-7.47 (m, 2H), 7.44-7.40 (m, 2H), 7.31-7.28 (m, 3H), 7.10-0.08 (m, 8H), 7.06-7.01 (m, 7H), 6.98-6.94 (m, 2H), 6.89 (bs, 2H), 6.28 (d, $J = 9.1$ Hz, 0.7H), 6.23 (d, $J = 10.0$ Hz, 0.3H), 5.80 (d, $J = 10.0$ Hz, 0.3H), 5.41 (d, $J = 9.1$ Hz, 0.7H), 1.75-1.68 (m, 2H), 1.52-1.47 (m, 23H), 1.39-1.37 (m, 4H). ^{13}C NMR (CDCl_3 , 100 MHz) δ (ppm) 181.2, 136.1, 135.7, 135.4, 134.8, 134.7, 134.3, 133.2, 132.4, 131.5, 129.6, 128.6, 128.5, 128.4, 128.2, 128.1, 128.0, 127.9, 127.8, 127.8, 127.6, 127.4, 127.3, 127.1, 126.9, 126.7, 126.3, 125.7, 125.6, 122.0, 121.9, 90.7, 88.4, 88.1, 87.7, 73.3, 72.0, 31.4, 9.5, 9.4, 9.3, 9.2. **MS** (ESI) found $[\text{M}+\text{H}]^+$ 1126.4.



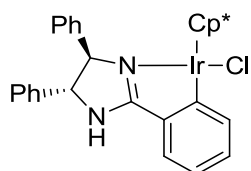
Ir 18

Yellow solid. $^1\text{H NMR}$ (CDCl_3 , 400 MHz) δ (ppm) 7.56-7.54 (m, 4H), 7.47 (d, $J = 8$ Hz, 3H), 7.43 (d, $J = 8.3$ Hz, 2H), 7.36 (d, $J = 8.3$ Hz, 2H), 7.31-7.28 (m, 3H), 7.24-7.18 (m, 9H), 6.84-6.83 (m, 1H), 6.70-6.67 (m, 1H), 6.27 (d, $J = 9.3$ Hz, 0.7H), 6.13 (d, $J = 9.9$ Hz, 0.3H), 5.7 (d, $J = 9.9$ Hz, 0.3H), 5.37 (d, $J = 9.3$ Hz, 0.7H), 2.96-2.90 (m, 4H), 1.30-1.25 (m, 24H), 1.21 (s, 15H). $^{13}\text{C NMR}$ (CDCl_3 , 100 MHz) δ (ppm) 181.0, 149.3, 149.1, 141.2, 141.2, 141.1, 140.1, 139.9, 139.8, 136.5, 130.4, 130.2, 129.9, 129.8, 129.5, 128.5, 128.0, 127.9, 127.7, 127.5, 127.0, 126.9, 126.8, 126.3, 126.1, 123.9, 123.4, 123.2, 123.1, 122.8, 90.4, 88.0, 87.2, 72.0, 34.4, 24.2, 9.2, 9.0. **MS** (ESI) found $[\text{M}+\text{H}]^+$ 1209.7. **CHN** $\text{C}_{73}\text{H}_{75}\text{ClIrNO}$ calculated C, 72.46; H, 6.25; N, 1.16; found C, 71.68; H, 6.24; N, 1.40.



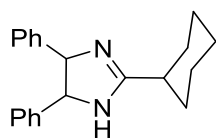
(4*R*,5*R*)-2,4,5-Triphenyl-4,5-dihydro-1*H*-imidazole¹⁸ In accordance with published data.

White solid. **¹H NMR** (CDCl₃, 400 MHz) δ (ppm) 7.93-7.90 (m, 2H), 7.50-7.24 (m, 13H) 4.86 (s, 2H). **¹³C NMR** (CDCl₃, 100 MHz) δ (ppm) 163.6, 143.9, 131.4, 130.5, 129.1, 126.0, 127.9, 127.8, 127.1, 75.3. **HRMS** (ESI) calculated [M+H]⁺ 299.1548; found [M+H]⁺ 299.1535.



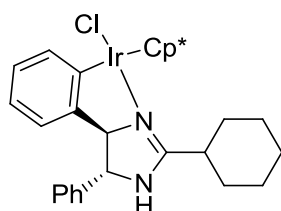
Ir 19¹⁸ In accordance with published data.

Yellow solid. **¹H NMR** (CDCl₃, 400 MHz) δ (ppm) 7.45-7.15 (m, 14H), 6.54 (dd, J = 8.0, 4.0Hz, 0.4H), 6.43 (dd, J = 8.0, 4.0 Hz, 0.6H), 5.65 (s, 0.6H), 5.31 (s, 0.4H), 5.04 (d, J = 4.0 Hz, 0.4H), 4.89 (d, J = 12 Hz, 0.6H), 4.72 (d, J = 12Hz, 0.6H), 4.60 (s, 0.4H), 3.80 (s, 3H), 1.37 (s, 15H). **¹³C NMR** (CDCl₃, 100 MHz) δ (ppm) 176.7, 176.0, 166.4, 162.1, 161.6, 143.8, 142.0, 140.1, 139.4, 128.9, 128.8, 128.7, 128.2, 127.5, 127.3, 127.2, 126.0, 120.6, 120.2, 87.7, 87.1, 79.3, 72.3, 72.0, 55.0, 31.5, 22.6, 14.1, 9.3, 9.1.



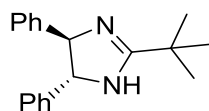
2-Cyclohexyl-4,5-diphenyl-4,5-dihydro-1H-imidazole⁵ In accordance with published data.

White solid. ¹H NMR (CDCl₃, 400 MHz) δ (ppm) 7.35-7.31 (m, 5H), 7.28-7.26 (m, 2H + CDCl₃), 7.23-7.21 (m, 3H), 4.69 (s, 2H), 2.49-2.42 (m, 1H), 2.09-2.04 (m, 1H), 1.86-1.83 (m, 2H), 1.74-1.68 (m, 2H), 1.60-1.52 (m, 2H), 1.40-1.25 (m, 3H). ¹³C NMR (CDCl₃, 100 MHz) δ (ppm) 170.3, 143.9, 138.8, 128.7, 127.4, 126.4, 38.8, 31.0, 26.0, 25.9. HRMS (ESI) calculated [M+H]⁺ 305.2018, found [M+H]⁺ 305.2024.



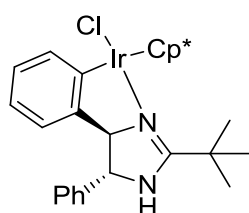
Ir 20⁵ In accordance with published data.

Orange solid. ¹H NMR (CDCl₃, 400 MHz) δ (ppm) 7.50 (m, 3H), 7.44 (t, J = 8.0 Hz, 2H), 7.36 (t, J = 8.0 Hz, 1H), 6.98 (td, J = 8.0, 2.0 Hz, 1H), 6.80 (m, 2H), 5.20 (s, br, 1H), 4.90 (m, 2H), 2.95 (tt, J = 12.0, 4.0 Hz, 1H), 2.38 (d, J = 16.0 Hz, 1H), 2.10-0.8 (m, 9H), 1.71 (s, 15H). ¹³C NMR (CDCl₃, 100 MHz) δ (ppm) 173.7, 156.2, 147.0, 142.0, 136.8, 129.2, 128.4, 127.5, 127.4, 122.4, 118.4, 86.8, 83.0, 67.7, 40.4, 32.7, 31.3, 26.2, 26.0, 25.9, 9.6.



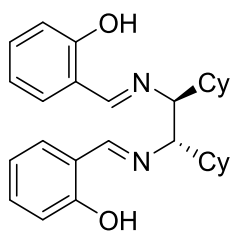
(4*R*,5*R*)-2-(*Tert*-butyl)-4,5-diphenyl-4,5-dihydro-1*H*-imidazole

White solid. $^1\text{H NMR}$ (CDCl_3 , 400 MHz) δ (ppm) 7.30-7.14 (m, 10H), 4.73 (s, 2H), 1.29 (s, 9H). $^{13}\text{C NMR}$ (CDCl_3 , 100 MHz) δ (ppm) 129.3, 129.2, 129.2, 127.4, 126.7, 85.7, 28.8, 9.8.



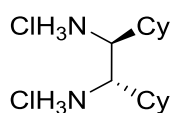
Ir 21

Orange solid. $^1\text{H NMR}$ (CDCl_3 , 400 MHz) δ (ppm) 7.25-7.14 (m, 9H), 5.0 (d, $J = 7.0$ Hz, 1H), 4.51 (d, $J = 7.0$ Hz, 1H), 1.33 (s, 6H), 1.30-1.29 (m, 18H). $^{13}\text{C NMR}$ (CDCl_3 , 100 MHz) δ (ppm) 129.6, 129.3, 129.2, 129.1, 128.7, 128.6, 128.4, 128.1, 128.0, 127.8, 127.6, 127.4, 126.7, 87.55, 85.7, 42.4, 28.8, 9.9, 9.8.



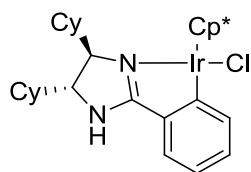
2,2'-((1E,1'E)-(((1S,2S)-1,2-Dicyclohexylethane-1,2-diyl)bis(azanylylidene))bis(methanylylidene))diphenol²⁴

White solid. ¹H NMR (CDCl₃, 400 MHz) δ (ppm) 8.24 (s, 2H), 7.31-7.2 (m, 4 + CD₃), 7.08-7.00 (m, 2H), 6.85-6.81 (m, 4H), 3.54 (m, 2H), 1.83-1.6 (m, 12H), 1.33-1.03 (m, 10H).



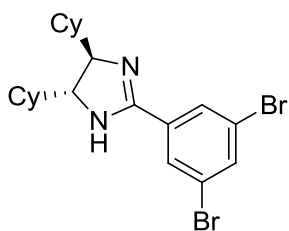
(1S,2S)-1,2-Bis(chloro-l5-azanyl)-1,2-dicyclohexylethane²⁴

White solid. ¹H NMR (CDCl₃, 400 MHz) δ (ppm) 3.43 (s, 2H), 1.88-1.61 (m, 12H), 1.41-0.89 (m, 10H).

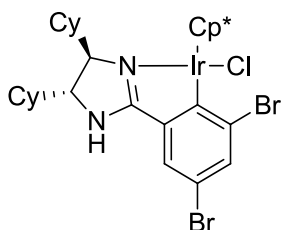


Ir 22

Yellow solid. ¹H NMR (CDCl₃, 400 MHz) δ (ppm) 7.76 (d, J = 8.0 Hz, 1H), 7.15 (d, J = 8.0 Hz, 2H), 6.94 (m, 1H), 3.76 (bs, 1H), 3.70 (m, 1H), 1.73 (s, 15H), 1.59 (bs, 6H), 1.34-1.04 (m, 14H), 0.88 (bs, 2H). ¹³C NMR (CDCl₃, 100 MHz) δ (ppm) 173.9, 136.1, 131.3, 124.0, 121.2, 87.0, 72.3, 62.4, 30.7, 29.7, 28.7, 27.0, 26.5, 26.1, 25.9, 25.5, 9.4. HRMS (ESI, EtOAc) [M]⁺ 673.2856.

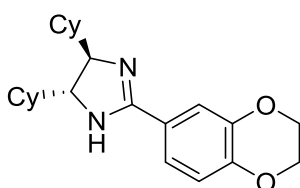


Yellow solid. $^1\text{H NMR}$ (CDCl_3 , 400 MHz) δ (ppm) 7.86 (d, J = 1.8 Hz, 2H), 7.71 (t, J = 1.8 Hz, 1H), 4.80 (bs, 1H), 3.70 (s, 1H), 3.40 (s, 1H), 0.9-1.80 (m, 22H).



Ir 23

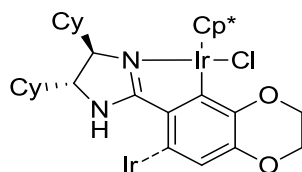
Yellow solid. $^1\text{H NMR}$ (CDCl_3 , 400 MHz) δ (ppm) 6.63 (d, J = 8.7 Hz, 1H), 6.35 (d, J = 8.7 Hz, 1H), 6.30 (s, 1H), 3.63 (m, 1H), 3.56 (m, 1H), 0.6-1.8 (m, 37H). $^{13}\text{C NMR}$ (CDCl_3 , 100 MHz) δ (ppm) 173.7, 157.9, 156.9, 153.2, 123.9, 116.0, 104.9, 87.7, 71.0, 55.8, 43.6, 40.1, 30.2, 29.3, 29.1, 27.1, 26.9, 26.8, 26.5, 26.4, 10.0.



(4*R*,5*R*)-4,5-Dicyclohexyl-2-(2,3-dihydrobenzo[*b*][1,4]dioxin-6-yl)-4,5-dihydro-1*H*-imidazole

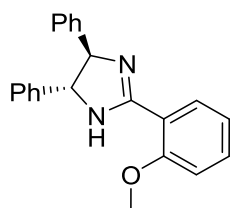
Yellow solid. $^1\text{H NMR}$ (CDCl_3 , 400 MHz) δ (ppm) 7.29-7.32 (dd+s, 2H), 6.85 (d, J = 8.7 Hz, 1H), 4.26 (m, 4H), 3.52 (d, J = 3.8 Hz, 2H), 1.80-1.60 (m, 10H), 1.40-0.92 (m,

12H). **¹³C NMR** (CDCl₃, 100 MHz) δ (ppm) 161.5, 146.1, 143.7, 124.2, 121.2, 117.6, 116.9, 64.6, 60.8, 43.8, 29.1, 29.0, 27.0, 26.7, 26.0. **MS** (CI) [M+H]⁺ 369.0.



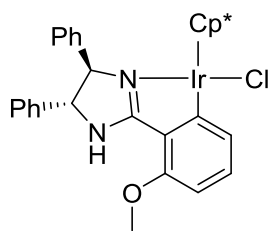
Ir 25

Yellow solid. **¹H NMR** (CDCl₃, 400 MHz) δ (ppm) 7.19 (s, 0.3H), 6.78 (d, J = 8.4 Hz, 0.7H), 6.74 (s, 0.3H), 6.54 (d, J = 8.4 Hz, 0.7H), 5.12 (bs, 0.7H), 5.02 (bs, 0.3H), 4.33-4.22 (m, 4H), 3.81-3.79 (m, 0.7H), 3.76-3.74 (m, 0.3H), 3.68-3.63 (m, 1H), 1.99-1.84 (m, 6H), 1.76 (s, 8H), 1.74 (s, 7H), 1.65-1.59 (m, 8H), 1.35-1.21 (m, 8H). **HRMS** (ESI) found [M+H]⁺ 730.2875.



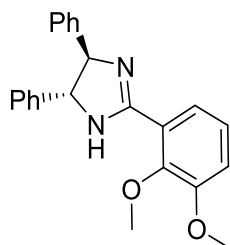
(4*R*,5*R*)-2-(2-Methoxyphenyl)-4,5-diphenyl-4,5-dihydro-1*H*-imidazole

Yellow oil. **¹H NMR** (CDCl₃, 400 MHz) δ (ppm) 8.33 (dd, J = 7.8, 1.7 Hz, 1H), 7.46 (dt, J = 7.8, 1.7 Hz, 1H), 7.37-7.25 (m, 11H, CHCl₃ included), 7.08 (t, J = 7.6 Hz, 1H), 7.01 (d, J = 8.4 Hz, 1H), 6.39 (bs, 1H), 4.89 (s, 2H), 3.91 (s, 3H). **¹³C NMR** (CDCl₃, 100 MHz) δ (ppm) 162.3, 157.8, 143.7, 132.4, 131.8, 128.7, 127.5, 126.7, 121.4, 118.0, 111.5, 74.3, 55.9. **MS** (CI) found [M+H]⁺ 329.17.



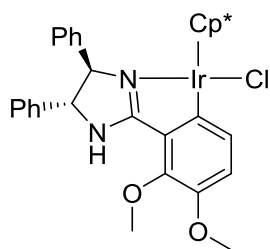
Ir 26

Yellow solid. ^1H NMR (CDCl_3 , 400 MHz) δ (ppm) 7.58-7.18 (m, 13H), 6.76 (s, 0.5H), 6.72 (s, 0.2H), 6.53-6.5 (m, 0.9H), 5.01 (d, $J = 6.2$ Hz, 0.3H), 4.96 (s, 0.18H), 4.93 (s, 0.41H), 4.86 (s, 0.17H), 4.73 (d, $J = 6.2$ Hz, 0.3H), 3.82 (s, 3H), 1.16 (s, 10H), 1.14 (s, 5H). ^{13}C NMR (CDCl_3 , 100 MHz) δ (ppm) 176.9, 175.8, 168.2, 167.0, 157.7, 144.0, 142.4, 140.5, 139.7, 133.3, 132.3, 129.2, 128.9, 128.9, 128.8, 128.8, 128.3, 128.2, 128.1, 128.0, 127.5, 127.4, 123.5, 122.5, 103.8, 103.7, 87.8, 87.2, 78.7, 78.2, 72.5, 72.3, 55.0, 55.0, 9.4, 9.2. HRMS (ESI) found $[\text{M}+\text{H}]^+$ 690.1995. CHN $\text{C}_{32}\text{H}_{34}\text{ClIrN}_2\text{O}$ calculated C, 55.35; H, 4.96; N, 4.06; found C, 53.86; H 4.85; N, 3.35.



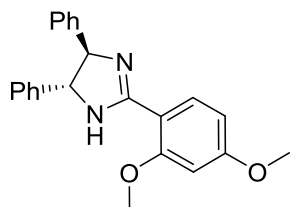
(4*R*,5*R*)-2-(2,3-Dimethoxyphenyl)-4,5-diphenyl-4,5-dihydro-1*H*-imidazole

Yellow oil. ^1H NMR (CDCl_3 , 400 MHz) δ (ppm) 7.85 (dd, $J = 8.1, 1.5$ Hz, 1H), 7.37-7.28 (m, 10H), 7.15 (t, $J = 7.5$ Hz, 1H), 7.05 (dd, $J = 8.1, 1.5$ Hz, 1H), 4.89 (s, 2H), 3.92 (s, 3H), 3.91 (s, 3H). ^{13}C NMR (CDCl_3 , 100 MHz) δ (ppm) 161.9, 152.9, 148.1, 143.9, 128.7, 126.6, 124.5, 123.6, 122.7, 114.7, 61.6, 56.0. HRMS (ESI) calculated $[\text{M}+\text{H}]^+$ 359.1760; found $[\text{M}+\text{H}]^+$ 359.1750.



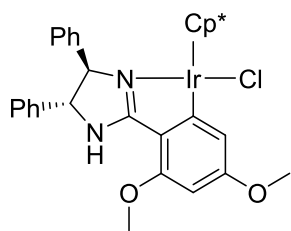
Ir 27

Yellow solid. $^1\text{H NMR}$ (CDCl_3 , 400 MHz) δ (ppm) 7.52 (d, $J = 6.8$ Hz, 1H), 7.43-7.3 (m, 9H), 7.00 (d, $J = 8.1$ Hz, 1H), 6.78 (s, 1H), 4.99 (d, $J = 6.1$ Hz, 0.36H) 4.96-4.88 (m, 1.33H), 4.74 (d, $J = 6.1$ Hz, 0.35H), 3.98 (s, 2H), 3.96 (s, 1H), 3.86 (s, 1H), 3.85 (s, 2H), 1.45 (s, 10H), 1.43 (s, 5H). $^{13}\text{C NMR}$ (CDCl_3 , 100 MHz) δ (ppm) 176.8, 175.9, 155.9, 147.7, 146.9, 140.5, 139.6, 130.7, 130.3, 128.9, 128.8, 128.4, 128.2, 128.1, 127.6, 127.3, 126.9, 119.1, 118.2, 87.5, 87.0, 78.8, 78.3, 72.2, 71.9, 61.2, 56.6, 53.5, 9.4, 9.2. **HRMS** (ESI) found $[\text{M}+\text{H}]^+$ 721.2127. **CHN** $\text{C}_{33}\text{H}_{36}\text{ClIrN}_2\text{O}_2$ calculated C, 55.03; H, 5.04; N, 3.89; found C, 52.33; H, 4.86; N, 2.92.



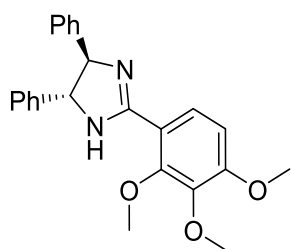
(4*R*,5*R*)-2-(2,4-Dimethoxyphenyl)-4,5-diphenyl-4,5-dihydro-1*H*-imidazole

Yellow solid. $^1\text{H NMR}$ (CDCl_3 , 400 MHz) δ (ppm) 8.29 (d, $J = 8.7$ Hz, 1H), 7.35-7.26 (m, 12H, CHCl_3 included), 6.59 (dd, $J = 8.7, 2.2$ Hz, 1H), 6.52 (d, $J = 2.2$ Hz, 1H), 3.87 (s, 3H), 3.84 (s, 3H). $^{13}\text{C NMR}$ (CDCl_3 , 100 MHz) δ (ppm) 163.0, 162.0, 159.1, 144.1, 133.0, 128.6, 127.3, 126.7, 111.4, 105.5, 98.8, 55.8, 55.6. **HRMS** (ESI) calculated $[\text{M}+\text{H}]^+$ 359.1760; found $[\text{M}+\text{H}]^+$ 359.1751.



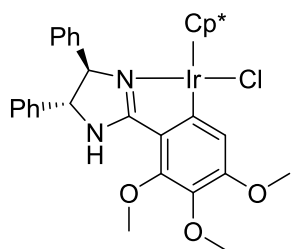
Ir 28

Yellow solid. $^1\text{H NMR}$ (CDCl_3 , 400 MHz) δ (ppm) 7.51 (d, $J = 6.9$ Hz, 1H), 7.44-7.3 (m, 9H), 7.03-6.98 (m, 1H), 6.61 (s, 1H), 6.12-6.08 (m, 1H), 4.98 (d, $J = 6.0$ Hz, 0.37H), 4.93-4.82 (m, 1.37H), 4.7 (d, $J = 6.0$ Hz, 0.37H), 3.92 (s, 3H), 3.80 (s, 3H), 1.46 (s, 10H), 1.44 (s, 5H). $^{13}\text{C NMR}$ (CDCl_3 , 100 MHz) δ (ppm) 176.3, 175.4, 169.7, 168.5, 163.6, 163.0, 159.0, 158.9, 144.3, 142.5, 140.5, 139.9, 128.8, 128.7, 128.3, 128.2, 128.0, 127.9, 127.5, 127.4, 116.7, 115.8, 112.7, 112.4, 92.7, 92.5, 87.7, 87.1, 86.3, 78.4, 77.9, 77.3, 72.4, 72.3, 55.2, 55.1, 55.0, 9.9, 9.5, 9.2. **MS** (ESI) found $[\text{M}+\text{H}]^+$ 721.2. **CHN** $\text{C}_{33}\text{H}_{36}\text{ClIrN}_2\text{O}_2$ calculated C, 55.03; H, 5.04; N, 3.89; found C, 53.65; H, 5.96; N, 3.16.



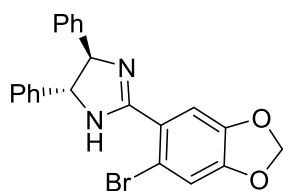
(4*R*,5*R*)-4,5-Diphenyl-2-(2,3,4-trimethoxyphenyl)-4,5-dihydro-1*H*-imidazole

Yellow solid. $^1\text{H NMR}$ (CDCl_3 , 400 MHz) δ (ppm) 8.04 (d, $J = 8.9$ Hz, 1H), 7.36-7.25 (m, 11H CHCl_3 included), 6.78 (d, $J = 8.9$ Hz, 1H), 4.86 (s, 2H), 3.97 (s, 3H), 3.91 (s, 3H), 3.89 (s, 3H). $^{13}\text{C NMR}$ (CDCl_3 , 100 MHz) δ (ppm) 161.6, 155.9, 152.9, 144.0, 142.0, 128.7, 127.4, 126.6, 126.1, 116.1, 107.9, 61.8, 61.0, 56.2. **HRMS** (ESI) calculated $[\text{M}+\text{H}]^+$ 389.1865; found $[\text{M}+\text{H}]^+$ 389.1868.



Ir 29

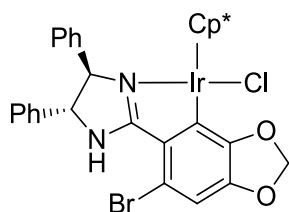
Yellow solid. ^1H NMR (CDCl_3 , 400 MHz) δ (ppm) 7.51 (d, $J = 6.9\text{ Hz}$, 1H), 7.41-7.28 (m, 9H), 7.1 (m, 1H), 6.61 (s, 1H), 4.97 (d, $J = 6.0\text{ Hz}$, 0.35H), 4.92-4.84 (m, 1.3H), 4.71 (d, $J = 6.0\text{ Hz}$, 0.35H), 4.04 (s, 2H), 4.01 (s, 1H), 4.00 (s, 2H), 3.99 (s, 1H), 3.83 (s, 1H), 3.79 (s, 2H), 1.46 (s, 10H), 1.44 (s, 5H). ^{13}C NMR (CDCl_3 , 100 MHz) δ (ppm) 176.7, 175.7, 161.4, 160.2, 156.7, 156.2, 151.5, 151.4, 144.1, 142.4, 140.4, 139.7, 136.0, 135.8, 128.9, 128.7, 128.3, 128.2, 128.1, 128.0, 127.5, 127.3, 120.1, 118.9, 113.9, 113.4, 87.6, 87.1, 78.5, 78.0, 72.3, 72.1, 61.2, 61.1, 60.4, 55.8, 9.5, 9.2. HRMS (ESI) found $[\text{M}+\text{H}]^+$ 750.2206. CHN calculated C 54.42, H 5.10, N 3.73, found 53.92, H 5.34, N 3.33.



(4*R*,5*R*)-2-(6-Bromobenzo[*d*][1,3]dioxol-5-yl)-4,5-diphenyl-4,5-dihydro-1*H*-imidazole

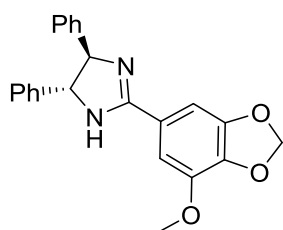
Yellow solid. ^1H NMR (CDCl_3 , 400 MHz) δ (ppm) 7.35-7.26 (m, 11H plus CHCl_3), 7.01 (s, 1H), 5.99 (s, 1H), 4.82 (s, 2H). ^{13}C NMR (CDCl_3 , 100 MHz) δ (ppm) 162.8, 149.8, 147.4, 143.3, 128.7, 127.5, 126.8, 125.7, 113.3, 111.1, 102.3, 75.3. HRMS (ESI) calculated $[\text{M}+\text{H}]^+$ 421.0552 and 423.0531; found $[\text{M}+\text{H}]^+$ 421.0546 and 423.0529.

CHN C₂₂H₁₇ClIrN₂O₂ calculated C, 62.72; H, 4.07; N, 6.65; found C, 63.17; H, 4.06; N, 6.71.



Ir 30

Yellow solid. ¹H NMR (CDCl₃, 400 MHz) δ (ppm) 7.47-7.40 (m, 5H), 7.34-7.30 (m, 5H), 6.78 (s, 0.35H), 6.76 (s, 0.65H), 6.13 (s, 0.65H), 6.01 (s, 0.75H), 5.98 (s, 0.56H), 5.01 (d, J = 5.6 Hz, 0.3H), 4.93-4.86 (m, 1.3H), 4.70 (d, J = 5.6 Hz, 0.3H), 1.51 (s, 10H), 1.47 (s, 5H). ¹³C NMR (CDCl₃, 100 MHz) δ (ppm) 175.8, 175.0, 151.3, 150.9, 148.7, 148.1, 144.1, 143.7, 141.8, 140.4, 139.4, 129.0, 128.9, 128.5, 128.4, 128.4, 128.2, 128.1, 128.0, 127.6, 127.3, 127.2, 126.6, 113.7, 113.4, 108.8, 108.7, 100.2, 99.9, 88.9, 88.3, 79.1, 78.2, 72.1, 71.2, 9.8, 9.5. **HRMS** (ESI) found [M+H]⁺ 782.0875. **CHN** C₃₂H₃₁ClIrN₂O₂ calculated C, 49.07; H, 3.99; N, 3.58; found C, 48.58; H, 4.10; N, 3.54.

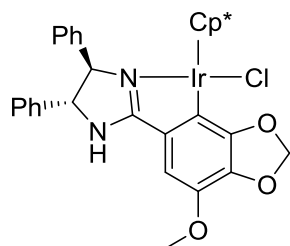


(4*R*,5*R*)-2-(7-Methoxybenzo[*d*][1,3]dioxol-5-yl)-4,5-diphenyl-4,5-dihydro-1*H*-imidazole

Yellow solid. ¹H NMR (CDCl₃, 400 MHz) δ (ppm) 7.35-7.27 (m, 11H), 7.06 (s, 1H), 6.04 (s, 2H), 4.88 (s, 2H), 3.95 (s, 3H). ¹³C NMR (CDCl₃, 100 MHz) δ (ppm) 171.1,

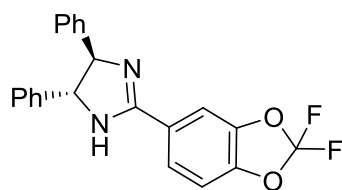
162.9, 148.9, 143.7, 143.2, 137.9, 128.8, 127.6, 126.6, 107.8, 102.1, 101.7, 56.9. **MS**

(ESI) calculated 372.15; found $[M+H]^+$ 373.2.



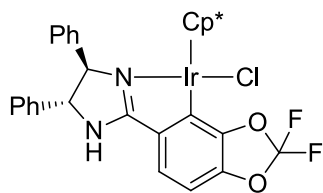
Ir 31

Yellow solid. **¹H NMR** (CDCl₃, 400 MHz) δ (ppm) 7.44 (d, J = 6.4 Hz, 1H), 7.36-7.18 (m, 9H), 6.83 (s, 1H), 6.06 (bs, 1H), 5.97 (bs, 1H), 5.08 (bs, 0.3H), 4.93 (d, J = 10.8 Hz, 0.7H), 4.73 (d, J = 10.8 Hz, 0.7H), 4.62 (bs, 0.3H), 3.78 (s, 3H), 1.46 (bs, 15H). **¹³C NMR** (CDCl₃, 100 MHz) δ (ppm) 177.4, 171.2, 151.5, 140.5, 140.0, 139.8, 137.3, 131.2, 129.0, 128.9, 128.7, 128.4, 128.2, 128.1, 127.4, 106.9, 100.0, 88.2, 87.5, 79.6, 71.6, 56.5, 9.9, 9.6, 9.4. **HRMS** (ESI) found $[M+H]^+$ 734.1880. **CHN** C₃₃H₃₄ClIrN₂O₃ calculated C, 53.98; H, 4.67; N, 3.81; found C, 53.08; H, 4.66; N, 3.42.



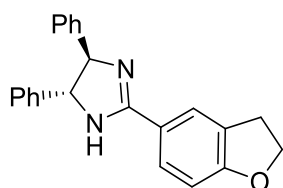
(4*R*,5*R*)-2-(2,2-difluorobenzo[*d*][1,3]dioxol-5-yl)-4,5-diphenyl-4,5-dihydro-1*H*-imidazole

Yellow solid. **¹H NMR** (CDCl₃, 400 MHz) δ (ppm) 7.92 (d, J = 7.4 Hz, 2H), 7.53-7.42 (m, 2H), 7.36-7.26 (m, 9H), 4.89 (s, 2H). **¹³C NMR** (CDCl₃, 100 MHz) δ (ppm) 171.1, 163.4, 143.1, 131.3, 129.5, 128.7, 128.6, 127.6, 127.6, 126.6, 74.7.



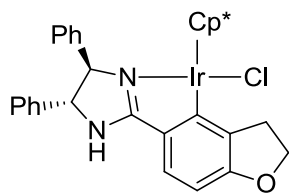
Ir 32

Brown solid. $^1\text{H NMR}$ (CDCl_3 , 400 MHz) δ (ppm) 7.83 (dd, $J = 7.4$ Hz, 1H), 7.51 (d, $J = 6.7$ Hz, 1H), 7.45 (d, $J = 6.7$ Hz, 1H), 7.38-7.23 (m, 8H), 8.0 (td, $J = 7.4$ Hz, 1H), 5.13 (d, $J = 5.5$ Hz, 0.35H), 4.99 (d, $J = 11.3$ Hz, 0.64H), 4.84 (d, $J = 11.3$ Hz, 0.63H), 4.71 (d, $J = 5.5$ Hz, 0.37H), 1.45 (s, 9H), 1.44 (s, 6H). $^{13}\text{C NMR}$ (CDCl_3 , 100 MHz) δ (ppm) 177.4, 176.6, 165.2, 143.6, 141.9, 140.1, 139.3, 136.1, 135.8, 134.1, 132.3, 131.4, 129.0, 128.8, 128.5, 128.4, 128.1, 127.7, 127.4, 127.3, 124.8, 124.7, 121.6, 121.5, 87.3, 82.9, 79.5, 72.3, 72.0, 9.5, 9.4, 9.2.



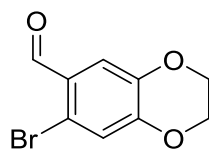
(4*R*,5*R*)-2-(2,3-dihydrobenzofuran-5-yl)-4,5-diphenyl-4,5-dihydro-1*H*-imidazole

Yellow solid. $^1\text{H NMR}$ (CDCl_3 , 400 MHz) δ (ppm) 7.86 (s, 1H), 7.63 (d, $J = 8.3$ Hz, 1H), 7.35-7.25 (m, 10H), 6.78 (d, $J = 8.3$ Hz, 1H), 4.84 (s, 2H), 4.63 (t, $J = 8.7$ Hz, 2H), 3.21 (t, $J = 8.7$ Hz, 2H). $^{13}\text{C NMR}$ (CDCl_3 , 100 MHz) δ (ppm) 171.1, 163.2, 162.7, 143.5, 128.8, 128.7, 128.1, 128.0, 127.8, 127.5, 126.7, 126.6, 124.8, 122.1, 109.1, 74.8, 71.9. **HRMS** (CI) calculated $[\text{M}+\text{H}]^+$ 341.1648. found $[\text{M}+\text{H}]^+$ 341.1651.



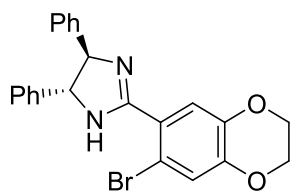
Ir 33

Orange solid. $^1\text{H NMR}$ (CDCl_3 , 400 MHz) δ (ppm) 7.5 (d, J = 6.9 Hz, 1H), 7.45-7.16 (m, 11H), 5.77 (bs, 0.5H), 5.43 (s, 0.25H), 5.10 (d, J = 5.1 Hz, 0.37H), 4.94 (d, J = 10 Hz, 0.7H), 4.75-4.68 (m, 0.7H), 4.64 (d, J = 5.1 Hz, 0.35H), 4.60-4.49 (m, 2H), 3.19-3.04 (m, 2H), 1.43 (s, 13H), 1.41 (s, 2H). $^{13}\text{C NMR}$ (CDCl_3 , 100 MHz) δ (ppm) 176.7, 176.0, 166.9, 163.6, 163.2, 143.9, 142.2, 140.4, 139.8, 128.9, 128.8, 128.7, 128.4, 128.3, 128.2, 128.1, 128.0, 127.5, 127.4, 127.3, 126.5, 121.9, 121.0, 120.8, 116.4, 116.0, 88.8, 88.1, 87.7, 87.3, 87.1, 79.3, 72.2, 71.9, 71.4, 21.1, 10.1, 9.6, 9.5, 9.4, 9.2.



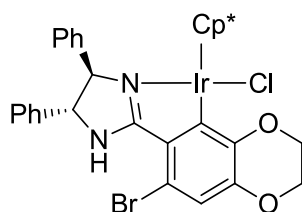
7-bromo-2,3-dihydrobenzo[*b*][1,4]dioxine-6-carbaldehyde

White solid. $^1\text{H NMR}$ (CDCl_3 , 400 MHz) δ (ppm) 10.16 (s, 1H), 7.46 (s, 1H), 7.13 (s, 1H), 4.34-4.26 (m, 4H). $^{13}\text{C NMR}$ (CDCl_3 , 100 MHz) δ (ppm) 190.6, 149.5, 143.4, 127.3, 121.8, 118.7, 118.2, 64.8, 64.0. **HRMS** (CI) found $[\text{M}+\text{H}]^+$ 242.9655.



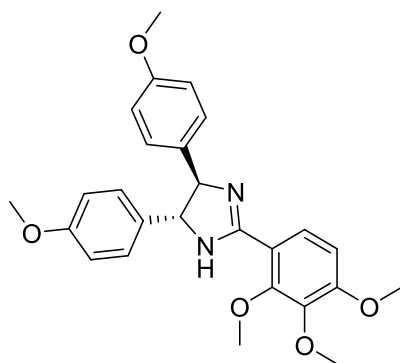
(4*R*,5*R*)-2-(7-bromo-2,3-dihydrobenzo[*b*][1,4]dioxin-6-yl)-4,5-diphenyl-4,5-dihydro-1*H*-imidazole

White solid. $^1\text{H NMR}$ (CDCl_3 , 400 MHz) δ (ppm) 7.46 (s, 1H), 7.36-7.32 (m, 10H), 7.14 (s, 1H), 4.88 (s, 2H), 4.41-4.39 (m, 1H), 4.29-4.26 (m, 3H). **HRMS** (ESI) found $[\text{M}+\text{H}]^+$ 435.0702.



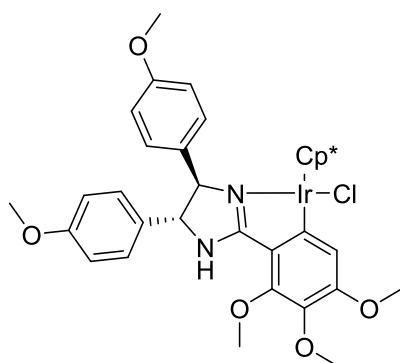
Ir 34

Yellow solid. $^1\text{H NMR}$ (CDCl_3 , 400 MHz) δ (ppm) 7.45-7.38 (m, 5H), 7.34-7.29 (m, 5H), 7.08 (s, 0.4H), 6.81 (s, 0.6H), 5.03-5.00 (m, 0.3H), 4.94-4.86 (m, 1.3H), 4.69-4.66 (m, 0.3H), 4.37-4.21 (m, 4H), 1.47 (s, 10H), 1.43 (s, 5H). $^{13}\text{C NMR}$ (CDCl_3 , 100 MHz) δ (ppm) 176.1, 158.8, 146.1, 144.9, 141.9, 140.7, 139.5, 129.1, 129.0, 128.9, 128.5, 128.4, 128.3, 128.1, 128.0, 127.5, 127.1, 127.0, 124.7, 117.1, 111.8, 88.9, 88.7, 88.2, 87.9, 87.4, 82.9, 78.8, 78.0, 72.1, 71.0, 70.8, 64.5, 64.4, 63.8, 63.7, 53.5, 9.9, 9.5. **HRMS** (ESI) found $[\text{M}+\text{H}]^+$ 809.1536.



(4*R*,5*R*)-4,5-bis(4-methoxyphenyl)-2-(2,3,4-trimethoxyphenyl)-4,5-dihydro-1*H*-imidazole

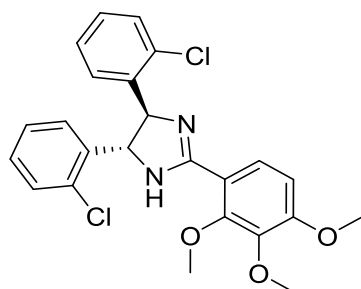
Yellow solid. ^1H NMR (CDCl_3 , 400 MHz) δ (ppm) 8.02 (d, J = 8.9 Hz, 1H), 7.89 (d, J = 8.9 Hz, 1H), 7.22 (d, J = 8.6 Hz, 4H), 6.87 (d, J = 8.6 Hz, 4H), 4.77 (s, 2H), 3.96 (s, 3H), 3.92 (s, 3H), 3.89 (s, 3H), 3.85 (s, 6H). ^{13}C NMR (CDCl_3 , 100 MHz) δ (ppm) 161.4, 159.0, 156.0, 152.9, 142.0, 136.0, 127.7, 126.1, 114.1, 114.0, 107.9, 61.9, 61.0, 56.1, 55.3.



Ir 35

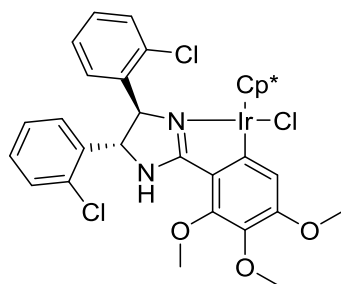
Yellow solid. ^1H NMR (CDCl_3 , 400 MHz) δ (ppm) 7.44-7.34 (m, 2H), 7.13-7.02 (m, 2H), 6.93- 6.82 (m, 3H), 6.59-6.38 (m, 2H), 5.64-5.51 (m, 0.35H), 5.13-5.04 (m, 0.25H), 4.90 (d, J = 10.5 Hz, 0.3H), 4.83-4.74 (m, 0.5H), 4.62-4.53 (m, 0.2H), 4.02-4.0 (m, 3H), 3.89-3.79 (m, 9H), 3.65-3.46 (m, 2H), 3.27-3.15 (m, 1H), 1.46 (s, 13H), 1.40

(s, 2H). **¹³C NMR** (CDCl₃, 100 MHz) δ (ppm) 176.4, 159.0, 156.7, 151.5, 135.8, 132.4, 132.0, 130.0, 128.6, 128.4, 114.1, 113.9, 113.3, 88.2, 87.6, 87.2, 88.0, 78.0, 71.7, 61.1, 60.7, 55.8, 55.4, 55.3, 55.0, 53.5, 9.5, 9.3, 9.3. **HRMS** (ESI) found [M+H]⁺ 810.2417.



(4*R*,5*R*)-4,5-bis(2-chlorophenyl)-2-(2,3,4-trimethoxyphenyl)-4,5-dihydro-1*H*-imidazole

Yellow solid. **¹H NMR** (CDCl₃, 400 MHz) δ (ppm) 8.04 (d, *J* = 9.0 Hz, 1H), 7.55 (d, *J* = 6.5 Hz, 2H), 7.35 (d, *J* = 7.9 Hz, 2H), 7.3-7.26 (m, 2.5H, CHCl₃ included), 7.23-7.19 (m, 2H), 6.80 (d, *J* = 8.9 Hz, 1H), 5.42 (bs, 2H), 3.93 (s, 3H), 3.91 (s, 3H), 3.89 (s, 3H). **¹³C NMR** (CDCl₃, 100 MHz) δ (ppm) 162.2, 156.1, 152.9, 142.1, 141.1, 133.0, 129.5, 128.5, 127.3, 126.0, 115.8, 107.9, 61.8, 61.0, 56.2. **HRMS** (CI) calculated [M+H]⁺ 457.1080. found [M+H]⁺ 457.1095.



Ir 36

Yellow solid. $^1\text{H NMR}$ (CDCl_3 , 400 MHz) δ (ppm) 7.69 (d, $J = 7.8$ Hz, 1H), 7.42-7.29 (m, 5H), 7.24-7.17 (m, 2H), 7.11 (s, 0.4H), 7.07 (s, 0.6H), 6.52 (s, 1H), 5.62 (d, $J = 10.7$ Hz, 0.65H), 5.52 (d, $J = 4.5$ Hz, 0.35H), 5.43 (d, $J = 10.7$ Hz, 0.63H), 5.27 (d, $J = 4.5$ Hz, 0.37H), 4.02 (s, 2H), 4.01 (m, 3H), 3.99 (s, 1H), 3.82 (s, 1H), 3.79 (s, 2H), 1.49 (s, 9H), 1.48 (s, 6H). $^{13}\text{C NMR}$ (CDCl_3 , 100 MHz) δ (ppm) 177.0, 176.2, 161.6, 133.0, 132.7, 130.1, 129.9, 129.3, 129.0, 128.9, 128.7, 128.3, 128.3, 127.4, 127.2, 113.9, 113.4, 87.8, 87.1, 73.2, 67.8, 61.2, 60.8, 55.8, 53.4, 9.3, 9.1. **HRMS** (ESI) found $[\text{M}+\text{H}]^+$ 818.1422.

2.6 References

- 1 Y.-F. Han and G.-X. Jin, *Chem. Soc. Rev.*, 2014, **43**, 2799.
- 2 Y. Boutadla, D. L. Davies, R. C. Jones and K. Singh, *Chemistry (Weinheim an der Bergstrasse, Germany)*, 2011, **17**, 3438–48.
- 3 C. Wang, A. Pettman, J. Basca and J. Xiao, *Angew. Chemie Intd Ed*, 2010, **49**, 7548–52.
- 4 C. Wang, H.-Y. T. Chen, J. Bacsa, C. R. a. Catlow and J. Xiao, *Dalton Trans*, 2012, 935–940.
- 5 J. H. Barnard, C. Wang, N. G. Berry and J. Xiao, *Chem. Sci*, 2013, **4**, 1234.
- 6 Q. Lei, Y. Wei, D. Talwar, C. Wang, D. Xue and J. Xiao, *Chem. Euro. J.* 2013, **19**, 4021–4029.
- 7 Y. Wei, D. Xue, Q. Lei, C. Wang and J. Xiao, *Green Chem*, 2013, **15**, 629–634.
- 8 J. Wu, J. H. Barnard, Y. Zhang, D. Talwar, C. M. Robertson and J. Xiao, *Chem. Comm*, 2013, **49**, 7052–4.
- 9 J. Wu, D. Talwar, S. Johnston, M. Yan and J. Xiao, *Angew. Chemie Intd. Ed.* 2013, **52**, 6983–6987.
- 10 D. Talwar, N. P. Salguero, C. M. Robertson and J. Xiao, *Chem. Euro J.* 2014, **20**, 245–252.
- 11 D. Talwar, A. Gonzalez-de-Castro, H. Y. Li and J. Xiao, *Angew Chemie Intd Ed.* 2015, **54**, 5223–5227.
- 12 D. Talwar, H. Y. Li, E. Durham and J. Xiao, *Chem. Eur J.* 2015, **21**, 5370–5379.
- 13 Q. Zou, C. Wang, J. Smith, D. Xue and J. Xiao, *Chem. Eur J.* 2015, **21**, 9656–9661.

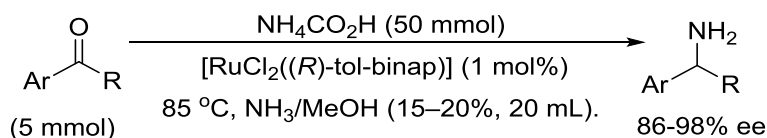
- 14 E. Kirsten and F. Glorius, *Synthesis*, 2006, 2996–3002.
- 15 A. J. Wilkinson, H. Puschmann, J. K. Howard, C. E. Foster and J. G. Williams, *InorgChem*. 2006, **45**, 8685–99.
- 16 WO 2008/137102 A2, 2008.
- 17 H. C. Aspinall, O. Beckingham, M. D. Farrar, N. Greeves and C. D. Thomas, *Tet. Lett*, 2011, **52**, 5120–5123.
- 18 C. Wang, Transfer Hydrogenation of Imino Bonds, University of Liverpool, 2011, PhD.
- 19 B. Villa-Marcos, Chiral Amines *via* Asymmetric Reduction of Imino Bonds, University of Liverpool, 2011, PhD
- 20 R. Martin and S. L. Buchwald, *Acc. Chem. Res.*, 2008, **41**, 1461–1473.
- 21 C. F. Du, H. Hart and K. D. Ng, *J. Org Chem*. 1986, **51**, 3162–3165.
- 22 A. Saednya and H. Hart, *Synthesis*, 1996, 1455–1458.
- 23 U. I. Zakai, A. Bzoch-mechkour, N. E. Jacobsen, L. Abrell, G. Lin, G. S. Nichol, T. Bally and R. S. Glass, *J. Org. Chem*. 2010, **75**, 8363–8371.
24. H. Kim, M. Staikova, A. Lough, and J. Chin, *Org. Lett.*, 2009, **11**, 157–160.

Chapter 3: Development of a Direct Asymmetric Reductive Amination System.

3.1 Introduction

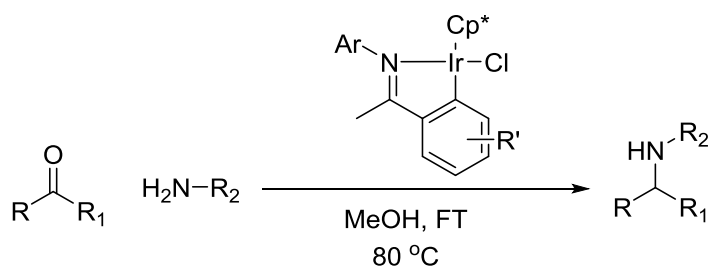
Direct asymmetric reductive amination (DARA) is a highly appealing method for the synthesis of chiral amines but has long been a challenge. Whilst many racemic methods have been developed,^{1–9} the challenge of a chiral system has still remained. This is due in part to the difficulty in developing a selective catalyst for imine over carbonyl reduction, as well as the challenge of forming the imine in conditions suitable for the reduction.

There have been several systems that have overcome these challenges and produced high selectivity. Most of these systems require high pressures of hydrogen gas,^{10,11} have a limited substrate scope^{12–14} or require the use of an additional chiral phosphoric acid.^{15,16} This highlighted the need for a new simple and universal system, preferably under TH conditions. There has been only one successful system developed utilising ATH conditions.¹⁷ Although successful in terms of ee and yield, this system still requires high temperatures and a large excess of ammonium formate in an ammonia-methanol solution (Scheme 3.1).



Scheme 3.11 Best reported example of DARA under ATH conditions.

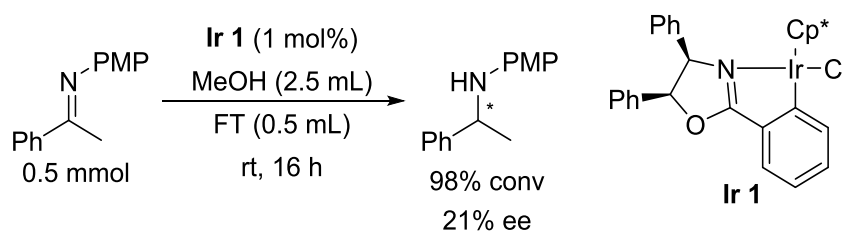
The aim of this work was to build a chiral system for DARA based on the racemic version previously developed by Xiao *et al*,^{7–9} shown in Scheme 3.2, which has a large substrate scope and is active under TH conditions. This system uses high temperatures, but complete conversion can be achieved in very short times, which is promising for developing a mild chiral system.



Scheme 3.12 Racemic conditions reported for reductive amination.

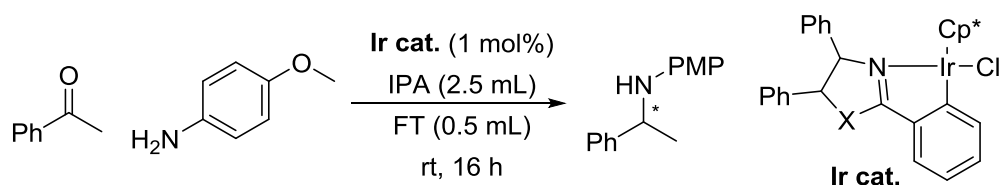
3.2 Screening Iridicycles

An initial test was done to determine if the chiral catalysts developed (see Chapter 2) would be active under TH conditions. A test reaction was initiated using the imine, shown in Scheme 3.3. A simple oxazoline catalyst was chosen and subjected to the conditions reported for the achiral reaction, except at a lower temperature. This result was promising; a high conversion was attained overnight, along with a moderate enantioselectivity. As the developed catalyst motif was active for reduction under mild TH conditions, a range of the synthesised complexes were screened under these conditions.



Scheme 3.13 Testing conditions for imine ATH.

Initially the simple imidazoline and oxazoline iridicycles were examined as a basis for comparison. These results, shown in Table 3.1, showed that oxazolines were able to afford higher ee's than the corresponding imidazoline, with the *R,S*-ligand showing the greatest ee.



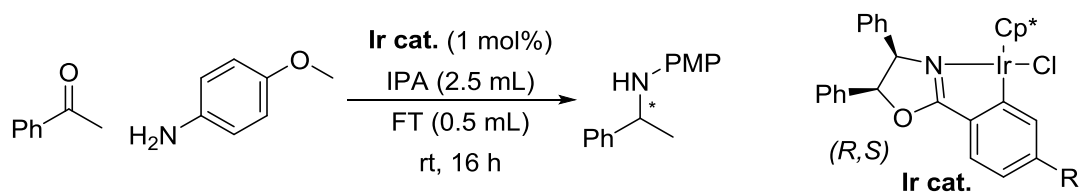
Entry	Catalyst	Conv (%)	ee (%)
1	 Ir 2	83	14
2	 Ir 1	68	23
3	 Ir 19	50	4

Reaction conditions: 0.5 mmol acetophenone, 0.6 mmol *p*-methoxy aniline, 1 mol% Ir cat, 2.5 mL anhydrous IPA, 0.5 mL FT, sealed in air, overnight.

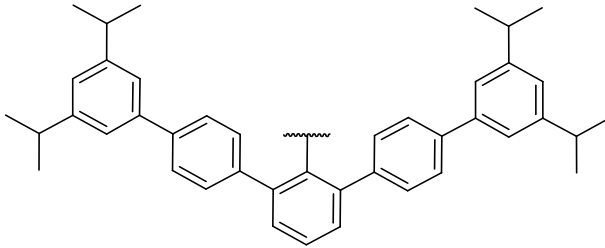
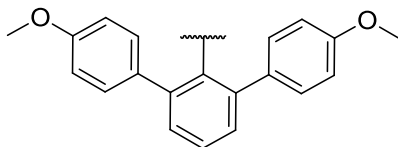
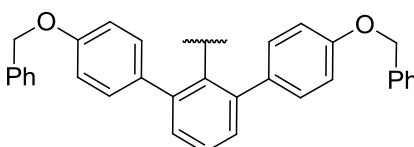
Table 3.1 Basic complexes tested for DARA.

A range of bulky oxazoline complexes were tested for their activity in this reaction, to determine if the steric bulk on the ligand would improve the selectivity. These produced underwhelming results, shown in Table 3.2, providing little difference in ee from the un-substituted complex **Ir 1** (Entry 2, Table 3.1). Further extending the bulky groups demonstrated both a slower rate of reaction, as well as a reduction in ee. Surprisingly it was the least bulky complex **Ir 10** that yielded the

best ee, indicating that steric hindrance at this position was not the key to high enantioselectivity for this system.



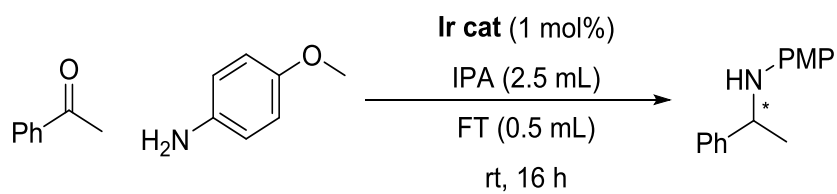
Entry	R	Conv (%)	ee (%)
1	^t Bu Ir 10	87	40
2	 Ir 11	95	25
3	 Ir 12	90	25
4	 Ir 13	70	22
5	 Ir 16	71	17
6	 Ir 17	62	10

7		60	10
	Ir 18		
8		60	0
	Ir 14		
9		89	14
	Ir 15		

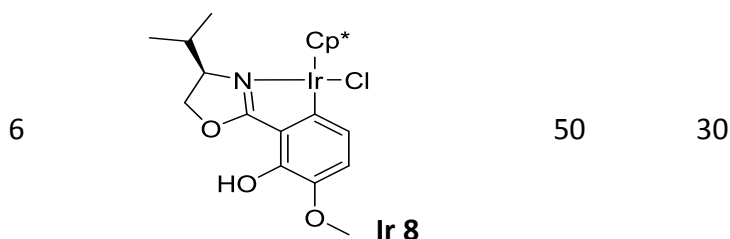
Reaction conditions: 0.5 mmol acetophenone, 0.6 mmol *p*-methoxy aniline, 1 mol% Ir cat, 2.5 mL anhydrous IPA, 0.5 mL FT, sealed in air, overnight.

Table 3.2 Screening of bulky oxazolines for DARA.

Having ruled out steric effects as the key to achieving a high ee, electronic effects were investigated with a range of less bulky oxazoline complexes (Table 3.3). These complexes showed varying results, with electron withdrawing groups showing a decrease in ee (Entry 1, Table 3.3). Electron donating groups in certain substitution patterns (Entries 2-6, Table 3.3) offered some improvement in ee compared to the un-substituted oxazoline complex (Entry 1, Table 3.1), although these results weren't very promising, with a maximal ee of 30% being obtained.



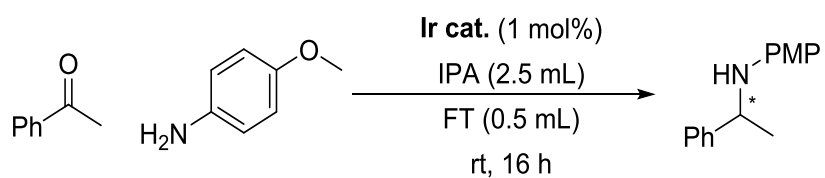
Entry	Catalyst	Conv (%)	ee (%)
1	 Ir 3	15	7
2	 Ir 4	74	22
3	 Ir 5	95	26
4	 Ir 6	80	30
5	 Ir 7	50	17



Reaction conditions: 0.5 mmol acetophenone, 0.6 mmol *p*-methoxy aniline, 1 mol% Ir cat, 2.5 mL anhydrous IPA, 0.5 mL FT, sealed in air, overnight.

Table 3.3 Screening of small oxazoline complexes for DARA.

Looking back at the imidazoline complex **Ir 19** screened (Entry 3, Table 3.1) it was known that three inseparable isomers had formed during cyclometalation, as opposed to two with the oxazoline, which may account for the reduced selectivity. It was decided to test those complexes formed in just 1 or 2 isomers, to determine which of these complexes were active. Complexes that lost their conjugation (**Ir 20** and **Ir 21**) also lost activity, producing < 5% conversion, even with a 3 day reaction time (Entries 1 and 2, Table 3.4). Complexes that maintained their conjugation, but were forced to cyclometalate on just the one ring maintained high activity (Entries 3-6, Table 3.4), with the cyclohexane diamine complex offering a moderate enantioselectivity. Bulky substituents *ortho* to the iridium centre (**Ir 23**) showed a reduction in ee once more (Entry 4, Table 3.4). The presence of the dioxane ring (**Ir 25**) also showed a reduced ee (Entry 6, Table 3.4), potentially due to the two regioisomers present. The highest selectivity was achieved with the dioxole containing complex **Ir 24** (Entry 6, Table 3.4).



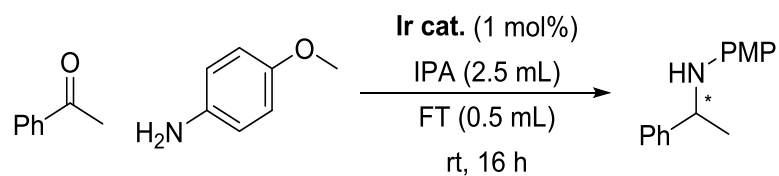
Entry	Catalyst	Conv (%)	ee (%)
1	Ir 20	0	-
2	Ir 21	0	-
3	Ir 22	41	27
4	Ir 23	43	28
5	Ir 24	49	50
6	Ir 25	95	39

Reaction conditions: 0.5 mmol acetophenone, 0.6 mmol *p*-methoxy aniline, 1 mol% Ir cat, 2.5 mL anhydrous IPA, 0.5 mL FT, sealed in air, overnight.

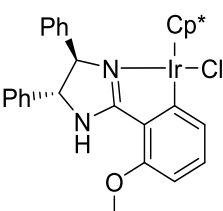
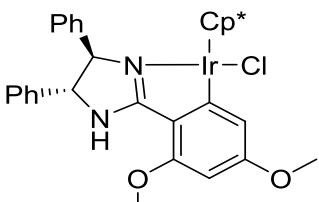
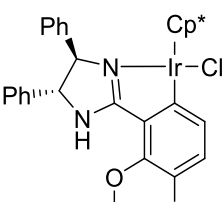
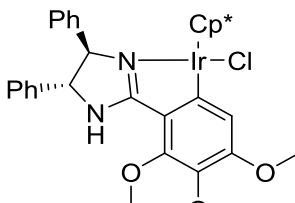
Table 3.4 Screening of non-aryl imidazoline containing complexes for DARA.

Analogues of the dioxole ligands were then screened to determine if the ee could be further improved upon. It was firstly shown that the aryl imidazoline analogue (**Ir 30**) could be used just as successfully with the dioxole functional group present (Entry 1, Table 3.5), despite forming three isomers (Chapter 2.3). Further modified dioxole-containing complexes (**Ir 31** - **Ir 33**) were screened; however these all showed a decrease in ee. The most significant loss in ee was observed in correlation with a loss of electron donating groups (Entries 3 and 4, Table 3.5). Whilst expanding the ring size (**Ir 34**) or adding an additional electron donating methoxy (**Ir 31**) offered little change in ee (Entries 2 and 5, Table 3.5).

To determine if the dioxole ring, or simply the presence of electron donating groups, were crucial, a range of simple methoxy containing complexes were screened. These once more showed that varying the position of the electron rich groups had a significant impact upon the ee (Entries 6-9, Table 3.5). A relatively low ee of just 27% was achieved by the 6-methoxy complex **Ir 26** (Entry 6, Table 3.5), the addition of a second methoxy to the 4-position (**Ir 27**) showed great improvement to 42% (Entry 7, Table 3.5). Moving the second group to the 5 position (**Ir 28**) had no effect on ee (Entry 8, Table 3.5). The highest ee was achieved with the 4,5,6-trimethoxy complex, **Ir 29** (Entry 9, Table 3.5), indicating a narrow band where the electron density is optimal for this reaction.



Entry	Catalyst	Conv (%)	ee(%)
1	 Ir 30	72	50
2	 Ir 34	75	43
3	 Ir 33	70	28
4	 Ir 32	73	28
5	 Ir 31	65	43

6		67	27
	Ir 26		
7		75	42
	Ir 27		
8		84	27
	Ir 28		
9		78	56
	Ir 29		

Reaction conditions: 0.5 mmol acetophenone, 0.6 mmol *p*-methoxy aniline, 1 mol% Ir cat, 2.5 mL anhydrous IPA, 0.5 mL FT, sealed in air, overnight.

Table 3.5 Screening of oxygen rich phenyl imidazoline complexes for DARA.

Variation of the aryl groups on the imidazoline was also investigated, **Ir 35** and **Ir 36**, to determine the impact upon the selectivity, in combination with the best 4,5,6-trimethoxy group. These complexes showed no further improvement to the ee (Table 3.6), with both an electron withdrawing and donating group producing a significant reduction in selectivity. These results further indicate that there is a narrow band where steric and electronic effects are optimal for this reaction.

Entry	Catalyst	Conv (%)	ee (%)
1	 Ir 35	78	21
2	 Ir 36	75	39

Reaction conditions: 0.5 mmol acetophenone, 0.6 mmol *p*-methoxy aniline, 1 mol% Ir cat, 2.5 mL anhydrous IPA, 0.5 mL FT, sealed, overnight.

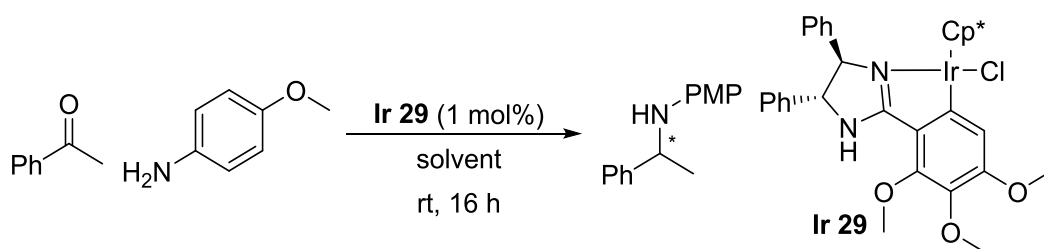
Table 3.6 Varying the diamine in trimethoxy complexes for DARA.

Having completed an extensive screening of complexes, it was determined that the 4,5,6-trimethoxy imidazoline complex (**Ir 29**) produced the greatest ee (56%), with a high conversion (78%). This complex was therefore taken forward for further optimisation of the reaction conditions.

3.3 Optimisation of reaction conditions

To improve the ee and conversion obtained, a range of conditions were screened. Initial screenings were done by varying the solvent (Table 3.7). An initial

test was performed to ensure that both solvent and FT were required for the conversions and ee previously obtained. In neat FT a slight drop in conversion along with a decrease in ee was observed. The IPA was shown to be an inactive hydride source for this transformation, yielding no conversion in neat IPA.



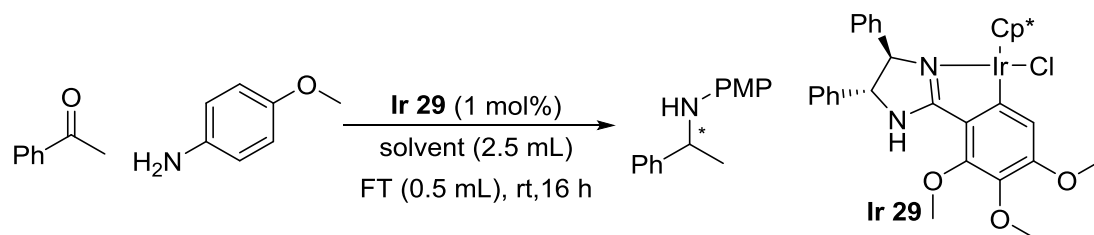
Entry	Solvent	Co-solvent	Conv (%)	ee (%)
1	IPA (2.5 mL)	FT (0.5 mL)	78	56
2	FT (1 mL)	-	70	27
3	IPA (2.5 mL)	-	0	-

Reaction conditions: 0.5 mmol acetophenone, 0.6 mmol *p*-methoxy aniline, 1 mol% Ir 29, sealed in air, overnight.

Table 3.7 Initial solvent test.

A range of other solvents were also screened, from these results it was seen that non-protic solvents such as toluene and acetonitrile were ineffective (Entries 1 and 2, Table 3.8), indicating that polar alcohol solvents were required. Simple MeOH gave a reduced ee, when compared to bulkier IPA (Entries 4 and 5, Table 3.8); *t*-amyl alcohol, however also produced a lower conversion and ee (Entry 6, Table 3.8). Poly ethylene glycols and *t*-butanol offered no improvement on the conversion or ee (Entries 7-12, Table 3.8), possibly due to their viscosity leading to poor mixing of substrates with the complex. The best results were obtained in the

moderately bulky IPA (Entry 4, Table 3.8), in the presence of FT, with the best ee obtained in a moderate conversion at room temperature.



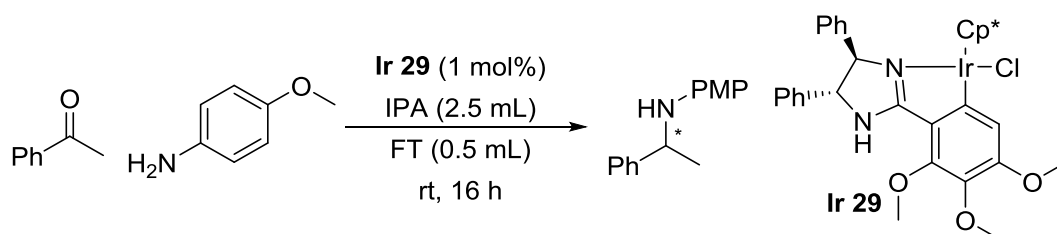
Entry	Solvent	Conv (%)	ee (%)	Entry	Solvent	Conv (%)	ee (%)
1	PhMe	0	-	7	<i>t</i> BuOH	42	50
2	MeCN	0	-	8	Polyethyleneglycol (200)	57	53
3	TFE	25	-	9	Polyethyleneglycol (300)	53	51
4	IPA	78	56	10	Polyethyleneglycol (400)	47	50
5	MeOH	58	43	11	Ethylene glycol	80	44
6	<i>t</i> amyl alcohol	30	42	12	Ethylene glycol : IPA (1:1)	73	48

Reaction conditions: 0.5 mmol acetophenone, 0.6 mmol *p*-methoxy aniline, 1 mol% Ir 29, 2.5 mL solvent, 0.5 mL FT, sealed in air, overnight, (Room temperature was determined to be between 8 and 15 °C).

Table 3.8 Solvent screening for DARA.

To improve the conversion, 4Å MS were added, these yielded a positive effect in small amounts showing a 10% increase in conversion (Table 3.9). A large amount of 4Å MS proved detrimental to the reaction, potentially due to the acidity

of sieves leading to interactions between them and the amine substrate, resulting in a decrease in the concentration of free aniline and preventing the condensation reaction from occurring readily.

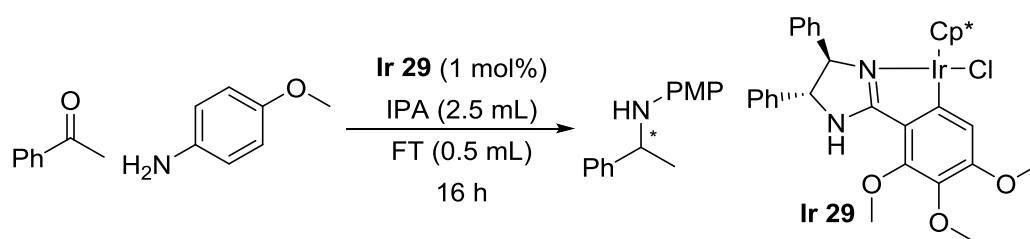


Entry	Additive	Conv (%)
1	-	78
2	4Å MS – 30 mg	88
3	4Å MS – 60 mg	84
4	4Å MS – 100 mg	62

Reaction conditions: 0.5 mmol acetophenone, 0.6 mmol *p*-methoxy aniline, 1 mol% Ir 29, 2.5 mL anhydrous IPA, 0.5 mL FT, sealed in air, overnight.

Table 3.9 Effect of molecular sieves on conversion.

In a further attempt to optimise the conversion and ee, various temperatures were investigated. Increasing the temperature slightly offered an increase in conversion, whilst maintaining the ee (Entry 1, Table 3.10), providing the optimal conditions. Reduced temperatures were also investigated to determine whether the selectivity could be increased. A detrimental effect was observed on both the conversion and ee (Entries 3 and 4, Table 3.10), potentially due to the limited solubility of the complex and amine at low temperatures.

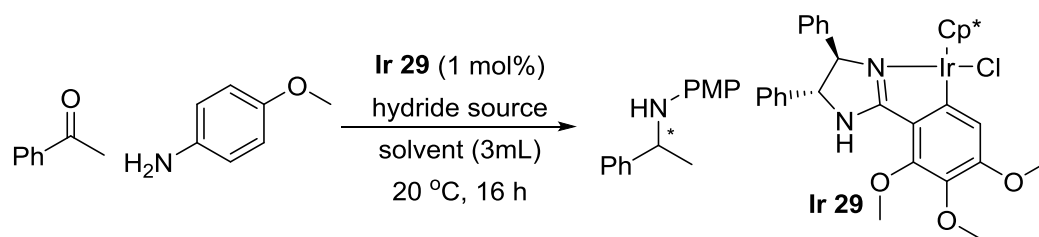


Entry	Temp (°C)	Conv (%)	ee (%)
1	20	97	56
2	15	78	56
3	5	70	54
4	-10	18	40

Reaction conditions: 0.5 mmol acetophenone, 0.6 mmol *p*-methoxy aniline, 1 mol% Ir **29**, 2.5 mL anhydrous IPA, 0.5 mL FT, sealed in air, overnight.

Table 3.10 Effect of temperature variation on DARA.

Other hydride sources were also screened. Hantzsch esters (HEH) have been commonly used as a hydride source; when screened under standard conditions it provided no conversion (Entry 2, Table 3.11). This was thought to be due to the insolubility of the HEH in the reaction media. Toluene was therefore tested as solvent, which has been previously reported,¹⁸ once more this offered no conversion (Entry 3, Table 3.11). Aqueous conditions were also tested, with a NaCO₂H/HCO₂H buffered solution (pH 4.5, which was shown to be active in the racemic studies).⁸ These conditions provided a much faster rate of reaction but offered a slight drop in ee (Entry 1, Table 3.11).



Entry	Hydride source	Solvent	Conv (%)	ee (%)
1	NaCO ₂ H/HCO ₂ H	H ₂ O (pH 4.5)	100	40
2		IPA	0	-
3		PhMe	0	-

Reaction conditions: 0.5 mmol acetophenone, 0.6 mmol *p*-methoxy aniline, 1 mol% Ir 29, 3 mL solvent, hydride source, sealed in air, overnight.

Table 3.11 Variation of hydride source for DARA.

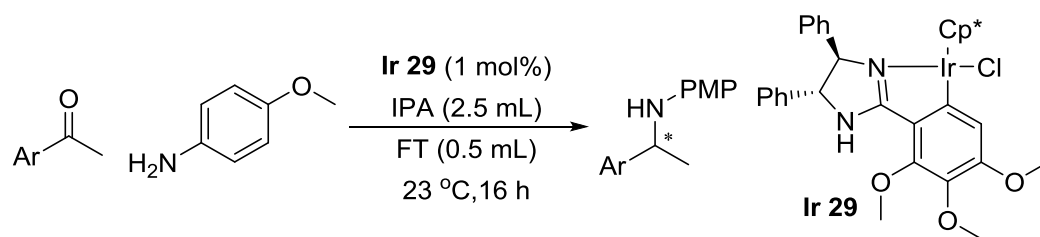
After the extensive screening of conditions it was determined that FT in IPA was the optimal reaction medium. A temperature of 20-25°C was also determined to give the best conversion and ee, in just 16 h. These conditions were carried forward to probe the range of substrates suitable for this system.

3.4 Substrate scope

3.4.1 Ketone variation

The substrate scope was initiated by varying the acetophenone used and the results showed promise (Table 3.12). Placing substituents in the *para* position offered similar results to the un-substituted acetophenone, with electron donating and electron withdrawing groups being tolerated, (Entries 2 and 3, Table 3.12). However, an exception was observed in the case of a methoxy group which produced a lower conversion (Entry 3, Table 3.12). This may be due to the resonance forms possible with the methoxy group present, rendering the ketone less active towards the condensation reaction. *Meta* substitutions also proved to have little impact on the conversion and ee (Entries 5-7, Table 3.12), yielding above 95% conversions and similar ee to standard acetophenone.

Switching to an *ortho* substitution pattern afforded a significant drop in ee (Entries 8 and 9, Table 3.12). These results also showed a switch in the major enantiomer formed, indicating that the *ortho* substituents interfere with reduction step, especially during the enantioselectivity determining step. Although a high conversion was obtained with an electron withdrawing chloride, a very poor conversion was obtained with an electron donating methyl group.



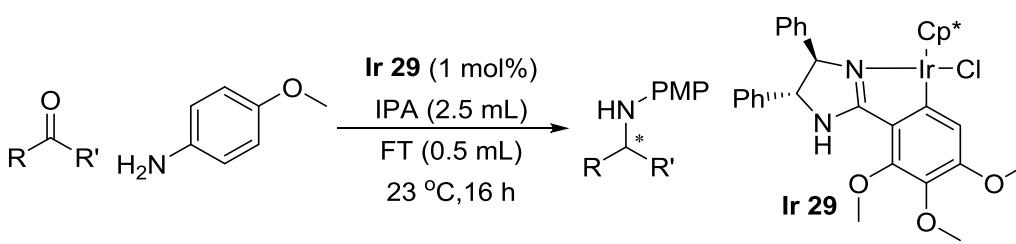
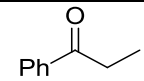
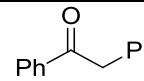
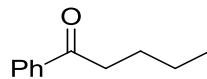
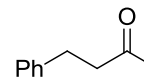
Entry	Acetophenone	Conv (%)	ee (%)	Entry	Acetophenone	Conv (%)	ee (%)
1		92	56	6		100	56
2		96	50	7		100	56
3		96	54	8		50	20
4		60	58	9		94	34
5		82	54				

Reaction conditions: 0.5 mmol ketone, 0.6 mmol *p*-methoxy aniline, 1 mol% Ir 29, 2.5 mL anhydrous IPA, 0.5 mL FT, sealed in air, overnight.

Table 3.12 Variation of acetophenone substrates scope.

Lengthening the alkyl chain of the ketone from a methyl to ethyl produced a higher ee than seen previously (Entry 1, Table 3.13), showing this system (unlike some biological systems)¹⁸ can tolerate alteration at this position and could even

offer improved results. The ee was also improved by adding a phenyl group into this position (Entry 3, Table 3.13), agreeing with the above observations; however the bulkiness of this group resulted in a slower rate of reaction. Unfortunately adding a longer alkyl chain into this position caused a decrease in ee (Entry 2, Table 3.13), demonstrating a limit to the functionalisation that can be tolerated in this position, although it had less of an impact on the rate.

							
Entry	Ketone	Conv (%)	ee (%)	Entry	Ketone	Conv (%)	ee (%)
1		90	63	3		41	63
2		78	38	4		100	0

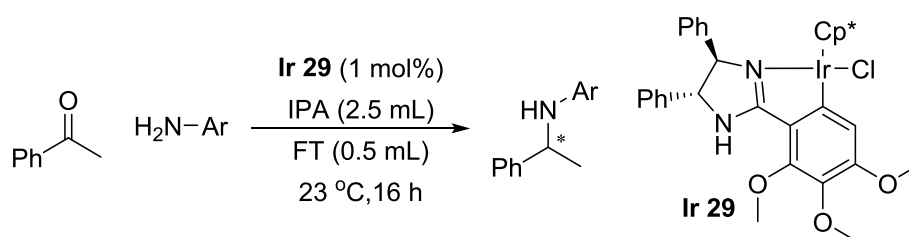
Reaction conditions: 0.5 mmol ketone, 0.6 mmol *p*-methoxy aniline, 1 mol% Ir 29, 2.5 mL anhydrous IPA, 0.5 mL FT, sealed in air, overnight.

Table 3.13 Variation of ketone for DARA

Switching from an aryl to an alkyl ketone afforded complete conversion (Entry 4, Table 3.13). However, this improved rate of reaction was accompanied by formation of racemic products, indicating that this catalytic system is not suitable for alkyl ketones.

3.4.2 Amine variation

Varying the aniline was next investigated to determine the versatility of the catalytic system regarding the amine partner. These results revealed a new problem, whilst the ee's achieved were similar to those previously produced, the conversions all showed a dramatic reduction (Table 3.14). This indicated that the electron donating methoxy group was crucial to the rate of reaction, probably increasing the rate of imine formation, due to the increased electron density on the nitrogen.

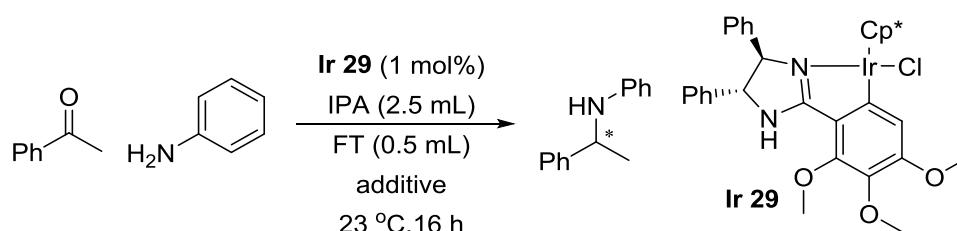


Entry	Aniline	Conv (%)	ee (%)	Entry	Aniline	Conv (%)	ee (%)
1		92	56	4		10	52
2		40	53	5		51	53
3		40	55	6		53	62

Reaction conditions: 0.5 mmol acetophenone, 0.6 mmol aniline, 1 mol% **Ir 29**, 2.5 mL anhydrous IPA, 0.5 mL FT, sealed in air, overnight.

Table 3.14 Screening of anilines for DARA under standard conditions

To overcome this issue, further screening was undertaken for the aniline substrates. This was initially done by testing a range of additives for promoting imine formation. Altering the pH of the solution with the addition of catalytic amounts of formic acid or triethylamine offered little impact upon the rate of reaction or the ee observed (Entries 3 and 4, Table 3.15). The addition of catalytic amounts of PTSA or 4Å MS, although commonly used for imine formation, resulted in a drop in the conversion (Entries 1 and 3, Table 3.15). This may again be due to the solution becoming too acidic for the condensation reaction to readily occur.



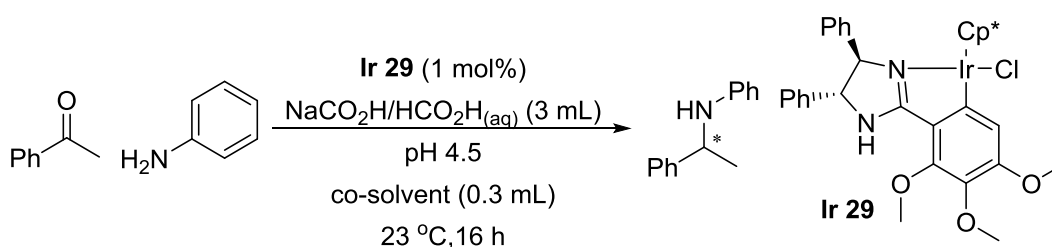
Entry	Additive (10 mol%)	Conv (%)	ee (%)	Entry	Additive (10 mol%)	Conv (%)	ee (%)
1	4Å MS (50 mg)	31	42	3	HCO ₂ H	55	51
2	PTSA	26	54	4	NEt ₃	51	50

Reaction conditions: 0.5 mmol acetophenone, 0.6 mmol aniline, 1 mol% Ir 29, 10 mol% additive, 2.5 mL anhydrous IPA, 0.5 mL FT, sealed in air, overnight.

Table 3.15 Additives for DARA on aniline.

As these methods offered no improvement on the conversions obtained, it was necessary to refer back to the previous optimisation reactions and re-examine the aqueous system briefly tested. Previously this system offered a faster rate of reaction but a slight drop in ee (Entry 3, Table 3.11). As such it was decided to test the aniline substrates under these conditions. As observed previously the

conversion showed significant improvement under the aqueous conditions, though as before the ee was reduced slightly (Entry 2, Table 3.14 vs. Entry 1, Table 3.16). An improvement in ee was offered by the addition of a co-solvent, whilst maintaining a high conversion. Use of DCM caused a significant drop in conversion (Entry 2, Table 3.16), whilst IPA, MeOH and 2-methyltetrahydrofuran (2-MeTHF) all offered similarly high conversions (Entries 3-5, Table 3.16). Although all solvents screened resulted in some drop in ee from the FT system, the smallest drop was seen with 2-MeTHF, showing this to be the optimal co-solvent for use in this biphasic reduction.



Entry	Co-solvent	Conv (%)	ee (%)	Entry	Co-solvent	Conv (%)	ee (%)
1	-	78	46	4	MeOH	82	47
2	DCM	25	-	5	2-MeTHF	80	55
3	IPA	83	50				

Reaction conditions: 0.5 mmol acetophenone, 0.6 mmol aniline, 1 mol% Ir 29, 3 mL NaCO₂H/HCO₂H pH 4.5, 0.3 mL co-solvent, sealed in air, overnight.

Table 3.16 Screen of co-solvents for a biphasic system.

The same range of anilines was once more studied using this optimised system (Table 3.17). Under these conditions all the conversions greatly improved. Although the conversion of the electron withdrawing 4-bromo species was still moderate, a significant improvement from that seen in the FT system was observed.

Pleasingly there was also little to no drop in ee seen with these anilines, showing that this biphasic system holds great promise.

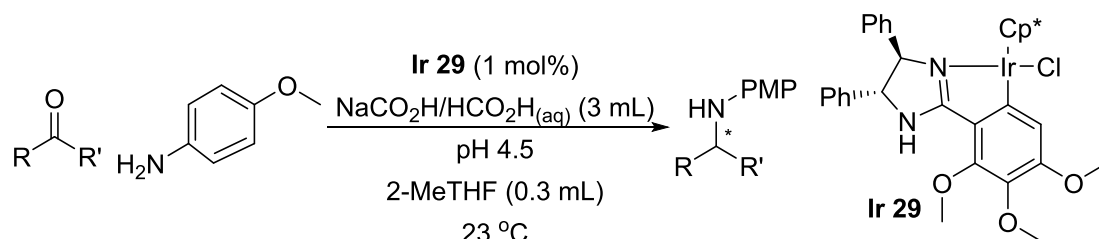
Entry	Aniline	Conv (%)	ee (%)	Entry	Aniline	Conv (%)	ee (%)
1		86	48	3		45	54
2		90	53	4		70	60

Reaction conditions: 0.5 mmol acetophenone, 0.6 mmol aniline, 1 mol% Ir 29, 3 mL NaCO₂H/HCO₂H pH 4.5, 0.3 mL co-solvent, sealed in air, overnight.

Table 3.17 Testing of anilines under a biphasic system.

To determine how versatile this aqueous system was, these conditions were tested on a variety of previously screened ketones with *p*-anisidine. It was of particular interest to determine if this could achieve similar results in shorter times, improving the lower conversions seen in some of the previous examples. The results showed great potential (Table 3.18), with similar ee's afforded and an improvement in most conversions being observed, in half the time (just 8 hours compared to those achieved in 16 hours under FT conditions). The alkyl chain was able to gain some ee, although only to a very poor 5% (Entry 3, Table 3.18). The only

disappointing result was achieved with the 2-methylacetophenone where the conversion remained the same but the ee dropped further (Entry 6, Table 3.18).

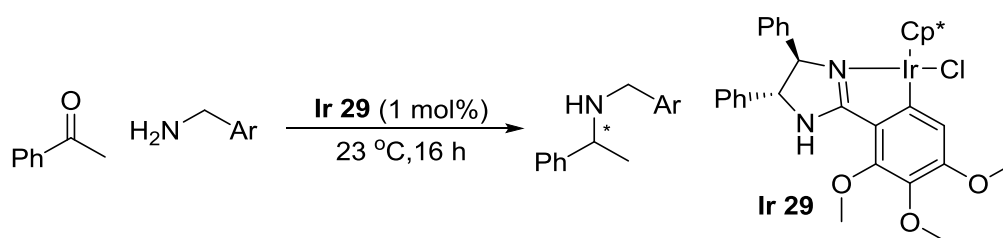


Entry	Time (h)	Ketone	NaCO ₂ H/HCO ₂ H		IPA FT*	
			Conv (%)	ee (%)	Conv (%)	ee (%)
1	16		80	59	41	63
2	16		86	36	78	38
3	8		100	5	100	0
4	8		81	48	96	54
5	8		79	55	100	56
6	8		50	15	50	20

Reaction conditions: 0.5 mmol acetophenone, 0.6 mmol aniline, 1 mol% **Ir 29**, 3 mL $NaCO_2H/HCO_2H$ pH 4.5, 0.3 mL co-solvent, sealed in air, overnight. *results from Tables 3.12 and 3.13 above.

Table 3.18 Comparison of various ketones under biphasic system and the FT system.

Further variation of the amine was undertaken by screening of benzylamines, in both the original FT and the aqueous conditions (Table 3.19). These results showed that the benzylamine was in fact active in this system with both conditions giving high to full conversion. This was a pleasing result as it was feared that the benzylamine may bind to the iridium centre, inhibiting the reaction. The ee's, however, were disappointing with the highest ee achieved being just 22%. Again little variation was observed between the ee's obtained under the two conditions.



Entry	Benzylamine	IPA/FT		NaCO ₂ H/HCO ₂ H	
		Conv (%)	ee (%)	Conv (%)	ee (%)
1	<chem>Nc1ccccc1</chem>	83	16	100	10
2	<chem>Nc1ccc(C)cc1</chem>	71	14	100	16
3	<chem>Nc1ccc(OC)cc1</chem>	80	17	100	22
4	<chem>Nc1ccccc1Cl</chem>	97	10	100	2

Reaction conditions: 0.5 mmol acetophenone, 0.6 mmol benzylamine, 1 mol% Ir 29, 3 mL NaCO₂H/HCO₂H pH 4.5, 0.3 mL co-solvent, sealed in air, overnight.

Table 3.19 Screen of benzylamines for DARA.

3.5 Conclusions

The results presented above show great promise for the chiral iridicycles, after an extensive complex screen, the electron rich 4,5,6-trimethoxy imidazoline complex, showed great activity and moderate to high enantioselectivity towards direct reductive amination. The transformation was shown to be successful under two different conditions; an organic system utilising IPA in the presence of FT and an aqueous system utilising formic acid and sodium formate in water. It was observed that the organic system produced the highest enantioselectivity, whilst the biphasic system provided a greater rate of reaction. It was demonstrated that a range of ketones and amines were active in this system, with only aliphatic ketones producing racemic products. Although lower ee's were achieved than in previously published work, the reaction conditions used are milder.

3.6 Experimental

The iridium complexes were synthesised as described in Chapter 2. IPA, DCM and toluene were dried on a MB-SPS 800 and methanol was dried over magnesium and iodine. All other chemicals were obtained commercially and used without further purification. NMR spectra were recorded on a Bruker 400 MHz NMR spectrometer, with TMS as internal standard. HPLC analysis was recorded on an Agilent 1260 Infinity equipped with either Chiralpak IB-3 or Chiralcel OJ-H.

3.6.1 Standard Procedures

Standard procedure for DARA under FT conditions

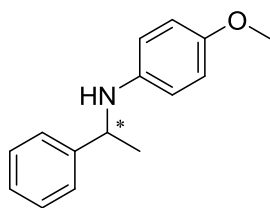
A glass vial was charged with the iridium catalyst (1 mol%), amine (0.6 mmol) and ketone (0.5 mmol) along with a stirring bar, IPA (2.5 mL) was added, followed by FT

(0.5 mL) to initiate the reaction. The glass vial was sealed and stirred at the stated temperature and time. After the reaction time was complete, the reaction mixture was quenched by the addition of aq 10% NaOH and extracted into EtOAc. The organic phase was dried over MgSO_4 , filtered and evaporated under vacuum. The resulting residue was purified by column chromatography, in 15% EtOAc in hexane, upon which HPLC analysis was performed.

Standard procedure for DARA under aqueous conditions

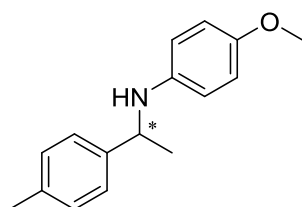
A glass vial was charged with the iridium catalyst (1 mol%), amine (0.6 mmol) and ketone (0.5 mmol) along with a stirring bar, 2-MeTHF (0.3 mL) was added, followed finally by an aqueous solution of sodium formate/formic acid (3 mL) to initiate the reaction. The glass vial was sealed and stirred at the stated temperature and time. After the reaction time was complete the reaction mixture was quenched by the addition of saturated aq K_2CO_3 and extracted into EtOAc. The organic phase was dried over MgSO_4 , filtered and evaporated under vacuum. The resulting residue was purified by column chromatography, in 15% EtOAc in hexane, upon which HPLC analysis was performed.

3.6.2 Analytical data



4-Methoxy-*N*-(1-phenylethyl)aniline⁷ In accordance with published data.

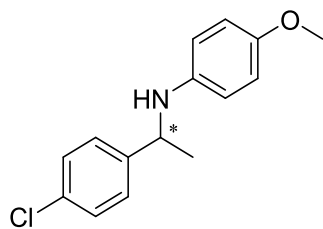
White solid isolated in 90% yield. **¹H NMR** (CDCl₃, 400 MHz) δ (ppm) 7.37-7.29 (m, 4H), 7.23-7.20 (m, 1H), 6.79 (d, J = 8.4 Hz, 2H), 6.49 (d, J = 8.4 Hz, 2H), 4.21 (q, J = 6.6 Hz, 1H), 3.69 (s, 3H), 1.51 (d, J = 6.6 Hz, 3H). **¹³C NMR** (CDCl₃, 100 MHz) δ (ppm) 152.1, 145.2, 141.2, 128.6, 126.9, 126.0, 114.9, 114.8, 55.7, 54.5, 25.0. **HRMS** (CI) [M+H]⁺ Calculated 228.1383; [M+H]⁺ found 228.1386. **CHN** C₁₅H₁₇NO calculated C, 79.26; H, 7.54; N, 6.16; found C, 79.42; H, 7.50; N, 5.95. **HPLC** (Chiralpak IB-3, 98:2 Hex:IPA + 0.1% HNEt₂, 1 mL/min, 25 °C, 254 nm) 7.14 min (major) and 8.61 min.



4-Methoxy-*N*-(1-(*p*-tolyl)ethyl)aniline⁸ In accordance with published data.

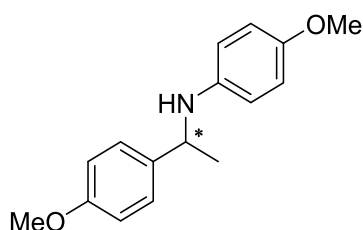
White solid isolated in 95% yield. **¹H NMR** (CDCl₃, 400 MHz) δ (ppm) 7.24 (d, J = 7.9 Hz, 2H), 7.12 (d, J = 7.9 Hz, 2H), 6.69 (d, J = 8.8 Hz, 2H), 6.48 (d, J = 8.8 Hz, 2H), 4.38 (q, J = 6.7 Hz, 1H), 3.69 (s, 3H), 3.32 (s, 3H), 1.48 (d, J = 6.7 Hz, 3H). **¹³C NMR** (CDCl₃, 100 MHz) δ (ppm) 142.5, 141.7, 136.3, 129.3, 128.5, 125.8, 114.8, 114.6, 55.8, 54.0, 25.1, 21.1. **HRMS** (CI) [M+H]⁺ Calculated 242.1539; [M+H]⁺ found 242.1544. **CHN** C₁₆H₁₉NO calculated C, 79.63; H, 7.94; N, 5.80; found C, 79.88; H, 7.81; N, 4.7. **HPLC**

(Chiralpak IB-3, 98:2 Hex:IPA + 0.1% HNEt₂, 1 mL/min, 25 °C, 254 nm) 11.16 min and 11.99 min (major).



***N*-(1-(4-Chlorophenyl)ethyl)-4-methoxyaniline**⁸ In accordance with published data.

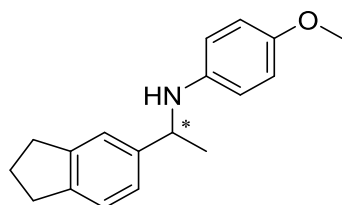
Orange oil isolated in 94% yield (from the organic system) and 80% (in the aqueous system). ¹H NMR (CDCl₃, 400 MHz) δ (ppm) 7.31-7.25 (m, 4H), 6.69 (d, J = 8.9 Hz, 2H), 6.43 (d, J = 8.9 Hz, 2H), 4.37 (q, J = 6.7 Hz, 1H), 3.69 (s, 3H), 1.47 (d, J = 6.7 Hz, 3H). ¹³C NMR (CDCl₃, 100 MHz) δ (ppm) 152.1, 144.0, 141.1, 132.3, 128.8, 127.3, 114.8, 114.7, 55.7, 53.8, 25.1. HRMS (CI) [M+H]⁺ Calculated 262.0993; [M+H]⁺ found 262.0992. CHN C₁₅H₁₆ClNO calculated C, 68.83; H, 6.16; N, 5.35; found C, 69.73; H, 6.33; N, 5.12. HPLC (Chiralpak IB-3, 98:2 Hex:IPA + 0.1% HNEt₂, 1 mL/min, 25 °C, 254 nm) 17.23 min and 18.83 min (major).



4-Methoxy-*N*-(1-(4-methoxyphenyl)ethyl)aniline⁷ In accordance with published data.

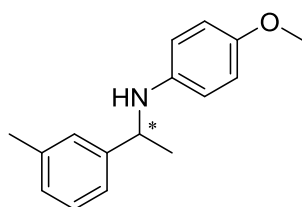
White solid isolated in 59% yield. ¹H NMR (CDCl₃, 400 MHz) δ (ppm) 7.29-2.76 (m, 2H), 6.87-6.84 (m, 2H), 6.70-6.68 (m, 2H), 6.49-6.46 (m, 2H), 4.37 (q, J = 6.7 Hz, 1H),

3.78 (s, 3H), 3.69 (s, 3H), 1.47 (d, $J = 6.7$ Hz, 3H). **^{13}C NMR** (CDCl_3 , 100 MHz) δ (ppm) 158.4, 151.8, 141.7, 137.5, 114.7, 114.6, 114.0, 113.7, 55.7, 55.5, 55.2, 25.2. **CHN** $\text{C}_{16}\text{H}_{19}\text{NO}_2$ calculated C, 74.68; H, 7.44; N, 5.44; found C, 74.25; H, 7.41; N, 3.65. **HPLC** (Chiralpak IB-3, 98:2 Hex:IPA + 0.1% HNEt_2 , 1 mL/min, 25 °C, 254 nm) 16.05 min and 16.93 min (major).



***N*-(1-(2,3-Dihydro-1*H*-inden-5-yl)ethyl)-4-methoxyaniline**

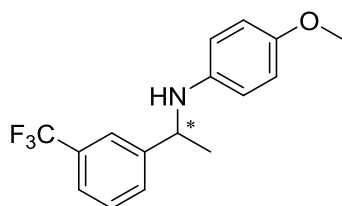
Orange oil isolated in 80% yield. **^1H NMR** (CDCl_3 , 400 MHz) δ (ppm) 7.22 (s, 1H), 7.13 (q, $J = 7.7$ Hz, 2H), 6.69 (d, $J = 8.9$ Hz, 2H), 6.49 (d, $J = 8.9$ Hz, 2H), 4.38 (q, $J = 6.7$ Hz, 1H), 3.69 (s, 3H), 2.87 (t, $J = 7.7$ Hz, 4H), 2.05 (quin, $J = 7.5$ Hz, 2H), 1.48 (d, $J = 6.7$ Hz, 3H). **^{13}C NMR** (CDCl_3 , 100 MHz) δ (ppm) 151.9, 144.7, 143.4, 142.9, 124.4, 123.8, 121.8, 114.8, 114.6, 55.8, 54.3, 32.9, 32.5, 25.5, 25.3. **HRMS** (CI) $[\text{M}+\text{H}]^+$ Calculated 268.1696; $[\text{M}+\text{H}]^+$ found 268.1706. **HPLC** (Chiralpak IB-3, 98:2 Hex:IPA + 0.1% HNEt_2 , 1 mL/min, 25 °C, 254 nm) 10.85 min and 11.80 min (major).



4-Methoxy-*N*-(1-(*m*-tolyl)ethyl)aniline¹⁵ In accordance with published data.

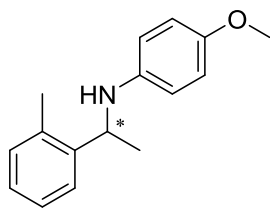
Yellow oil isolated in 96% yield. **^1H NMR** (CDCl_3 , 400 MHz) δ (ppm) 7.21-7.14 (m, 3H), 7.03 (d, $J = 7.1$ Hz, 1H), 6.69 (d, $J = 8.5$ Hz, 2H), 6.48 (d, $J = 8.9$ Hz, 2H), 4.36 (q, J

= 6.7 Hz, 1H), 3.69 (s, 3H), 2.33 (s, 3H), 1.48 (d, J = 6.7 Hz, 3H). **¹³C NMR** (CDCl₃, 100 MHz) δ (ppm) 152.0, 145.4, 141.5, 138.2, 128.5, 127.7, 126.6, 123.0, 114.8, 114.7, 55.8, 54.4, 25.0, 21.5. **HRMS** (CI) [M+H]⁺ Calculated 242.1539; [M+H]⁺ found 242.1536. **CHN** C₁₆H₁₉NO calculated C, 79.63; H, 7.94; N, 5.80; found C, 80.43; H, 7.98; N, 5.57. **HPLC** (Chiralpak IB-3, 98:2 Hex:IPA + 0.1% HNEt₂, 1 mL/min, 25 °C, 254 nm) 11.12 min and 12.25 min (major).



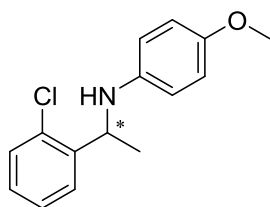
4-Methoxy-N-(1-(3-(trifluoromethyl)phenyl)ethyl)aniline¹⁵ In accordance with published data.

Yellow oil isolated in 95% yield. **¹H NMR** (CDCl₃, 400 MHz) δ (ppm) 7.63 (bs, 1H), 7.55 (d, J = 6.4 Hz, 1H), 7.48 (d, J = 6.4 Hz, 1H), 7.42 (d, J = 7.1 Hz, 1H), 6.69 (d, J = 6.9 Hz, 2H), 6.43 (d, J = 7.0 Hz, 2H), 4.45 (m, 1H), 3.69 (s, 3H), 1.49 (d, J = 6.2 Hz, 3H). **¹³C NMR** (CDCl₃, 100 MHz) δ (ppm) 152.2, 146.8, 141.1, 129.3, 129.1, 123.8, 123.8, 122.8, 122.8, 114.8, 114.6, 55.7, 54.2, 25.2. **HRMS** (CI) [M+H]⁺ Calculated 296.1257; [M+H]⁺ found 296.1267. **CHN** C₁₆H₁₆F₃NO calculated C, 65.08; H, 5.46; N, 4.74; found C, 65.78; H, 5.52; N, 4.33. **HPLC** (Chiralpak IB-3, 98:2 Hex:IPA + 0.1% HNEt₂, 1 mL/min, 25 °C, 254 nm) 15.81 min and 20.08 min (major).



4-Methoxy-*N*-(1-(*o*-tolyl)ethyl)aniline¹⁵ In accordance with published data.

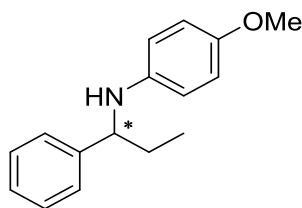
Orange liquid isolated in 45% yield. ¹H NMR (CDCl₃, 400 MHz) δ (ppm) 7.42 (d, J = 7.3 Hz, 1H), 7.17-7.12 (m, 3H), 6.68 (d, J = 8.9 Hz, 2H), 6.40 (d, J = 8.9 Hz, 2H), 4.60 (q, J = 6.6 Hz, 1H), 3.69 (s, 3H), 2.43 (s, 3H), 1.45 (d, J = 6.6 Hz, 3H). ¹³C NMR (CDCl₃, 100 MHz) δ (ppm) 151.8, 143.0, 141.6, 134.6, 130.6, 126.6, 126.5, 124.7, 114.8, 114.2, 55.8, 50.5, 23.1, 19.0. **CHN** C₁₆H₁₉NO calculated C, 79.63; H, 7.94; N, 5.80; found C, 80.80; H, 8.00; N, 5.66. **HPLC** (Chiralpak IB-3, 98:2 Hex:IPA + 0.1% HNEt₂, 1 mL/min, 25 °C, 254 nm) 10.01 min (major) and 12.17 min.



***N*-(1-(2-Chlorophenyl)ethyl)-4-methoxyaniline**¹⁵ In accordance with published data.

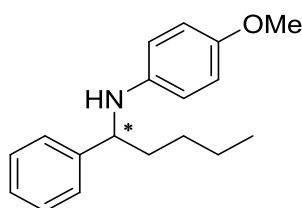
Orange oil isolated in 88% yield. ¹H NMR (CDCl₃, 400 MHz) δ (ppm) 7.45 (dd, J = 7.5, 1.8 Hz, 1H), 7.34 (dd, J = 7.5, 0.9 Hz, 1H), 7.20-7.12 (m, 2H), 6.68 (d, J = 8.8 Hz, 2H), 6.40 (d, J = 8.8 Hz, 2H), 4.83 (q, J = 6.6 Hz, 1H), 3.86 (bs, 1H), 3.68 (s, 3H), 1.48 (d, J = 6.6 Hz, 3H). ¹³C NMR (CDCl₃, 100 MHz) δ (ppm) 152.0, 142.3, 141.0, 132.5, 129.7, 128.0, 127.2, 126.8, 114.8, 114.3, 55.7, 50.9, 23.0. **HRMS** (CI) [M+H]⁺ Calculated 262.0993; [M+H]⁺ found 262.1002. **CHN** C₁₅H₁₆ClNO calculated C, 68.83; H, 6.16; N,

5.35; found C, 68.75; H, 6.20; N, 4.94. **HPLC** (Chiralpak IB-3, 98:2 Hex:IPA + 0.1% HNEt₂, 1 mL/min, 25 °C, 254 nm) 10.38 min (major) and 11.56 min.



4-Methoxy-N-(1-phenylpropyl)aniline¹⁵ In accordance with published data.

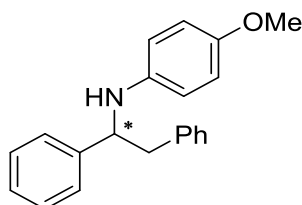
Orange oil isolated in 88% yield. ¹H NMR (CDCl₃, 400 MHz) δ (ppm) 7.34-7.28 (m, 4H), 7.23-7.20 (m, 1H), 6.70-6.66 (m, 2H), 6.79-6.45 (m, 2H), 4.15 (t, J = 6.7 Hz, 1H), 3.68 (s, 3H), 1.80 (dq, J = 16.1, 7.4 Hz, 2H), 0.94 (t, J = 7.4 Hz, 3H). ¹³C NMR (CDCl₃, 100 MHz) δ (ppm) 151.8, 144.2, 141.8, 128.5, 126.8, 126.6, 114.8, 114.4, 60.6, 55.8, 31.7, 10.9. **HRMS** (CI) [M+H]⁺ Calculated 242.1539; [M+H]⁺ found 242.1547. **CHN** C₁₆H₁₉NO calculated C, 79.63; H, 7.94; N, 5.80; found C, 80.94; H, 8.03; N, 5.58. **HPLC** (Chiralpak IB-3, 98:2 Hex:IPA + 0.1% HNEt₂, 1 mL/min, 25 °C, 254 nm) 8.57 min and 9.21 min (major).



4-Methoxy-N-(1-phenylpentyl)aniline²⁰ In accordance with published data.

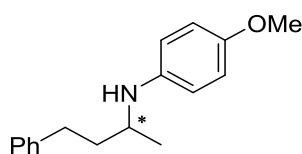
Yellow oil isolated 75% yield (in the organic system) and 84% yield (in the aqueous system). ¹H NMR (CDCl₃, 400 MHz) δ (ppm) 7.34-7.20 (m, 5H), 6.68-6.62 (m, 4H), 4.2 (t, J = 7.0 Hz, 1H), 3.68 (s, 3H), 1.96-1.87 (m, 2H), 1.31-1.21 (m, 4H), 0.84 (t, J = 7.0 Hz, 3H). ¹³C NMR (CDCl₃, 100 MHz) δ (ppm) 141.6, 128.6, 127.3, 127.0, 116.7, 114.6,

55.7, 45.7, 37.4, 28.4, 22.5, 14.7, 14.0, 6.6. **HRMS** (CI) $[M+H]^+$ Calculated 270.1852; $[M+H]^+$ found 270.1863. **CHN** $C_{18}H_{23}NO$ calculated C, 80.26; H, 8.61; N, 5.20; found C, 81.26; H, 8.64; N, 4.78 **HPLC** (Chiralpak IB-3, 98:2 Hex:IPA + 0.1% $HNEt_2$, 1 mL/min, 25 °C, 254 nm) 7.60 min and 8.16 min (major).



***N*-(1,2-Diphenylethyl)-4-methoxyaniline**²¹ In accordance with published data.

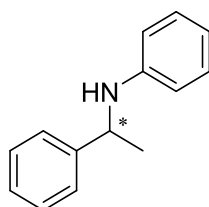
Yellow oil isolated in 38% yield (in the organic system) and 76% yield (in the aqueous system). **¹H NMR** ($CDCl_3$, 400 MHz) δ (ppm) 8.02-7.97 (m, 2H), 7.55-7.44 (m, 3H), 7.32-7.30 (m, 3H), 7.12 (d, J = 7.2 Hz, 2H), 6.64 (d, J = 8.8 Hz, 2H), 6.41 (d, J = 8.8 Hz, 2H), 4.50 (dd, J = 8.0, 5.9 Hz, 1H), 3.11 (dd, J = 13.9, 5.9 Hz, 1H), 2.99 (dd, J = 14.0, 8.3 Hz, 1H). **¹³C NMR** ($CDCl_3$, 100 MHz) δ (ppm) 129.9, 129.5, 129.2, 129.0, 128.7, 128.6, 128.5, 127.0, 126.7, 126.5, 114.9, 114.7, 60.1, 55.7, 45.3. **HRMS** (CI) $[M+H]^+$ Calculated 304.1696; $[M+H]^+$ found 304.1709. **HPLC** (Chiralpak IB-3, 98:2 Hex:IPA + 0.1% $HNEt_2$, 1 mL/min, 25 °C, 254 nm) 10.51 min and 13.99 min (major).



4-Methoxy-*N*-(4-phenylbutan-2-yl)aniline⁸ In accordance with published data.

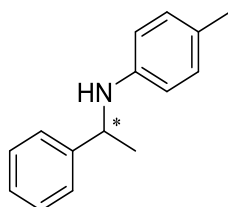
Yellow oil isolated in 97% yield. **¹H NMR** ($CDCl_3$, 400 MHz) δ (ppm) 7.30-7.28 (m, 2H), 7.19-7.17 (m, 3H), 6.78-6.74 (m, 2H), 6.53-6.50 (m, 2H), 3.74 (s, 3H), 3.42-3.37 (m, 1H), 2.78-2.70 (m, 2H), 1.89-1.71 (m, 2H), 1.19 (d, J = 6.2 Hz, 3H). **¹³C NMR**

(CDCl₃, 100 MHz) δ (ppm) 151.9, 142.1, 141.7, 128.5, 128.4 (q), 126.1, 125.8, 115.0, 114.8, 55.8, 49.0, 38.9, 32.5, 20.9. **HRMS** (CI) [M+H]⁺ Calculated 256.1696; [M+H]⁺ found 256.1703. **HPLC** (Chiralpak IB-3, 98:2 Hex:IPA + 0.1% HNEt₂, 1 mL/min, 25 °C, 254 nm) 11.84 min and 12.39 min.



***N*-(1-Phenylethyl)aniline**⁸ In accordance with published data.

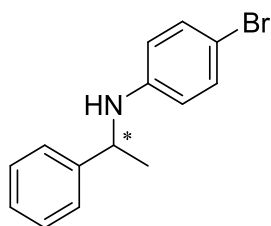
Yellow oil isolated in 37% and 82% yield (in the organic and aqueous system respectively). **¹H NMR** (CDCl₃, 400 MHz) δ (ppm) 7.38-7.30 (m, 4H), 7.24-7.20 (m, 1H), 7.11-7.06 (m, 2H), 6.64 (t, *J* = 7.3 Hz, 1H), 6.52-6.50 (m, 2H), 4.48 (q, *J* = 6.7 Hz, 1H), 1.52 (d, *J* = 6.7 Hz, 3H). **¹³C NMR** (CDCl₃, 100 MHz) δ (ppm) 129.1, 129.0, 128.7, 128.4, 126.9, 125.9, 119.4, 113.3, 53.5, 25.0. **HRMS** (CI) [M+H]⁺ calculated 198.1277; [M+H]⁺ found 198.1280. **CHN** C₁₄H₁₅N calculated C, 85.24; H, 7.66; N, 7.10; found C, 86.33; H, 7.91; N, 7.25. **HPLC** (Chiralpak IB-3, 98:2 Hex:IPA + 0.1% HNEt₂, 1 mL/min, 25 °C, 254 nm) 8.25 min (major) and 9.57 min.



4-Methyl-*N*-(1-phenylethyl)aniline⁸ In accordance with published data.

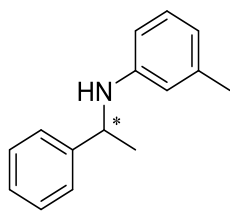
White solid isolated in 37% and 84% yield (in the organic and aqueous systems respectively). **¹H NMR** (CDCl₃, 400 MHz) δ (ppm) 7.37-7.29 (m, 4H), 7.23-7.20 (m,

1H), 6.90 (d, J = 8.2 Hz, 2H), 6.43 (d, J = 8.2 Hz, 2H), 4.45 (q, J = 6.7 Hz, 1H), 2.18 (s, 3H), 1.50 (d, J = 6.7 Hz, 3H). **¹³C NMR** (CDCl₃, 100 MHz) δ (ppm) 129.6, 129.5, 128.6, 127.1, 126.8, 125.8, 119.4, 113.5, 53.7, 25.1, 20.4. **HRMS** (CI) [M+H]⁺ Calculated 212.1434; [M+H]⁺ found 212.1442. **CHN** C₁₅H₁₇N calculated C, 85.26; H, 8.11; N, 6.63; found C, 85.01; H, 8.19; N, 6.60. **HPLC** (Chiralpak IB-3, 98:2 Hex:IPA + 0.1% HNEt₂, 1 mL/min, 25 °C, 254 nm) 7.96 min and 8.73 min (major).



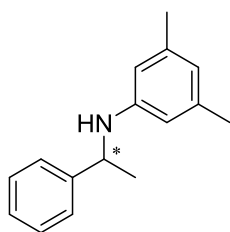
4-Bromo-N-(1-phenylethyl)aniline⁸ In accordance with published data.

Yellow oil isolated in 8% and 42% yield (in the organic and aqueous systems respectively). **¹H NMR** (CDCl₃, 400 MHz) δ (ppm) 7.32-7.29 (m, 4H), 7.23-7.21 (m, 1H), 7.14 (d, J = 8.5 Hz, 2H), 6.36 (d, J = 8.5 Hz, 2H), 4.42 (q, J = 6.7 Hz, 1H), 1.50 (d, J = 6.7 Hz, 3H). **¹³C NMR** (CDCl₃, 100 MHz) δ (ppm) 146.2, 144.6, 131.8, 128.8, 127.1, 125.8, 114.9, 108.9, 55.5, 25.0. **HRMS** (CI) [M+H]⁺ Calculated 276.0382; [M+H]⁺ found 276.0382. **CHN** C₁₄H₁₄BrN calculated C, 60.89; H, 5.11; N, 5.07; found C, 61.59; H, 5.43; N, 4.77. **HPLC** (Chiralpak IB-3, 98:2 Hex:IPA + 0.1% HNEt₂, 1 mL/min, 25 °C, 254 nm) 9.77 min and 11.59 min (major).



3-Methyl-*N*-(1-phenylethyl)aniline²² In accordance with published data.

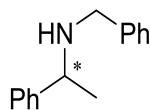
Orange oil isolated in 47% yield. **¹H NMR** (CDCl₃, 400 MHz) δ (ppm) 7.38-7.31 (m, 4H), 7.24-7.22 (m, 1H), 6.97 (t, *J* = 7.8 Hz, 1H), 6.47 (d, *J* = 7. Hz, 1H), 6.36 (s, 1H), 6.3 (dd, *J* = 8, 2.2 Hz, 1H), 4.47 (q, *J* = 6.7 Hz, 1H), 2.21 (s, 3H), 1.50 (d, *J* = 6.7 Hz, 3H). **¹³C NMR** (CDCl₃, 100 MHz) δ (ppm) 147.3, 145.4, 138.9, 129.0, 128.6, 126.8, 125.9, 118.2, 114.1, 110.3, 53.4, 25.0, 21.6. **HRMS** (CI) [M+H]⁺ Calculated 212.1434; [M+H]⁺ found 212.1443. **CHN** C₁₅H₁₇N calculated C, 85.26; H, 8.11; N, 6.63; found C, 85.19; H 8.27; N, 6.79. **HPLC** (Chiralpak IB-3, 98:2 Hex:IPA + 0.1% HNEt₂, 1 mL/min, 25 °C, 254 nm) 7.24 min (major) and 8.66 min.



3,5-Dimethyl-*N*-(1-phenylethyl)aniline²³ In accordance with published data.

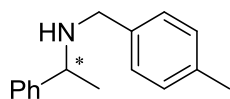
Yellow oil isolated in 50% and 65% yields (in the organic and aqueous systems respectively). **¹H NMR** (CDCl₃, 400 MHz) δ (ppm) 7.37-7.29 (m, 4H), 7.23-7.20 (m, 1H), 6.31 (s, 1H), 6.16 (s, 2H), 4.47 (q, *J* = 6.7Hz, 1H), 2.16 (s, 6H), 1.48 (d, *J* = 6.7Hz, 3H). **¹³C NMR** (CDCl₃, 100 MHz) δ (ppm) 147.4, 145.5, 138.8, 128.6, 126.8, 125.9, 119.3, 111.2, 53.3, 25.0, 21.5. **HRMS** (CI) [M+H]⁺ calculated 226.159; [M+H]⁺ found

226.1591. **HPLC** (Chiralpak IB-3, 98:2 Hex:IPA + 0.1% HNEt₂, 1 mL/min, 25 °C, 254 nm) 6.21 min (major) and 6.84 min.



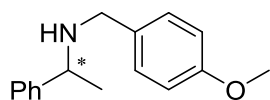
***N*-Benzyl-1-phenylethanamine**⁷ In accordance with published data.

Yellow oil isolated in 80 and 97% yields (in the organic and aqueous systems respectively). ¹H NMR (CDCl₃, 400 MHz) δ (ppm) 7.36-7.21 (m, 10H), 3.81 (q, J = 6.6 Hz, 1H), 3.62 (q, J = 13.1 Hz, 2H), 1.63 (bs, 1H), 1.37 (d, J = 6.6 Hz, 3H). ¹³C NMR (CDCl₃, 100 MHz) δ (ppm) 145.6, 140.6, 128.5, 128.4, 128.2, 127.0, 126.9, 126.7, 57.5, 51.7, 24.6. **HRMS** (CI) [M+H]⁺ Calculated 212.1434; [M+H]⁺ found 212.1444. **HPLC** (Chiralpak IB-3, 99:1 Hex:IPA + 0.1% HNEt₂, 1 mL/min, 25 °C, 254 nm) 5.65 min (major) and 6.09 min.



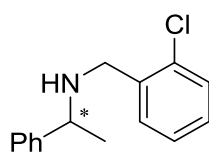
***N*-(4-Methylbenzyl)-1-phenylethanamine**²⁴ In accordance with published data.

Yellow oil isolated in 66% and 94% yields (in the organic and aqueous systems respectively). ¹H NMR (CDCl₃, 400 MHz) δ (ppm) 7.35-7.34 (m, 4H), 7.6-7.26 (m, 1H), 7.17-7.10 (m, 4H), 3.80 (q, J = 6.6 Hz, 1H), 3.58 (q, J = 13.0 Hz, 2H), 2.33 (s, 3H), 1.60 (bs, 1H), 1.35 (d, J = 6.6 Hz, 3H). ¹³C NMR (CDCl₃, 100 MHz) δ (ppm) 145.6, 137.6, 136.4, 129.1, 128.5, 128.1, 126.9, 126.8, 57.4, 51.4, 24.5, 21.3. **HRMS** (CI) [M+H]⁺ calculated 226.1590; [M+H]⁺ found 226.1596. **HPLC** (Chiralpak IB-3, 99.8:0.2 Hex:IPA (+ 0.1% HNEt₂), 0.5 mL/min, 25 °C, 254 nm) 16.83 min (major) and 17.72 min.



***N*-Benzyl-1-(4-nitrophenyl)ethanamine**²⁵ In accordance with published data.

Yellow oil isolated in 77% and 93% yields (in the organic and aqueous systems respectively). **¹H NMR** (CDCl₃, 400 MHz) δ (ppm) 7.35-7.33 (m, 4H), 7.26-7.25 (m, 1H), 7.19 (d, *J* = 8.5 Hz, 2H), 6.85 (d, *J* = 8.5 Hz, 2H), 3.82-3.77 (m, 4H), 3.56 (q, *J* = 12.9 Hz, 2H), 1.36 (d, *J* = 6.6 Hz, 3H). **¹³C NMR** (CDCl₃, 100 MHz) δ (ppm) 158.6, 145.7, 132.8, 129.3, 128.5, 126.9, 126.7, 113.8, 57.4, 55.3, 51.1, 24.6. **HRMS** (CI) [M+H]⁺ Calculated 242.1539; [M+H]⁺ found 242.1545. **HPLC** (Chiralpak IB-3, 99.8:0.2 Hex:IPA (+ 0.1% HNEt₂), 0.5 mL/min, 25 °C, 254 nm) 25.69 min (major) and 27.27 min.



***N*-(2-Chlorobenzyl)-1-phenylethanamine**

Yellow oil isolated in 90% and 93% yields (in the organic and aqueous systems respectively). **¹H NMR** (CDCl₃, 400 MHz,) δ (ppm) 7.39-7.30 (m, 6H), 7.26-7.23 (m, 1H), 7.22-7.16 (m, 2H), 3.82-3.67 (m, 3H), 1.8 (bs, 1H), 1.37 (d, *J* = 6.5 Hz, 3H). **¹³C NMR** (CDCl₃, 100 MHz) δ (ppm) 145.3, 137.8, 133.8, 130.5, 129.5, 128.5, 128.3, 127.0, 126.8, 57.4, 49.3, 24.6. **HRMS** (CI) [M+H]⁺ Calculated 246.1044; [M+H]⁺ found 246.1055. **HPLC** (Chiralpak IB-3, 99.8:0.2 Hex:IPA (+ 0.1% HNEt₂), 0.5 mL/min, 25 °C, 254 nm) 17.63 min (major) and 18.77 min.

3.7 References

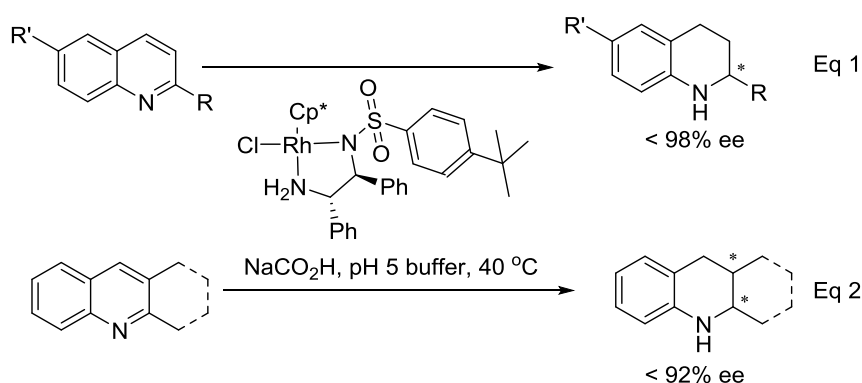
- 1 T. Gross, A. M. Seayad, M. Ahmad and M. Beller, *Org. Lett.*, 2002, **4**, 2055–8.
- 2 J. J. Kangasmetsä and T. Johnson, *Org. Lett.*, 2005, **7**, 5653–5655.
- 3 A. F. Abdel-magid and S. J. Mehrman, *Org. Process Res. Dev.*, 2006, **971**, 971–1031.
- 4 A. Robichaud and A. Nait Ajjou, *Tet. Lett.*, 2006, **47**, 3633–3636.
- 5 D. Menche, J. Hassfeld, J. Li, G. Menche, A. Ritter and S. Rudolph, *Org. Lett.*, 2006, **8**, 741–4.
- 6 D. Gnanamgari, A. Moores, E. Rajaseelan and R. H. Crabtree, *Organometallics*, 2007, **26**, 1226–1230.
- 7 C. Wang, A. Pettman, J. Basca and J. Xiao, *Angew. Chem. Int. Ed.*, 2010, **49**, 7548–52.
- 8 Q. Lei, Y. Wei, D. Talwar, C. Wang, D. Xue and J. Xiao, *Chem. Eur. J.*, 2013, **19**, 4021–4029.
- 9 D. Talwar, N. P. Salguero, C. M. Robertson and J. Xiao, *Chem. Eur. J.*, 2014, **20**, 245–252.
- 10 M. Chang, S. Liu, K. Huang and X. Zhang, *Org. Lett.*, 2013, **15**, 4354–4357.
- 11 S. Zhou, S. Fleischer, H. Jiao, K. Junge and M. Beller, *Adv. Synth. Catal.*, 2014, **365**, 3451–3455.
- 12 D. Steinhuebel, Y. Sun, K. Matsumura, N. Sayo and T. Saito, *J. Am. Chem. Soc.*, 2009, **131**, 11316–7.
- 13 O. Bondarev and C. Bruneau, *Tet. Asym.*, 2010, **21**, 1350–1354.

- 14 K. Matsumura, X. Zhang, K. Hori, T. Murayama, T. Ohmiya, H. Shimizu, T. Saito and N. Sayo, *Org. Process Res. Dev.*, 2011, **15**, 1130–1137.
- 15 C. Li, B. Villa-Marcos and J. Xiao, *J. Am. Chem. Soc.*, 2009, **131**, 6967–9.
- 16 B. Villa-Marcos, C. Li, K. R. Mulholland, P. J. Hogan and J. Xiao, *Molecules*, 2010, **15**, 2453–2472.
- 17 R. Kadyrov and T. H. Riermeier, *Angew. Chem. Int. Ed.*, 2003, **42**, 5472–4.
- 18 R. I. Storer, D. E. Carrera, Y. Ni and D. W. C. MacMillan, *J. Am. Chem. Soc.*, 2006, **128**, 84–6.
- 19 S. Werkmeister, S. Fleischer, S. Zhou, K. Junge and M. Beller, *ChemSusChem*, 2012, **5**, 777–782.
- 20 C. Denhez, J. L. Vasse and J. Szymoniak, *Synthesis*, 2005, **2**, 2075–2079.
- 21 H. Hikawa, K. Izumi, Y. Ino, S. Kikkawa, Y. Yokoyama and I. Azumaya, *Adv. Synth. Catal.*, 2015, **357**, 1037–1048.
- 22 S. Zhu, J. Xie, Y. Zhang, S. Li and Q. Zhou, *J. Am. Chem. Soc.*, 2006, **128**, 12886–12891.
- 23 A. J. Minnaard, B. L. Feringa and J. G. De Vries, *J. Am. Chem. Soc.*, 2009, **131**, 8358–8359.
- 24 S. Y. Shirai, H. Nara, Y. Kayaki and T. Ikariya, *Organometallics*, 2009, **28**, 802–809.
- 25 C. Wang, X. Wu, L. Zhou and J. Sun, *Chem. Eur. J.*, 2008, **14**, 8789–8792.

Chapter 4: Asymmetric Transfer Hydrogenation of Quinolines

4.1 Introduction

The reduction of quinolines has long been a desirable process, due to the biological activity of the tetrahydroquinoline motif.¹ Whilst a number of AH systems have been reported, the ATH of quinolines has proved a more challenging process, with the majority of systems utilising chiral phosphoric acids²⁻⁵ and only a few metal catalysed systems published.⁶⁻⁸ Of the metal catalysed systems a rhodium DPEN based complex proved the most successful, allowing for highly selective reduction of 2-substituted quinolines, as well as two 2,3-disubstituted quinolines (Scheme 4.1).⁷



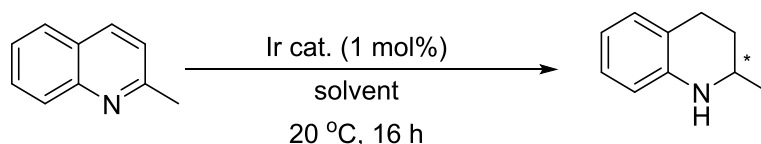
Scheme 4.14 Rhodium catalysed ATH of quinolines.

4.2 Complex Screening

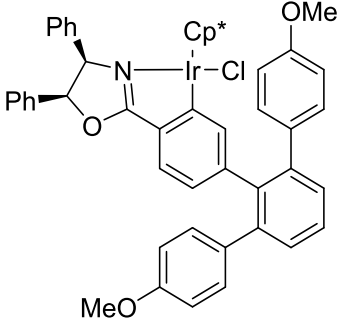
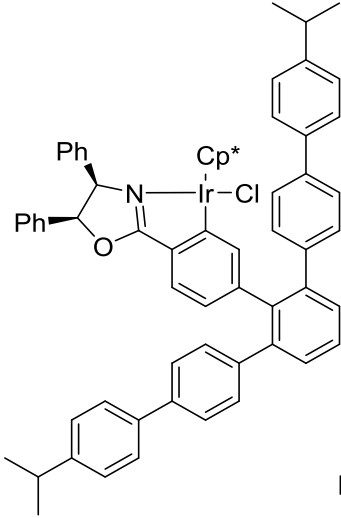
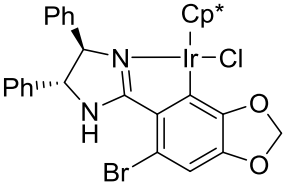
To further explore the activity of the chiral iridium complexes developed in Chapter 2, quinoline ATH was investigated. A test reaction showed activity in both the IPA/FT conditions, as well as the aqueous conditions previously reported for use with the racemic iridicycles.⁹ A variety of complexes were screened under both conditions to determine the impact upon the conversion and selectivity. With a range of complexes tested, IPA/FT conditions afforded the highest selectivity, although only low to moderate conversions were observed (Table 4.1). Aq

NaCO₂H/HCO₂H (pH 4.5) afforded a slight reduction in selectivity with complete conversion (Table 4.1). These aqueous conditions were therefore deemed favourable and taken forward for further complex screening.

The results in Table 4.1 show that the bulky oxazoline complexes were the most selective for this transformation, with both terphenyl complexes (**Ir 14** and **Ir 17**) screened providing the highest ee's of 55-60% (Entries 3 and 4, Table 4.1). Less bulky oxazolines (Entries 1 and 2, Table 4.1) yielded much lower selectivities, with the imidazoline complex (**Ir 30**) producing an almost racemic product (Entry 5, Table 4.1).



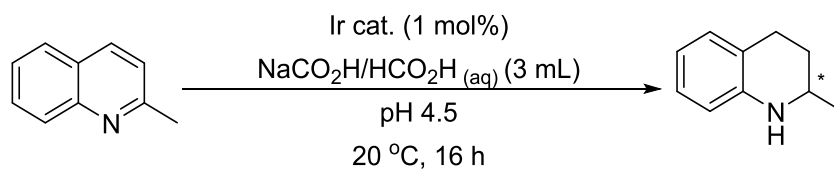
Entry	Catalyst	IPA (2 mL) FT		NaCO ₂ H/HCO ₂ H _(aq)	
		(0.5 mL)		(pH 4.5) (2.5 mL)	
		Conv (%)	ee (%)	Conv (%)	ee (%)
1	 Ir 7	42	20	100	14
2	 Ir 9	38	21	100	17

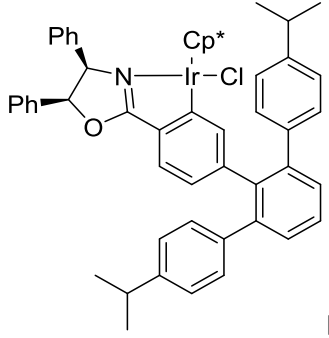
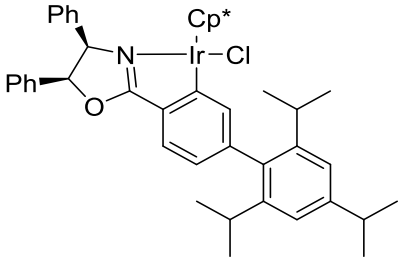
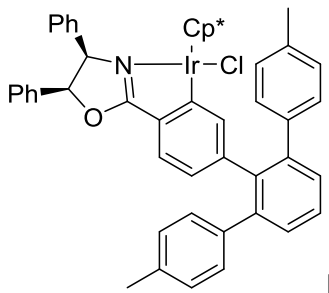
3	 Ir 14	35	60	100	57
4	 Ir 17	26	60	100	55
5	 Ir 30	40	5	-	-

Reaction conditions: 0.5 mmol quinoline, 1 mol% iridium complex, 2.5 mL solvent/hydride source, sealed, overnight.

Table 4.20 Comparison of organic and aqueous conditions for ATH of quinoline.

Further terphenyl complexes were screened to determine if the selectivity could be improved upon. The simple *p*-methyl terphenyl **Ir 12** yielded a surprisingly low ee (Entry 3, Table 4.2), whilst the 4-*iso*-propyl terphenyl **Ir 13** and 2,4,6-*iso*-propyl phenyl **Ir 11** complexes (Entries 1 and 2 respectively, Table 4.2) provided the greatest selectivities.



Entry	Catalyst	Conv (%)	ee (%)
1	 Ir 13	100	66
2	 Ir 11	100	58
3	 Ir 12	100	10

Reaction conditions: 0.5 mmol quinoline, 1 mol% iridium complex, 3 mL aq NaCO₂H/HCO₂H pH 4.5, sealed, overnight.

Table 4.21 Screening of bulky oxazoline complexes.

With a complex in hand able to produce moderate ee and complete conversion under mild conditions, the versatility of this system was investigated. Although higher selectivity was shown by the **Ir 13**, this catalyst is more expensive

and challenging to synthesise than **Ir 11**, which was the second best complex, therefore this is utilised for further screening of the substrate range.

4.3 Additive screening

Investigation of substrate scope was initiated with commercially available 8-chloroquinoline. This substrate provided just 30% conversion and 37% ee (Entry 1, Table 4.3) under the standard conditions. The lower conversion was attributed to the insolubility of the substrate in the aqueous reaction medium with both complex and substrate on the surface of the water with little interaction. In the racemic system, this problem was circumvented by heating the mixture at reflux.

A range of co-solvents were investigated for improving the solubility of the solid substrates. Apart from methanol and polyethylene glycol (Entries 1 and 6, Table 4.3) all co-solvents screened offered an increase in conversion and ee. The highest ee was observed when the reaction was carried out in the presence of 2-MeTHF (Entry 4, Table 4.3). Although the conversion was lower than with that achieved when DCM or IPA was used (Entries 3 and 4, Table 4.3), the conversion and ee were satisfactory for this co-solvent to be taken forward for further screening.

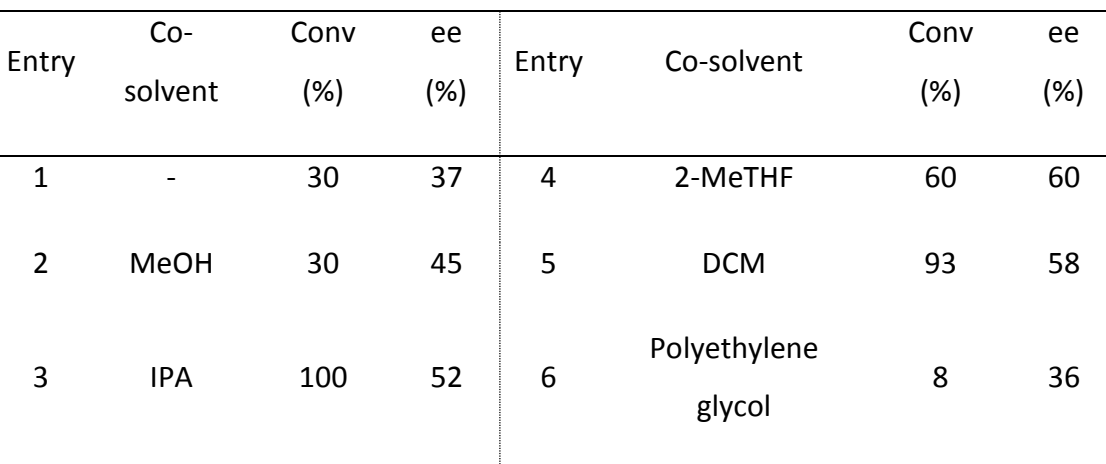
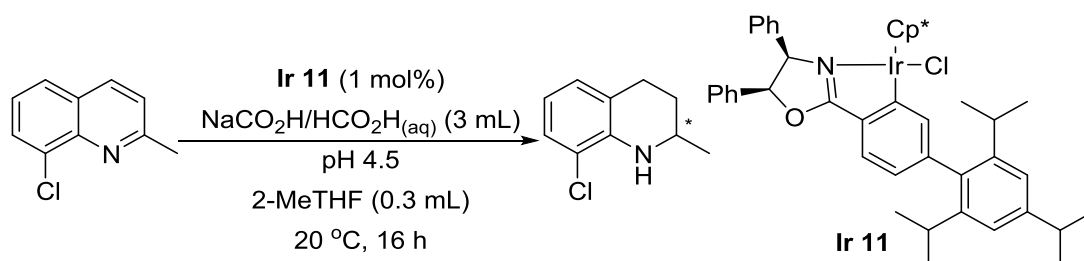


Table 4.22 Screening of co-solvents for ATH of 8-chloroquinaldine.

156

90% with 70% ee and so the combination of this with 2-MeTHF was taken forward to further explore the scope of this transformation.



Entry	Additive (10 mol%)	Conv (%)	ee (%)	Entry	Additive (10 mol%)	Conv (%)	ee (%)
1	SDS	90	70	5		30	57
2	Diethylmalonate	84	57	6		63	54
3	2,3-Butandiol	35	41	7		67	59
4		62	65	8		75	59

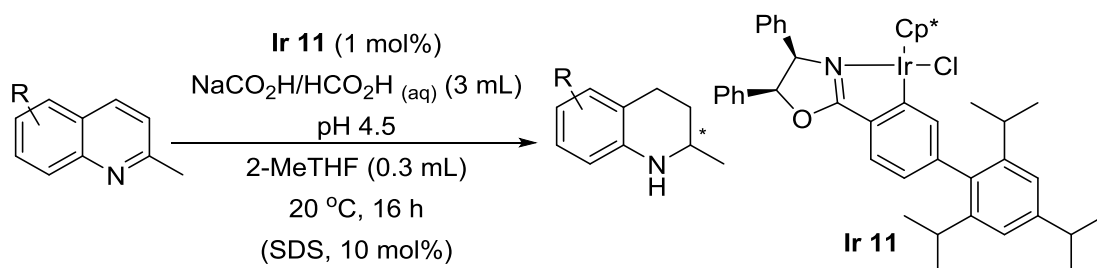
Reaction conditions: 0.5 mmol quinoline, 1 mol% Ir 11, 10 mol% additive, 0.3 mL 2-MeTHF, 3 mL aq NaCO₂H/HCO₂H pH 4.5, sealed, overnight.

Table 4.23 Screening of additives for ATH of 8-chloroquinoline.

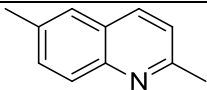
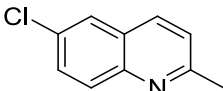
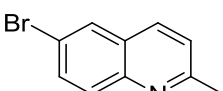
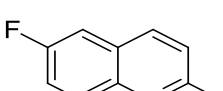
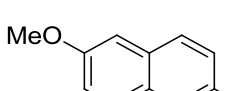
4.4 Substrate Scope

4.4.1 2-Substituted quinolines

A range of commercially available 2-substituted quinolines were screened to explore the activity of this ATH system. The addition of SDS had shown great benefit to the 8-chloroquinoline; however its presence with the liquid substrate quinaldine had a detrimental effect with little conversion being observed (Entries 1 and 2, Table 4.5). Further substrates were screened for both systems, in the presence and absence of SDS, using 2-MeTHF as a co-solvent (Table 4.5).



Entry	Substrate	Without SDS		With SDS	
		Conv (%)	ee (%)	Conv (%)	ee (%)
1		100*	68	5	-
2		60	60	90	70
3		90	-	/	/
4		95	-	/	/

5		100	66	100	60
6		100	51	100	36
7		100	50	100	36
8		100	52	100	40
9		100	73	100	65

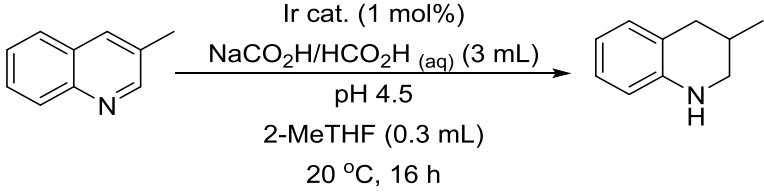
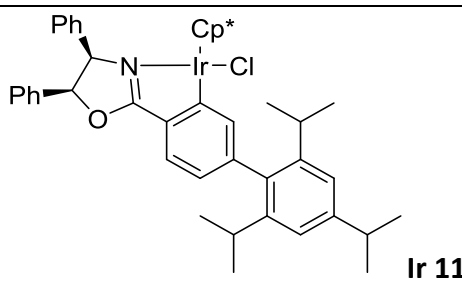
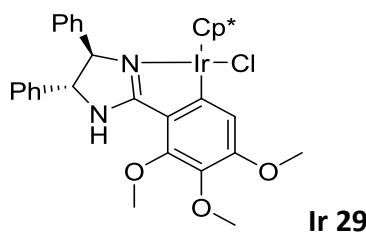
Reaction conditions: 0.5 mmol quinoline, 1 mol% Ir 11, (10 mol% SDS), 0.3 mL 2-MeTHF, 3 mL aq NaCO₂H/HCO₂H pH 4.5, sealed, overnight. (* ran for 7 h)

Table 4.24 Substrate scope for ATH of quinolines.

The most readily available substitution pattern available is 2,7-quinolines. From these it can be seen that the electronics of the substituents have an impact upon the selectivity although not conversion, with 7-methoxy and 7-methyl quinoline providing the highest ee's in the absence of SDS, 73% and 66% respectively (Entries 5 and 9, Table 4.5). Although lower in the presence of SDS the ee's were still moderately high (65% and 60% respectively). Electron withdrawing groups showed a larger drop in selectivity in the presence of SDS, down to roughly 35% ee from 50% (Entries 6-8, Table 4.5). 2,8-dimethyltetrahydroquinoline and 2-methyl-7-chlorotetrahydroquinoline proved active under the described system, however chiral HPLC analysis proved unsuccessful.

4.4.2 3- and 4-Substituted quinolines

With a range of 2-substituted quinolines investigated, attention was turned to the more challenging 3- and 4- substituted quinolines. Initially, the commercially available 3-methylquinoline was investigated. Under the standard conditions the rate of reaction remained high, although a racemic product was yielded (Entry 1, Table 4.6). Upon varying the catalyst to a less bulky, electron-rich imidazoline complex, the conversion was improved but once more a racemic product was obtained (Entry 2, Table 4.6), indicating the 3-substituted quinolines may not be a suitable substrates for this catalytic system.

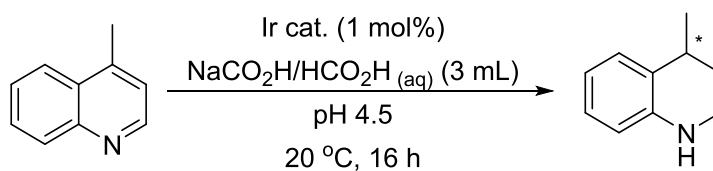
			
Entry	Catalyst	Conv (%)	ee (%)
1	 Ir 11	93	0
2	 Ir 29	100	0

Reaction conditions: 0.5 mmol quinoline, 1 mol% iridium complex, 0.3 mL 2-MeTHF, 3 mL aq NaCO₂H/HCO₂H pH 4.5, sealed, overnight.

Table 4.25 ATH of 3-methylquinoline.

Lepidine showed greater promise, however, under standard conditions, an ee of 15% and a low conversion of 20% was observed (Entry 1, Table 4.7). Removal of the 2-MeTHF offered a slight improvement in both selectivity and conversion by 5% (Entry 2, Table 4.7). Varying the iridicycle used to the less bulky imidazolines improved conversion, to < 90% (Entries 3-5, Table 4.7). The trimethoxy imidazoline complex also showed an improvement in selectivity up to 30% (Entries 4 and 5, Table 4.7). Although only a moderate ee, this proved to be only the second ATH system for reduction of 4-substituted quinolines reported, using milder conditions and shorter reaction times.¹⁰

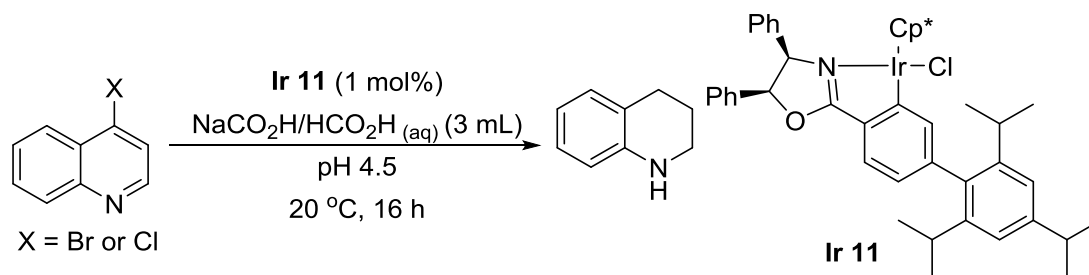
Variation of the substituent from a methyl group to an electron withdrawing halogen gave complete conversion, to 1,2,3,4-tetrahydroquinoline, arising from complete C-X bond cleavage during the reaction (Scheme 4.2). Indicating that halides, and potentially other good leaving groups, are unlikely to be suitable substrates for this transformation. This reaction potentially occurred *via* an initial 1,4-hydride addition, the aromaticity could then be reinstated by the loss of the 4-halide, allowing for a second 1,4-addition, isomerisation and a 1,2-hydride addition, as reported in the racemic system (Figure 4.1).⁹



Entry	Catalyst	2-MeTHF	Conv (%)	ee (%)
1	 Ir 11	0.3 mL	20	15
2		-	25	20
3	 Ir 30	-	97	16
4		0.3 mL	80	30
5	 Ir 29	-	90	30

Reaction conditions: 0.5 mmol quinoline, 1 mol% iridium complex, (0.3 mL 2-MeTHF), 3 mL aq NaCO₂H/HCO₂H pH 4.5, sealed, overnight.

Table 4.26 ATH of lepidine.



Scheme 4.15 Attempted ATH of 4-bromo and chloro quinoline.

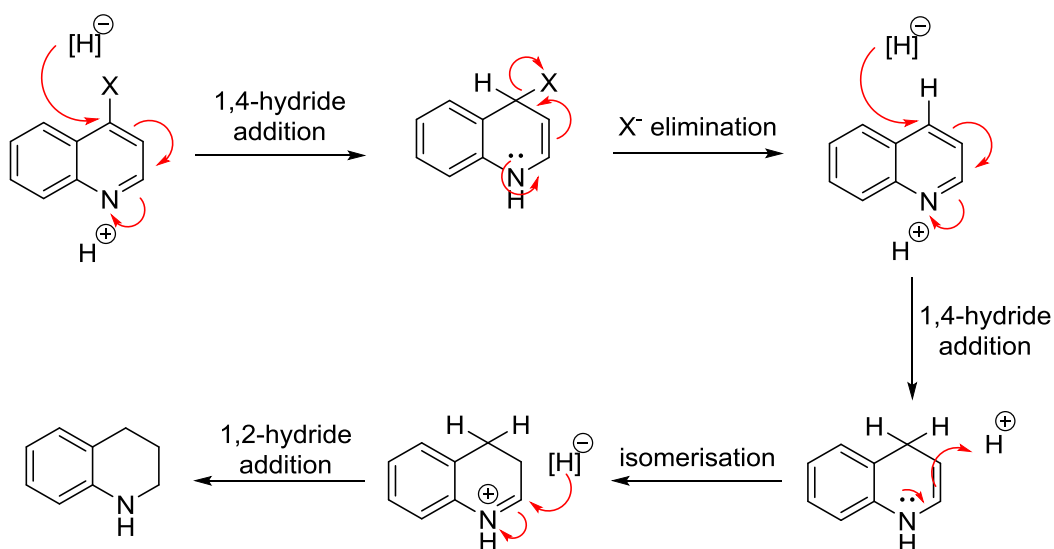


Figure 4.12 Proposed mechanism for halide elimination during ATH.

4.5 Conclusion

The asymmetric reduction of quinolines proved successful with the developed iridium complexes. The greatest results were seen in the presence of a bulky oxazoline complex on an aqueous medium. The presence of a co-solvent was able to further improve the conversion and enantioselectivities, particularly for solid substrates, which are insoluble in the aqueous medium. Although the conversions and ee's obtained were lower than other published systems, it demonstrated a further use for these asymmetric iridium complexes. Whilst 3-substituted quinolines proved to be inactive under these reaction conditions, greater promise was shown for 4-substituted quinolones, with low conversion and a moderate enantioselectivity being achieved under the standard conditions. Halide groups were shown to be unstable under the ATH conditions, resulting in exchange of the halide for a proton.

4.6 Experimental

The iridium complexes were synthesised as described in Chapter 2. IPA was dried on a MB-SPS 800. All other chemicals were obtained commercially and used without further purification. NMR spectra were recorded on a Bruker 400 MHz NMR spectrometer, with TMS as internal standard. HPLC analysis was recorded on an Agilent 1260 Infinity equipped with a Chiralcel OJ-H column.

4.6.1 General Procedures

ATH under organic conditions

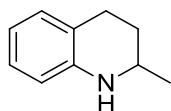
A glass vial was charged with the iridium catalyst (1 mol%) and quinoline (0.5 mmol), along with a stirrer bar. IPA (2.5 mL) was added, followed finally by FT (0.5 mL) to initiate the reaction. The glass vial was sealed and stirred at 20 °C for 16 h. After the reaction time, it was quenched by the addition of 10% NaOH and extracted into EtOAc. The organic phase was dried over MgSO₄, filtered and evaporated under vacuum. The resulting residue was purified by column chromatography, using 15% EtOAc in hexane, upon which HPLC analysis was performed.

ATH under aqueous conditions

A glass vial was charged with the iridium catalyst (1 mol%), quinoline (0.5 mmol) and an additive when desired (10 mol%) along with a stirrer bar and co-solvent (0.3 mL), followed by an aqueous solution of NaCO₂H/HCO₂H pH 4.5 (3 mL) to initiate the reaction. The glass vial was sealed and stirred at 20 °C for 16 h. After the reaction time it was quenched by the addition of saturated aq K₂CO₃ and extracted into EtOAc. The organic phase was dried over MgSO₄, filtered and evaporated under

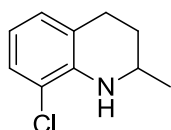
vacuum. The resulting residue was purified by column chromatography, using 15% EtOAc in hexane, upon which HPLC analysis was performed.

4.6.2 Analytical data



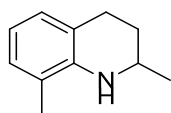
2-Methyl-1,2,3,4-tetrahydroquinoline⁷ In accordance with published data.

Yellow oil isolated in up to 98% yield. ¹H NMR (CDCl₃, 400 MHz) δ (ppm) 6.97-6.94 (t, J = 6.2 Hz, 2H), 6.60 (t, J = 7.3 Hz, 1H), 6.46 (d, J = 8.6 Hz, 1H), 3.68 (bs, 1H), 3.43-3.35 (m, 1H), 2.83 (ddd, J = 16.5, 11.3, 5.6 Hz, 1H), 2.72 (dt, J = 16.2, 4.4 Hz, 1H), 1.95-1.89 (m, 1H), 1.63-1.53 (m, 1H), 1.20 (d, J = 6.2 Hz, 3H). ¹³C NMR (CDCl₃, 100 MHz) δ (ppm) 144.8, 129.3, 126.7, 121.1, 117.0, 114.0, 47.2, 30.2, 26.6, 22.6. **HRMS** (CI) calculated [M+H]⁺ 148.1121. found [M+H]⁺ 148.1127. **HPLC** (Chiralcel OJ-H, 95:5 Hex:IPA +0.1% HNEt₂, 1 mL/min, 25 °C, 254 nm) 12.45 min and 13.70 min (major).



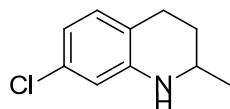
8-Chloro-2-methyl-1,2,3,4-tetrahydroquinoline⁹ In accordance with published data.

Yellow solid isolated in up to 87% yield. ¹H NMR (CDCl₃, 400 MHz) δ (ppm) 7.06 (d, J = 7.9 Hz, 1H), 6.86 (d, J = 7.4 Hz, 1H), 6.51 (t, J = 7.7 Hz, 1H), 4.26 (bs, 1H), 3.50-3.43 (m, 1H), 2.88-2.73 (m, 1H), 1.94 (ddt, J = 12.8, 5.4, 3.5 Hz, 1H), 1.58 (dddd, J = 12.8, 11.2, 9.9, 5.5 Hz, 1H), 1.27 (d, J = 6.2 Hz, 3H). ¹³C NMR (CDCl₃, 100 MHz) δ (ppm) 140.7, 127.4, 126.7, 122.4, 117.8, 116.3, 47.2, 29.6, 26.8, 22.5. **HPLC** (Chiralcel OJ-H, 95:5 Hex:IPA +0.1% HNEt₂, 1 mL/min, 25 °C, 254 nm) 5.03 min and 5.31 min (major).



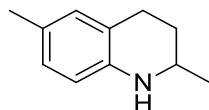
2,8-Dimethyl-1,2,3,4-tetrahydroquinoline

Yellow oil isolated in up to 85% yield. $^1\text{H NMR}$ (CDCl_3 , 400 MHz) δ (ppm) 6.86 (t, J = 6.3 Hz, 2H), 6.55 (t, J = 7.4 Hz, 1H), 3.47-3.40 (m, 2H), 2.90-2.82 (m, 1H), 2.08 (s, 3H), 1.96-1.90 (m, 1H), 1.63, 1.53 (m, 1H), 1.25 (d, J = 6.3 Hz, 3H). $^{13}\text{C NMR}$ (CDCl_3 , 100 MHz) δ (ppm) 142.7, 129.5, 127.9, 127.2, 125.5, 116.4, 47.4, 30.1, 26.9, 22.9, 17.2.



7-Chloro-2-methyl-1,2,3,4-tetrahydroquinoline¹¹ In accordance with published data.

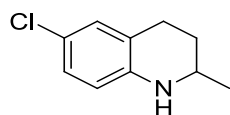
Yellow solid isolated in up to 93% yield. $^1\text{H NMR}$ (CDCl_3 , 400 MHz) δ (ppm) 6.83 (d, J = 7.9 Hz, 1H), 6.53 (dd, J = 8.0, 2.0 Hz, 1H), 6.41 (d, J = 2.0 Hz, 1H), 3.41-3.34 (m, 1H), 2.79-2.65 (m, 2H), 1.93-1.88 (m, 1H), 1.56-1.49 (m, 1H), 1.19 (d, J = 6.2 Hz, 3H). $^{13}\text{C NMR}$ (CDCl_3 , 100 MHz) δ (ppm) 145.8, 131.9, 130.2, 119.3, 116.6, 113.3, 47.0, 29.8, 26.1, 22.5.



2,6-Dimethyl-1,2,3,4-tetrahydroquinoline⁷ In accordance with published data.

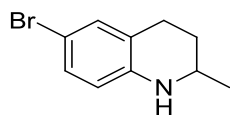
Yellow solid isolated in up to 97% yield. $^1\text{H NMR}$ (CDCl_3 , 400 MHz) δ (ppm) 6.78-6.77 (m, 2H), 6.4 (d, J = 7.9 Hz, 1H), 3.57 (bs, 1H), 3.35 (ddd, J = 9.7, 6.5, 2.8 Hz, 1H), 2.85-2.77 (m, 1H), 2.72-2.65 (m, 1H), 2.20 (s, 3H), 1.94-1.88 (m, 1H), 1.57 (tdd, J = 12.1,

10.1, 5.5 Hz, 1H), 1.19 (d, J = 6.3 Hz, 3H). **¹³C NMR** (CDCl₃, 100 MHz) δ (ppm) 141.5, 129.8, 127.2, 121.3, 114.3, 47.3, 30.4, 26.6, 22.6, 20.4. **HPLC** (Chiralcel OJ-H, 95:5 Hex:IPA +0.1% HNEt₂, 1 mL/min, 25 °C, 254 nm) 18.5 min (major) and 23.2min.



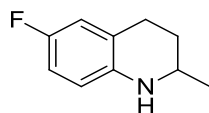
6-Chloro-2-methyl-1,2,3,4-tetrahydroquinoline⁷ In accordance with published data.

Yellow solid isolated in up to 98% yield. **¹H NMR** (CDCl₃, 400 MHz) δ (ppm) 6.91-6.87 (m, 2H), 6.37 (d, J = 8.4 Hz, 1H), 3.69 (bs, 1H), 3.37 (ddd, J = 9.7, 6.4, 2.9 Hz, 1H), 2.79 (ddd, J = 16.6, 11.3, 5.7 Hz, 1H), 2.68 (dt, J = 16.3, 4.5 Hz, 1H), 1.91-1.88 (m, 1H), 1.53 (m, 1H), 1.2 (d, J = 6.2 Hz, 3H). **¹³C NMR** (CDCl₃, 100 mHz) δ 143.3, 128.8, 126.5, 122.6, 121.3, 114.9, 47.2, 29.7, 26.5, 22.5. **HPLC** (Chiralcel OJ-H, 95:5 Hex:IPA +0.1% HNEt₂, 1 mL/min, 25 °C, 254 nm) 14.9 min (major) and 17.9 min.



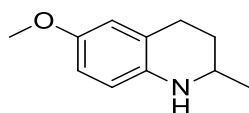
6-Bromo-2-methyl-1,2,3,4-tetrahydroquinoline⁷ In accordance with published data.

Yellow solid isolated in up to 94% yield. **¹H NMR** (CDCl₃, 400 MHz) δ (ppm) 7.06-7.01 (m, 2H), 6.34 (d, J = 8.5 Hz, 1H), 3.71 (bs, 1H), 3.37 (dq, J = 9.6, 6.4, 2.8 Hz, 1H), 2.84-2.75 (m, 1H), 2.72-2.66 (m, 1H), 1.94-1.88 (m, 1H), 1.59-1.49 (m, 2H), 1.20 (d, J = 6.2Hz, 3H). **¹³C NMR** (CDCl₃, 100 MHz) δ (ppm) 143.8, 131.7, 129.3, 123.1, 115.4, 108.3, 47.1, 29.6, 26.4, 22.5. **HPLC** (Chiralcel OJ-H, 95:5 Hex:IPA +0.1% HNEt₂, 1 mL/min, 25 °C, 254 nm) 17.1 min (major) and 21.28 min.



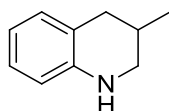
6-Fluoro-2-methyl-1,2,3,4-tetrahydroquinoline⁷ In accordance with published data.

Yellow solid. ¹H NMR (CDCl₃, 400 MHz) δ (ppm) 6.69-6.65 (m, 2H), 6.41-6.38 (m, 1H), 3.38-3.30 (m, 1H), 2.82 (ddd, J = 16.9, 11.4, 5.8 Hz, 1H), 2.73-2.66 m, 1H), 1.94-1.88 (m, 1H), 1.56 (tdd J = 12.8, 10.3, 5.5 Hz, 1H), 1.2 (d, J = 6.2 Hz, 3H). ¹³C NMR (CDCl₃, 100 MHz) δ (ppm) 156.7, 154.3, 140.9, 122.5, 122.5, 115.2, 115.3, 114.8, 114.7, 113.3, 133.1, 47.3, 29.9, 26.7, 26.7, 22.5. HPLC (Chiralcel OJ-H, 95:5 Hex:IPA +0.1% HNEt₂, 1 mL/min, 25 °C, 254 nm) 11.1 min (major) and 11.5 min.



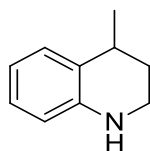
6-Methoxy-2-methyl-1,2,3,4-tetrahydroquinoline⁷ In accordance with published data.

Yellow oil isolated in up to 96% yield. ¹H NMR (CDCl₃, 400 MHz) δ (ppm) 6.61-6.58 (m, 2H), 6.49 (d, J = 8.4 Hz, 1H), 3.72 (s, 3H), 3.36-3.31 (m, 1H), 2.88-2.80 (m, 1H), 2.74-2.68 (m, 1H), 1.95-1.89 (m, 1H), 1.64-1.54 (m, 1H), 1.21 (d, J = 6.2 Hz, 3H). ¹³C NMR (CDCl₃, 100 MHz) δ (ppm) 152.1, 138.3, 122.9, 115.7, 114.6, 112.9, 55.8, 47.6, 30.2, 26.9, 22.4. HPLC (Chiralcel OJ-H, 95:5 Hex:IPA +0.1% HNEt₂, 1 mL/min, 25 °C, 254 nm) 24.8 min (major) and 31.4 min.



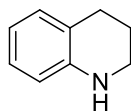
3-Methyl-1,2,3,4-tetrahydroquinoline⁹ In accordance with published data.

Yellow oil isolated in up to 96% yield. ¹H NMR (CDCl₃, 400 MHz) δ (ppm) 6.97-6.92 (m, 2H), 6.60 (t, J = 7.4 Hz, 1H), 6.47 (t, J = 7.9 Hz, 1H), 3.27-3.24 (m, 1H), 2.89 (t, J = 10.3 Hz, 1H), 2.77 (dd, J = 16.0, 4.6 Hz, 1H), 2.42 (dd, J = 16.0, 10.2 Hz, 1H), 2.09-2.02 (m, 1H), 1.04 (d, J = 6.6 Hz, 3H). ¹³C NMR (CDCl₃, 100 MHz) δ (ppm) 144.3, 129.5, 126.7, 121.1, 116.9, 113.9, 48.9, 35.5, 27.2, 19.1. HPLC (Chiracel IB-3, 98:2 Hex:IPA + 0.1% HNEt₂, 1 mL/min, 25 °C, 254 nm) 7.35 min and 8.27 min.



4-Methyl-1,2,3,4-tetrahydroquinoline⁹ In accordance with published data.

Yellow oil isolated in up to 90% yield. ¹H NMR (CDCl₃, 400 MHz) δ (ppm) 7.06 (d, J = 7.7 Hz, 1H), 6.96 (td, J = 7.7, 1.2 Hz, 1H), 6.63 (td, J = 7.4, 1.1 Hz, 1H), 6.48 (dd, J = 7.9, 1 Hz, 1H), 3.36-3.24 (m, 2H), 2.91 (sxt, J = 6.5 Hz, 1H), 2.02-1.95 (m, 1H), 1.68 (dtd, J = 13.0, 6.4, 3.6 Hz, 1H), 1.29 (d, J = 7.0 Hz, 3H). ¹³C NMR (CDCl₃, 100 MHz) δ (ppm) 144.3, 128.5, 126.7, 126.7, 116.9, 114.2, 39.0, 30.2, 29.9, 22.7. HRMS (CI) calculated [M+H]⁺ 148.1121. found [M+H]⁺ 148.1125. HPLC (Chiracel IB-3, 98:2 Hex:IPA + 0.1% HNEt₂, 1 mL/min, 25 °C, 254 nm) 8.09 min (major with Ir **11**) and 8.62 min (major with Ir **29** and **30**).



1,2,3,4-Tetrahydroquinoline⁹ In accordance with published data.

Yellow solid isolated in up to 95% yield. ¹H NMR (CDCl₃, 400 MHz) δ (ppm) 6.98-6.94 (m, 2H), 6.60 (td, J = 1.1, 7.4 Hz, 1H), 6.47 (d, J = 7.9 Hz, 1H), 3.30 (t, J = 5.4 Hz, 2H), 2.76 (t, J = 6.4 Hz, 2H), 1.98-1.91 (m, 2H).

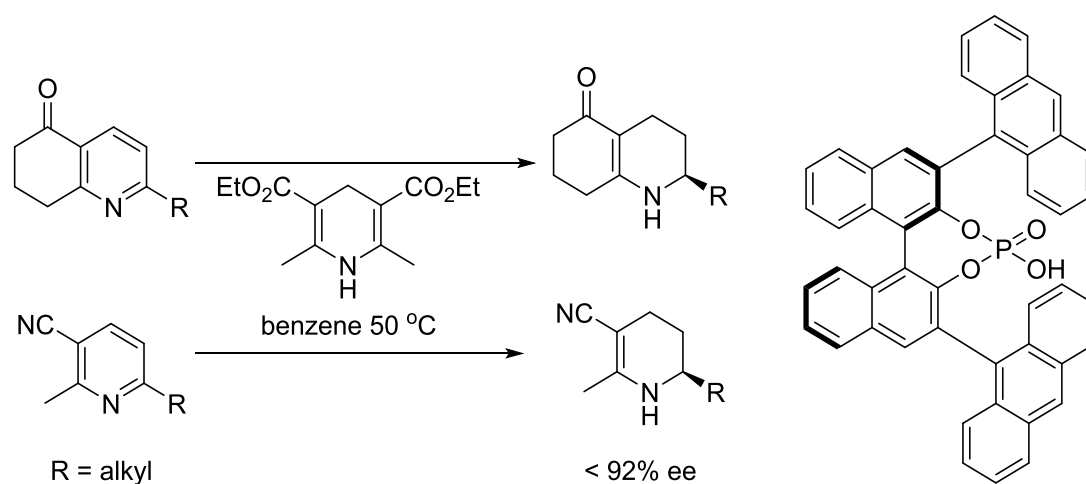
4.7 References

- 1 V. Sridharan, P. a. Suryavanshi and J. C. Menéndez, *Chem. Rev.*, 2011, **111**, 7157–7259.
- 2 M. Rueping, A. P. Antonchick and T. Theissmann, *Angew. Chem. Int. Ed.*, 2006, **45**, 3683–6.
- 3 Q.-S. Guo, D.-M. Du and J. Xu, *Angew. Chem. Int. Ed.*, 2008, **47**, 759–62.
- 4 L. Ren, T. Lei, J.-X. Ye and L.-Z. Gong, *Angew. Chem. Int. Ed.*, 2012, **51**, 771–4.
- 5 X.-F. Cai, R.-N. Guo, G.-S. Feng, B. Wu and Y.-G. Zhou, *Org. Lett.*, 2014, **16**, 2680–3.
- 6 D.-W. Wang, W. Zeng and Y.-G. Zhou, *Tett. Asym.*, 2007, **18**, 1103–1107.
- 7 C. Wang, C. Li, X. Wu, A. Pettman and J. Xiao, *Angew. Chem. Int. Ed.*, 2009, **48**, 6524–8.
- 8 X.-F. Tu and L.-Z. Gong, *Angew. Chem. Int. Ed.*, 2012, **51**, 11346–9.
- 9 D. Talwar, H. Y. Li, E. Durham and J. Xiao, *Chem. Eur. J.*, 2015, **21**, 5370–5379.
- 10 M. Rueping, T. Theissmann, M. Stoeckel and A. P. Antonchick, *Org. Biomol. Chem.*, 2011, **9**, 6844–6850.
- 11 F. R. Gou, W. Li, X. Zhang and Y. M. Liang, *Adv. Synth. Catal.*, 2010, **352**, 2441–2444.

Chapter 5: Asymmetric Transfer Hydrogenation of Pyridinium Salts

5.1 Introduction

The reduction of pyridine and derivatives is a desirable process, with the piperidine motif being found in many natural and pharmaceutical products. However, this remains one of the most challenging C=N bond reductions to achieve. Few successful systems have been reported for the hydrogenation of pyridine and its salts, all of which require pressurised hydrogen gas as the hydride source^{1–5} or a chiral auxiliary,⁶ with some achieving only partial reduction of the aromatic system.⁷ Only one ATH system has been reported (Scheme 5.1); this system is very substrate specific and is only able to partially hydrogenate a limited substrate motif.⁸

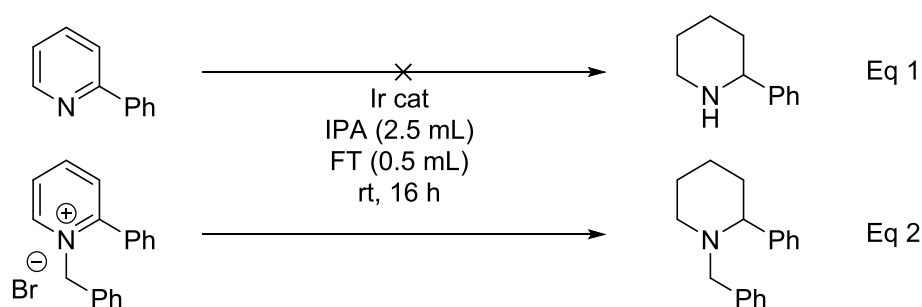


Scheme 5.16 Partial reduction of pyridines *via* phosphoric acid catalysed ATH.

The aim of this chapter is to build on the previous systems reported within Chapters 3 and 4, further extending the scope of the ATH conditions for the reduction of pyridines, with the intention of achieving this transformation under unprecedentedly mild ATH conditions.

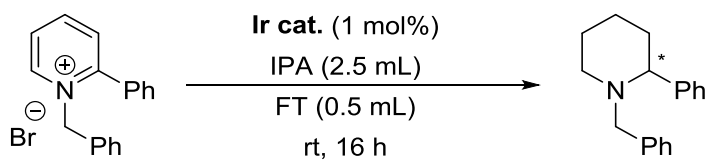
5.2 Screening of Chiral Iridacycles

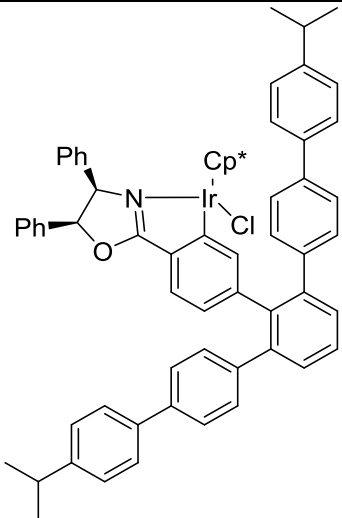
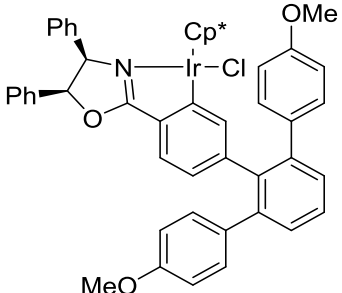
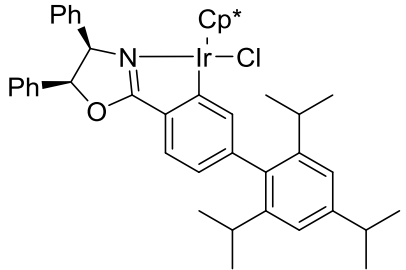
An initial test, using the conditions developed in Chapter 3 for DARA, was trialled for the ATH of 2-phenylpyridine (Eq 1, Scheme 5.2). Initial results showed no conversion, potentially due to the low electrophilicity of the substrate and its ability to bind to the iridium centre rendering it inactive. Therefore the 2-phenylpyridine was subjected to an alkylation reaction forming the *N*-benzyl-2-phenylpyridinium bromide salt, which has a greater activity towards nucleophilic attack. This species was treated to the same ATH conditions with much greater success (Eq 2, Scheme 5.2).

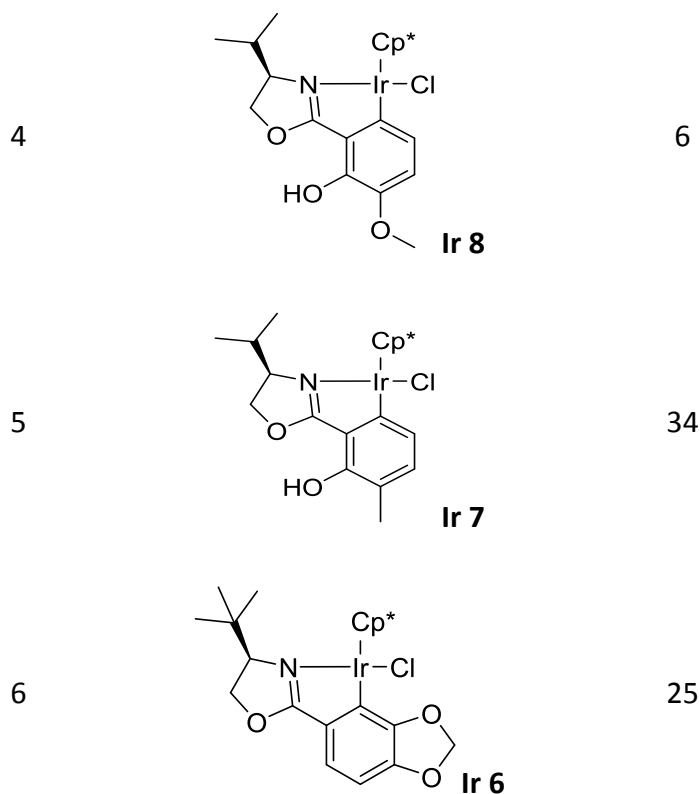


Scheme 5.17 Model ATH, showing alkylation of the pyridine is required.

A range of the developed iridacycles are screened, with a focus on the ee achieved. Initial results indicated that the bulky complexes (**Ir 11**, **Ir 14** and **Ir 17**) produced a low ee (Entries 1-3, Table 5.1). More promising results were seen with the less bulky oxygenated (**Ir 6** - **Ir 8**) complexes giving an ee up to 34% (Entry 5, Table 5.1). The aqueous workup, however, made conversion challenging to determine due to the solubility of any remaining starting salt; therefore conversions are not quoted.



Entry	Complex	ee (%)
1	 <p>Ir 17</p>	20
2	 <p>Ir 14</p>	10
3	 <p>Ir 11</p>	15

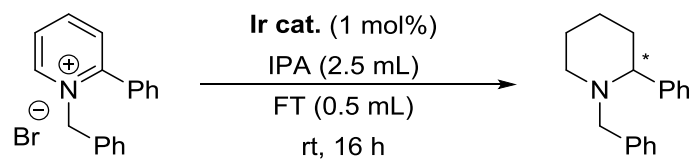


Reaction conditions: 0.5 mmol pyridinium salt, 1 mol% Ir cat, 2.5 mL anhydrous IPA, 0.5 mL FT, sealed, overnight.

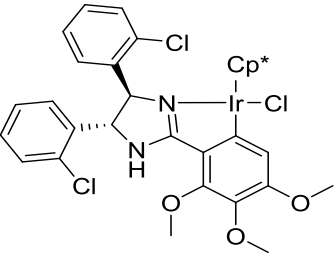
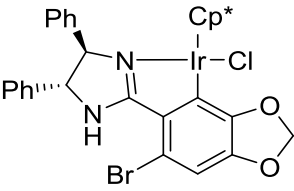
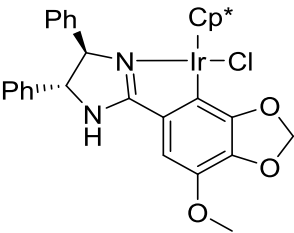
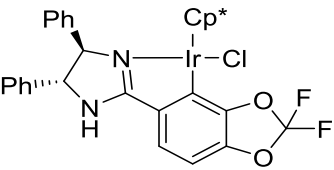
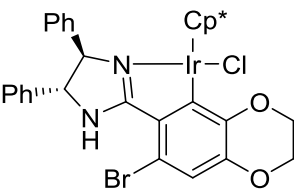
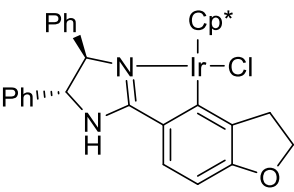
Table 5.27 Iridicycle screening for ATH of pyridinium salts.

Following the same trend as seen in the DARA (Chapter 3), the small electron rich imidazoline-containing complexes were tested to determine if the ee could be improved. Once more the 4,5,6-trimethoxy complex **Ir 29** offered an improved ee (Entry 1, Table 5.2). As seen in the DARA, modification of the phenyl rings of the imidazoline with either an electron donating (**Ir 35**) or electron withdrawing group (**Ir 36**) offered no improvement in ee, once more showing a small range for optimal electronic effects (Entry 4 and 5, Table 5.2). Further testing showed that the dioxole complex **Ir 30** provided the highest ee of 51% (Entry 6, Table 5.2). Further modification of the dioxole motif (**Ir 31** - **Ir 34**), with both

electron donating and withdrawing groups, had a negative effect on the ee (Entries 7-10, Table 5.2).



Entry	Complex	ee (%)
1	<p>Ir 29</p>	44
2	<p>Ir 27</p>	33
3	<p>Ir 21</p>	2
4	<p>Ir 35</p>	24

5	 Ir 36	20
6	 Ir 30	51
7	 Ir 31	46
8	 Ir 32	17
9	 Ir 34	38
10	 Ir 33	10

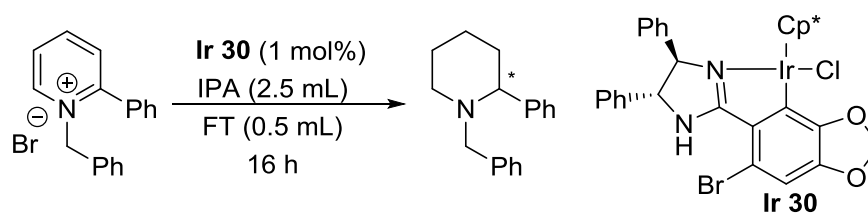
Reaction conditions: 0.5 mmol pyridinium salt, 1 mol% Ir cat, 2.5 mL anhydrous IPA, 0.5 mL FT, sealed, overnight.

Table 5.28 Further iridicycle screening for ATH of the pyridinium salt.

5.3 Condition Optimisation

In an attempt to further improve the ee, the conditions were modified utilising the best catalyst (**Ir 30**) shown above. An initial test was done to determine if the ATH would proceed with a greater selectivity under aqueous conditions. The reaction did progress, however, the ee showed a significant drop (down to 20% from 51%), a much greater difference than seen with aqueous conditions in Chapters 3 and 4. This difference may be due to the reduced interaction between substrate and complex, whilst the pyridine salt is soluble in these conditions, the catalyst is insoluble and therefore effectively sat on the water. As a result no further aqueous conditions were trialled.

Reduced temperatures were also investigated (Table 5.3) to determine the impact upon the selectivity, with an increase in ee expected. This showed great promise with an increase up to 76% ee at -10 °C (Entry 4, Table 5.3), further reduction in temperature offered little improvement.

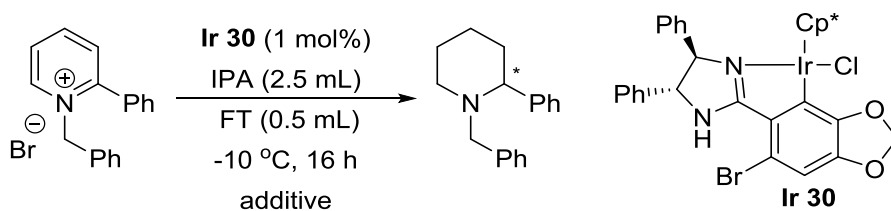


Entry	Temp (°C)	ee (%)
1	20	50
2	10	65
3	5	69
4	-10	76
5	-20	77

Reaction conditions: 0.5 mmol pyridinium salt, 1 mol% Ir 30, 2.5 mL anhydrous IPA, 0.5 mL FT, sealed, overnight.

Table 5.29 Effect of temperature upon ee.

A range of additives were next screened to determine the effect upon the ee (Table 5.3). The presence of water had a detrimental impact on the ee (Entry 1, Table 5.3), indicating that continued use of dry IPA was essential. Alteration of pH by addition of a small amount of formic acid resulted in a significant drop in ee (Entry 2, Table 5.4). Addition of triethylamine offered no improvement in ee, whilst the addition of a large excess of base resulted in complete loss of activity (Entries 3 and 4, Table 5.4). Further indicating that the presence of free amine may poison the catalyst, as previously observed with the unprotected pyridine. Alternatively, significant variation in pH may hinder the reaction, preventing decomposition of the FT to the desired hydride and carbon dioxide.

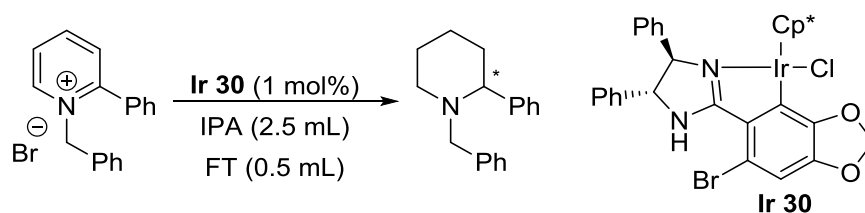


Entry	Additive	ee (%)
1	H ₂ O (0.1 mL)	52
2	HCO ₂ H (0.1 mL)	36
3	NEt ₃ (0.2 mL)	74
4	NEt ₃ (0.3 mL)	n.r

Reaction conditions: 0.5 mmol pyridinium salt, 1 mol% **Ir 30**, 2.5 mL anhydrous IPA, 0.5 mL FT, additive, -10 °C, sealed, overnight.

Table 5.30 Effect of additives on the ATH of pyridinium salt.

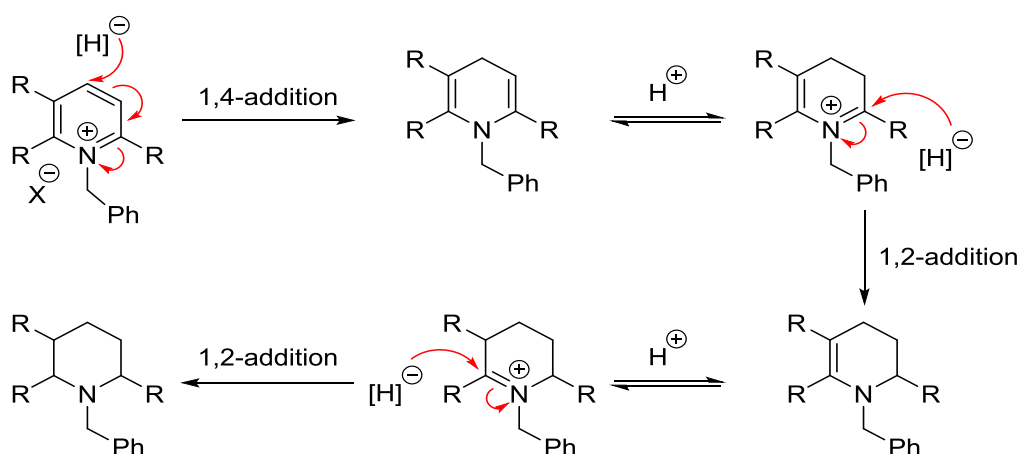
In an attempt to determine if the system required the low temperature of -10 °C to be maintained for the entire reaction in order to achieve high ee's, the time was shortened and two reactions were run simultaneously. The first was run for 9 h at -10 °C and the second was run initially at -10 °C for 4.5 hours, then the reaction temperature increased to 20 °C. These showed vastly different ee's, with the first maintaining the ee previous seen (Entry 1, Table 5.5), whilst the second returned to that previously seen at 20 °C (Entry 2, Table 5.5). These results show that the low temperature must be maintained in order to produce the high ee, indicating the ATH reaction is likely to proceed *via* the known mechanism:⁹ where the reaction occurs *via* a 1,4-addition, followed by isomerisation and finally a 1,2-addition (Scheme 5.3).



Entry	Temp (°C) / Time (h)	ee (%)
1	-10 °C / 9 h	76
2	-10 °C / 4.5 h + 20 °C / 4.5 h	56

Reaction conditions: 0.5 mmol pyridinium salt, 1 mol% Ir 30, 2.5 mL anhydrous IPA, 0.5 mL FT, -10 °C, sealed, 9 h.

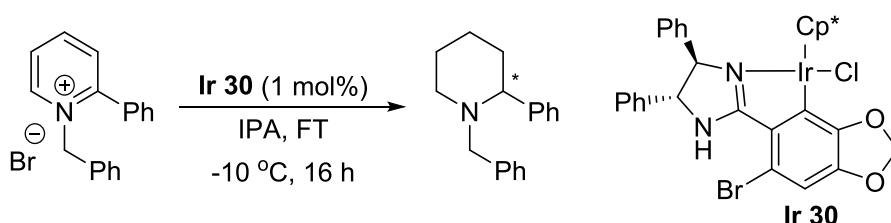
Table 5.31 Effect of varying temperature half way through reaction time.



Scheme 5.18 Potential mechanism of reduction for 2-substituted pyridinium salts.

With the ee optimised, the yield was next investigated using the optimised conditions. Under these conditions the yield was only moderate, with approximately 50% of the product isolated. To overcome this issue the solvent volumes and ratios were altered to improve the conversion. Initial attempts to concentrate the mixture down to 2 mL and vary the ratio of IPA to FT proved ineffective, maintaining the yield around 50% (Entries 1-4, Table 5.6). The low conversion was likely due to the insolubility of the starting salt in the reaction

media. Doubling the IPA volume offered an improvement in yield but caused a drop in ee (Entry 5, Table 5.6), maintaining the original IPA/FT ratio, whilst doubling the volume, showed great improvement allowing for 97% of the product to be isolated, with the same high ee as previous (Entry 6, Table 5.6).



Entry	IPA (mL)	FT (mL)	Yield (%)	ee (%)
1	2.5	0.5	52	77
2	2.5	0.2	56	66
3	2.5	1	58	73
4	1.5	0.5	50	74
5	5	0.5	60	68
6	5	1	97	77

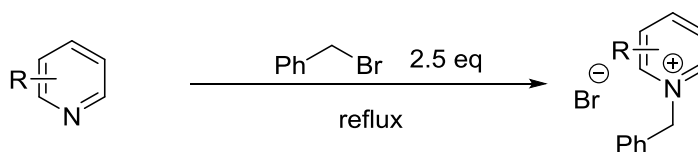
Reaction conditions: 0.5 mmol pyridinium salt, 1 mol% Ir 30, X mL anhydrous IPA, X mL FT, -10 °C, sealed, overnight.

Table 5.32 Optimisation of yield for ATH of pyridine salt.

These conditions were deemed optimal for the reaction as > 95% isolated yield could be attained with the high ee of 77%. The next stage was to determine how widely applicable the ATH could be.

5.4 Substrate Scope

To explore the substrate scope a range of pyridines were activated *via* an alkylation reaction. This was performed by reflux of the pyridine in benzyl bromide until a solid had formed (Scheme 5.4), followed by washing off the excess benzyl bromide.

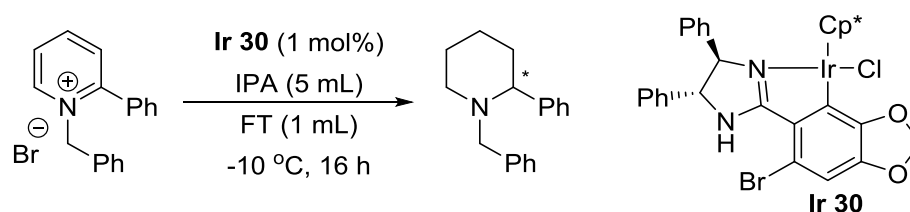


Scheme 5.19 Alkylation of pyridines to form the desired pyridinium salts.

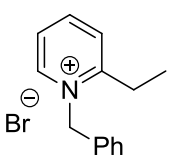
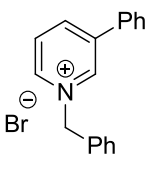
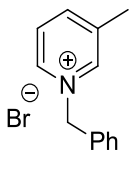
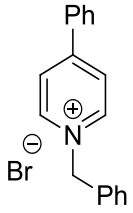
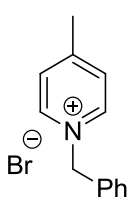
Initial salts synthesised were mono substituted and offered varying steric and electronic effects at the 2-position, with the phenyl ring being substituted with electron donating or withdrawing groups, also being replaced with a alkyl or benzyl group. 3-Substituted pyridines were synthesised, bearing different steric and electronic effects, using methyl and phenyl groups. Pyridines containing 4-substituents were prepared, to determine their activity, although the products could not be chiral.

Once subjected to the ATH conditions, the substrates screened showed great promise with good yields obtained in all reactions. Upon varying the substituent at the 2-position, the isolated yield was seen to decrease (Entries 1-6, Table 5.7), even for the less bulky 2-benzyl substituted pyridinium salt, which produced a very low ee of just 10% (Entry 4, Table 5.7). The addition of a methoxy group upon the phenyl ring produced a similarly high ee, in a moderate yield of 68% (Entry 2, Table 5.7). A similar drop in yield was also seen with various substituents at the 3-position (Entries 7 and 8, Table 5.7). The ee's for the remaining substrates

could not be determined, due to a lack of separation on the available chiral HPLC columns using various solvent systems. High yields could be achieved for 4-substituted pyridinium salts (Entries 9 and 10, Table 5.7); whilst these examples cannot be chiral, they indicate that substitution in this position is tolerable.



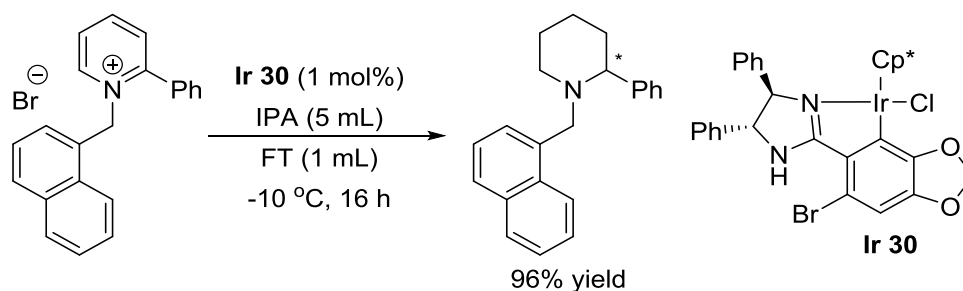
Entry	Substrate	Yield (%)	ee (%)
1		97	77
2		68	75
3		65	nd
4		75	10
5		40	nd

6		60	nd
7		60	nd
8		53	nd
9		75	NA
10		80	NA

Reaction conditions: 0.5 mmol pyridinium salt, 1 mol% Ir 30, 5 mL anhydrous IPA, 1 mL FT, -10 °C, sealed, overnight.

Table 5.33 ATH of various pyridinium salts.

Next, the alkylating group on the pyridine nitrogen was varied in an attempt to further improve the ee. The bulkier 1-(bromomethyl)naphthylene was chosen in the hope that the larger group would make the hydride addition more face selective, therefore improving the enantioselectivity. The 2-phenylpyridine was alkylated as before (Scheme 5.4) and subjected to the optimised conditions (Scheme 5.5). The ATH showed promising results with a high isolated yield (96%); however once more the HPLC trace could offer no separation of the peaks.



Scheme 5.20 Variation of alkylating group for ATH of pyridinium salt.

5.5 Conclusions

The first ATH system for the reduction of pyridinium salts to the corresponding fully hydrogenated piperidine. After an extensive complex screen of the iridicycles to hand it was determined an electron rich imidazoline containing iridicycle was the most active. The selected complex was able to yield high activity and moderate enantioselectivity under mild reaction conditions, with a greater enantioselectivity being observed when conducted at a reduced temperature whilst maintaining a moderate reaction rate. Although ee's could not be determined for all substrates tested, it is believed this would have been possible with the use of SFC.⁵

5.6 Experimental

The iridium complexes were synthesised as described in Chapter 2. Anhydrous IPA was purchased from Sigma Aldrich. All other chemicals were obtained commercially and used without further purification. NMR spectra were recorded on a Bruker 400 MHz NMR spectrometer, with TMS as internal standard. HPLC analysis was recorded on an Agilent machine equipped with Chiralcel OJ-3 column.

5.6.1 Standard procedures

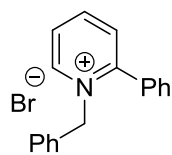
Preparation of pyridinium salts

A pyridine derivative (5-10 mmol) was weighed into a Schlenk tube loaded with a stirrer bar. Benzyl bromide was injected in excess (2.5 eq) and the reaction mixture was heated to reflux. Reaction was deemed complete when a solid had formed. The solid was washed with hexane until the excess benzyl bromide was removed. ^1H NMR was used to determine whether the salt had formed and was clean.

ATH of pyridinium salt

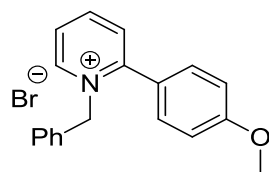
To a Schlenk tube charged with a stirrer bar, the benzyl protected pyridine (0.5 mmol) and an iridium complex (1 mol%) were loaded, followed by IPA (5 mL). The Schlenk tube was inserted into an Integrity 10 machine, pre-set to $-10\text{ }^{\circ}\text{C}$. FT (1 mL) was injected into the Schlenk tube and the reaction mixture left to stir for 16 h. The reaction was quenched by the addition of aq NaOH solution (5 mL); the reaction mixture was warmed to room temperature. The organics were extracted with EtOAc x 3, dried over MgSO_4 and concentrated under vacuum. The resulting residue was purified by column chromatography, using an eluent of 20% EtOAc in hexane, upon which HPLC analysis was performed.

5.6.2 Analytical data



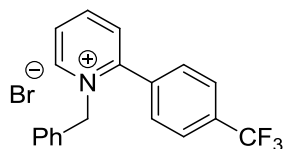
1-Benzyl-2-phenylpyridin-1-ium bromide

White solid. $^1\text{H NMR}$ (DMSO- d_6 , 400 MHz) δ (ppm) 9.34 (d, $J = 7.0$ Hz, 1H), 8.74 (td, $J = 7.9, 1.4$ Hz, 1H), 8.27 (ddd, $J = 7.9, 6.3, 1.5$ Hz, 1H), 8.13 (dd, $J = 7.9, 1.3$ Hz, 1H), 7.66-7.59 (m, 1H), 7.57-7.52 (m, 4H), 7.32-7.26 (m, 3H), 6.92-6.89 (m, 2H), 5.82 (s, 2H). $^{13}\text{C NMR}$ (DMSO- d_6 , 100 MHz,) δ (ppm) 155.56, 146.93, 146.84, 134.25, 132.12, 131.49, 131.34, 129.47, 129.45, 129.31, 129.17, 128.06, 127.95, 61.68.



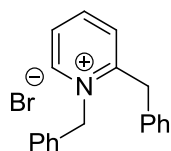
1-Benzyl-2-(4-methoxyphenyl)pyridin-1-ium bromide

White solid. $^1\text{H NMR}$ (CDCl_3 , 400 MHz) δ (ppm) 9.65 (d, $J = 6.3$ Hz, 1H), 8.57 (t, $J = 7.9$ Hz, 1H), 8.09 (ddd, $J = 7.9, 6.3, 1.5$ Hz, 1H), 7.86 (d, $J = 7.9$ Hz, 1H), 7.49 (d, $J = 8.7$ Hz, 2H), 7.30-7.27 (m, 3H), 7.07-7.05 (m, 4H), 6.16 (s, 2H), 3.80 (s, 3H). $^{13}\text{C NMR}$ (CDCl_3 , 100 MHz) δ (ppm) 162.06, 155.97, 147.21, 145.46, 133.37, 130.91, 130.31, 129.39, 129.34, 128.44, 126.94, 123.28, 115.00, 61.89, 55.68.



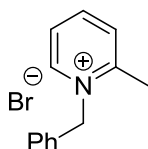
1-Benzyl-2-(4-(trifluoromethyl)phenyl)pyridin-1-ium bromide

White solid. $^1\text{H NMR}$ (CDCl_3 , 400 MHz) δ (ppm) 8.61 (td, $J = 7.9, 1.3$ Hz, 1H), 8.23 (ddd, $J = 7.9, 6.3, 1.5$ Hz, 1H), 7.85 (dd, $J = 7.9, 1.5$ Hz, 1H), 7.8 (s, 4H), 7.32-7.25 (m, 4H), 7.0 (d, $J = 7.9$ Hz, 2H), 6.08 (s, 2H). $^{13}\text{C NMR}$ (CDCl_3 , 100 MHz) δ (ppm) 154.24, 147.74, 145.83, 134.74, 132.57, 130.03, 129.96, 129.62, 129.46, 128.49, 128.04, 126.37, 126.63, 77.25, 63.02.



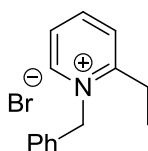
1,2-Dibenzylpyridin-1-ium bromide

White solid. $^1\text{H NMR}$ (CDCl_3 , 400 MHz) δ (ppm) 9.62 (d, $J = 6.1$ Hz, 1H), 8.39 (t, $J = 7.9$ Hz, 1H), 7.99 (t, $J = 6.8$ Hz, 1H), 7.62 (d, $J = 7.9$ Hz, 1H), 7.38-7.26 (m, 8H), 7.17-7.15 (m, 2H), 6.31 (s, 2H), 4.85 (s, 2H). $^{13}\text{C NMR}$ (CDCl_3 , 100 MHz) δ (ppm) 157.96, 147.07, 145.46, 133.22, 131.95, 129.68, 129.65, 129.62, 129.56, 129.53, 128.26, 128.23, 126.25, 61.46, 39.09.



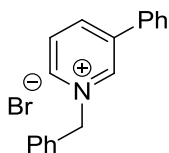
1-Benzyl-2-(4-(trifluoromethyl)phenyl)pyridin-1-ium bromide

White solid. ^1H NMR (CDCl_3 , 400 MHz) δ (ppm) 9.57 (d, J = 5.9 Hz, 1H), 8.43 (td, J = 7.8, 1.2 Hz, 1H), 8.0-7.96 (m, 2H), 7.37-7.30 (m, 5H), 6.22 (s, 2H), 2.93 (s, 3H). ^{13}C NMR (CDCl_3 , 100 MHz) δ (ppm) 155.77, 146.78, 145.59, 131.95, 130.54, 129.57, 129.37, 128.09, 126.14, 61.82, 21.51.



1-Benzyl-2-ethylpyridin-1-ium bromide

White solid. ^1H NMR (CDCl_3 , 400 MHz) δ (ppm) 9.68 (dd, J = 6.1, 1.3 Hz), 8.53 (dt, J = 7.9, 1.3 Hz, 1H), 8.01 (t, J = 6.90 Hz, 1H), 7.94 (d, J = 7.9 Hz, 1H), 7.37-7.29 (m, 5H), 6.27 (s, 2H), 3.24 (q, J = 7.4 Hz, 2H), 1.34 (t, J = 7.4 Hz, 3H). ^{13}C NMR (CDCl_3 , 100 MHz) δ (ppm) 159.96, 147.24, 145.81, 132.41, 129.58, 129.34, 127.80, 125.96, 61.31, 26.34, 11.91.



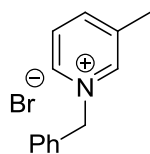
1-Benzyl-3-methylpyridin-1-ium bromide

White solid. ^1H NMR (CDCl_3 , 400 MHz) δ (ppm) 9.72 (s, 1H), 9.47 (d, J = 5.9 Hz, 1H), 8.48 (d, J = 8.3 Hz, 1H), 8.06 (dd, J = 8.3, 5.9 Hz, 1H), 7.84 (dd, J = 8, 1.5 Hz, 2H), 7.71

(dd, $J = 6.8, 2.5$ Hz, 2H), 7.53-7.45 (m, 3H), 7.35 (t, $J = 2.9$ Hz, 3H), 6.44 (s, 2H). ^{13}C

NMR (CDCl_3 , 100 MHz) δ (ppm) 142.37, 141.40, 133.14, 132.67, 130.62, 129.93,

129.85, 129.70, 129.60, 129.03, 128.13, 127.71, 64.18.



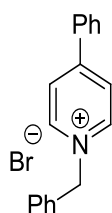
1-Benzyl-3-methylpyridin-1-ium bromide

White solid. ^1H **NMR** (CDCl_3 , 400 MHz) δ (ppm) 9.46 (s, 1H), 9.36 (d, $J = 5.4$ Hz, 1H),

8.15 (d, $J = 8.0$ Hz, 1H), 7.9 (t, $J = 7.0$ Hz, 1H), 7.69 (t, $J = 3.2$ Hz, 2H), 7.38 (d, $J = 1.6$

Hz, 3H), 6.25 (s, 2H), 2.58 (s, 3H). ^{13}C **NMR** (CDCl_3 , 100 MHz) δ (ppm) 145.63, 144.59,

142.17, 133.03, 129.96, 129.68, 129.60, 127.58, 63.96, 18.77.



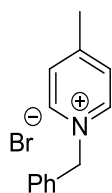
1-Benzyl-4-phenylpyridin-1-ium bromide

White solid. ^1H **NMR** (CDCl_3 , 400 MHz) δ (ppm) 9.58 (d, $J = 7.0$ Hz, 2H), 8.12 (d, $J =$

7.0 Hz, 2H), 7.72-1.69 (m, 4H), 7.59-7.53 (m, 3H), 7.4-7.35 (m, 3H), 6.31 (s, 2H). ^{13}C

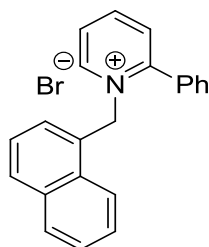
NMR (CDCl_3 , 100 MHz) δ (ppm) 156.58, 144.93, 133.55, 133.06, 132.48, 129.98,

129.96, 129.66, 129.65, 127.81, 124.84, 63.42.



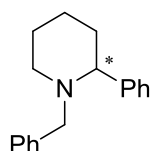
1-Benzyl-4-methylpyridin-1-ium bromide

White solid. $^1\text{H NMR}$ (CDCl_3 , 400 MHz) δ (ppm) 9.50 (d, J = 6.4 Hz, 2H), 7.79 (d, J = 6.4 Hz, 2H), 7.72-7.70 (m, 2H), 7.38-7.31 (m, 3H), 6.24 (s, 2H), 2.59 (s, 3H). $^{13}\text{C NMR}$ (CDCl_3 , 100 MHz) δ (ppm) 158.99, 144.17, 133.32, 129.80, 129.57, 129.52, 128.71, 63.10, 22.26.



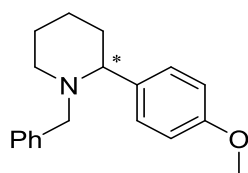
1-(Naphthalen-1-ylmethyl)-2-phenylpyridin-1-ium bromide

White solid. $^1\text{H NMR}$ (CDCl_3 , 400 MHz) δ (ppm) 9.82 (d, J = 6.1 Hz, 1H), 8.63 (t, J = 7.8 Hz, 1H), 8.16 (t, J = 7.0 Hz, 1H), 7.87 (d, J = 7.8 Hz, 1H), 7.76 (d, J = 7.8 Hz, 1H), 7.71 (d, J = 8.4 Hz, 2H), 7.62 (m, 1H), 7.56-7.45 (m, 7H), 7.1 (d, J = 8.4 Hz, 1H), 6.28 (s, 2H). $^{13}\text{C NMR}$ (CDCl_3 , 100 MHz) δ (ppm) 155.75, 147.36, 145.87, 133.22, 132.92, 131.60, 131.31, 130.26, 130.20, 129.52, 129.41, 129.17, 128.65, 127.70, 127.52, 127.21, 126.95, 124.98, 62.36.



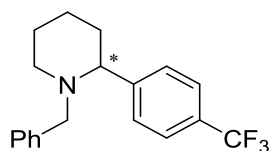
1-Benzyl-2-phenylpiperidine⁵ In accordance with published data.

White solid isolated in 97% yield. **¹H NMR** (CDCl₃, 400 MHz) δ (ppm) 7.45 (d, J = 7.3 Hz, 2H), 7.32 (t, J = 7.3 Hz, 2H), 7.27-7.18 (m, 6H), 3.76 (d, J = 13.6 Hz, 1H), 3.10 (dd, J = 11.0, 2.6 Hz, 1H), 2.96 (d, J = 11.5 Hz, 1H), 2.80 (d, J = 13.5 Hz, 1H), 1.96-1.90 (m, 1H), 1.77 (d, J = 12.5 Hz, 2H), 1.62-1.56 (m, 4H). **¹³C NMR** (CDCl₃, 100 MHz) δ (ppm) 148.73, 139.82, 128.70, 128.49, 128.00, 127.46, 126.87, 126.51, 69.20, 59.79, 53.36, 37.01, 26.00, 25.25. **HRMS** (CI) $[M+H]^+$ calculated 252.1747; found 252.1753. **HPLC** (Chiracel OJ-3, 100% EtOH, 1 mL/min, 25 °C, 220 nm) 1.31 min and 1.66 min.



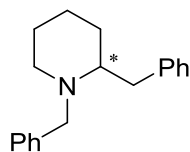
1-Benzyl-2-(4-methoxyphenyl)piperidine⁵ In accordance with published data.

White solid isolated in 68% yield. **¹H NMR** (CDCl₃, 400 MHz) δ (ppm) 7.36 (d, J = 9.0 Hz, 2H), 7.28-7.24 (m, 4H + CDCl₃), 6.87 (d, J = 7.9 Hz, 2H), 3.79 (s, 3H), 3.05 (d, J = 10.9 Hz, 1H), 2.95 (d, J = 11.4 Hz, 1H), 2.78 (d, J = 13.5 Hz, 1H), 1.92 (dt, J = 11.4, 3.1 Hz, 1H), 1.76 (t, J = 11.9 Hz, 2H), 1.60-1.56 (m, 4H), 1.37 (t, J = 13.3 Hz, 1H). **¹³C NMR** (CDCl₃, 100 MHz) δ (ppm) 158.48, 139.95, 137.85, 128.70, 128.41, 127.98, 126.47, 113.85, 68.46, 59.63, 55.26, 53.45, 37.05, 26.06, 25.30. **HPLC** (Chiralcel OJ-3, 100% EtOH, 1 mL/min, 25 °C, 220 nm) 1.19 min and 1.39 min.



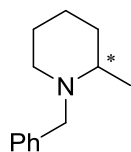
1-Benzyl-2-(4-(trifluoromethyl)phenyl)piperidine

White solid, isolated in 65% yield. $^1\text{H NMR}$ (CDCl_3 , 400 MHz) δ (ppm) 7.64-7.55 (m, 5H), 7.32-7.2 (m, 4H + CDCl_3), 3.69 (d, $J = 13.8$ Hz, 1H), 3.19 (d, $J = 11.4$ Hz, 1H), 2.99 (d, $J = 11.4$ Hz, 1H), 2.84 (d, $J = 13.6$ Hz, 1H), 1.96 (t, $J = 11.4$ Hz, 1H), 1.78 (t, $J = 13.7$ Hz, 3H), 1.61 (d, $J = 9.3$ Hz, 2H), 3.39 (t, $J = 12.0$ Hz, 1H). $^{13}\text{C NMR}$ (CDCl_3 , 100 MHz) δ (ppm) 149.93, 139.27, 128.57, 128.11, 127.70, 126.73, 125.52, 125.48, 77.23, 68.75, 29.90, 53.20, 36.99, 25.86, 25.06. **HRMS** (CI) calculated $[\text{M}+\text{H}]^+$ 320.1621; found $[\text{M}+\text{H}]^+$ 320.1625.



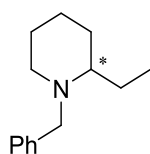
1,2-Dibenzylpiperidine⁵ In accordance with published data.

White solid isolated in 75% yield. $^1\text{H NMR}$ (CDCl_3 , 400 MHz) δ (ppm) 7.37-7.27 (m, 5H), 7.24-7.13 (m, 5H), 4.05 (d, $J = 13.6$ Hz, 1H), 3.49 (d, $J = 13.6$ Hz, 1H), 3.70 (d, $J = 9.7$ Hz, 1H), 2.8-2.74 (m, 1H), 2.68-2.59 (m, 2H), 2.22 (dt, $J = 11.7, 6.0$ Hz, 1H), 1.66-1.61 (m, 1H), 1.54-1.5 (m, 3H), 1.36-1.26 (m, 2H). $^{13}\text{C NMR}$ (CDCl_3 , 100 MHz) δ (ppm) 129.4, 129.3, 128.8, 128.3, 128.2, 128.1, 128.0, 61.71, 58.5, 50.8, 36.5, 29.3, 25.4, 22.4. **HRMS** (ESI) $[\text{M}+\text{H}]^+$ calculated 266.1909; found 266.1910. **HPLC** (Chiracel OJ-3, 100% EtOH, 1 mL/min, 25 °C, 220 nm) 1.41 min and 1.99 min.



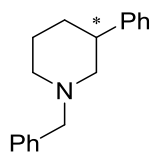
1-Benzyl-2-methylpiperidine⁵ In accordance with published data.

White solid isolated in 40% yield. ¹H NMR (CDCl₃, 400 MHz) δ (ppm) 7.32-7.29 (m, 4H), 7.24-7.21 (m, 1H), 4.00 (d, J = 13.4 Hz, 1H), 3.48 (s, 1H), 3.2 (d, J = 13.4 Hz, 1H), 2.73 (d, J = 11.3 Hz, 1H), 2.32-2.29 (m, 1H), 1.95 (t, J = 10.9 Hz, 1H), 1.64 (d, J = 9.6 Hz, 3H), 1.55-1.47 (m, 2H), 1.17 (d, J = 6.3 Hz, 3H). ¹³C NMR (CDCl₃, 100 MHz) δ (ppm) 129.17, 128.05, 126.63, 60.41, 58.52, 52.18, 34.73, 26.05, 24.04, 21.06, 14.22. HRMS (CI) calculated [M+H]⁺ 190.1590; found [M+H]⁺ 190.1595.



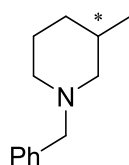
1-Benzyl-2-ethylpiperidine⁹ In accordance with published data.

White solid isolated in 60% yield. ¹H NMR (CDCl₃, 400 MHz) δ (ppm) 7.34-7.29 (m, 4H), 7.24-7.19 (m, 1H), 3.98 (d, J = 13.5 Hz, 1H), 3.2 (d, J = 13.5 Hz, 1H), 2.74 (dt, J = 11.6, 3.8 Hz, 1H), 2.23-2.17 (m, 1H), 2.0 (ddd, J = 11.7, 9.5, 4.0 Hz, 1H), 1.71-1.61 (m, 4H), 1.50-1.42 (m, 3H), 1.31-1.28 (m, 1H), 0.92 (t, J = 7.5 Hz, 3H). ¹³C NMR (CDCl₃, 100 MHz) δ (ppm) 139.96, 128.95, 128.08, 126.57, 61.87, 57.59, 51.97, 29.76, 25.37, 24.45, 23.87, 9.1. HRMS (CI) calculated [M+H]⁺ 204.1747. found [M+H]⁺ 204.1752.



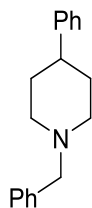
1-Benzyl-3-phenylpiperidine

White solid isolated in 60% yield. $^1\text{H NMR}$ (CDCl_3 , 400 MHz) δ (ppm) 7.39-7.16 (m, 10H), 3.54 (s, 2H), 2.98 (ddt, $J = 15.7, 11.0, 1.8$ Hz, 1H), 2.84 (tt, $J = 12.0, 3.6$ Hz, 1H), 2.07-1.90 (m, 2H), 1.77-1.70 (m, 2H), 1.61 (bs, 1H), 1.45 (dq, $J = 12.0, 5.0$ Hz, 1H), 1.26 (s, 1H). $^{13}\text{C NMR}$ (CDCl_3 , 100 MHz) δ (ppm) 144.9, 138.3, 129.2, 128.3, 128.2, 127.3, 127.0, 126.3, 63.5, 61.0, 53.8, 42.9, 31.7, 25.8. **HRMS** (CI) calculated $[\text{M}+\text{H}]^+$ 252.1747; found $[\text{M}+\text{H}]^+$ 252.1755.



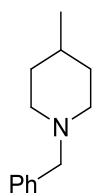
1-Benzyl-3-methylpiperidine

White solid isolated in 53% yield. $^1\text{H NMR}$ (CDCl_3 , 400 MHz) δ (ppm) 7.31-7.28 (m, 4H), 7.25-7.21 (m, 1H), 3.47 (s, 2H), 2.79 (t, $J = 10.9$ Hz, 2H), 1.86 (td, $J = 11, 3.6$ Hz, 1H), 1.71-1.50 (m, 6H), 0.83 (d, $J = 6.4$ Hz, 3H). $^{13}\text{C NMR}$ (CDCl_3 , 100 MHz) δ (ppm) 138.7, 129.2, 128.1, 126.8, 63.6, 62.0, 54.0, 33.0, 31.1, 25.6, 19.8. **HRMS** (CI) calculated $[\text{M}+\text{H}]^+$ 190.1590. found $[\text{M}+\text{H}]^+$ 190.1587.



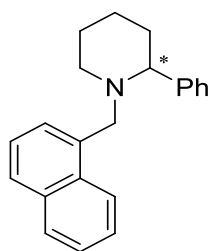
1-Benzyl-4-phenylpiperidine

White solid isolated in 75% yield. **¹H NMR** (CDCl₃, 400 MHz) δ (ppm) 7.39-1.30 (m, 9H), 7.24-7.20 (m, 1H), 6.06 (dt, J = 3.4, 1.8 Hz, 1H), 3.64 (s, 2H), 3.18 (q, J = 2.8 Hz, 2H), 2.72 (t, J = 5.8 Hz, 2H), 2.58-2.55 (m, 2H), 1.83-1.80 (m, 1H), 1.58-1.56 (m, 1H). **¹³C NMR** (CDCl₃, 100 MHz) δ (ppm) 135.00, 129.26, 128.29, 128.27, 127.12, 124.92, 121.93, 62.76, 53.35, 49.99, 28.06. **HRMS** (CI) calculated [M+H]⁺ 252.1747. found [M+H]⁺ 252.1753.



1-Benzyl-4-methylpiperidine

White solid isolated in 80% yield. **¹H NMR** (CDCl₃, 400 MHz) δ (ppm) 7.32-7.29 (m, 4H), 7.24-7.22 (m, 1H), 3.48 (s, 2H), 2.93 (quin, J = 2.05 Hz, 1H), 2.83 (dt, J = 11.9 3.0 Hz, 2H), 2.55 (t, J = 5.8 Hz, 1H), 1.93 (td, J = 11.5, 2.4 Hz, 2H), 1.67 (d, J = 1.2 Hz, 1H), 1.58 (dd, J = 12.6, 1.6 Hz, 2H), 0.91 (d, J = 6.3 Hz, 3H). **¹³C NMR** (CDCl₃, 100 MHz) δ (ppm) 129.24, 128.19, 128.10, 126.82, 63.59, 53.98, 53.98, 34.39, 30.81, 21.94. **HRMS** (CI) calculated [M+H]⁺ 190.1590. found [M+H]⁺ 190.1594.



1-(Naphthalen-1-ylmethyl)-2-phenylpiperidine

White solid isolated in 96% yield. $^1\text{H NMR}$ (CDCl_3 , 400 MHz) δ (ppm) 7.78-7.73 (m, 3H), 7.65 (s, 1H), 7.5 (d, $J = 7.2$ Hz, 2H), 7.44-7.39 (m, 3H), 7.34 (t, $J = 7.4$ Hz, 2H), 7.22 (t, $J = 7.4$ Hz, 1H), 3.91 (d, $J = 13.5$ Hz, 1H), 3.14 (d, $J = 10.8$ Hz, 1H), 3.00-2.93 (m, 2H), 2.03-1.93 (m, 1H), 1.79 (d, $J = 11.6$ Hz, 2H), 1.7-1.58 (m, 3H), 1.42-1.34 (m, 1H). $^{13}\text{C NMR}$ (CDCl_3 , 100 MHz) δ (ppm) 145.78, 137.49, 133.37, 132.65, 128.59, 127.66, 127.64, 127.55, 127.28, 127.13, 129.96, 125.80, 125.31, 69.40, 60.05, 53.50, 37.10, 26.08, 25.33. **HRMS** (ESI) $[\text{M}+\text{H}]^+$ calculated 302.1909; found 302.1904.

5.7 References

- 1 M. Struder, C. Wedemeyer-exl, F. Spindler and H.-U. Blaser, *Monatshefte für Chemie*, 2000, **131**, 1335–1343.
- 2 C. Y. Legault and A. B. Charette, *J. Am. Chem. Soc.*, 2005, 8966–8967.
- 3 Y. Liu and H. Du, *J. Am. Chem. Soc.*, 2013, **135**, 12968–71.
- 4 Z.-S. Ye, M.-W. Chen, Q.-A. Chen, L. Shi, Y. Duan and Y.-G. Zhou, *Angew. Chem. Int. Ed.*, 2012, **51**, 10181–4.
- 5 M. Chang, Y. Huang, S. Liu, Y. Chen, S. W. Krska, I. W. Davies and X. Zhang, *Angew. Chem. Int. Ed.*, 2014, **53**, 12761–4.
- 6 F. Glorius, N. Spielkamp, S. Holle, R. Goddard and C. W. Lehmann, *Angew. Chem. Int. Ed.*, 2004, **43**, 2850–2.
- 7 X.-B. Wang, W. Zeng and Y.-G. Zhou, *Tet. Lett.*, 2008, **49**, 4922–4924.
- 8 M. Rueping and A. P. Antonchick, *Angew. Chem. Int. Ed.*, 2007, **46**, 4562–5.
- 9 J. Wu, W. Tang, A. Pettman and J. Xiao, *Adv. Synth. Catal.*, 2013, **355**, 35–40.

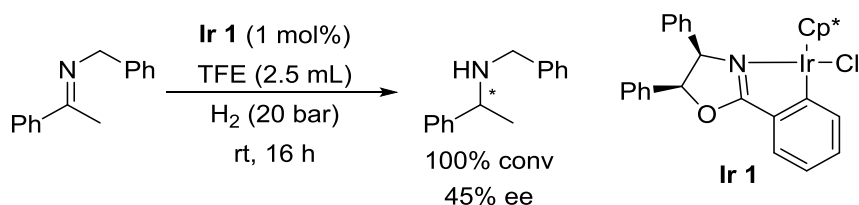
Chapter 6: Asymmetric Hydrogenation of Acyclic Imines

6.1 Introduction

The reduction of acyclic imines has long been investigated, with chiral systems reported as early as the 1970s.¹ Although a difficult process to achieve, great effort has been put into this area of research,² leading to a number of successful systems. A range of hydrogenation systems have been published with iridium the most common and successful metal for the transformation,^{3–7} although a range of metal free ATH systems have also been established.^{8–12}

6.2 Catalyst Screening

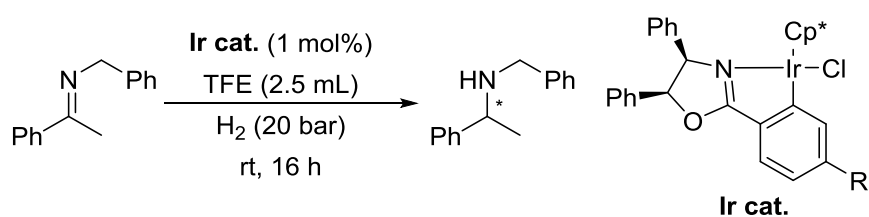
Using the range of complexes described in Chapter 2, an initial reaction was performed for the AH of benzyl imine. This was initiated by screening of the small simple oxazoline complex (**Ir 1**) shown in Scheme 6.1, to determine if these iridicycles were active. This test proved successful, producing complete conversion with 45% ee, in 2,2,2-trifluoroethanol (TFE) under 20 bar hydrogen.

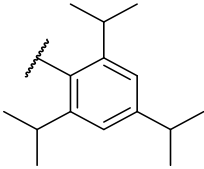
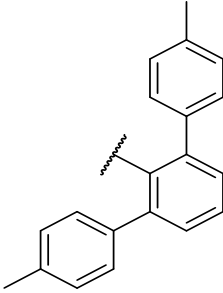
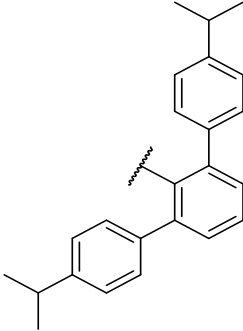
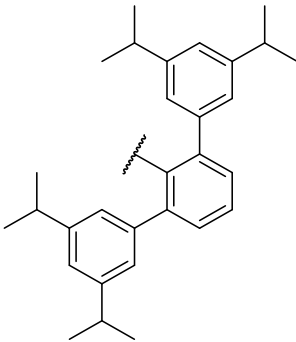


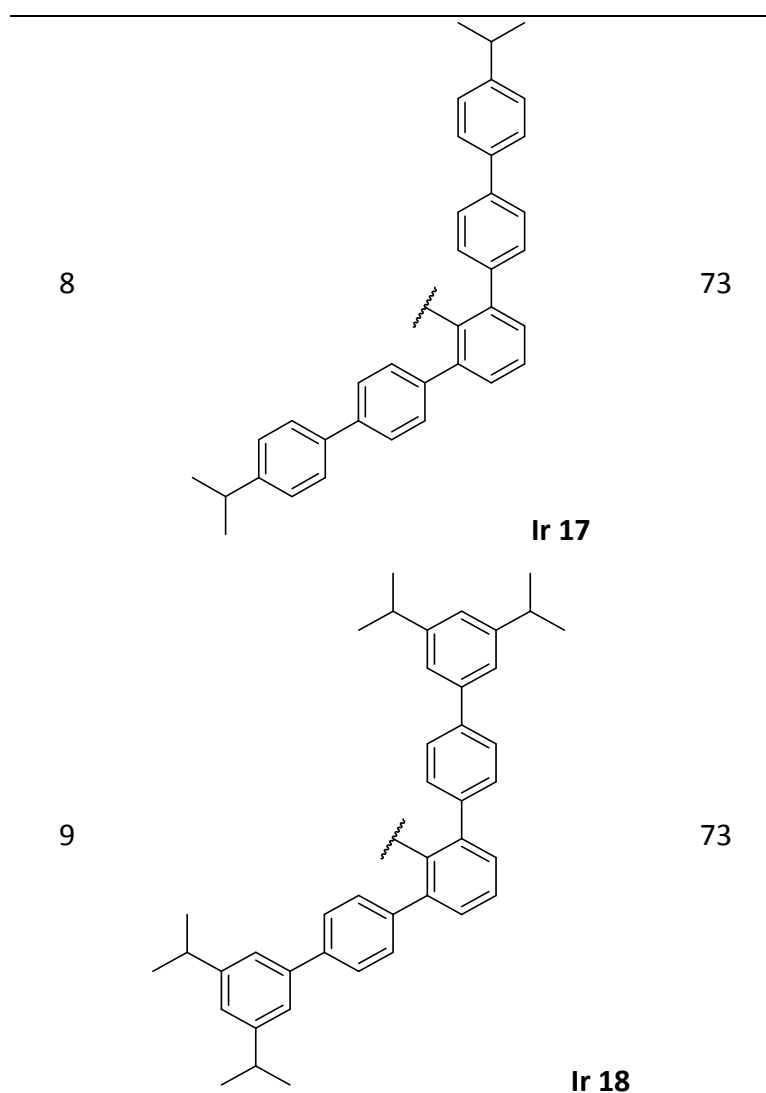
Scheme 6.21 Test reaction for benzyl imine reduction.

An extensive screening was undertaken, with a focus on the bulky oxazoline complexes described in Chapter 2, all of these provided greater than 90% conversion to the desired product. The addition of bulky groups *para* to the oxazoline showed an increase in ee, with a trend of H (**Ir 1**) < iPr (**Ir 9**) < ^tBu (**Ir 10**), with 45%, 70% and 75% respectively (Entries 1-3, Table 6.1). Additional groups on the terphenyl ring had varying effects, with most offering no improvement, with

ee's around 50% as shown in Entries 4 and 5 in Table 6.1. The 4-*iso*-propyl terphenyl complex (**Ir 13**) showed a significant improvement in ee, achieving 77% (Entry 6, Table 6.1). Further extension of the terphenyl group (**Ir 17** and **Ir 18**) offered no improvement, with ee's maintained between 70 and 75% (Entries 8 and 9, Table 6.1). The best ee of 78%, was achieved using the much smaller 2,4,6-*iso*-propyl complex **Ir 11** (Entry 4, Table 6.1).



Entry	R	ee (%)
1	H Ir 1	45
2	^t Bu Ir 10	70
3	iPr Ir 9	70
4	 Ir 11	78
5	 Ir 12	52
6	 Ir 13	77
7	 Ir 16	52

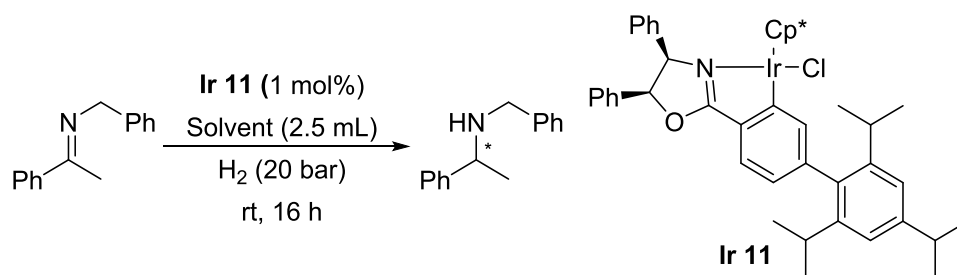


Reaction conditions: 0.5 mmol benzyl imine, 1 mol% Ir cat, 2.5 mL TFE, 20 bar H₂, overnight.

Table 6.1 Screening of complexes for AH of benzyl imine.

6.3 Condition Optimisation

Further examination of the conditions was undertaken to determine if the TFE was necessary, or if the transformation could be performed in a cheaper solvent. A range of alcohols were screened, as well as other common laboratory solvents, none of which showed any conversion (Table 6.2). These results indicated that the acidity of the TFE is crucial for the reactivity observed, potentially assisting in chloride dissociation from the iridium centre and shifting the equilibrium in favour of the active species (Figure 6.1).



Entry	Solvent	Conv (%)	ee (%)	Entry	Solvent	Conv (%)	ee (%)
1	TFE	100	78	8	Hexane	0	-
2	MeOH	0	-	9	PhMe	0	-
3	EtOH	0	-	10	Benzene	0	-
4	IPA	< 1	-	11	Heptane	0	-
5	^t BuOH	0	-	12	CHCl ₃	0	-
6	Ethoxy ethanol	0	-	13	EtOAc	0	-
7	Ethylene glycol	0	-	14	DMSO	0	-

Reaction conditions: 0.5 mmol benzyl imine, 1 mol% Ir 11, 2.5 mL solvent, 20 bar H₂, overnight.

Table 6.2 Screening of solvents for benzyl imine AH.

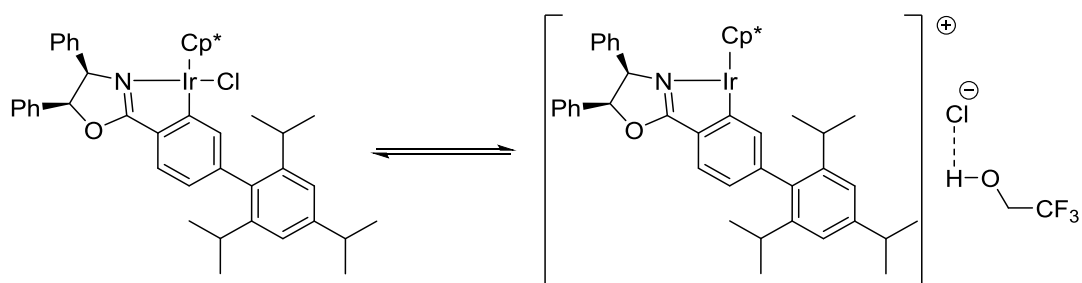
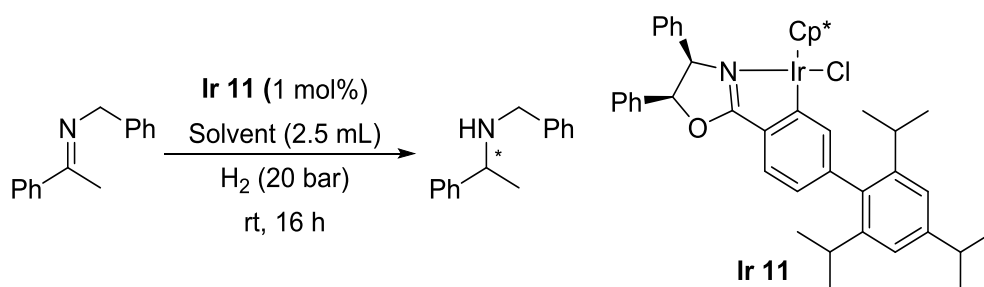


Figure 6.13 Potential activation pathway of iridium complex by TFE.

A range of fluorinated solvents were screened to further investigate this effect. Pleasingly, all of the fluorinated alcohols tested showed great activity for the desired reaction with greater than 95% conversion; however the non-protic α,α,α -trifluorotoluene showed no activity, further indicating that the acidity of the alcohol groups is crucial. The longer chain alcohols (trifluorobutanol and trifluoropentanol) showed a reduction in ee to 62% and 56% respectively (Entries 4 and 5, Table 6.3).

The shorter chain 2,2-difluoroethan-1-ol once more showed a reduction in ee to 68% (Entry 3, Table 6.3). Increasing the number of fluorides present on the alcohol had little impact on the observed ee, with hexafluoro-*iso*-propanol producing an ee of 71% similar to that observed with TFE (Entries 1 and 2, Table 6.3).



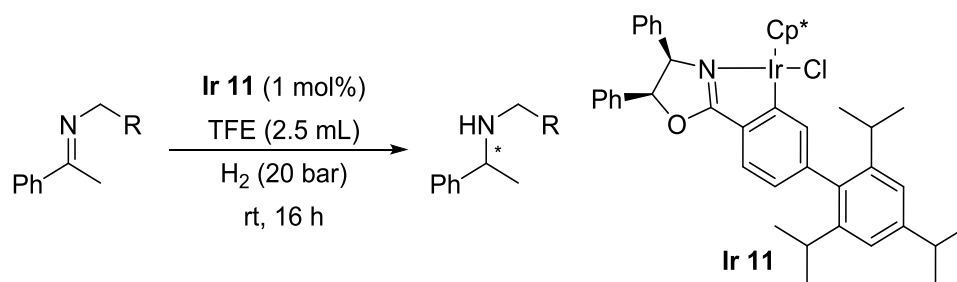
Entry	Solvent	Conv (%)	ee (%)
1	TFE	> 99	78
2	Hexafluoro- <i>iso</i> -propanol	> 95	71
3	2,2-difluoroethan-1-ol	> 95	68
4	4,4,4-trifluorobutan-1-ol	> 95	62
5	5,5,5-trifluoropentan-1-ol	> 95	56
6	Perfluoro- <i>tert</i> -butanol	> 95	40
7	α,α,α -trifluoro toluene	0	-

Reaction conditions: 0.5 mmol benzyl imine, 1 mol% Ir 11, 2.5 mL solvent, 20 bar H₂, overnight

Table 6.3 Screening of fluorinated solvents for AH.

6.4 Substrate Screening

Substrate scope was investigated using the optimised conditions determined above, by varying the benzylamine used; this was a good starting point as the benzyl group has the potential to be cleaved allowing for the formation of the chiral primary amine. Electronics in the *para* position had little influence upon the enantioselectivity with both electron donating (Entries 2 and 4, Table 6.4) and electron withdrawing (Entry 3, Table 6.4) groups producing high ee's, of 71% and 70% respectively. Having a substituent in the *meta* position caused a significant decrease in ee (Entries 5 and 6, Table 6.4); with the 3,5-ditrifluoromethyl substituted imine being reduced down to 16% ee, whilst the electron donating dioxole group showed less of a drop in ee, to 34%. *Ortho* substituents were well tolerated, with an electron donating methyl group producing once more a high ee of 72% (Entry 7, Table 6.4). Electron withdrawing groups had a similar effect, showing only a slight reduction of ee (Entries 8 and 9, Table 6.4). The addition of a methoxy group in the *ortho* position showed a significant drop in conversion, although a moderately high ee of 60% was maintained (Entry 10, Table 6.4).



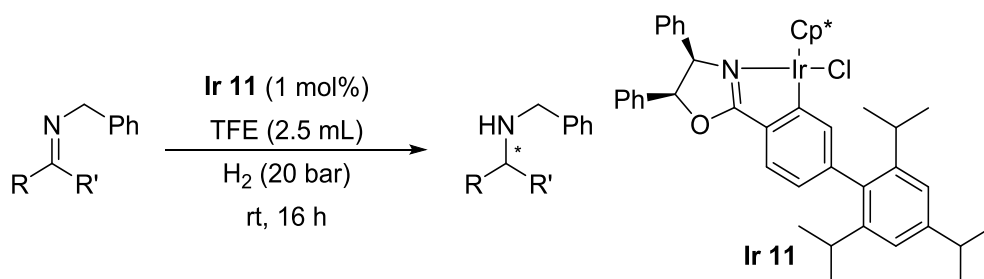
Entry	R	Conv (%)	ee (%)	Entry	R	Conv (%)	ee (%)
1		100	78	7		100	72
2		100	71	8		100	65
3		100	70	9		100	68
4		100	77	10		40	60
5		100	34	11		100	70
6		100	16				

Reaction conditions: 0.5 mmol benzyl imine, 1 mol% Ir 11, 2.5 mL TFE, 20 bar H₂, overnight

Table 6.4 Effect of variation of the benzyl group on AH.

Having established that variation of the benzyl group of the imine showed good results, variation of the ketone group was next investigated. Once again addition of *para* groups showed similarly high ee's whilst maintaining complete conversion (Entries 1 and 2, Table 6.5). Variation of the *meta* group showed more varied results with an electron donating group providing a high ee (Entry 3, Table

6.5), whilst the use of the electron withdrawing 3-trifluoromethyl group resulted in a drop in ee to 50% (Entry 4, Table 6.5). Extension of the R' group to an ethyl had a detrimental impact upon the ee, reducing it to 24% (Entry 5, Table 6.5).

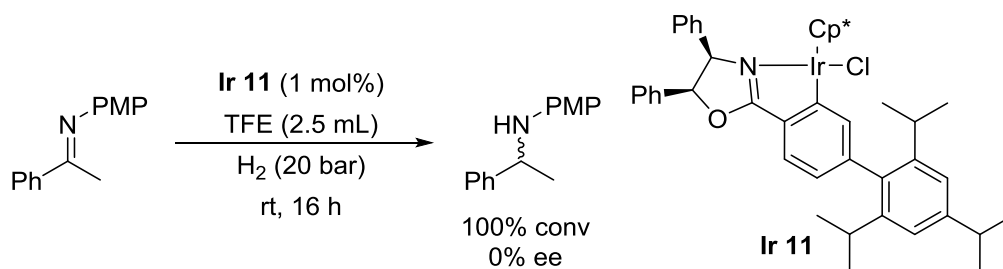


Entry	R	R'	Conv (%)	ee (%)
1		Me	100	71
2		Me	100	77
3		Me	100	70
4		Me	100	50
5	Ph	Et	100	24

Reaction conditions: 0.5 mmol benzyl imine, 1 mol% Ir 11, 2.5 mL TFE, 20 bar H₂, overnight.

Table 6.5 Effect of varying substrates on selectivity.

To further probe the range of substrates suitable for this system, aniline-based imines were prepared. Upon being subjected to these standard conditions complete conversion was obtained, however, a racemic product was produced (Scheme 6.2). This intriguing result led to a mechanistic investigation.

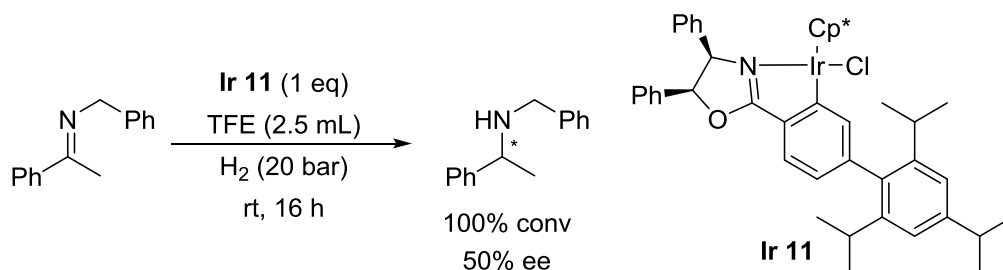


Scheme 6.22 Hydrogenation of aniline based imines.

6.5 Mechanistic Investigation

6.5.1 Benzyl Imine AH

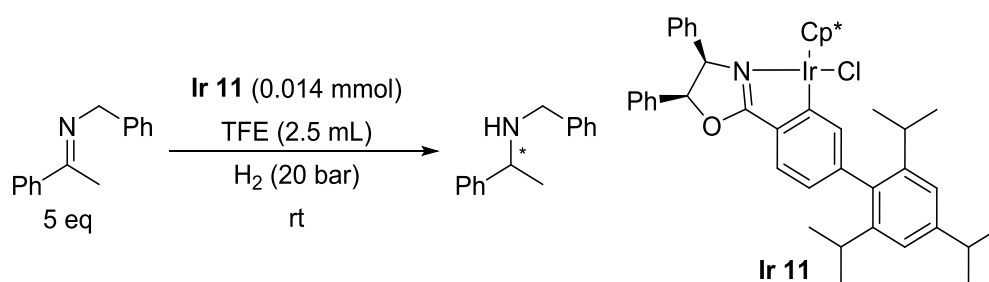
An initial reaction, utilising 1 eq of catalyst with respect to the imine, showed a decrease in ee to 50%, although 100% conversion was still obtained (Scheme 6.3). After the reaction was complete, the starting iridicycle was no longer present, with the free oxazoline ligand being observed, indicating the ligand is susceptible to reductive elimination in the presence of hydrogen.



Scheme 6.23 AH of benzylimine using 1 eq of complex.

An NMR investigation was initiated to probe the mechanistic route and identify any intermediates formed. The iridium complex was dissolved in non-deuterated TFE in a sapphire NMR tube equipped for high pressure experiments¹³ (Scheme 6.4). A standard 1D ^1H spectra was run, with solvent suppression around the 3.88 and 5.02 ppm regions. This removed some areas of the complex spectra, but key diagnostic peaks were unaffected (Figure 6.2). 5 eq of imine was then

added; upon this addition the iridium complex peaks shifted and a new set of resonances, indicative of a new complex was observed. Once the hydrogen pressure had reached 20 bar and stabilised (approximately 10 min) the imine was consumed, but the new iridium complex remained intact. Hydride peaks were observed at -15.1 and -15.4 ppm after the reaction was complete (bottom spectra, Figure 6.2), these however did not integrate with respect to the complex, indicating a second minor iridium species is present. Hydrides around -15 ppm have previously been reported for the non-chiral cyclometallated iridium complexes, implying this minor species maybe the hydride species of the initial complex (**Ir 11**).¹⁴



Scheme 6.24 High pressure imine hydrogenation for an *in situ* study.

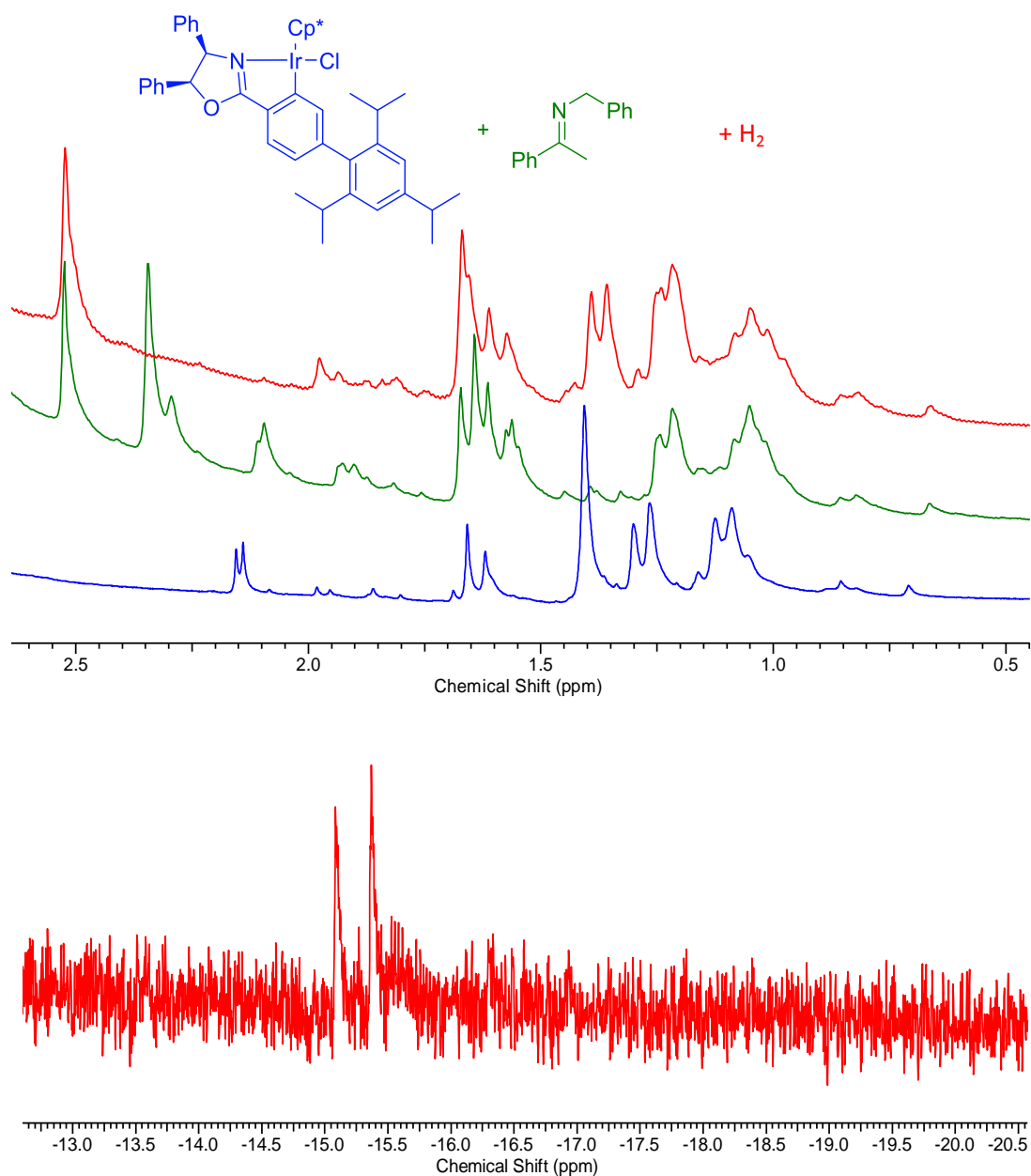


Figure 6.14 Complex in TFE, + 5 eq's of imine, + 20 bar H_2 over 10 min at 298 K.

Repeating this high pressure reaction at a lower temperature of 253 K, a hydride peak can be observed at -8.45 ppm (Figure 6.3). This hydride is only seen in a few spectra and at varying intensities with respect to the TFE quartet, indicating this may potentially be the active hydride forming and being used in the catalytic cycle. Once more the hydride peak did not integrate with respect to the iridium

imine complex, indicating a second minor iridium hydride species is present during the catalytic cycle.

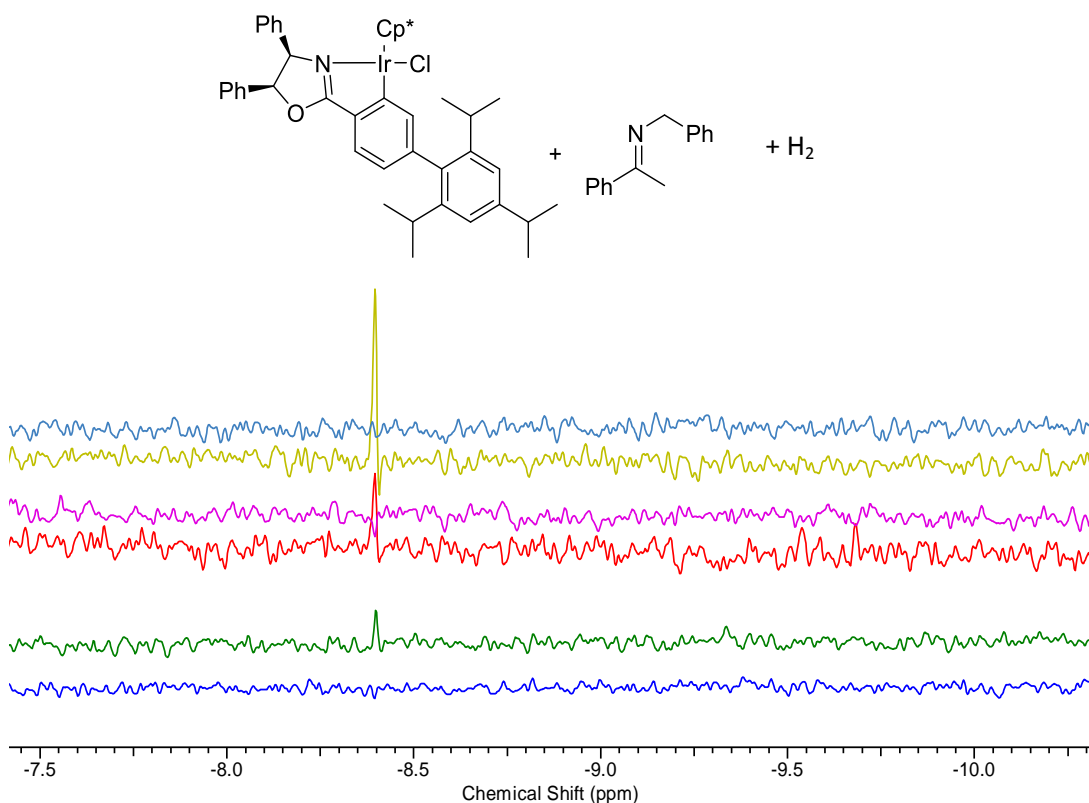


Figure 6.15 Low temperature, high pressure imine hydrogenation at 2.5 min intervals.

To probe the reaction occurring *in situ*, the iridium complex was dissolved in $\text{d}^3\text{-TFE}$, with 1 eq of the imine and the ^1H NMR spectrum recorded (Figure 6.4). This showed the formation of a new species. Splitting of the CH_2 protons of the benzyl group was observed to an AB quartet, with the two peaks shifting upfield to 3.23 and 3.50 ppm, indicating the formation of one distinct diastereoisomer. The *iso*-propyl groups from the ligand also became better defined into distinctly separate peaks, as well as showing the downfield shift of the Cp* protons seen previously. In TFE, only one set of resonances for the complex is observed (compared to the 2 seen in CDCl_3), showing a loss of chirality at the iridium centre, through loss of chloride from the iridium centre forming a pro-chiral species (Figure 6.1).

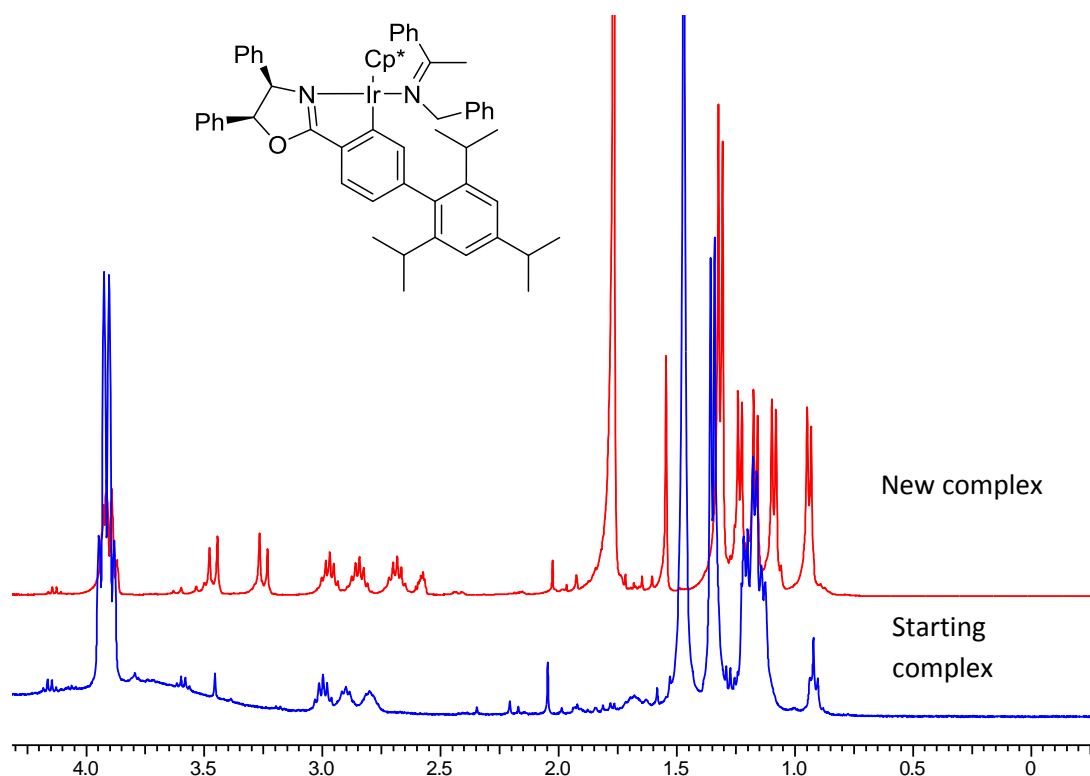
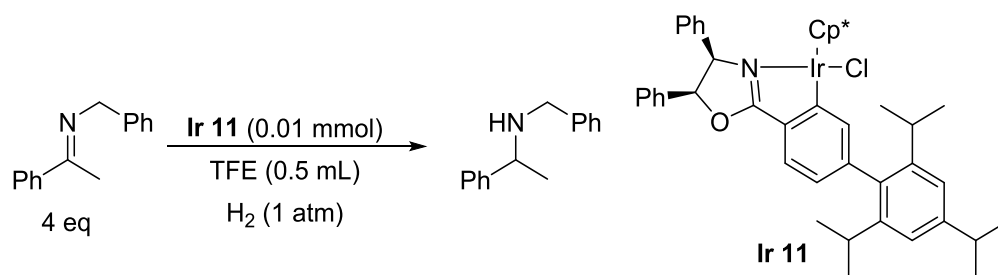


Figure 6.16 Original Ir complex, Ir complex bound to 1 eq of imine after 2 days.

Low pressure and temperature *in situ* NMR reactions were conducted to sufficiently slow the rate of reaction in order to better observe the intermediates formed in this transformation. The first combined 4 eq of imine with the iridium complex (Scheme 6.5), which showed complete formation of a new catalytic species. The mixture was cooled to 253 K and sealed under an atmospheric H₂ pressure, before being warmed to 298 K over 6 h. The newly formed complex did not appear to alter during the reaction although reduction of the imine was observed from 253 K (Figure 6.5 and 6.6). No hydride species were observed, at the low pressure, possibly due to the low concentration of hydrogen in the system.



Scheme 6.25 Low pressure *in situ* imine hydrogenation.

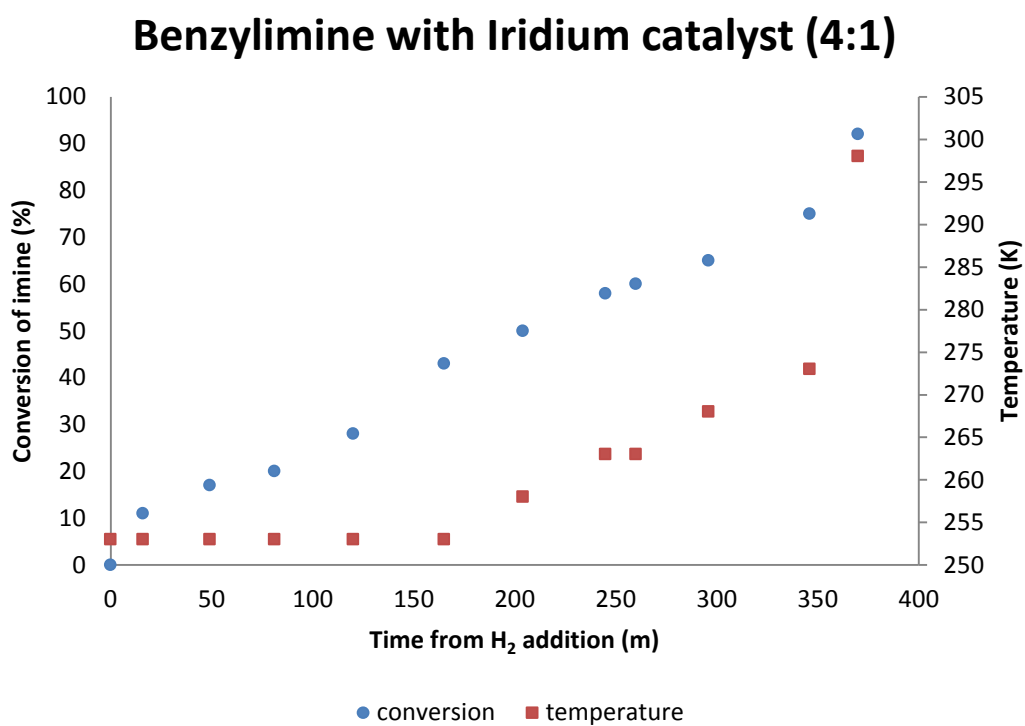


Figure 6.17 Atmospheric pressure reduction of benzyl imine.

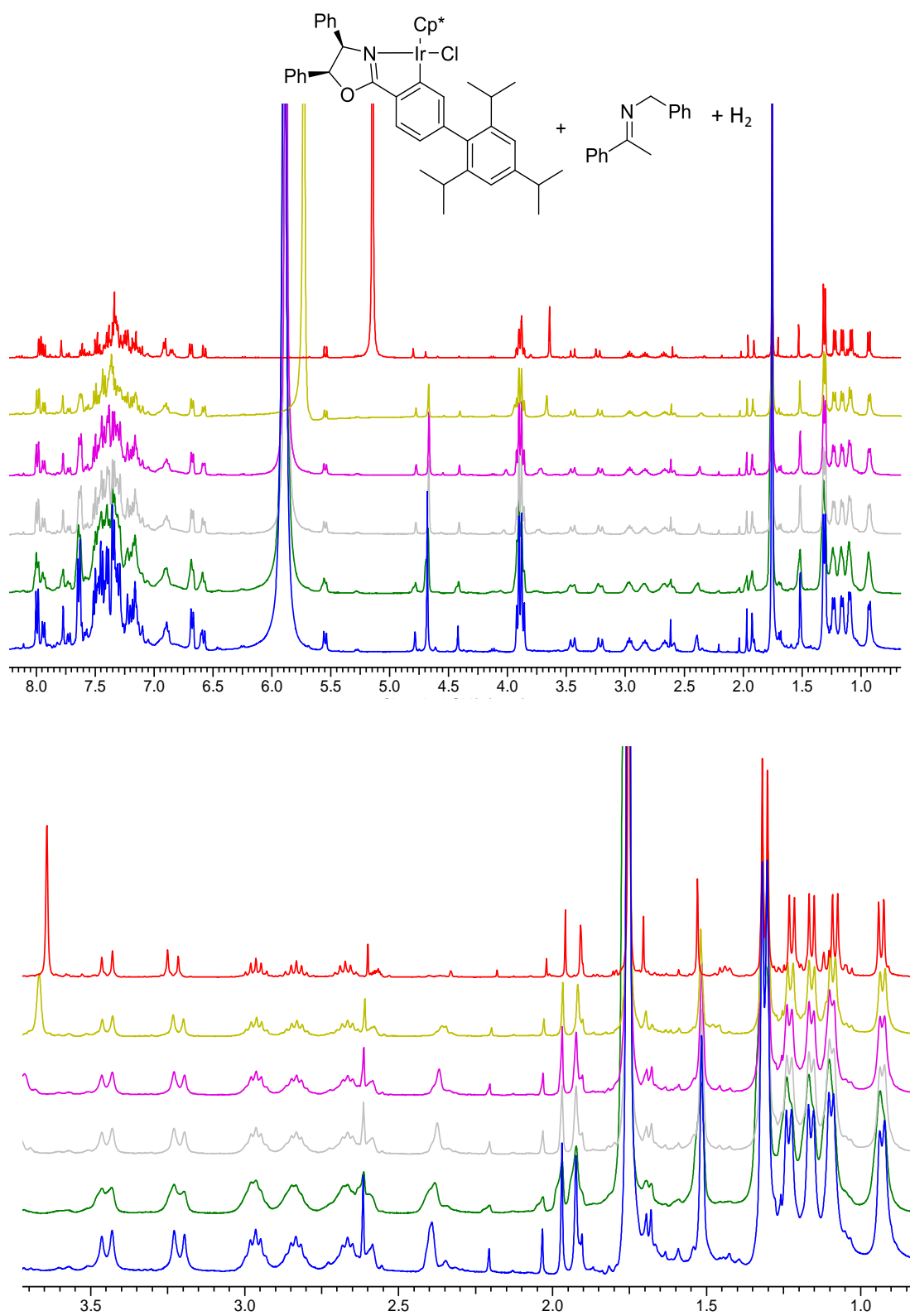


Figure 6.18 Ir cat + 4 eq imine at atmospheric H_2 pressure cooled to 253 K, warmed to 263 K, 298 K, Below spectra is close up of new complex peaks remaining intact and product forming.

6.5.2 Modelling of the New Iridium Species

After running ^1H , ^{13}C , COSY, HMQC and ^1H - ^1H NOESY NMR analysis upon the new complex in d^3 -TFE, it could be determined how the two species lay in relation to one another. This data was compared to a molecular mechanics (MM) model of the iridium imine complex, with both iridium diastereoisomers being modelled. The lowest energy structures that were in agreement with the proton-proton correlations observed in the NOESY NMR, i.e. $< 3 \text{ \AA}$ apart, were carried forward for DFT calculations by Dr Neil Berry. Three structures were selected; two *E* imines as an energy difference was observed, dependent upon the face of the iridium it was bound to and one *Z* imine, as no energy difference was observed between these structures. The structures obtained by DFT calculations are shown below (Figure 6.7 and 6.8). The *Z* imine showed the lowest energy with the imine group on the opposite face from the chiral groups. The top *E* imine showed an energy difference of +2.55 kcal/mol from the *Z* imine, once more with the imine on the opposite face to the chiral groups. The structure, shown on the bottom, shows an energy difference of +13.41 kcal/mol from the *Z* imine, this structure also shows the imine group in close proximity to the chiral groups, indicating this species may be the chiral inducing form, whilst the others enable the formation of the racemic product.

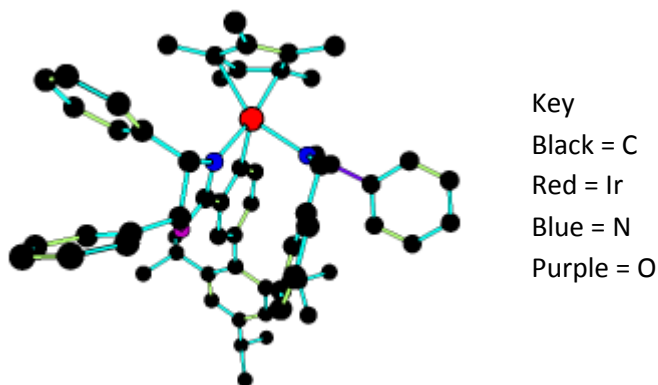


Figure 6.19 *Z* imine bound to the iridium complex with an energy of -1639042.89 kcal/mol.

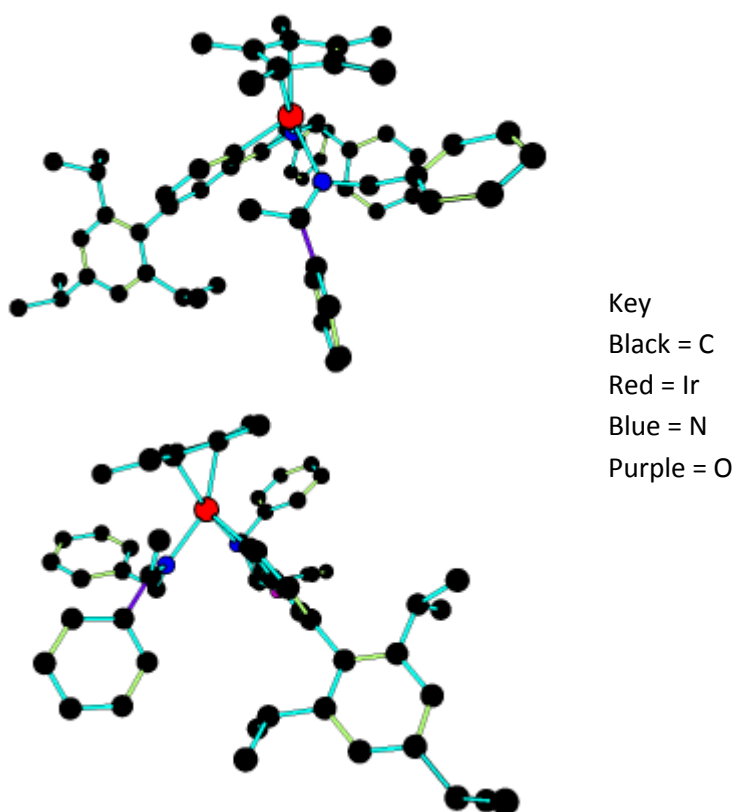


Figure 6.20 *E* imine on opposite faces of the iridium; Top showing an energy of -1639040.333 kcal/mol, Bottom with an energy of -1639029.482 kcal/mol.

Once bound the imine could undergo either intramolecular hydrogenation, reducing the bound imine, or intermolecular hydrogenation, in which the imine would stay bound and a second molecule of imine would be reduced. To determine

the feasibility both the *S* and *R* amine were modelled bound onto the iridium (Figure 6.9). Although both the *R* and *S* amines showed similar energies an energy difference of 4.12 kcal/mol was observed between them. A much greater difference in energy from the starting imine was observed at +25413.38 kcal/mol. This shows a significantly large energy difference, indicating the intramolecular pathway would be slow to occur.

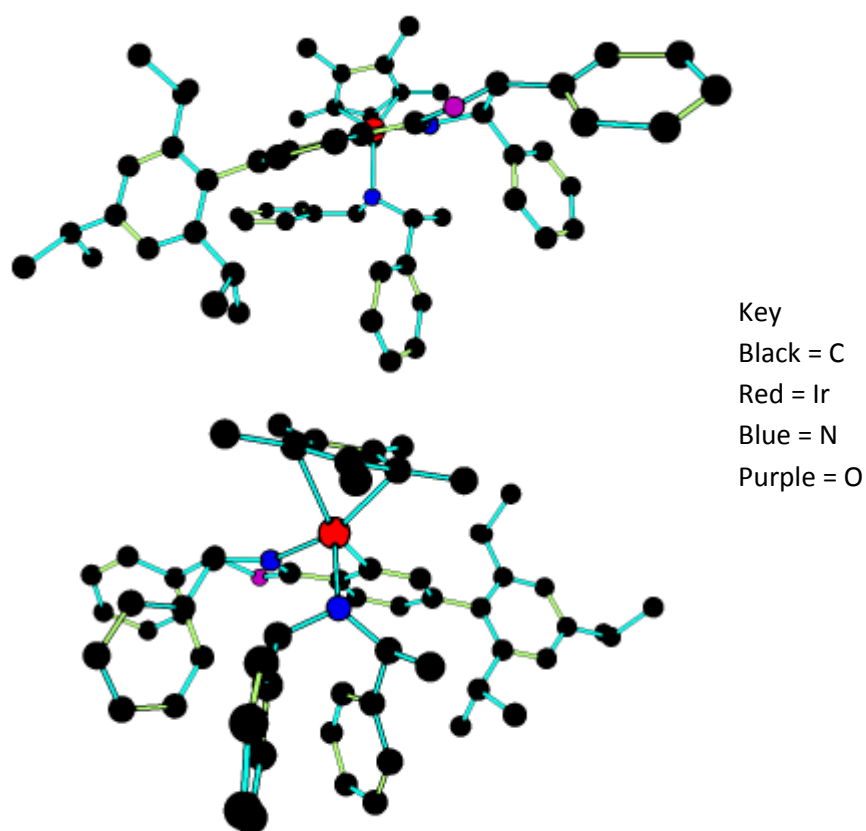
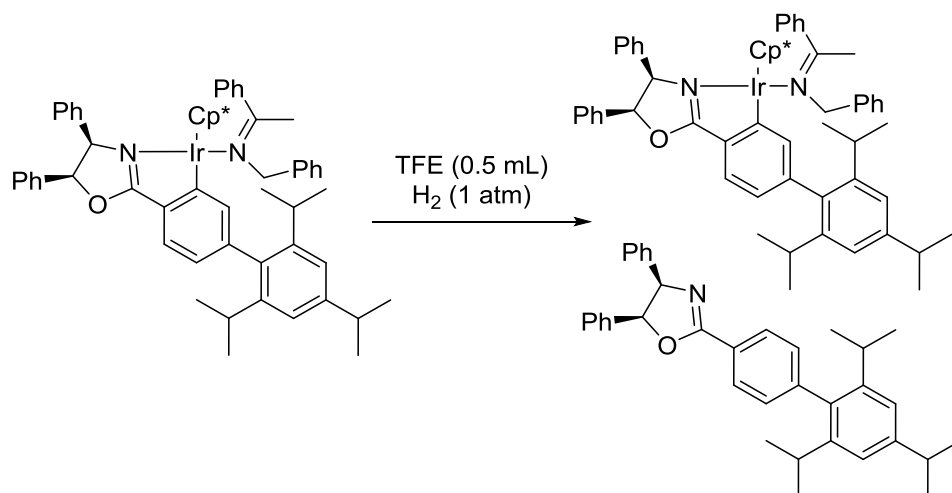


Figure 6.21 Top R amine bearing an energy of -1664429.454 kcal/mol, Bottom S amine with an energy of -1664433.572 kcal/mol.

The pre-formed imine iridium complex was subjected to atmospheric H_2 at 298 K, however, no reduction of the bound imine was observed, although the small excess of free imine was reduced. After 24 h a small amount of iridium complex had decomposed, with free ligand being observed (Scheme 6.6). After decomposition

had been observed, several hydride species could be detected around -15 ppm (Figure 6.10), indicating multiple inactive hydride formed on the free iridium centre.



Scheme 6.26 Attempted hydrogenation of the imine bound complex.

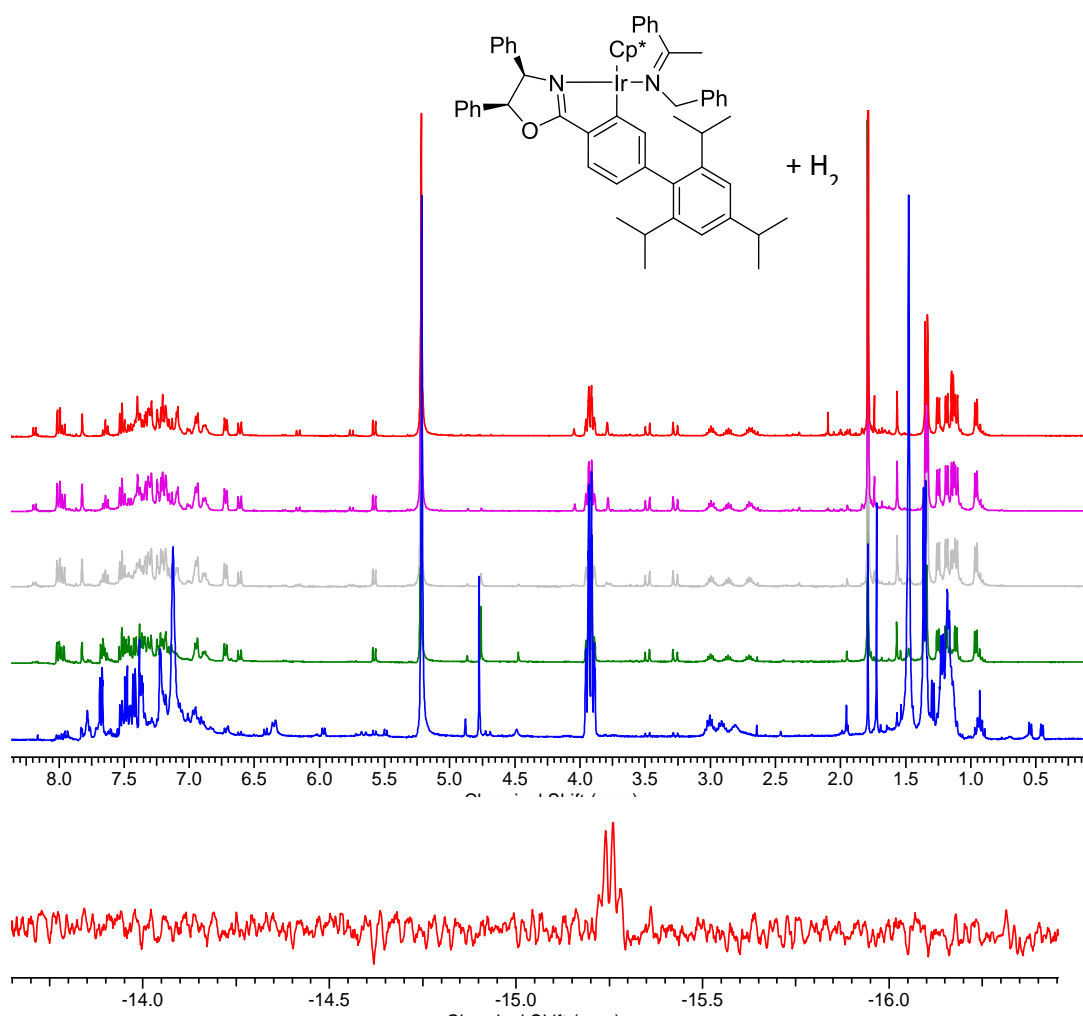


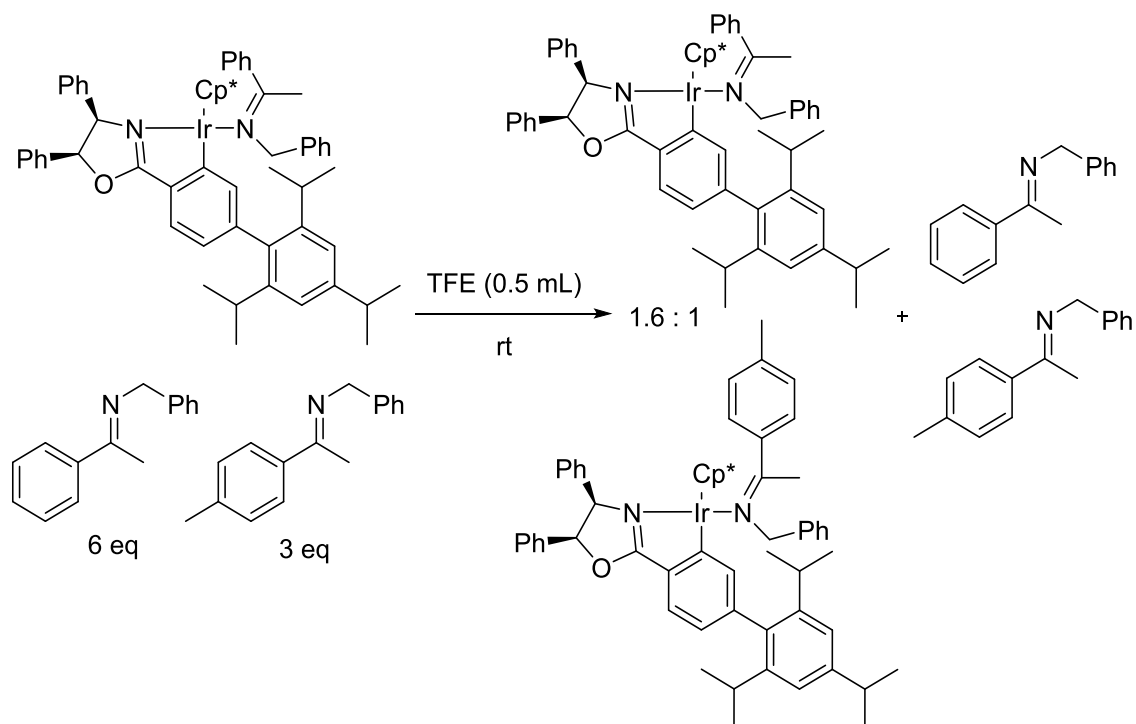
Figure 6.22 Ir cat + 1eq of imine, left 2 days for complex formation, add H₂, 10 hours later₂

7 hours later.

6.5.3 Changing Benzyl imine

To further determine if the hydrogenation would occur *via* an intra- or intermolecular mechanism the iridium complex was mixed with 6 eq of the benzyl imine until complete formation of the new species was observed by ¹H NMR. 3 eq of *p*-methylbenzyl imine was then added (Scheme 6.7) and monitored for an hour at room temperature. During this time it was observed that scrambling of the bound imine iridium complex occurred, shown by the formation of additional doublets

between 3.0 and 3.5 ppm, demonstrating at room temperature the bound imine is labile, without decomposition of the complex (Figure 6.11).



Scheme 6.27 Scrambling of the benzyl imine bound complex with *p*-methylbenzylimine.

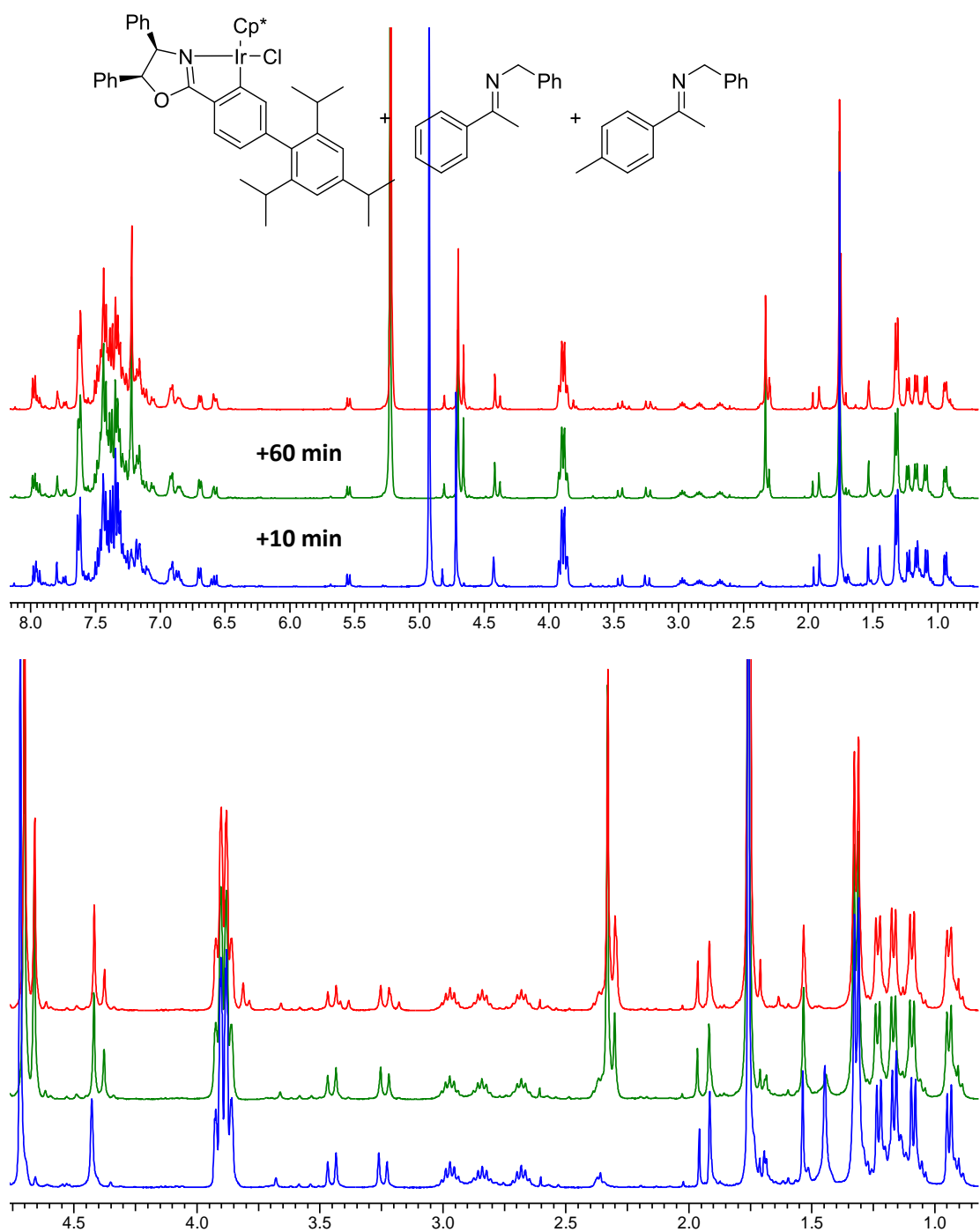


Figure 6.23 6 eq of Benzyl imine with iridium complex, + 3 eq *p*-Methylbenzylamine,

Mixture of both imine bound complexes (6:1 ratio).

After cooling to 253 K and the addition of hydrogen gas at an atmospheric pressure, it can be seen that both species are reduced at a similar rate, whilst

maintaining the ratio of bound benzyl imine to *p*-methylbenzyl imine complex (Figure 6.12).

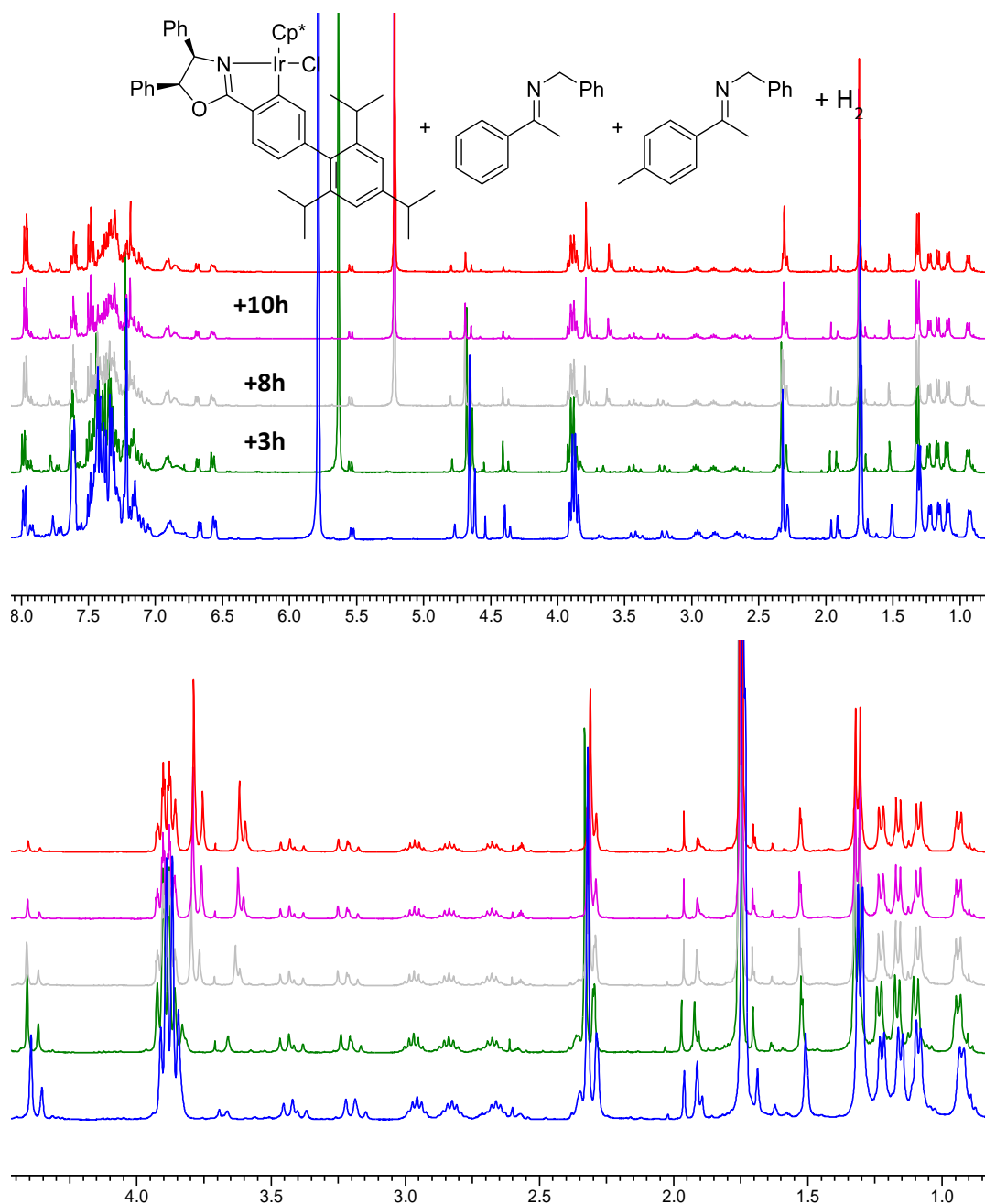
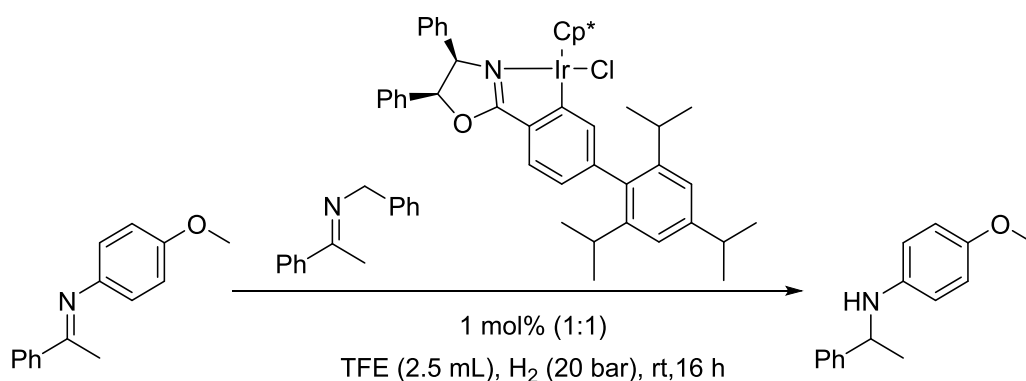


Figure 6.24 The scrambled benzyl imine/*p*-methyl benzyl imine complex from above with addition of H₂ 253K, Increase to 273K, then upto 298K.

A further experiment of reducing the temperature for the pre-formed benzyl imine iridium complex, prior to the addition of the *p*-methylbenzyl imine was run (Figure 6.13). This showed that at a low temperature of 253 K, conversion of just the

p-methyl benzyl imine occurred, with the low rate of conversion potentially being caused by the low pressure and temperature. Upon warming it was seen that scrambling occurred once more, such that both complexes were present. During scrambling the bound benzyl imine was not reduced but removed intact, indicating that an intermolecular hydrogenation is occurring, rather than an intramolecular hydrogenation.

(Scheme 6.8). Complete conversion was obtained with an ee of 10% for the aniline product, compared to 0% ee during screening. This indicates that this complex is responsible for the chiral induction to the product; it was later shown that 30 min was insufficient time to completely form the new complex at 1 eq of imine to iridium complex, indicating a higher enantioselectivity may be observed if a longer pre-mixing time was used.



Scheme 6.28 AH of aniline imine, utilising the benzyl imine bound complex.

In an attempt to further understand the system, similar ¹H NMR experiments were performed on the aniline imine. No new species was observed upon addition of the aniline imine to the iridium complex, as was seen with the benzyl imine. The conversion occurred at a faster rate initially, before slowing down, which may be due to a lack of H₂. This suggested that the standard iridicycle was able to perform the reaction, the same TFE hydride was also formed initially (-10 ppm). Multiple hydrides were seen in the final spectra after the reaction was complete, indicating the standard complex is less stable and decomposes to a large number of iridium hydride species, with those around -15 ppm once more being observed (bottom spectra, Figure 6.14).

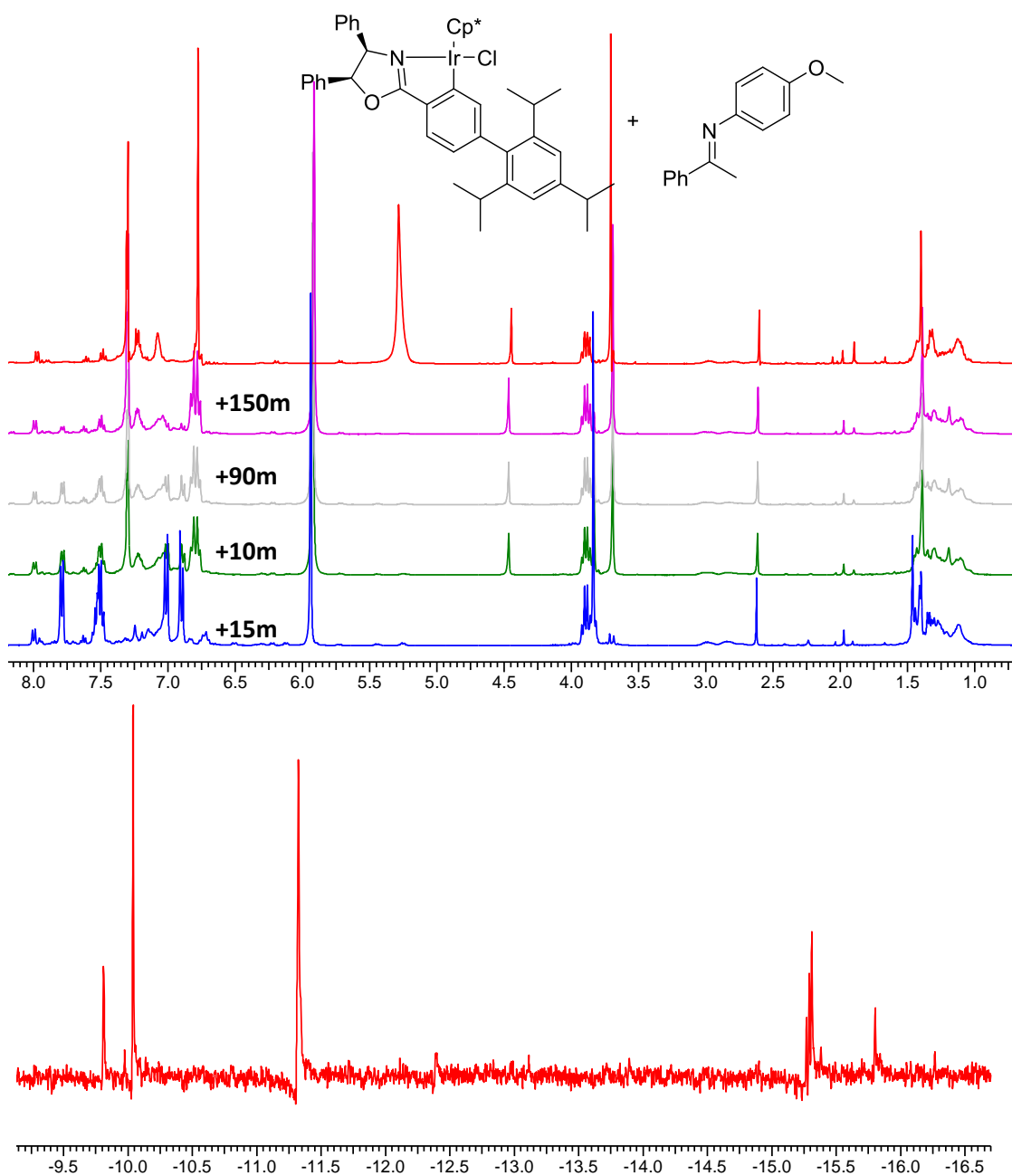


Figure 6.26 Iridium catalyst with 5 eq of aniline at 253 K, additions of atmospheric H₂, heated to 298 K.

A pre-formed sample of the benzyl imine iridium complex was treated with 5 eq of the aniline-based imine and subjected to the above conditions (Figure 6.15). This showed a much slower rate of reaction than previously observed for the aniline imine, indicating the benzyl imine bound complex is stable. After 24 hours complete

Figure 1 displays the ^1H NMR spectra of the Ir complex **1** and its reaction with 2-methoxy-1-phenylvinyl. The top panel shows the ^1H NMR spectrum of complex **1** in CDCl_3 , with peaks for the complex and a reference peak at 3.7 ppm. The bottom panel shows the ^1H NMR spectra of the reaction mixture at various time points: +0.25h (red), +0.5h (green), +4h (grey), +1h (magenta), and +26h (yellow). The spectra show the formation of a new product over time, with the reference peak at 3.7 ppm remaining constant.

230

6.5.5 Solvent Test

It was previously observed (Table 6.2) that the AH was inactive in common laboratory solvents, such as MeOH and CHCl_3 . These solvents were therefore investigated *via* ^1H NMR for their varied effect upon the iridium complex. Chloroform was trialled initially; this showed no change in the complex upon addition of the benzyl imine (Figure 6.16). After treatment with atmospheric H_2 gas, no change was observed in the complex or conversion of imine, even after being sealed at room temperature for 3 days.

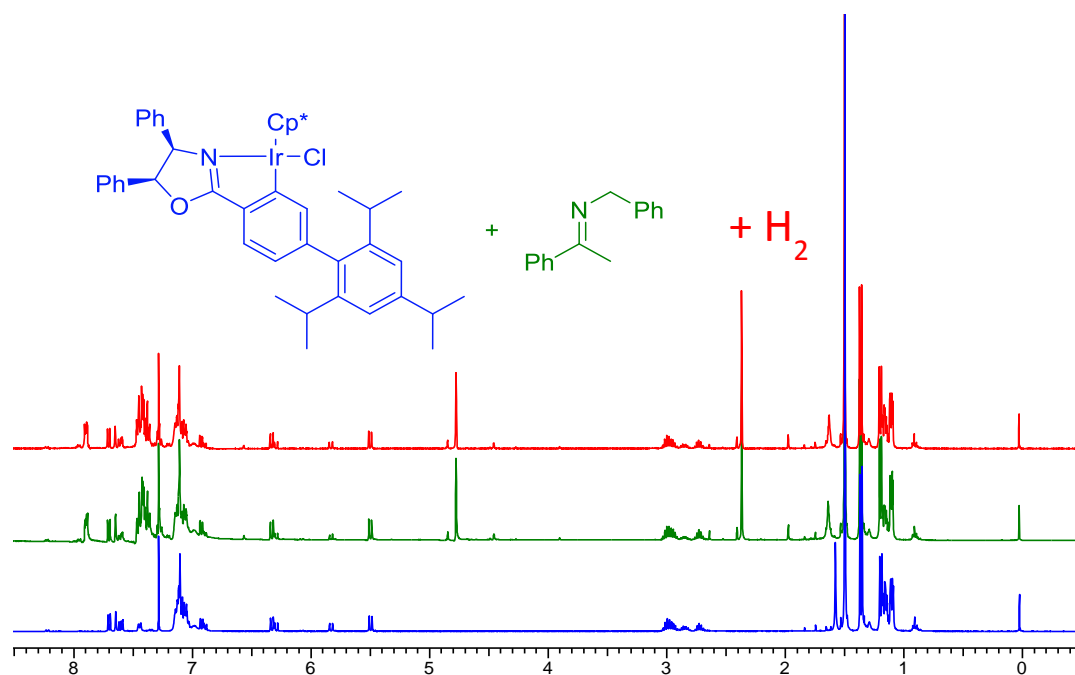


Figure 6.28 Ir cat in CDCl_3 , addition of imine, addition of atmospheric pressure H_2 left for 3 days.

Methanol was also examined, this showed no alteration of the standard Ir **11** complex, although it was rapidly seen that the key CH_2 imine peak was lost (Figure 6.17). There was no formation of new peaks observed to specify product synthesis. This indicates the formation of the new complex is unique to the TFE

system, emphasising the formation of this new species *in situ* may be crucial for the AH to occur.

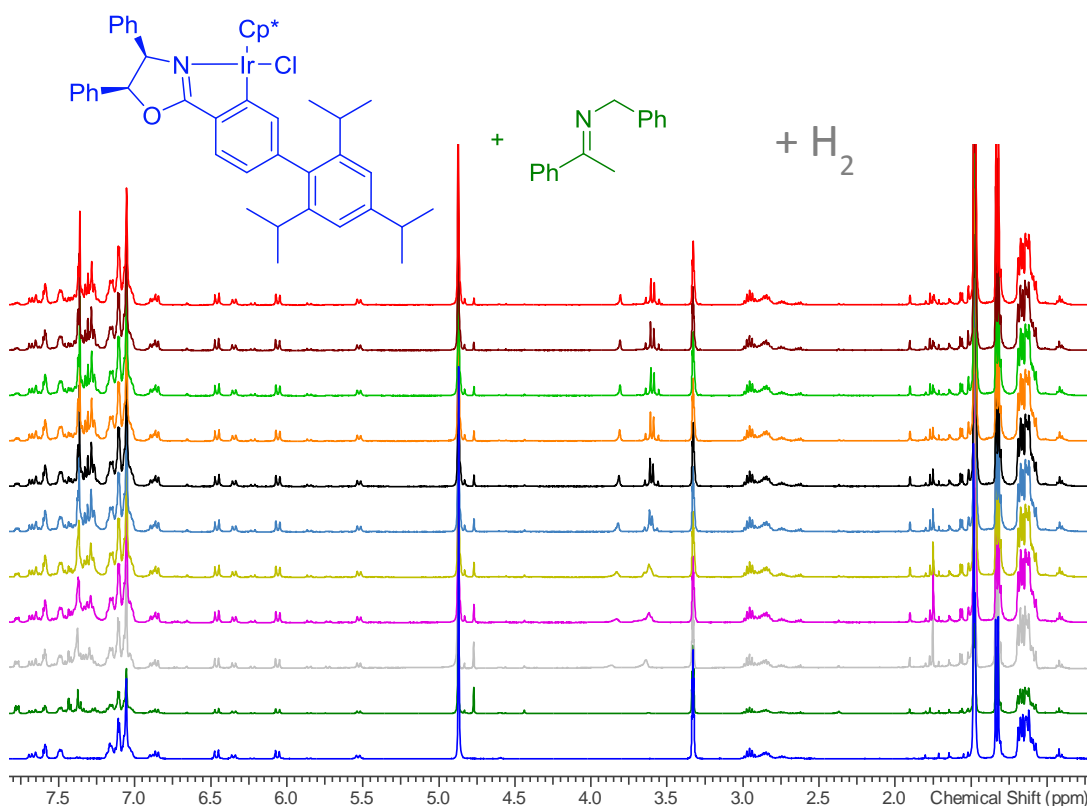


Figure 6.29 Ir cat In MeOD, plus 1 eq of imine, addition of H₂ (1 atm) 7.5 min apart.

6.5.6 Proposed mechanism

Considering the output from the modelling and experimental observations an intermolecular mechanism appeared to be likely (Figure 6.18). The hydrogenation is only possible in TFE as no other solvent allows for removal of the chloride and is therefore shown to be inactive. It is clear that the major form of the iridium species is bound to the imine and that the bound imine is not hydrogenated, but maybe removed intact at room temperature. The presence of this imine bound species also offers an increase in the enantioselectivity observed, indicating this species plays a key role in the reduction step. A second minor iridium species is present, which appears to be the hydride species, though this species was too weak

to be fully observed and characterised, from the high pressure NMR it was seen that hydride species of -15 ppm were formed, consistent with an iridacycle hydride species (such as **Ir 11**). For the minor hydride species observed to have resulted from the bound imine iridium complex, ligand dissociation would have to occur; either through the dissociation of the cyclometallated nitrogen, or through the slippage of the cyclopentadienyl species, to allow a hydride to bind. An interaction between the two iridium species would account for the increased enantioselectivity observed for the aniline imine, as well as the reduction in ee at a 1:1 imine iridium ratio, although the nature of this coordination could not be observed. The decomposition of the complex has been observed after the reaction was complete *via* reductive elimination, to yield free ligand and multiple iridium hydride species.

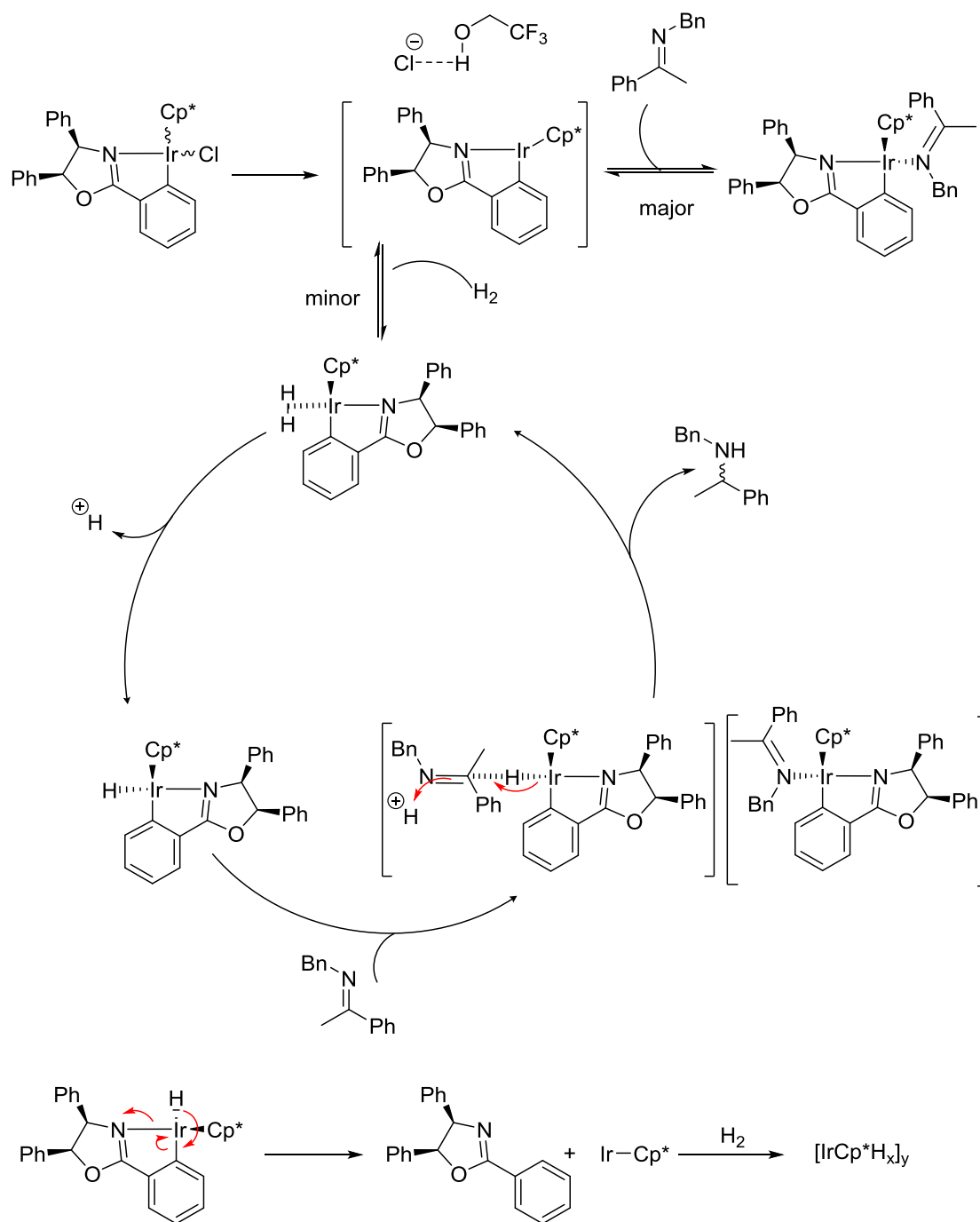


Figure 6.30 Proposed mechanism.

6.6 Conclusions

The results presented in this chapter demonstrate further utility for the bulky oxazoline containing complexes. Proving highly active under mild hydrogenation conditions for the asymmetric reduction of benzyl imines, yielding

the desired amines in both high conversions and moderate to high ees. The corresponding complex however, showed high conversion but racemic amines when utilised for the reduction of aryl imines. This observation initiated a mechanistic investigation, identifying the formation of a novel iridium species upon subjection to the catalytic conditions. The *in-situ* formed species was revealed to have formed *via* the co-ordination of the imine onto the existing iridium species. Further mechanistic and modelling investigation indicated the hydrogenation occurred *via* an intermolecular hydrogenation pathway in which the un-bound imine is hydrogenated in preference over the iridium bound imine species.

6.7 Experimental

IPA, toluene and DCM were dried on a MB-SPS 800 and methanol was dried over magnesium and iodine; all other chemicals were used as purchased. Standard NMR spectra were recorded on a Bruker 400 MHz NMR spectrometer, with TMS as internal standard. High pressure mechanistic NMRs were run on a Bruker 200 MHz spectrometer in non-deuterated TFE. Low pressure mechanistic NMRs were run on a BrukerAvance 400 MHz spectrometer using d³-TFE. COSY and HSQC were run on a BrukerAvance 500 MHz. NOESY was run on a BrukerAvance 400 MHz spectrometer with mixing time of 0.5 s. Modelling studies were conducted on Spartan '08 and presented using Chemcraft software.

6.7.1 Standard Procedures

Imine synthesis

Imines were synthesised by the literature procedure. Ketone (1 eq) and amine (1.1eq) were refluxed in toluene in the presence of a catalytic amount of PTSA. The imines were purified by recrystallisation or distillation.

Imine hydrogenation

A glass lined autoclave was charged with a stirrer bar, the imine (1 eq, 0.5 mmol) and iridicycle (1 mol%), followed by TFE (2.5 mL). The autoclave was sealed and flushed three times with hydrogen gas, then charged to 20 bar and allowed to stir at room temperature for 16 h. The resulting mixture was concentrated under vacuum. The residue was purified by column chromatography in 10% EtOAc in hexane, in quantitative yields.

High pressure NMR hydrogenation

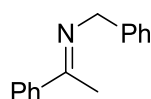
A Sapphire NMR tube was charged with catalyst (0.012 mmol, 10 mg), to which 2 mL TFE was added. An NMR spectrum was obtained, to allow for solvent suppression to be conducted. The imine (0.06 mmol, 2.5 mg) in TFE (0.5 mL) was charged into the tube. Another spectrum was run. Hydrogen gas was bubbled through the solution until a pressure of 20 bar was achieved. The hydrogen flow was reduced and multiple spectra were run.

Low pressure NMR hydrogenation

A Schlenk NMR tube was charged with imine and catalyst (0.0097 mmol, 8.4 mg, ratios described above) and 0.5 mL d^3 -TFE was added. The tube was sealed and

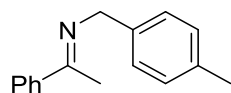
cooled to 253 K. After a lock and shim was completed the NMR tube was removed from the machine and maintained at 253 K in a cardice/acetonitrile bath. Balloon pressure H₂ was added *via* a long needle and bubbled through the solution. The tube was sealed once more and inserted into the NMR machine and multiple NMR spectra ran. The temperature was slowly raised by 5 to 10 K every hour, until room temperature was reached or the reaction was complete.

6.7.2 Analytical data



(E)-1-Phenyl-N-(1-phenylethylidene)methanamine

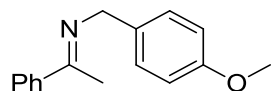
Yellow solid. **¹H NMR** (CDCl₃, 400 MHz) δ (ppm) 7.88-7.85 (m, 2H), 7.44-7.32 (m, 8H), 4.82 (s, 0.3H, minor isomer), 4.75 (s, 1.77H, major isomer), 2.38 (s, 0.4H, minor isomer), 2.34 (s, 2.6H, major isomer). **¹³C NMR** (CDCl₃, 100 MHz) δ (ppm) 166.09, 141.09, 140.53, 129.63, 128.41, 128.24, 127.71, 126.76, 126.57, 55.70, 15.90. **HRMS** (CI) [M+H]⁺ calculated 210.1277 [M+H]⁺ found 210.1286. **CHN** C₁₅H₁₅N calculated C, 86.08; H, 7.22; N, 6.69; found C, 86.65; H, 7.03; N, 5.43.



(E)-N-(1-Phenylethylidene)-1-(p-tolyl)methanamine

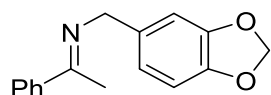
Yellow solid. **¹H NMR** (CDCl₃, 400 MHz) δ (ppm) 7.87-7.83 (m, 2H), 7.39-7.37 (m, 3H), 7.31 (d, J = 7.9 Hz, 2H), 7.16 (d, J = 7.9 Hz, 2H), 4.70 (s, 2H), 2.34 (s, 3H), 3.32 (s, 3H). **¹³C NMR** (CDCl₃, 100 MHz) δ (ppm) 165.87, 141.15, 137.49, 136.07, 129.58,

129.10, 128.23, 127.64, 126.77, 55.50, 21.15, 15.85. **HRMS** (CI) $[M+H]^+$ calculated 244.1434, $[M+H]^+$ found 224.1439.

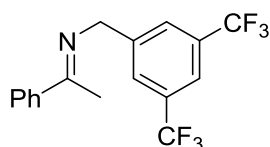


1-Phenyl-N-(1-(*m*-tolyl)ethylidene)methanamine (mixture of *E* and *Z*)

Yellow solid. $^1\text{H NMR}$ (CDCl_3 , 400 MHz) δ (ppm) 7.87-7.84 (m, 2H), 7.40-7.36 (m, 4H), 6.91-6.86 (m, 3H), 4.73 (s, 0.2H, minor isomer), 4.68 (s, 1.8H, major isomer), 3.84 (s, 0.3H, minor isomer), 3.81 (s, 2.7H, major isomer), 2.36 (s, 0.3H, minor isomer), 2.33 (s, 2.7H, major isomer). $^{13}\text{C NMR}$ (CDCl_3 , 100 MHz) δ (ppm) 165.76, 158.36, 141.14, 132.73, 129.58, 128.78, 128.22, 126.75, 113.83, 55.32, 45.93, 15.84. **HRMS** (CI) $[M+H]^+$ calculated 240.1383 $[M+H]^+$ found 240.1392. **CHN** $\text{C}_{16}\text{H}_{17}\text{NO}$ calculated C, 80.30; H, 7.16; N, 5.85; found C, 79.15; H, 7.08; N, 5.65.

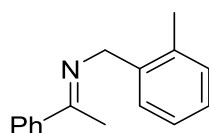


Cream solid. $^1\text{H NMR}$ (CDCl_3 , 400 MHz) δ (ppm) 7.86-7.84 (m, 2H), 7.40-7.37 (m, 3H), 6.97 (d, $J = 1.27$ Hz, 1H), 6.88-6.76 (m, 2H), 5.94 (s, 2H), 4.68 (s, 0.2H minor isomer), 4.63 (s, 1.8H, major isomer), 2.36 (s, 0.3H, minor isomer), 2.33 (s, 2.7H, major isomer). $^{13}\text{C NMR}$ (CDCl_3 , 100 MHz) δ (ppm) 165.88, 147.71, 146.19, 141.01, 134.59, 129.64, 128.23, 126.74, 120.55, 108.48, 108.12, 100.84, 55.44, 15.90. **HRMS** (CI) $[M+H]^+$ calculated 254.1176, $[M+H]^+$ found 254.1186.



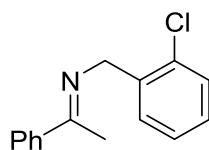
(E)-1-(3,5-Bis(trifluoromethyl)phenyl)-N-(1-phenylethylidene)methanamine

Yellow solid. ^1H NMR (CDCl_3 , 400 MHz) δ (ppm) 7.97 (s, 2H), 7.89-7.87 (m, 2H), 7.79 (s, 1H), 7.45-7.41 (m, 3H), 4.78 (s, 2H), 2.39 (s, 3H). ^{13}C NMR (CDCl_3 , 100 MHz) δ (ppm) 167.26, 143.43, 140.39, 131.68, 131.35, 130.10, 128.41, 128.00, 126.72, 120.68, 54.67, 16.30.



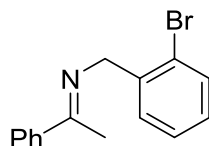
(E)-N-(1-Phenylethylidene)-1-(o-tolyl)methanamine

Cream solid. ^1H NMR (CDCl_3 , 400 MHz) δ (ppm) 7.88-7.86 (m, 2H), 7.40-7.38 (m, 4H), 7.20-7.17 (m, 3H), 4.69 (s, 2H), 2.39 (s, 3H), 2.34 (s, 3H). ^{13}C NMR (CDCl_3 , 100 MHz) δ (ppm) 165.98, 141.11, 138.49, 136.06, 130.08, 129.61, 128.24, 126.74, 126.64, 125.98, 53.82, 19.43, 15.78.



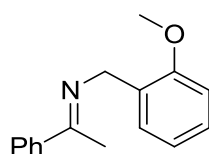
(E)-N-(1-Phenylethylidene)-1-(o-chlorophenyl)methanamine

Yellow solid. ^1H NMR (CDCl_3 , 400 MHz) δ (ppm) 7.90-7.87 (m, 2H), 7.66 (d, J = 6.4 Hz, 1H), 7.42-7.37 (m, 4H), 7.28-7.17 (m, 2H), 4.77 (s, 2H), 2.36 (s, 3H). ^{13}C NMR (CDCl_3 , 100 MHz) δ (ppm) 166.77, 140.97, 138.11, 133.15, 129.77, 129.33, 128.30, 127.76, 126.86, 126.78, 53.04, 16.12.



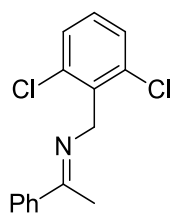
(E)-1-(2-Bromophenyl)-N-(1-phenylethylidene)methanamine

Orange solid. $^1\text{H NMR}$ (CDCl_3 , 400 MHz) δ (ppm) 7.91-7.88 (m, 2H), 7.66 (d, $J = 7.6$ Hz, 1H), 7.58 (dd, $J = 7.9, 0.8$ Hz, 1H), 7.43-7.41 (m, 3H), 7.33 (td, $J = 7.61, 0.7$ Hz, 1H), 7.13 (td, $J = 7.6, 1.3$ Hz, 1H), 4.75 (s, 2H), 2.37 (s, 3H). $^{13}\text{C NMR}$ (CDCl_3 , 100 MHz) δ (ppm) 166.75, 140.94, 129.67, 132.40, 129.78, 129.54, 128.30, 128.09, 127.47, 126.78, 123.48, 55.61, 16.19. **HRMS** (CI) $[\text{M}+\text{H}]^+$ calculated 288.0382 $[\text{M}+\text{H}]^+$ found 288.0375.



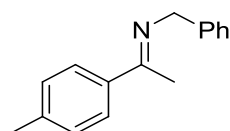
(E)-1-(2-Methoxyphenyl)-N-(1-phenylethylidene)methanamine

Yellow solid. $^1\text{H NMR}$ (CDCl_3 , 400 MHz) δ (ppm) 7.89-7.87 (m, 2H), 7.51 (d, $J = 7.4$ Hz, 1H), 7.39 (dd, $J = 4.0, 2.6$ Hz, 3H), 6.99-6.85 (m, 3H), 4.83 (s, 0.2H, minor isomer), 4.74 (s, 1.8H, major isomer), 3.86 (s, 3H), 2.39 (s, 0.3H, minor isomer), 2.33 (s, 2.7H, major isomer). $^{13}\text{C NMR}$ (CDCl_3 , 100 MHz) δ (ppm) 166.17, 156.88, 141.32, 129.52, 128.79, 126.47, 128.22, 127.43, 126.78, 120.58, 109.94, 55.34, 50.05, 15.85. **HRMS** (CI) $[\text{M}+\text{H}]^+$ calculated 240.1383 $[\text{M}+\text{H}]^+$ found 240.1392. **CHN** $\text{C}_{16}\text{H}_{17}\text{NO}$ calculated C, 80.30; H, 7.16; N, 5.85; found C, 79.04; H, 7.02; N, 5.59.



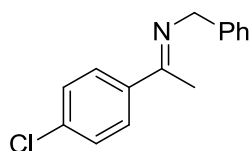
(E)-1-(2-Bromophenyl)-N-(1-phenylethylidene)methanamine

Yellow solid. ^1H NMR (400 MHz, CDCl_3) δ (ppm) 7.78-7.75 (m, 2H), 7.37-7.35 (m, 5H), 7.16 (t, $J = 7.80$ Hz, 1H), 4.88 (s, 2H), 2.43 (s, 3H). ^{13}C NMR (CDCl_3 , 100 MHz) δ (ppm) 177.5, 140.8, 128.3, 128.2, 127.9, 127.4, 126.7, 126.3, 56.5, 39.2, 20.2.



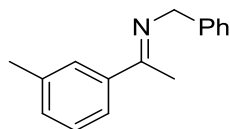
(E)-1-Phenyl-N-(1-(p-tolyl)ethylidene)methanamine

Yellow solid. ^1H NMR (CDCl_3 , 400 MHz) δ (ppm) 7.86-7.84 (m, 2H), 7.38-7.36 (m, 3H), 7.31 (d, $J = 7.8$ Hz, 2H), 7.15 (d, $J = 7.8$ Hz, 2H), 4.76 (s, 0.2H, minor isomer), 4.70 (s, 1.8H, major isomer), 2.36 (d, $J = 0.8$ Hz, 0.4H, minor isomer), 2.34 (s, 2.8H, major isomer), 2.31 (s, 2.8H, major isomer). ^{13}C NMR (CDCl_3 , 100 MHz) δ (ppm) 165.86, 141.16, 137.51, 136.07, 129.59, 129.11, 128.23, 127.65, 126.78, 55.51, 21.16, 15.84. HRMS (CI) $[\text{M}+\text{H}]^+$ calculated 244.1434, $[\text{M}+\text{H}]^+$ found 224.1437. CHN $\text{C}_{16}\text{H}_{17}\text{N}$ calculated C, 86.05; H, 7.67; N, 6.27; found C, 85.23; H, 7.46; N, 5.85.



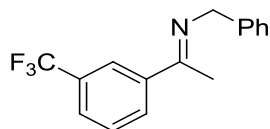
(E)-N-(1-(4-Chlorophenyl)ethylidene)-1-phenylmethanamine

Yellow solid. $^1\text{H NMR}$ (CDCl_3 , 400 MHz) δ (ppm) 7.81 (d, $J = 8.7$ Hz, 2H), 7.43-7.39 (m, 2H), 7.37-7.34 (m, 4H), 7.28-7.24 (m, 1H), 4.83 (s, 0.12H, minor isomer), 4.72 (s, 1.88H major isomer), 2.36 (s, 0.15H minor isomer), 2.31 (s, 2.85H, major isomer). $^{13}\text{C NMR}$ (CDCl_3 , 100 MHz) δ (ppm) 164.75, 140.33, 139.34, 135.71, 128.46, 128.39, 128.13, 127.79, 126.67, 55.76, 15.72. **HRMS** (CI) $[\text{M}+\text{H}]^+$ calculated 244.0888, $[\text{M}+\text{H}]^+$ found 244.0892. **CHN** $\text{C}_{15}\text{H}_{14}\text{ClN}$ calculated C, 73.92; H, 5.79; N, 5.75; found C, 73.43; H, 5.61; N, 4.65.



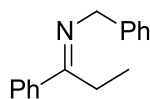
(E)-1-Phenyl-N-(1-(m-tolyl)ethylidene)methanamine

Yellow solid. $^1\text{H NMR}$ (CDCl_3 , 400 MHz) δ (ppm) 7.70 (s, 1H), 7.63 (d, $J = 7.7$ Hz, 1H), 7.43-7.29 (m, 5H), 7.25-7.20 (m, 2H), 4.83 (s, 0.1H, minor isomer), 4.74 (s, 1.9H major isomer), 2.41 (s, 0.2H minor isomer), 2.39 (s, 2.8H major isomer), 2.36 (s, 0.2H, minor isomer), 2.32 (s, 2.8H major isomer). $^{13}\text{C NMR}$ (CDCl_3 , 100 MHz) δ (ppm) 166.41, 141.12, 140.52, 137.87, 130.40, 128.41, 128.12, 127.72, 127.36, 123.96, 55.71, 21.52, 16.01. **HRMS** (CI) $[\text{M}+\text{H}]^+$ calculated 244.1434, $[\text{M}+\text{H}]^+$ found 224.1436.



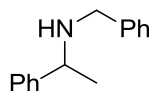
(E)-1-Phenyl-N-(1-(*m*-tolyl)ethylidene)methanamine

Yellow solid. $^1\text{H NMR}$ (CDCl_3 , 400 MHz) δ (ppm) 8.12 (s, 1H), 8.05 (d, $J = 7.8$ Hz, 1H), 7.64 (d, $J = 7.7$ Hz, 1H), 7.50 (t, $J = 7.8$ Hz, 1H), 7.44-7.35 (m, 5H), 4.83 (s, 0.2H, minor isomer), 4.75 (s, 1.8H, major isomer), 2.39 (s, 0.3H, minor isomer), 2.36 (s, 2.7H, major isomer). $^{13}\text{C NMR}$ (100 MHz, CDCl_3) δ (ppm) 161.51, 141.64, 140.12, 128.75, 128.51, 128.30, 128.00, 127.72, 126.76, 126.26, 126.22, 126.18, 126.15, 123.66, 123.62, 123.58, 123.54, 55.91, 15.83. **HRMS** (CI) $[\text{M}+\text{H}]^+$ calculated 278.1151, $[\text{M}+\text{H}]^+$ found 278.1155.



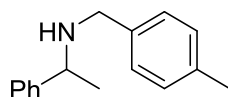
(E)-1-Phenyl-N-(1-phenylpropylidene)methanamine

Yellow liquid. $^1\text{H NMR}$ (CDCl_3 , 400 MHz) δ (ppm) 7.88-7.85 (m, 2H), 7.42-7.34 (m, 7H), 7.14 (m, 1H), 4.81 (s, 2H), 2.82 (q, $J = 7.5$ Hz, 2H), 1.16 (t, $J = 7.5$ Hz, 3H). $^{13}\text{C NMR}$ (CDCl_3 , 100 MHz) δ (ppm) 129.56, 128.51, 128.39, 128.31, 127.99, 127.65, 127.02, 126.54, 126.35, 54.81, 22.14, 11.63. **HRMS** (CI) $[\text{M}+\text{H}]^+$ calculated 244.1434, $[\text{M}+\text{H}]^+$ found 244.1438.



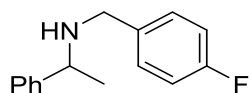
***N*-Benzyl-1-phenylethanamine**

Yellow oil. **¹H NMR** (CDCl₃, 400 MHz) δ (ppm) 7.36-7.21 (m, 10H), 3.81 (q, *J* = 6.5 Hz, 1H), 3.62 (q, *J* = 13.1 Hz, 2H), 1.63 (bs, 1H), 1.37 (d, *J* = 6.5 Hz, 3H). **¹³C NMR** (CDCl₃, 100 MHz) δ (ppm) 145.57, 140.64, 128.50, 128.40, 128.17, 126.97, 126.88, 126.74, 57.51, 51.67, 24.55. **HRMS** (CI) [M+H]⁺ Calculated 212.1434, [M+H]⁺ found 212.1444. **CHN** calculated C, 85.26; H, 8.11; N, 6.63; found C, 85.41; H, 8.17; N, 6.61. **HPLC** (Chiralpak IB-3, 99:1 Hex:IPA + 0.1% HNEt₂, 1 mL/min, 25 °C, 254 nm) 5.65 min (major) and 6.09 min.



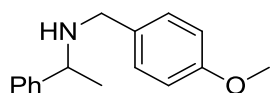
***N*-(4-Methylbenzyl)-1-phenylethanamine**

Yellow oil. **¹H NMR** (CDCl₃, 400 MHz) δ (ppm) 7.35-7.34 (m, 4H), 7.6-7.26 (m, 1H), 7.17-7.10 (m, 4H), 3.80 (q, *J* = 6.6 Hz, 1H), 3.58 (q, *J* = 13.0 Hz, 2H), 2.33 (s, 3H), 1.60 (bs, 1H), 1.35 (d, *J* = 6.6 Hz, 3H). **¹³C NMR** (CDCl₃, 100 MHz) δ (ppm) 145.62, 137.57, 136.44, 129.08, 128.49, 128.13, 126.94, 126.76, 57.41, 51.36, 24.53, 21.31. **HRMS** (CI) [M+H]⁺ calculated 226.1590, [M+H]⁺ found 226.1596. **CHN** C₁₆H₁₉N calculated C, 85.28; H, 8.50; N, 6.22; found C, 86.21; H, 8.58; N, 6.41. **HPLC** (Chiralpak IB-3, 99.8:0.2 Hex:IPA (+ 0.1% HNEt₂), 0.5 mL/min, 25 °C, 254 nm) 16.83 min (major) and 17.72 min.



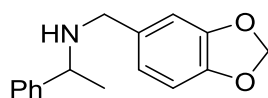
***N*-(4-Fluorobenzyl)-1-phenylethanamine**

Yellow solid. $^1\text{H NMR}$ (CDCl_3 , 400 MHz) δ (ppm) 7.35-7.33 (m, 4H), 7.25-7.22 (m, 2H), 7.08 (dt, $J = 28.5, 8.8$ Hz, 1H), 6.98 (t, $J = 8.8$ Hz, 2H), 3.79 (q, $J = 6.6$ Hz, 1H), 3.58 (q, $J = 12.4$ Hz, 2H), 1.65 (bs, 1H), 1.37 (d, $J = 6.6$ Hz, 3H). $^{13}\text{C NMR}$ (CDCl_3 , 100 MHz) δ (ppm) 145.42, 129.70, 129.62, 128.53, 127.02, 126.68, 115.22, 115.01, 57.53, 50.91, 24.48. **MS** (CI) $[\text{M}+\text{H}]^+$ Calculated 230.3, $[\text{M}+\text{H}]^+$ found 230.1. **HPLC** (Chiralpak IB-3, 99.8:0.2 Hex:IPA (+ 0.1% HNEt_2), 0.5 mL/min, 25 $^\circ\text{C}$, 254 nm) 15.12 min (major) and 15.71 min.

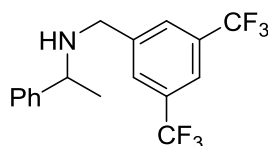


***N*-Benzyl-1-(4-nitrophenyl)ethanamine**

Yellow oil. $^1\text{H NMR}$ (CDCl_3 , 400 MHz) δ (ppm) 7.35-7.33 (m, 4H), 7.26-7.25 (m, 1H), 7.19 (d, $J = 8.5$ Hz, 2H), 6.85 (d, $J = 8.6$ Hz, 2H), 3.82-3.77 (m, 4H), 3.56 (q, $J = 12.9$ Hz, 2H), 1.36 (d, $J = 6.6$ Hz, 3H). $^{13}\text{C NMR}$ (CDCl_3 , 100 MHz) δ (ppm) 158.55, 145.65, 132.80, 129.32, 128.48, 126.93, 126.74, 113.76, 57.40, 55.30, 51.05, 24.55. **HRMS** (CI) $[\text{M}+\text{H}]^+$ Calculated 242.1539, $[\text{M}+\text{H}]^+$ found 242.1545. **CHN** $\text{C}_{16}\text{H}_{21}\text{NO}$ calculated C, 79.63; H, 7.94; N, 5.80; found C, 79.86; H, 8.04; N, 5.83. **HPLC** (Chiralpak IB-3, 99.8:0.2 Hex:IPA (+ 0.1% HNEt_2), 0.5 mL/min, 25 $^\circ\text{C}$, 254 nm) 25.69 min (major) and 27.27 min.

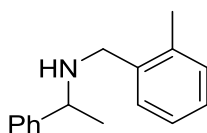


Yellow oil. $^1\text{H NMR}$ (CDCl_3 , 400 MHz) δ (ppm) 7.35-7.34 (m, 4H), 7.26-7.23 (m, 1H), 6.8 (d, $J = 1.3$ Hz, 1H), 6.75-6.69 (m, 2H), 5.93 (s, 2H), 3.79 (q, $J = 6.6$ Hz, 1H), 3.52 (q, $J = 13.0$ Hz, 2H), 1.59 (bs, 1H), 1.36 (d, $J = 6.5$ Hz, 3H). $^{13}\text{C NMR}$ (CDCl_3 , 100 MHz,) δ (ppm) 147.64, 146.41, 145.52, 134.62, 128.50, 126.97, 126.71, 121.18, 108.74, 108.06, 100.87, 57.33, 51.41, 24.53. **HRMS** (CI) calculated $[\text{M}+\text{H}]^+$ 256.1332, found $[\text{M}+\text{H}]^+$ 256.1325. **HPLC** (Chiralpak IB-3, 99.8:0.2 Hex:IPA + 0.1% HNEt_2 , 0.5 mL/min, 25 $^\circ\text{C}$, 254 nm) 26.39 min (major) and 30.42 min.



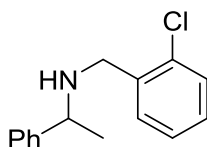
***N*-(3,5-Bis(trifluoromethyl)benzyl)-1-phenylethanamine**

Orange oil. $^1\text{H NMR}$ (CDCl_3 , 400 MHz) δ (ppm) 7.76 (s, 2H), 7.74 (s, 1H), 7.38-7.29 (m, 5H), 3.80 (q, $J = 6.6$ Hz, 1H), 3.75 (s, 2H), 1.42 (d, $J = 6.6$ Hz, 3H). $^{13}\text{C NMR}$ (CDCl_3 , 100 MHz) δ (ppm) 144.84, 143.41, 131.59, 131.26, 128.64, 128.18, 127.26, 126.61, 120.81, 58.00, 50.81, 24.47. **HRMS** (CI) calculated $[\text{M}+\text{H}]^+$ 348.1181, found $[\text{M}+\text{H}]^+$ 348.1190. **HPLC** (Chiralpak IB-3, 99.8:0.2 Hex:IPA (+ 0.1% HNEt_2), 0.5 mL/min 25 $^\circ\text{C}$, 254 nm) 12.63 min (major) and 13.66 min.



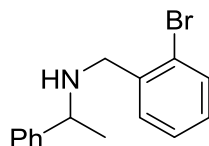
***N*-Benzyl-1-phenylethylamine**

Yellow oil. ^1H NMR (CDCl_3 , 400 MHz) δ (ppm) 7.40-7.33 (m, 4H), 7.28-7.24 (m, 2H + CDCl_3), 7.17-7.13 (m, 3H), 3.84 (q, J = 6.6 Hz, 1H), 3.60 (s, 2H), 2.26 (s, 3H), 1.53 (bs, 1H), 1.38 (d, J = 6.5 Hz, 3H). ^{13}C NMR (CDCl_3 , 100 MHz) δ (ppm) 145.70, 138.56, 136.45, 130.28, 158.58, 128.47, 126.97, 126.47, 125.90, 58.23, 49.67, 30.98, 24.60, 18.96. HRMS (CI) calculated $[\text{M}+\text{H}]^+$ 226.1590, found $[\text{M}+\text{H}]^+$ 226.1591. HPLC (Chiralpak IB-3, 99.5:0.5 Hex:IPA (+ 0.1% HNEt_2), 1 mL/min, 25 $^\circ\text{C}$, 254 nm) 7.70 min and 8.23 min (major).



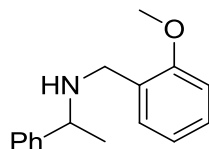
***N*-(2-Chlorobenzyl)-1-phenylethylamine**

Yellow oil. ^1H NMR (CDCl_3 , 400 MHz,) δ (ppm) 7.39-7.30 (m, 6H), 7.26-7.23 (m, 1H), 7.22-7.16 (m, 2H), 3.82-3.67 (m, 3H), 1.8 (bs, 1H), 1.37 (d, J = 6.5 Hz, 3H). ^{13}C NMR (CDCl_3 , 100 MHz) δ (ppm) 145.28, 137.80, 133.81, 130.45, 129.53, 128.50, 128.31, 127.03, 126.76, 57.43, 49.34, 24.58. HRMS (CI) $[\text{M}+\text{H}]^+$ Calculated 246.1044, $[\text{M}+\text{H}]^+$ found 246.1055. CHN $\text{C}_{16}\text{H}_{19}\text{NO}_2$ calculated C, 73.31; H, 6.56; N, 5.70; found C, 74.27; H, 6.65; N, 5.78. HPLC (Chiralpak IB-3, 99.8:0.2 Hex:IPA (+ 0.1% HNEt_2), 0.5 mL/min, 25 $^\circ\text{C}$, 254 nm) 17.63 min (major) and 18.77 min.



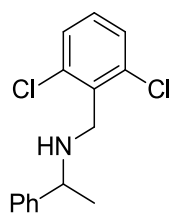
***N*-(2-Bromobenzyl)-1-phenylethanamine**

Yellow oil. $^1\text{H NMR}$ (CDCl_3 , 400 MHz) δ (ppm) 7.53 (dd, $J = 7.9, 0.9$ Hz, 1H), 7.39-7.24 (m, 7H + CDCl_3), 7.11 (dt, $J = 7.51, 1.56$ Hz, 1H), 3.79 (q, $J = 6.54$ Hz, 1H), 3.71 (q, $J = 13.76$ Hz, 2H), 1.75 (bs, 1H), 1.37 (d, $J = 6.6$ Hz, 3H). $^{13}\text{C NMR}$ (CDCl_3 , 100 MHz) δ (ppm) 145.29, 139.44, 132.82, 130.61, 128.58, 128.49, 127.38, 127.03, 126.82, 124.04, 57.36, 51.72, 24.59. **MS** (CI) $[\text{M}+\text{H}]^+$ calculated 289.05, $[\text{M}+\text{H}]^+$ found 290.10. **HPLC** (Chiralpak IB-3, 99.5:0.5 Hex:IPA (+ 0.1% HNEt_2), 1 mL/min, 25 $^\circ\text{C}$, 254 nm) 8.33 min (major) and 8.67 min.



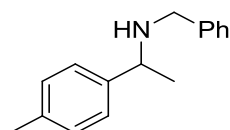
***N*-(2-Methoxybenzyl)-1-phenylethanamine**

Yellow oil. $^1\text{H NMR}$ (CDCl_3 , 400 MHz) δ (ppm) 7.38-7.32 (m, 4H), 7.27-7.25 (m, 2H), 7.15 (dd, $J = 7.3, 1.6$ Hz, 1H), 6.91-6.85 (m, 2H), 3.82 (s, 3H), 3.78 (q, 6.5 Hz, 1H), 3.72-3.69 (m, 1H), 3.59-3.56 (m, 1H), 1.35 (d, $J = 6.5$ Hz, 3H). $^{13}\text{C NMR}$ (CDCl_3 , 100 MHz) δ (ppm) 157.72, 145.75, 129.99, 128.48, 128.38, 128.16, 126.84, 120.36, 110.23, 57.16, 55.21, 47.26, 24.62. **HPLC** (Chiralpak IB-3, 99.8:0.2 Hex:IPA (+ 0.1% HNEt_2), 0.5 mL/min, 25 $^\circ\text{C}$, 254 nm) min (major) and min.



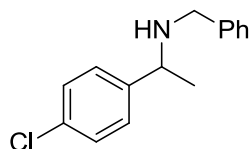
N-(2,6-Dichlorobenzyl)-1-phenylethanamine

Yellow oil. $^1\text{H NMR}$ (CDCl_3 , 400 MHz) δ (ppm) 7.40-7.38 (m, 2H), 7.33 (t, $J = 7.5$ Hz, 2H), 7.26-7.22 (m, 3H), 7.10 (t, $J = 7.6$ Hz, 1H), 3.89 (s, 2H), 3.84 (q, $J = 6.5$ Hz, 1H), 1.37 (d, $J = 6.5$ Hz, 3H). $^{13}\text{C NMR}$ (CDCl_3 , 100 MHz) δ (ppm) 145.27, 136.13, 135.97, 132.49, 128.80, 128.36, 126.36, 126.98, 126.74, 58.13, 47.04, 26.69. **HRMS** (CI) calculated $[\text{M}+\text{H}]^+$ 280.1654, found $[\text{M}+\text{H}]^+$ 280.0644. **HPLC** (Chiralpak IB-3, 99:1 Hex:IPA (+ 0.1% HNEt_2), 0.3 mL/min, 25 $^\circ\text{C}$, 254 nm) 25.96 min and 27.64 min.



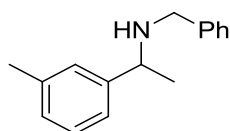
N-Benzyl-1-(p-tolyl)ethanamine

Yellow oil. $^1\text{H NMR}$ (CDCl_3 , 400 MHz) (ppm) δ 7.36-7.32 (m, 4H), 7.26-7.23 (m, 1H), 7.18-7.11 (m, 4H), 3.80 (q, $J = 6.6$ Hz, 1H), 3.58 (q, $J = 12.6$ Hz, 2H), 2.33 (s, 3H), 1.58 (bs, 1H), 1.36 (d, $J = 6.5$ Hz, 3H). $^{13}\text{C NMR}$ (CDCl_3 , 100 MHz) δ (ppm) 145.62, 137.57, 136.43, 129.07, 128.47, 128.12, 126.75, 57.39, 51.34, 24.54, 21.13. **HRMS** (CI) calculated $[\text{M}+\text{H}]^+$ 226.1590, found $[\text{M}+\text{H}]^+$ 226.1599. **HPLC** (Chiralpak IB-3, 99.8:0.2 Hex:IPA (+ 0.1% HNEt_2), 0.5 mL/min, 25 $^\circ\text{C}$, 254 nm) 14.62 min (major) and 15.25 min.



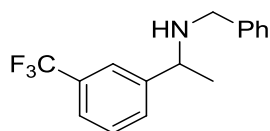
N-Benzyl-1-(4-chlorophenyl)ethanamine

Yellow oil. $^1\text{H NMR}$ (CDCl_3 , 400 MHz) δ (ppm) 7.34-7.24 (m, 9H), 3.79 (q, J = 6.6 Hz, 1H), 3.60 (q, J = 13.2 Hz, 2H), 1.33 (d, J = 6.5 Hz, 3H). $^{13}\text{C NMR}$ (CDCl_3 , 100 MHz) δ (ppm) 144.08, 140.39, 132.45, 128.63, 128.44, 128.14, 128.12, 126.97, 56.90, 51.63, 24.60. **HRMS** (CI) $[\text{M}+\text{H}]^+$ calculated 246.1044, found 246.1045. **HPLC** (Chiralpak IB-3, 99:1 Hex:IPA (+ 0.1% HNEt_2), 1 mL/min, 25 °C, 254 nm) 6.3 min (major) and 7.2 min.



N-Benzyl-1-(*m*-tolyl)ethanamine

Yellow oil. $^1\text{H NMR}$ (CDCl_3 , 400 MHz) δ (ppm) 7.33-7.22 (m, 6H), 7.17-7.14 (m, 2H), 7.07 (d, J = 7.3 Hz, 1H), 3.78 (q, J = 6.5 Hz, 1H), 3.63 (q, J = 13.2 Hz, 2H), 2.37 (s, 3H), 1.36 (d, J = 6.8 Hz, 3H). $^{13}\text{C NMR}$ (CDCl_3 , 100 MHz) δ (ppm) 145.56, 140.71, 138.07, 128.63, 128.40, 128.16, 127.72, 127.40, 126.86, 123.79, 57.49, 51.72, 24.52, 21.55. **HPLC** (Chiralpak IB-3, 99:1 Hex:IPA (+ 0.1% HNEt_2), 1 mL/min, 25 °C, 254 nm) 5.40 min (major) and 5.71 min.

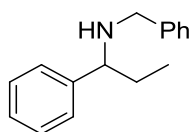


***N*-Benzyl-1-(3-(trifluoromethyl)phenyl)ethanamine**

Yellow solid. $^1\text{H NMR}$ (CDCl_3 , 400 MHz) δ (ppm) 7.64 (s, 1H), 7.50-7.45 (m, 3H), 7.30-7.23 (m, 5H), 3.88 (q, $J = 6.5$ Hz, 1H), 3.62 (q, $J = 13.2$ Hz, 2H), 1.37 (d, $J = 6.5$ Hz, 3H).

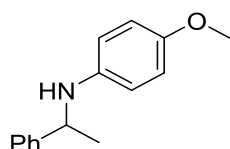
$^{13}\text{C NMR}$ (CDCl_3 , 100 MHz) δ (ppm) 146.71, 140.29, 130.93, 130.62, 130.30, 128.93, 128.47, 128.11, 127.03, 125.66, 123.86, 123.82, 123.60, 123.56, 57.28, 51.74, 24.63.

HRMS (CI) calculated $[\text{M}+\text{H}]^+$ 280.1308, found $[\text{M}+\text{H}]^+$ 280.1320. **HPLC** (Chiralpak IB-3, 99:1 Hex:IPA (+ 0.1% HNEt_2), 1 mL/min, 25 $^\circ\text{C}$, 254 nm) 5.87 min (major) and 6.80 min.



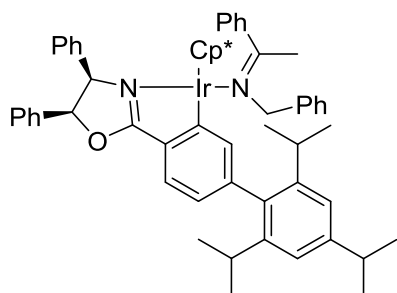
***N*-Benzyl-1-phenylpropan-1-amine**

Yellow oil. $^1\text{H NMR}$ (CDCl_3 , 400 MHz) δ (ppm) 7.37-7.24 (m, 10H), 3.67-3.63 (m, 1H), 3.56-3.52 (m, 2H), 1.79-1.65 (m, 2H), 0.81 (td, $J = 7.4, 2.4$ Hz, 3H). $^{13}\text{C NMR}$ (CDCl_3 , 100 MHz) δ (ppm) 144.09, 140.81, 128.36, 128.34, 128.17, 127.48, 126.95, 126.82, 64.23, 51.59, 31.16, 10.82. **HRMS** (CI) calculated $[\text{M}+\text{H}]^+$ 226.1590; found $[\text{M}+\text{H}]^+$ 226.1595. **CHN** $\text{C}_{16}\text{H}_{19}\text{N}$ calculated C, 85.28; H, 8.50; N, 6.22; found C, 85.88; H, 8.46; N, 6.51. **HPLC** (Chiralpak IB-3, 99.8:0.2 Hex:IPA (+ 0.1% HNEt_2), 0.5 mL/min, 25 $^\circ\text{C}$, 254 nm) 13.15 min (major) and 15.10 min.



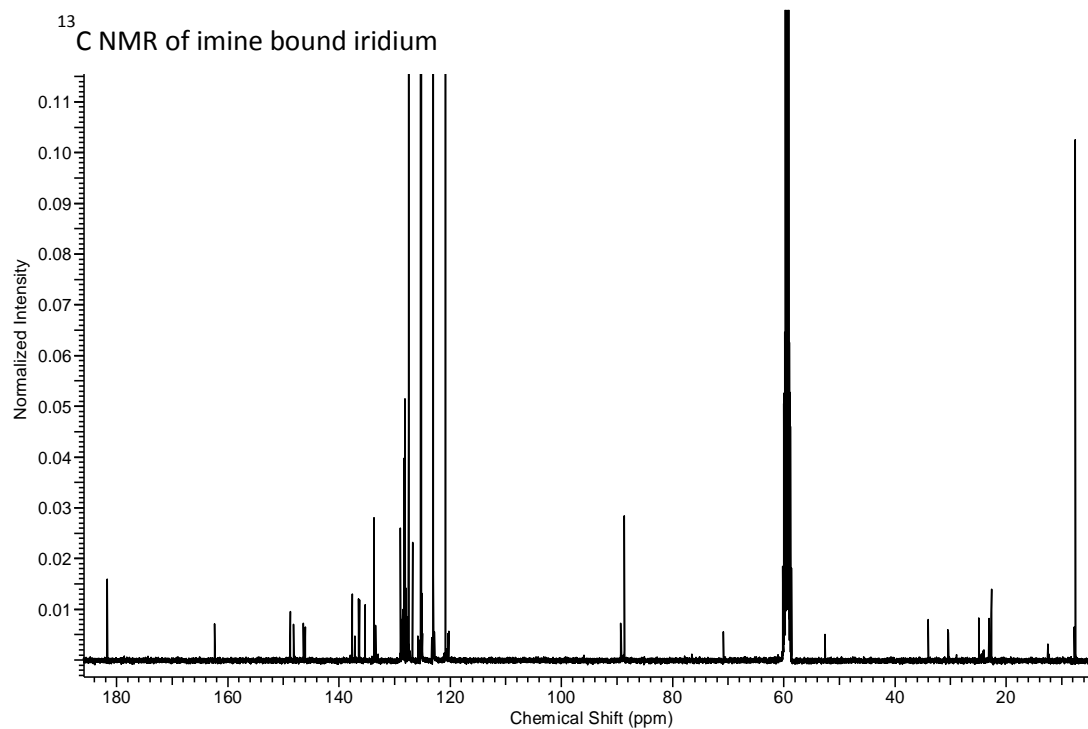
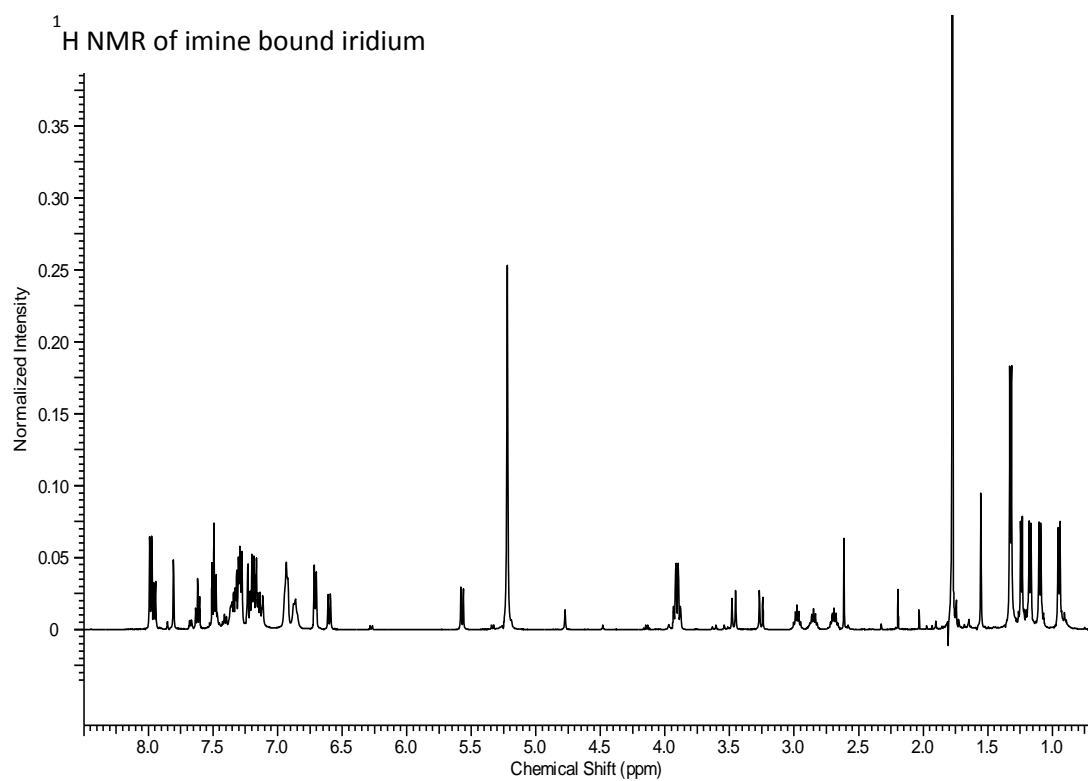
4-Methoxy-*N*-(1-phenylethyl)aniline¹⁵

White solid. **¹H NMR** (CDCl₃, 400 MHz) δ (ppm) 7.37-7.29 (m, 4H), 7.23-7.20 (m, 1H), 6.79 (d, *J* = 8.4 Hz, 2H), 6.49 (d, *J* = 8.5 Hz, 2H), 4.21 (q, *J* = 6.6 Hz, 1H), 3.69 (s, 3H), 1.51 (d, *J* = 6.6 Hz, 3H). **¹³C NMR** (CDCl₃, 100 MHz) δ (ppm) 152.1, 145.2, 141.2, 128.6, 126.9, 126.0, 114.9, 114.8, 55.7, 54.5, 25.0. **HRMS** (CI) [M+H]⁺ Calculated 228.1383, [M+H]⁺ found 228.1386. **CHN** C₁₅H₁₇NO calculated C, 79.26; H, 7.54; N, 6.16; found C, 79.42; H, 7.50; N, 5.95. **HPLC** (Chiralpak IB-3, 98:2 Hex:IPA + 0.1% HNEt₂, 1 mL/min, 25 °C, 254 nm) 7.14 min and 8.61 min.

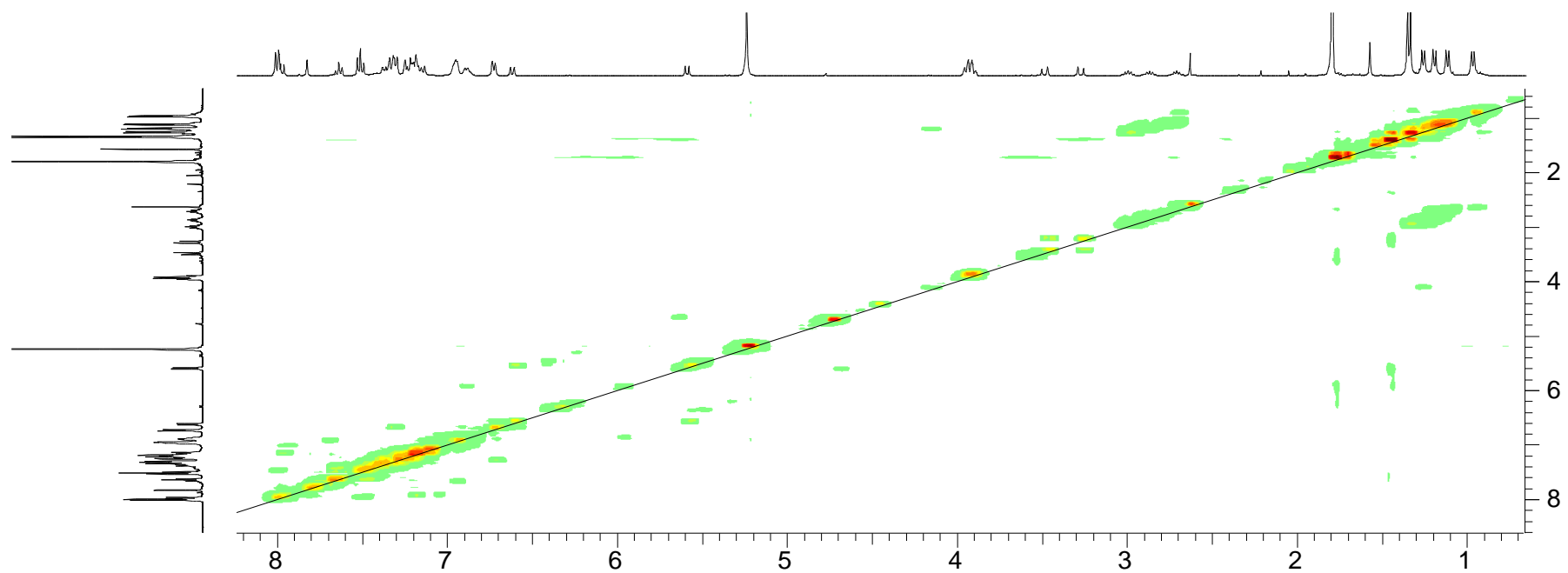


¹H NMR (d³-TFE, 400 MHz) δ (ppm) 7.98 (d, *J* = 7.3 Hz, 2H), 7.95 (d, *J* = 7.8 Hz, 1H), 7.81 (s, 1H), 7.62 (t, *J* = 7.3 Hz, 1H), 7.49 (t, 7.8 Hz, 3H), 7.34-7.28 (m, 6H), 7.23-7.11 (m, 7H), 6.94-6.92 (m, 2H), 6.71 (d, *J* = 7 Hz, 2H), 6.60 (d, *J* = 8.7 Hz, 1H), 5.57 (d, *J* = 8.9 Hz, 1H), 3.47 (d, *J* = 13.4 Hz, 1H), 3.26 (d, *J* = 13.4 Hz, 1H), 2.98 (dt, *J* = 13.8, 6.9 Hz, 1H), 2.85 (dt, *J* = 13.6, 6.7 Hz, 1H), 2.69 (dt, *J* = 13.7, 6.9 Hz, 1H), 1.78 (s, 15H), 1.32 (d, *J* = 7.0 Hz, 6H), 1.24 (d, *J* = 6.9 Hz, 3H), 1.17 (d, *J* = 6.7 Hz, 3H), 1.10 (d, *J* = 6.9 Hz, 3H), 0.95 (d, *J* = 6.9 Hz, 3H). **¹³C NMR** (CDCl₃, 100 MHz) δ (ppm) 181.7, 162.3, 148.7, 148.1, 146.4, 146.1, 137.6, 136.4, 136.3, 135.3, 133.7, 133.4, 128.9, 128.7,

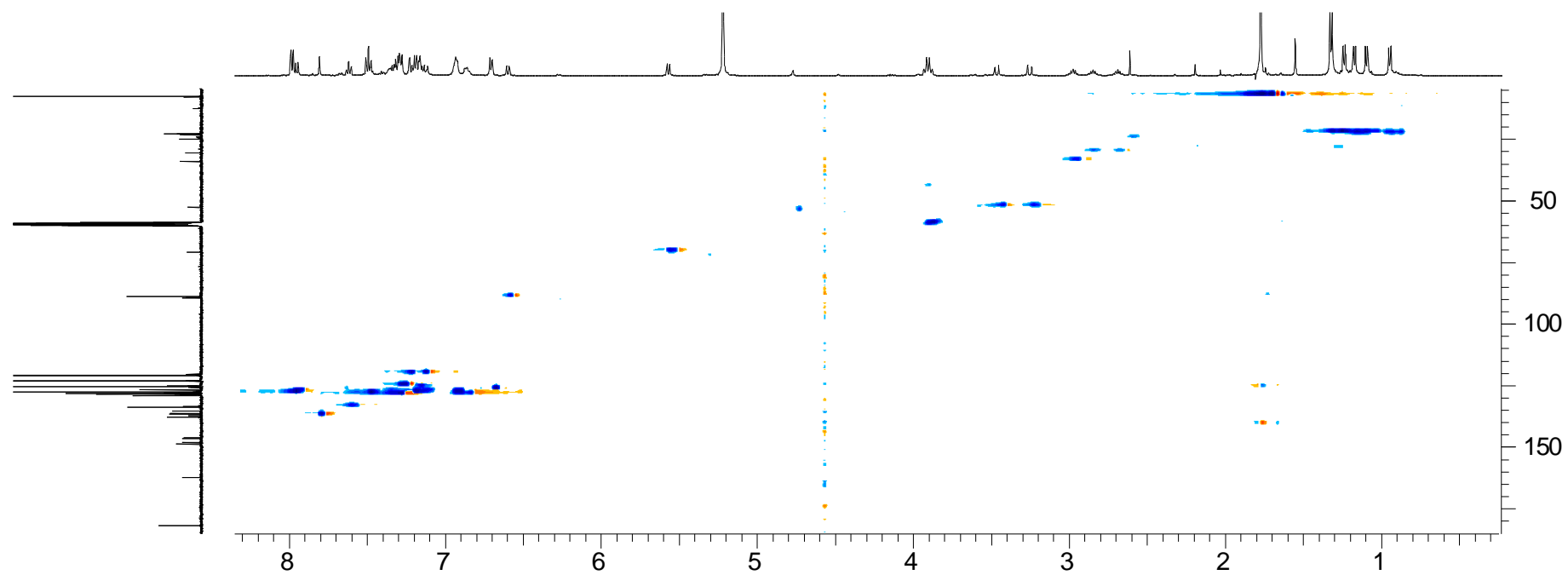
128.6, 128.5, 128.3, 128.1, 127.9, 127.7, 126.7, 120.4, 120.3, 89.3, 89.2, 88.7, 70.9,
52.6, 34.0, 30.4, 24.9, 23.1, 23.0, 22.7, 22.6, 7.8, 7.6.



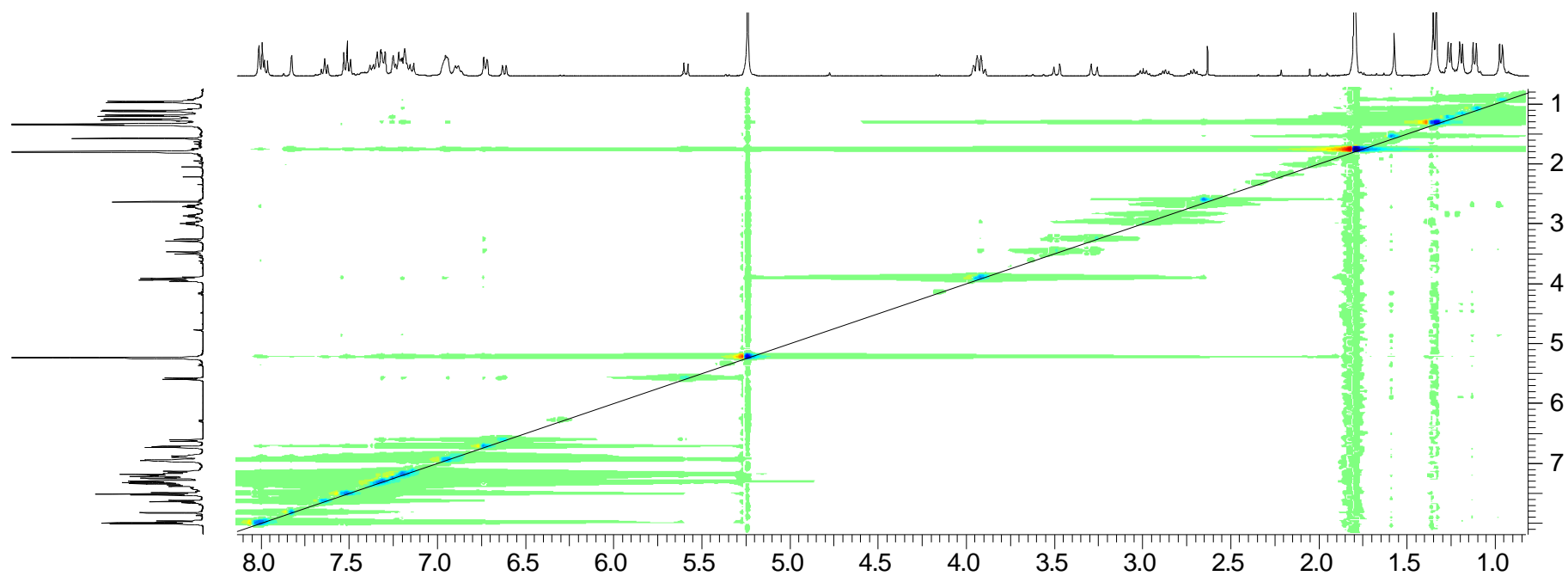
^1H - ^1H COSY NMR of imine bound iridium complex



HSQC NMR of imine bound iridium complex



NOESY NMR of imine bound iridium complex



6.8 References

- 1 A. Levi, G. Modena and G. Scorrano, *J. Chem. Soc*, 1975, **1975**, 6.
- 2 N. Fleury-Brégeot, V. de la Fuente, S. Castellón and C. Claver, *ChemCatChem*, 2010, **2**, 1346–1371.
- 3 W. Tang, S. Johnston, C. Li, J. a. Iggo, J. Bacsá and J. Xiao, *Chem Euro J*, 2013, **19**, 14187–14193.
- 4 C. J. Hou, Y. H. Wang, Z. Zheng, J. Xu and X. P. Hu, *Org Lett*, 2012, **14**, 3554–3557.
- 5 S. Y. Shirai, H. Nara, Y. Kayaki and T. Ikariya, *Organometallics*, 2009, **28**, 802–809.
- 6 S. Zhu, J. Xie, Y. Zhang, S. Li and Q. Zhou, *J. Am. Chem. Soc*, 2006, **128**, 12886–12891.
- 7 A. Dervisi, C. Carcedo and L. L. Ooi, *Ad. Synth and Catal*, 2006, **348**, 175–183.
- 8 M. Rueping, E. Sugiono, C. Azap, T. Theissmann and M. Bolte, *Org lett*, 2005, **7**, 3781–3.
- 9 Q. Kang, Z.-A. Zhao and S.-L. You, *Adv. Synth & Cat*, 2007, **349**, 1657–1660.
- 10 G. Li, Y. Liang and J. C. Antilla, *J. Am. Chem. Soc*, 2007, **129**, 5830–1.
- 11 T. B. Nguyen, H. Bousserouel, Q. Wang and F. Guéritte, *Org Lett*, 2010, **12**, 4705–4707.
- 12 J. G. de Vries and N. Mršić, *Catal. Sci & Tech*, 2011, **1**, 727.
- 13 A. Torres, N. Molina Perez, G. Overend, N. Hodge, B. T. Heaton, J. A. Iggo, J. Satherley, R. Whyman, G. R. Eastham and D. Gobby, *ACS Catal* 2012, **2**, 2281–2289.

- 14 J. H. Barnard, C. Wang, N. G. Berry and J. Xiao, *Chem Sci*, 2013, **4**, 1234.
- 15 C. Wang, A. Pettman, J. Basca and J. Xiao, *Angew Chem Int ed.* 2010, **49**, 7548–52.

Chapter 7: Conclusions and Future Work

During this project great progress was made in the areas of chiral iridicyclic synthesis and asymmetric reduction. A large number of novel chiral ligands and their corresponding iridicyclics were synthesised and characterised. These complexes all bore an iridium cyclopentadienyl chloride center, varying in the cyclometalated ligand bound to the metal center which could be split into two groups, oxazoline and imidazoline complexes. A number of bulky complexes were synthesised based on a terphenyl motif, to determine the effect of bulk on the observed enantioselectivities. For comparison smaller complexes were also synthesised, from these the electronic effects could also be investigated, with the presence of electron withdrawing and donating groups in various substitution patterns.

These novel iridicyclics were screened for a range of asymmetric reductions under mild transfer hydrogenation conditions. Reductive amination (the reduction of an imine formed *in-situ*) was investigated, the less bulky electron rich complexes proved highly successful, selectively reducing the imine in the presence of the ketone. The enantioselectivities achieved were moderate to high for the substrates screened, under mild conditions. These complexes also showed activity towards pyridinium salt reduction, yielding a number of asymmetric piperidines. Whilst high activity was observed for all substrates screened, not all enantioselectivities could be determined with the equipment available, however those determined showed great promise for this system. Several of the bulky oxazoline complexes synthesised showed great activity towards quinoline reductions, under aqueous transfer

hydrogenation conditions. Improved enantioselectivities and conversions could be obtained in the presence of a small amount of 2-methyl tetrahydrofuran.

The same bulky complexes proved active under hydrogenation conditions. Benzyl imines could be successfully reduced under mild hydrogenation conditions, with complete conversion and moderate to high enantioselectivities. A mechanistic study of this system was undertaken, indicating a key intermediate is synthesised for the asymmetric reduction, by coordination of the substrate to the iridium center, which is stable at low temperatures.

To further improve on the catalytic results obtained with these complexes modification of the ligands present could be undertaken. For example varying the steric and electronic properties of the cyclopentadienyl ligand, the enantioselectivities achieved in these catalytic transformations may show significant improvement. The addition of a solid support to either ligand may also allow for a heterogeneous complex to be synthesised. This may offer the opportunity for the iridicycle to be recycled, affording less waste and a greater atom economy.

A diverse range of reductive reactions were achieved in the presence of these complexes, affording moderate to high enantioselectivities. This included difficult transformations such as the DARA and the asymmetric reduction of pyridinium salts, both under transfer hydrogenation conditions. Further transformations may also be investigated utilising these complexes, such as ketone reduction, *N*-alkylation of alcohols and amines, as well as other transformations the non-chiral iridicycles have shown activity for.